

General Disclaimer

One or more of the Following Statements may affect this Document

- This document has been reproduced from the best copy furnished by the organizational source. It is being released in the interest of making available as much information as possible.
- This document may contain data, which exceeds the sheet parameters. It was furnished in this condition by the organizational source and is the best copy available.
- This document may contain tone-on-tone or color graphs, charts and/or pictures, which have been reproduced in black and white.
- This document is paginated as submitted by the original source.
- Portions of this document are not fully legible due to the historical nature of some of the material. However, it is the best reproduction available from the original submission.

(NASA-CR-169708) STRENGTH AND MECHANICS OF
BONDED SCARF JOINTS FOR REPAIR OF COMPOSITE
MATERIALS Final report, Jun. 1981 - May
1982 (Delaware Univ.) 190 p HC A09/MF A01

N83-15359

Unclassified
CSCL 11D G3/24 02332



DAMAGE REPAIR TECHNOLOGY FOR
COMPOSITE MATERIALS

NSG 1304

FINAL REPORT
JUNE 1981 - MAY 1982

R. BYRON PIPES
PRINCIPAL INVESTIGATOR
DAVID W. ADKINS

CENTER FOR COMPOSITE MATERIALS

College of Engineering
University of Delaware
Newark, Delaware

**Damage Repair Technology for
Composite Materials**

NSG 1304

**Final Report
June 1981 - May 1982**

**STRENGTH AND REPAIR OF BONDED SCARF JOINTS
FOR REPAIR OF COMPOSITE MATERIALS**

**R. Byron Pipes
Principal Investigator**

David W. Adkins

**Center for Composite Materials
College of Engineering
University of Delaware
Newark, Delaware 19711**

Jerry Deaton

**NASA Langley Research Center
Hampton, Virginia 23665**

December 1982

STRENGTH AND MECHANICS OF BONDED SCARF JOINTS
FOR REPAIR OF COMPOSITE MATERIALS

By

David W. Adkins

A dissertation submitted to the Faculty of the University of
Delaware in partial fulfillment of the requirements for the degree of
Doctor of Philosophy in Applied Sciences

December, 1982

ORIGINAL PAGE IS
OF POOR QUALITY.

ACKNOWLEDGEMENT

The research described in this dissertation was supported by a grant from the National Aeronautics and Space Administration for the study of repair of composite materials. It was also supported by E. I. duPont de Nemours and Co. through the use of their computers and other equipment.

PRECEDING PAGE BLANK NOT FILMED

ORIGINAL PAGE IS
OF POOR QUALITY

TABLE OF CONTENTS

	Page
NOMENCLATURE	v
ABSTRACT	1
INTRODUCTION AND BACKGROUND	3
EXPERIMENTS ON SCARF JOINTS WITHOUT DOUBLERS	16
Strength Data	18
Failure Modes	22
Other Experiments	28
ANALYSIS OF SCARF JOINTS WITHOUT DOUBLERS	35
SOLUTION OF THE GOVERNING DIFFERENTIAL EQUATION	45
ADHESIVE STRESSES IN THE SCARF JOINT	55
TWO-DIMENSIONAL STRESS DISTRIBUTION AT THE ADHESIVE ENDS	73
SCARF JOINTS WITH DOUBLERS	84
REFERENCES	98
APPENDICES	
Appendix i. BENDING OF A SPECIMEN WITH A THICK SECTION IN THE MIDDLE	103
Appendix ii. METHOD OF MAKING SCARF JOINT SPECIMENS	108
Appendix iii. EXPERIMENTAL DATA	116
Appendix iv. FORTRAN PROGRAMS SCARF3 AND SCARF4	120
Appendix v. FORTRAN PROGRAM SF3	171
Appendix vi. FORTRAN PROGRAM DEFLCOMP	176

ORIGINAL PAGE IS
OF POOR QUALITY.

NOMENCLATURE

A_{ij}	Elements of the laminate extensional stiffness matrix
E	Modulus of elasticity
F	Force
F_{ext}	External force, i.e. joint load
F	Dimensionless force
G	Modulus of elasticity in shear
k	Laminate curvature
t	Thickness
u	Displacement
w	Width
x, y	Coordinates
\bar{x}	Dimensionless coordinate
α	Scarf angle
ϵ	Strain
ν	Poisson's ratio
σ	Normal stress
σ_{max}	Maximum normal stress
τ	Shear stress
τ_{max}	Maximum shear stress

Subscripts, which are used singly and in combinations:

adher **Adherend**

adhes **Adhesive**

avg **Average over the laminate thickness**

extens **Extensional strain or stress**

l **Lower adherend**

u **Upper adherend**

x,y,z **Coordinate directions**

1,2 **Coordinate directions**

**ORIGINAL PAGE IS
OF POOR QUALITY**

ORIGINAL PAGE IS
OF POOR QUALITY

ABSTRACT

The experimental and analytical investigation of scarf joints described in this paper indicates that

- o slight bluntness of adherend tips induces adhesive stress concentrations which significantly reduce joint strength, and
- c the stress distribution through the adhesive thickness is non-uniform and has significant stress concentrations at the ends of the joint.

Also, the laminate stacking sequence can have important effects on the adhesive stress distribution. Three other results are worth mentioning. First, a significant improvement in joint strength is possible by increasing overlap at the expense of raising the repair slightly above the original surface. Second, although a surface grinder was used to make most experimental specimens, a hand held rotary bur can make a surprisingly good scarf. And third, scarf joints with doublers on one side, such as might be used for repair, bend under tensile loads and may actually be weaker than joints without doublers.

Bluntness results from breakage during fabrication where the adherends are only a few microns thick. The stress concentrations occur for all scarf joints but are much more pronounced for small scarf angles, i.e. around 20 milliradians (one degree). Experimental data suggest that there is an upper limit to scarf joint strength.

The scarf joint adhesive stress comprises two components. One is due to gross extension of the entire joint and is predominantly a tensile stress. It is simple to calculate. The other component is due to load transfer between the adherends and is predominantly a shear stress. The governing equation for the load transfer stress is a second order ordinary differential equation with two singular points. The solution to this equation exhibits boundary layer structure. WKB expansions and Frobenius series expansions provide very efficient and straight forward methods for solving it.

Stress concentrations are also induced through the adhesive thickness by the sudden change in shear loading at the ends of the adherends. Two dimensional equilibrium requires a large normal stress gradient to balance the shear stress gradient. This results in high normal stresses under the adherend tip. This phenomenon is analysed by a stress function solution for a rectangular region with Fourier series boundary conditions.

ORIGINAL PAGE IS
OF POOR QUALITY

INTRODUCTION AND BACKGROUND

This paper describes experiments and analyses of scarf joints with and without doublers. The majority of the work involved joints without doublers. The first part describes a number of ideas and models of joint behavior found in the literature. The second part describes making and tensile testing scarf joints of an 18-ply carbon/epoxy laminate with scarf angles between 20 milliradians and 160 milliradians (one degree and nine degrees). This part includes grinding scarfs with a hand-held bur, trying a suggestion from the literature to reduce adhesive singularities, and increasing joint overlap by letting the repair extend slightly above the surface. Next is a discussion of the two analyses: the effect of slight bluntness of the adherend tips and the stresses induced by the sudden change in adhesive shear loading at the ends of the adherends. Finally, experiments and a bending model of scarf joints with doublers are described.

The double scarf joint shown in Figure 1 is the joint geometry selected for this study. It was chosen as a typical repair for damaged laminates on commercial aircraft. The repair is made by first cutting out the damaged part of the laminate, Figure 2. Next the cut edges are beveled to form scarfs and adhesively bonded to a matching replacement piece. An optional doubler may be bonded over the scarf joint. The scarf joint repair is potentially very strong and has a smooth surface

ORIGINAL PAGE IS
OF POOR QUALITY

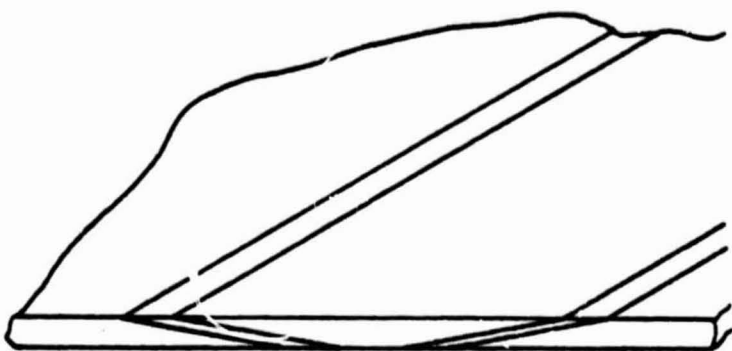


Figure 1. Scarf joint geometry.

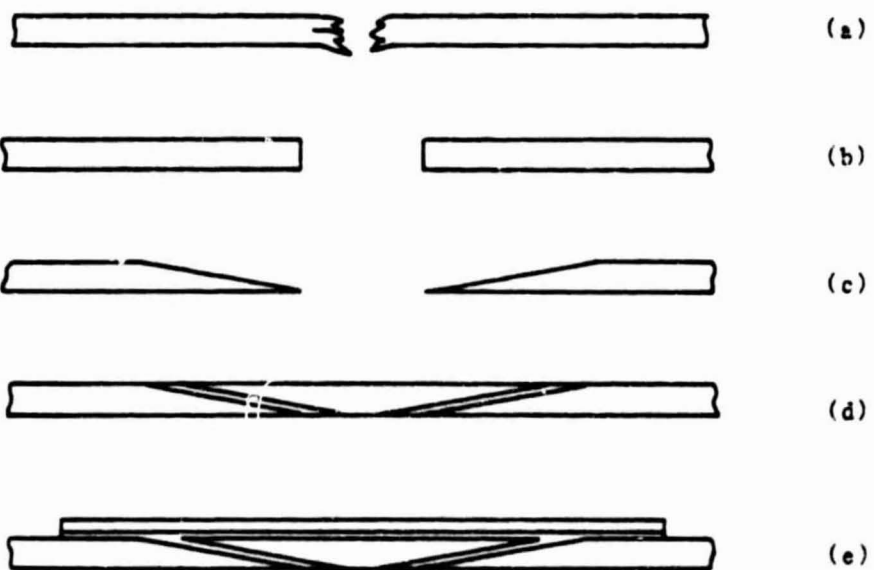


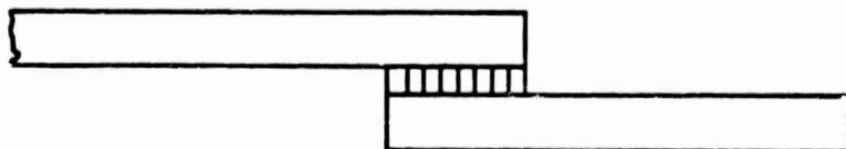
Figure 2. The steps in repairing a damaged plate with a scarf joint:
(a) damaged plate, (b) plate with damage removed, (c) beveled edges,
(d) replacement piece bonded to original laminate, (e) repair with an
optional doubler.

which is good for aerodynamics.

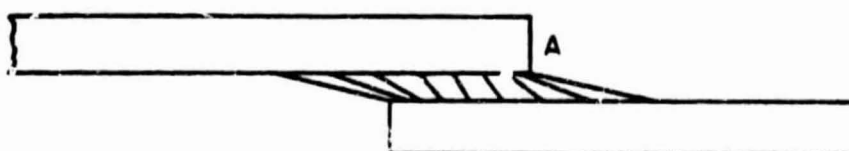
Several important models of joint mechanics have been developed in earlier studies. Perhaps the most important is a mechanism of load transfer between adherends by adhesive shear. In this model the adhesive shear stress is determined by the relative displacement of the adherends on either side of the adhesive. At the same time the adherend displacements depend on the load transferred to them by the adhesive. The mechanism is demonstrated in Figure 3.

When the lap joint in Figure 3 is loaded, different parts of the joint stretch different amounts. At location A, for example, the bottom adherend is stretched a lot because it carries nearly all of the load. In contrast, the top adherend at location A is stretched very little because it carries very little load. The result, as the figure shows, is that the adhesive is strained a lot in shear at the ends of the bond but very little in the middle. So the bond breaks at the ends before the middle is fully loaded. This model of load transfer was first published by Volkerson (Ref. 1) in 1938 and used in a well known paper by Goland and Reissner (Ref. 2) in 1943.

The adhesive strain can be made more uniform along the bond if the adherends are tapered, or scarfed, as shown in Figure 4. When the scarf joint is loaded the adherends stretch the same amount all along the bond. At location B, for example, the top adherend carries little of the load. However, it stretches the same as the bottom adherend, which carries more load but is proportionally thicker.



Unloaded



Loaded

Figure 3. Unloaded and loaded lap joint.



Unloaded



Loaded

Figure 4. Unloaded and loaded scarf joint.

This uniform shear distribution depends on proper joint design and several phenomena must be considered. Any joint design in which strains of the two adherends are not identical along the adhesive will have shear stress concentrations. Adherend section stiffness (thickness times elastic modulus), thermal expansion and moisture absorption can all be important. The effect of adherend section stiffness is demonstrated by Figures 3 and 4. In addition, if the adherends in Figure 4 have non-identical thicknesses or moduli the shear strain will be higher at the ends than in the middle. And it will be highest at one end. This shear stress distribution can be improved, although not necessarily made uniform, by using adherends with specially changing thickness along the adhesive. This approach has been studied by Ramamurthy and Rao (Refs. 3,4), Sainsbury-Carter (Ref. 5), Cherry and Harrison (Ref. 6) and by Thamm (Ref. 7). Lubkin in a study of scarf joints (Ref. 8) calculated the scarf angle for which no stress concentration would occur between two dissimilar adherends. The angles are large enough that it is not a practical way to design joints.

Adherends with different thermal or moisture expansion coefficients can have shear concentrations even when the joint is unloaded. In this case one adherend expands more than the other causing shear concentrations of opposite sign at the adhesive ends. Thermal expansion stresses are usually present in the unloaded joint because the adhesive sets at an elevated temperature. Also, temperature and especially moisture expansion can vary with both time and position in the adherend. These problems have been studied by Hart-Smith

(Ref. 9,10,11), Wetherhold and Vinson (Ref. 12), Sinha and Reddy (Ref. 13), Chen and Nelson (Ref. 14), and Vinson and Zumsteg (Ref. 15).

A limitation of this load transfer model is that it does not satisfy the zero shear stress boundary condition at the adhesive end. Since the adhesive end is a free surface, no shear stresses or normal stresses perpendicular to the adhesive end surface are possible. The adhesive end can not be strained in shear, as shown in Figures 3 and 4. The load transfer model still holds everywhere but near the end of the adhesive, however. So it is a useful model of joint mechanics, especially for thin adhesives.

Composite adherends are frequently orthotropic and this also effects their behavior in joints. The edge conditions, e.g. plane stress, and adherend physical properties determine the effective load-direction modulus of elasticity. Erdogan and Ratwani (Ref. 16), Reddy and Sinha (Ref. 17), and Renton and Vinson (Refs. 18,19) have developed models for such orthotropic materials. The model developed by Renton and Vinson also accounts for through-the-thickness shear of the adherends.

Adhesive thickness also influences the adhesive shear distribution (Ref. 20). A small displacement across a thin adhesive results in a higher shear strain than the same displacement across a thick adhesive. For this reason thick adhesive at the ends of the joint can reduce stress concentrations (Ref. 21).

Width-wise contraction of the adherends can cause a somewhat different type of shear stress concentration. The fully loaded (bottom) adherend at location A in Figure 3 will contract in width and thickness in proportion to the load and its Poisson's ratio. The adjacent unloaded adherend will not contract at all. This causes adhesive shear strains across the specimen, perpendicular to the strains shown in Figure 3. These strains are most pronounced at the adherend corners as discussed by Adams and Peppiatt (Ref. 22).

Another way of maintaining uniform shear stress is by using very thick adherends. The idea is to make them thick enough that their strains are small at loads up to the failure stress of the adhesive. This is not an efficient way to design structures because the strength of the adherend is not used. However, the idea has been applied to making specimens for testing adhesive properties (Refs. 23,24,25).

Another important idea about joints is that they sometimes bend when loaded only in tension. This happens because part of the joint is unsymmetrical about the plane of the applied load. For example, the lap joint of Figure 5 will bend when loaded in tension. A free body diagram of the adhesive and adjacent adherends shows that the force F must be held by parts that are away from the over-all plane of loading. Because of this offset, moments are created in the joint and it bends as shown in the figure. As the joint bends the offset is reduced. At equilibrium the moment of the offset applied force equals the moment required to bend the adherends.

ORIGINAL PAGE IS
OF POOR
QUALITY

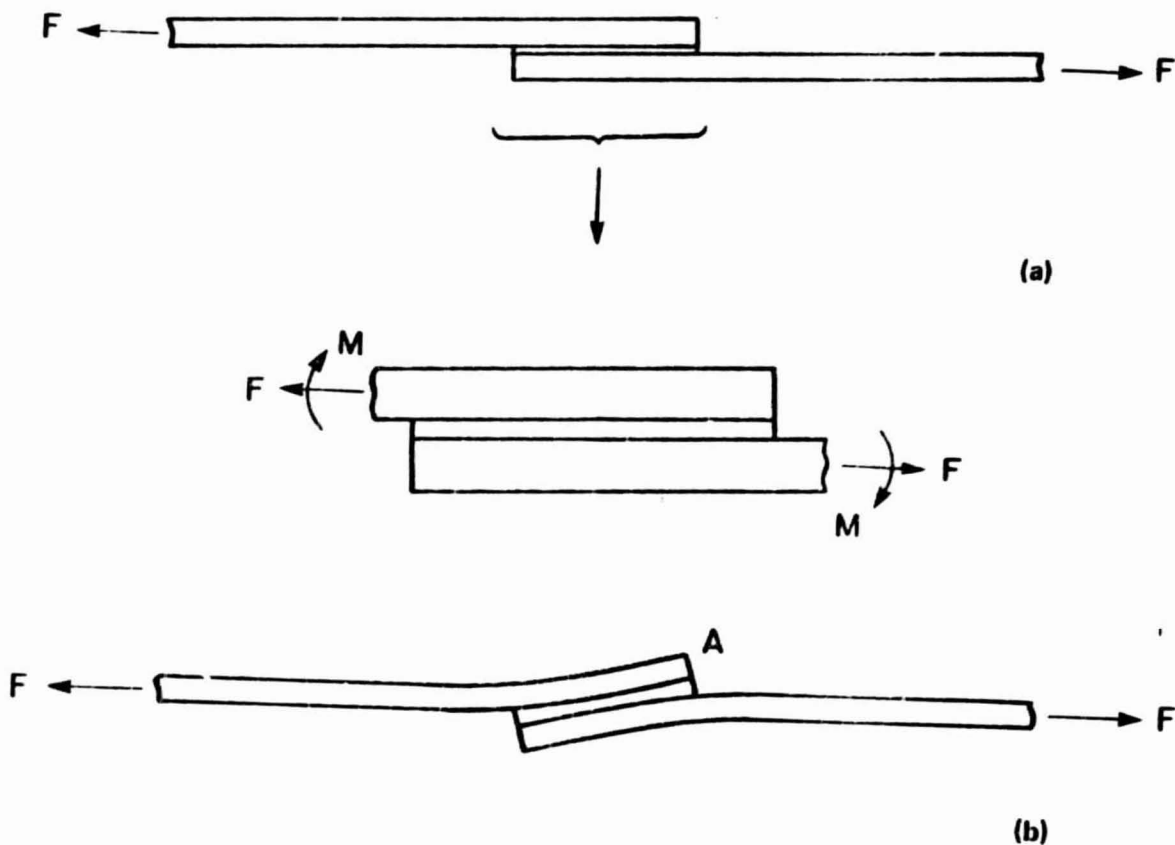


Figure 5. Bending of a lap joint loaded only in tension: (a) free body diagram of the adhesive and adjacent adherends, (b) exaggerated shape of the loaded joint.

ORIGINAL PAGE IS
OF POOR QUALITY

This bending is nonlinear with applied load. With application of a small load the joint will move rapidly toward the position shown in Figure 5. But once the joint approaches that position very large increases in load cause very little additional bending deflection.

Bending under tension is most pronounced in single lap joints, although even scarf joints bend some. Bending under tension, because it is so important to lap joints, has been studied by many authors (Refs. 9,18,19,20).

Bending under tension is important to joint strength because it induces forces perpendicular to the load-plane at the ends of the adhesive. For example, at point A of the loaded lap joint in Figure 5(b) the bottom adherend is bent a lot. And the nearby end of the top adherend is nearly straight. The adhesive must stretch in the vertical direction to remain bonded to both adherends. The resulting tensile, or peel, stresses can cause breaking in either the adhesive, the bottom adherend, or at the interface, as shown in Figure 6 (Ref. 9). Sawyer and Cooper have published a way of reducing bending effects by preforming (prebending) the adherends (Ref. 26).

Bending also increases tensile stresses at the outside of the specimen, just as a beam loaded in bending has higher stresses at the outer surfaces. This is important for scarf joints with doublers on only one side. Where the joint ends on the side away from the doubler the adhesive must accomodate the extra bending strain.

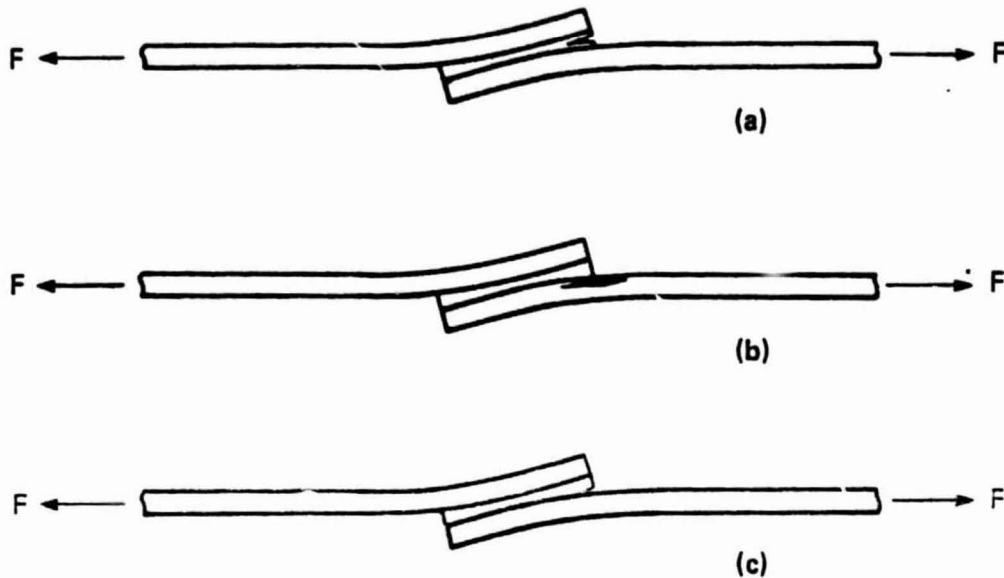


Figure 6. Peel stress induced failure: (a) cohesive failure, (b) adherend delamination, (c) adhesive failure.

There is another more subtle source of peel stresses. Adhesive shear forces can cause bending at the end of a bonded adherend. This bending happens even in joints which are symmetric about the load plane, such as double lap joints. A free body diagram of the upper adherend end of a double lap joint is shown in Figure 7. The horizontal shear forces on the bottom must be balanced. In the horizontal direction, the shear force can be balanced only by a force on the left hand side. However, this results in a couple which bends the adherend tip upward. The upward bending is resisted by bending stresses on the left hand side and normal stresses on the bottom. Note that both tensile and compressive adhesive stresses are required to maintain vertical equilibrium. This bending has been modeled by Hertz-Smith (Ref. 10).

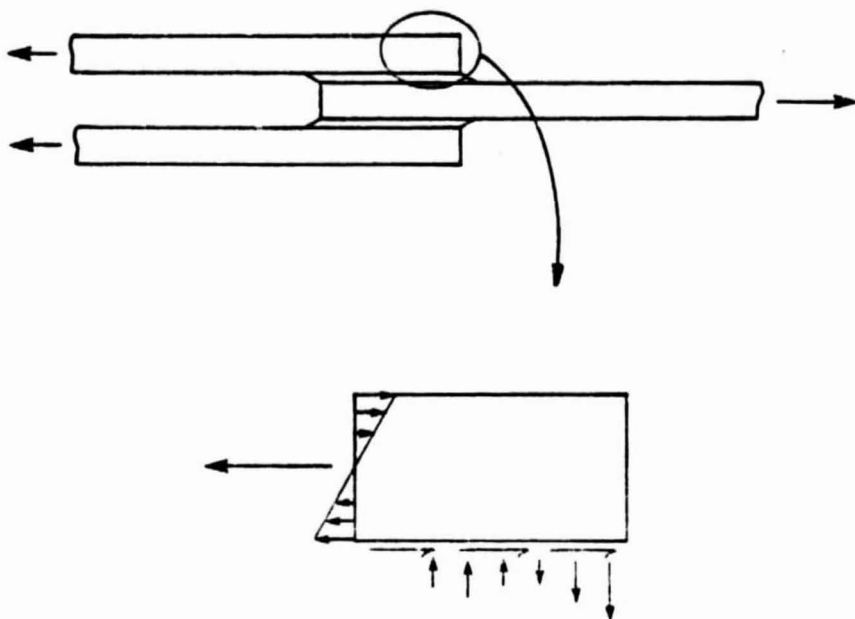


Figure 7. Peel stresses in the adhesive of a double lap joint.

Adherend bending, such as in Figure 7, also changes the adhesive shear strain at the end of the joint. This shear strain adds to the adhesive shear strain induced by load transfer discussed earlier. It is shown without the load transfer shear strain in Figure 8. The slope of the curved adherend tip strains the adhesive in shear, as shown by the upper small adhesive element. Ojalvo and Eidinoff (Ref. 20) discuss this effect and conclude that the shear strain must be different on the upper and lower surfaces of the adhesive.

A third important idea about joint mechanics is that stress concentrations sometimes happen at the adhesive-adherend interface. Few studies have been done on this effect for actual joint geometries.

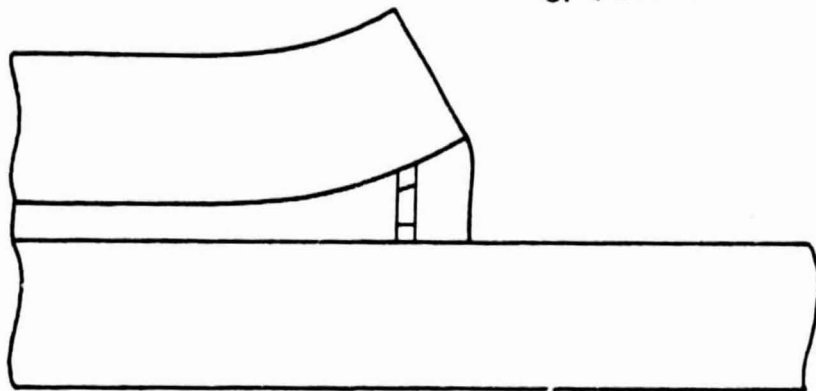
ORIGINAL PAGE IS
OF POOR QUALITY

Figure 8. Adhesive shear strain caused by bending of the adherend end.

Most analyses have dealt with stress fields at the interface of bonded wedges. Rao (Ref. 27), for example, has shown that elastic stress singularities occur and their intensity and order are functions of wedge angle. Hein and Erdogan (Ref. 28), and Bogy (Ref. 29) have also considered this problem.

Non-elastic adhesive behavior can also be very important to the adhesive stress distribution. This includes such effects as non-linear stress-strain behavior and viscoelasticity. Hart-Smith (Refs. 9,10,11) has approximated non-linear behavior with elastic-plastic and bilinear models. These models predict a nearly constant adhesive stress zone near the adherend ends with significantly higher predicted joint strength. Ralamurthy and Rao (Ref. 30) have used elastic-plastic, bilinear and trilinear approximations. Several finite element and finite difference analyses have also accounted for adhesive non-linearity (Refs. 31,32,33).

The complexity of viscoelastic analysis generally requires

numerical solutions. Nagaraja and Alwar (Ref. 34) have used the finite element method. Sen and Jones (Refs. 35,36) and Delale and Erdogan (Ref. 37) have used Laplace transform methods with numerical inversion.

Several of the papers mentioned deal specifically with scarf joints. Hart-Smith (Ref. 11) accounted for non-linear adhesive and adherends with different stiffnesses and thermal expansion coefficients. He also concluded that bond shear strength increases indefinitely as the scarf overlaps are made bigger. Erdogan and Ratwani (Ref. 16) developed a model for an orthotropic adherend bonded to an isotropic adherend. Reddy and Sinha extended that model to account for two orthotropic adherends (Ref. 17) and also for thermal expansion (Ref. 13). In addition, Thamm calculated the shear stress distribution in a lap joint with partially thinned (scarfed) adherends (Ref. 7).

Wah calculated the two dimensional stress distribution in a scarf joint adhesive using stress functions (Ref. 38). However, he considered scarf angles only between sixty degrees and ninety degrees (butt joint). Wright (Ref. 39) and Adams and Peppiatt (Ref. 32) using the finite element method found that there are stress concentrations in scarf joints between identical adherends. Also, in the same paper, Adams and Peppiatt calculate the stress distribution of a scarf joint with slightly blunted tips.

There are several surveys of the literature in adhesively bonded joints. The most recent and thorough are by Vinson (Ref. 40) and Mathews, Kilty and Godwin (Ref. 41).

ORIGINAL PAGE IS
OF POOR QUALITY

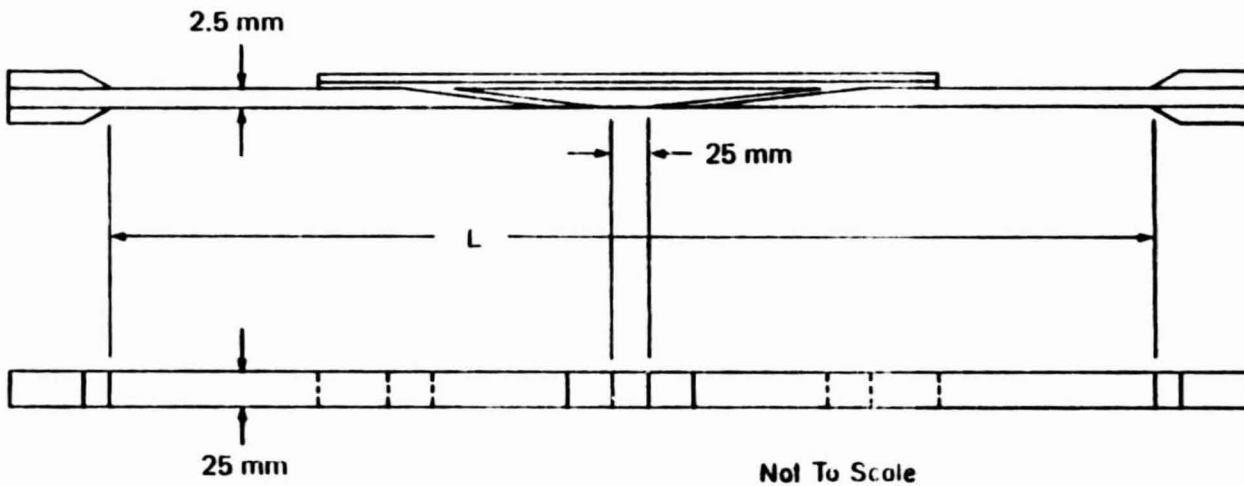
EXPERIMENTS ON SCARF JOINTS WITHOUT DOUBLERS

All of the experimental specimens were made from laminates of Hercules AS1/3501-6 carbon/epoxy. Since the primary purpose of this study was to evaluate the selected geometry, rather than the repair procedure itself, all experimental specimens were made directly from undamaged laminates. The stacking sequence was $[0_2/\pm45/90/\pm45/0_2]_S$. Ten specimens of this laminate were tested in tension to measure its strength. The data are tabulated in Appendix iii. The average ultimate force resultant was 2.21 ± 0.84 GN/m (12,600 \pm 480 lb/in) at 95% confidence level. Since the joint should be as strong as the adherends the goal strength is 2.21 GN/m.

The dimensions of the experimental specimens are shown in Figure 9. The eighteen ply laminate is 2.5mm thick. The width was selected as about ten times the thickness so that edge effects would be small. Specimen length was determined by worst case bending behavior. When a specimen with a doubler is loaded in tension it bends as explained on page 9. This bending induces moments at the test machine grips which might change the load at which the specimen breaks. Although the moments cannot be eliminated the specimens can be made long enough that the moments at the grips are insignificant.

Bending can be easily calculated for a specimen with a thick

ORIGINAL PAGE IS
OF POOR
QUALITY



Scarf angle (milliradians)	Specimen length, L (millimeters)
19	500
33	380
52	300
110	220
160	200

Figure 9. Dimensions of the experimental scarf joint specimens.

section in the middle, Appendix i. This is a good approximation to the scarf joint with a doubler, which is the worst bending case. Based on this analysis, the specimen length was chosen so that the slope at the grips would be zero to three significant figures.

The specimens were made by grinding scarfs on the cured laminates. The laminates were held onto a wedge-shaped block mounted on the table of a surface grinder. This method gave very smooth, accurate scarfs. The scarfed panels were then bonded together with film adhesive. The adhesive was autoclave cured with the joint pieces pinned onto a laminate of the same material and stacking sequence. This minimized loading the adhesive by thermal expansion of the scarfed adherends. The final panels were cut into tensile test specimens with a diamond saw. Panels and specimens were ultrasonically scanned at each stage to detect any defects. Details of the cutire process are in Appendix ii.

This procedure worked very well for all but the 160 milliradian (9.2 degree) scarf joints. These joints were difficult to bond despite their short overlap. It turns out that these joints are very unforgiving of misfit. The short overlap (15 mm) and high bending stiffness restrain deflection perpendicular to the specimen plane. So they don't easily deflect to compensate for machining or alignment errors. Surprisingly, the long joints are the easiest to fit.

Strength Data

Average strength data for five groups of joint specimens are

listed in Table I. The strengths are given as stress resultants because the laminates are thin (plikelike) and inhomogeneous. The efficiency is the joint strength divided by the laminate strength from page 16. Detailed data for the thirty-three specimens tested are in Appendix iii.

Table I. SCARF JOINT STRENGTH

(Strength ranges are for 95% confidence level)

Scarf Angle (m rad)	Scarf Angle (deg)	Number of Specimens	Average Ultimate Force Resultant (GN/m)	Efficiency (1bf/in)
19	1.1	6	1.35 \pm 0.086	7710 \pm 490
33	1.9	4	1.40 \pm 0.092	8000 \pm 520
52	3.0	5	0.990 \pm 0.062	5650 \pm 350
110	6.2	13	0.648 \pm 0.032	3700 \pm 180
160	9.2	4	0.510 \pm 0.048	2900 \pm 270

A striking feature of these data is that they don't fit conventional models of joint behavior. The joint strength would be expected to increase without limit as the scarf angle is made smaller. In principle, the load is born by a larger adhesive area which should be subject to lower stress. To the contrary, the 19 milliradian scarf joints supported only 1.35 GN/m compared to 1.40 GN/m for 33 milliradian scarf joints. Since the 19 milliradian joints were expected to be about 1.4 to 1.6 times as strong as the 33 milliradian joints two sets of 19 milliradian joints were made and tested. Both sets had the same strength.

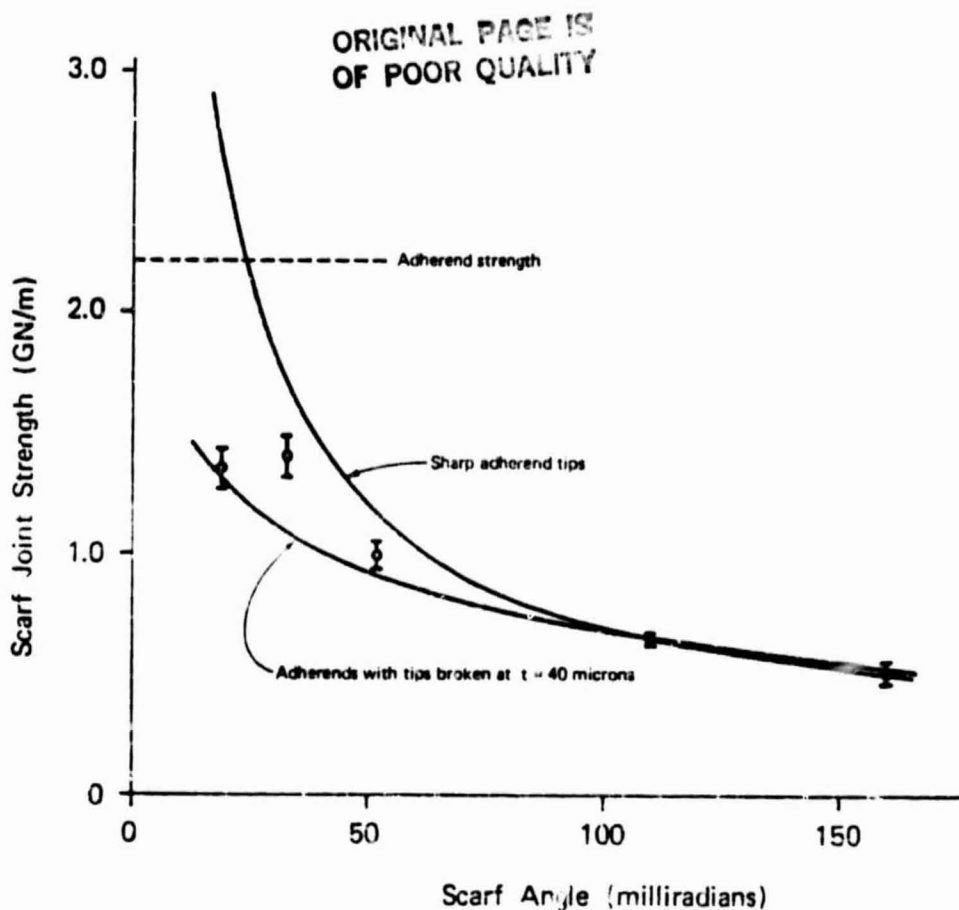


Figure 10. Experimental and predicted scarf joint strength. The predicted values are based on maximum shear stress.

The scarf joint strength data are plotted in Figures 10 and 11 along with some calculated strength curves. The maximum shear stress failure criterion is used for the curves in Figure 10 and maximum normal stress for Figure 11. The calculated strengths account for the stiffness of the zero degree plies at the adherend tips and for load-direction strain of the whole joint. These calculations are described in detail in the section on adhesive stresses in the scarf joint.

The strengths predicted for sharp tipped adherends are much

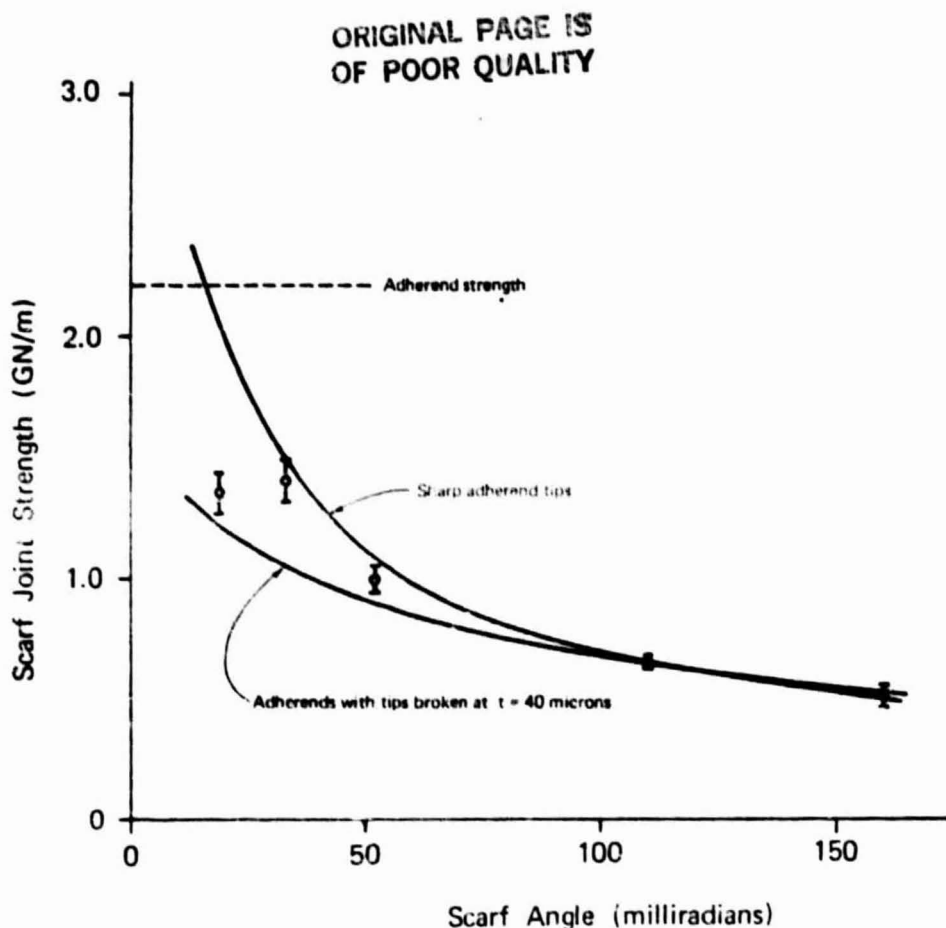


Figure 11. Experimental and predicted scarf joint strength. The predicted values are based on maximum normal stress.

higher than the experimental data for small scarf angles. However, as shown in the figures, the experimental data can be explained by adherends with tips broken off a short distance from the end. The lower curves represent the strength predicted for adherends with the tips broken where the adherend is only 40 microns (0.0016 in.) thick. This is the thickness of five carbon reinforcing fibers. As the curve shows, making the scarf angle even smaller for such adherends still may not attain the strength of the undamaged laminate.

Failure ModesORIGINAL PAGE IS
OF POOR QUALITY

The failures range from a relatively simple break through the adhesive for the 160 milliradian (9.2 degree) scarf joints to a complicated break with considerable adherend damage for the 19 milliradian (1.1 degree) joints. Both 110 milliradian (6.2 degree) and 160 milliradian (9.2 degree) joints broke mainly in the adhesive (Figures 12 and 13). The fracture surface had adhesive separated from itself with regions where the separation was in the adherend. All had

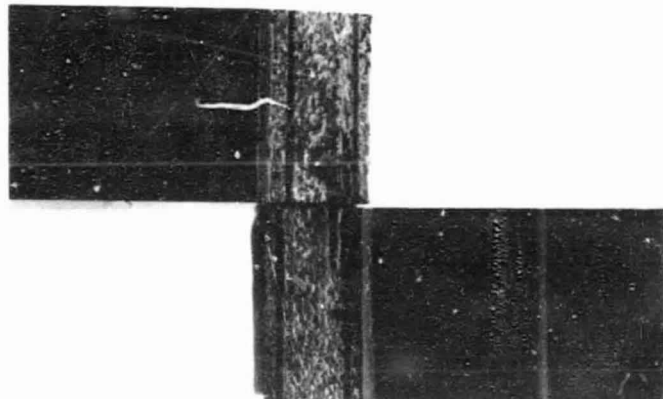


Figure 12. Fracture surface of a 160 milliradian scarf joint, specimen number 3-136-4.

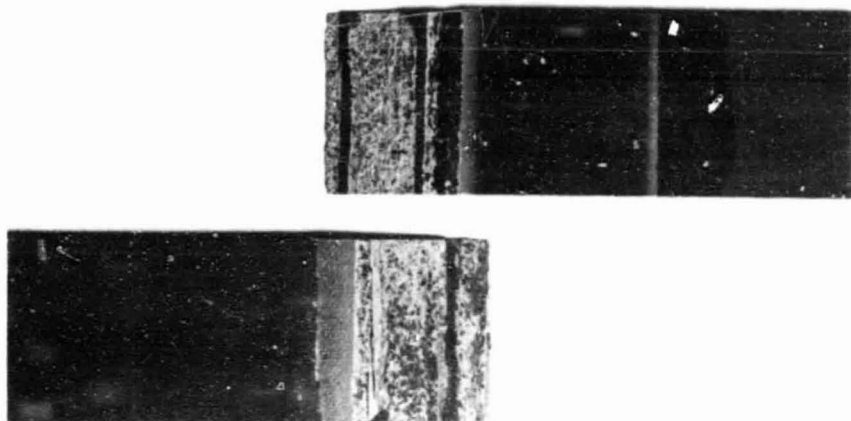


Figure 13. Fracture surface of a 110 milliradian scarf joint, specimen number 4-96-2.

pull-out of 45 degree and 90 degree adherend reinforcing fibers, although pullout was more pronounced in the 110 milliradian (6.2 degree) scarf joints.

Scanning electron micrographs of one of these regions (Figures 14 and 15) confirm that the failure is actually in the adherend. A thin layer of matrix resin and fibers has pulled off of the composite adherend and can be seen on a micrograph of the mating piece in Figure 15.

Micrographs also show two other interesting aspects of the adhesive. Figure 16 shows filaments in the adhesive from the knit tricot mat that is manufactured into it. This mat is used to control bond line thickness. The second feature is the small holes visible in Figure 17. They are caused by the small rubber particles used to

ORIGINAL PAGE IS
OF POOR QUALITY

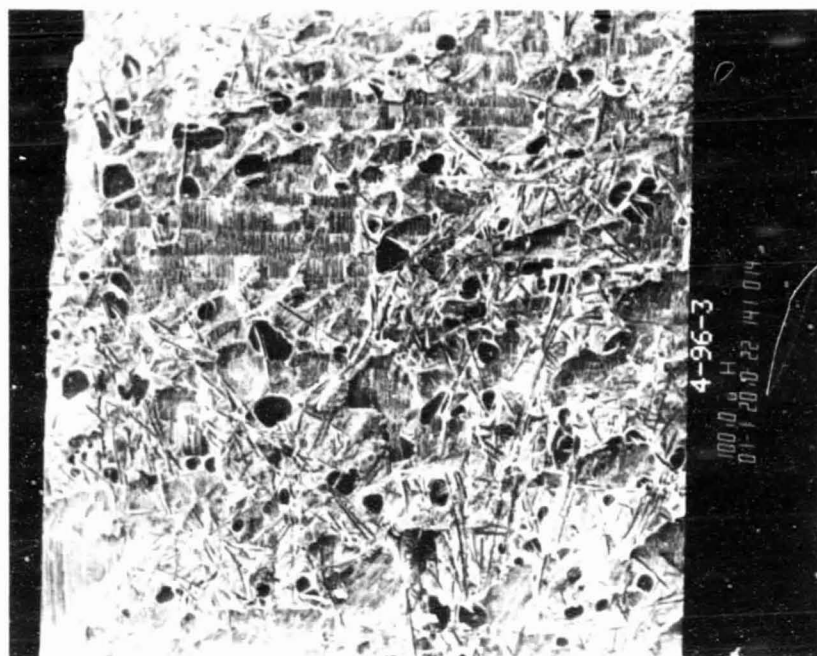


Figure 14. Scanning electron micrograph at 10x of the fracture surface of 110 milliradian scarf joint specimen number 4-96-3. Reinforcing fibers have broken from the adherend in the striated region in the upper left quadrant.

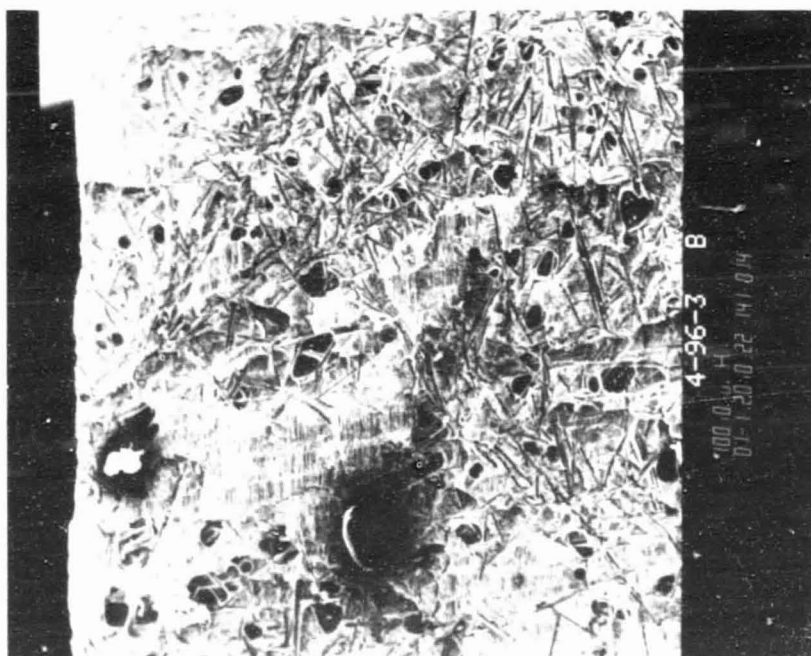


FIGURE 15. Scanning electron micrograph of the mating fracture surface to the one in Figure 14. The reinforcing fibers pulled from that adherend can be seen in the lower left quadrant.

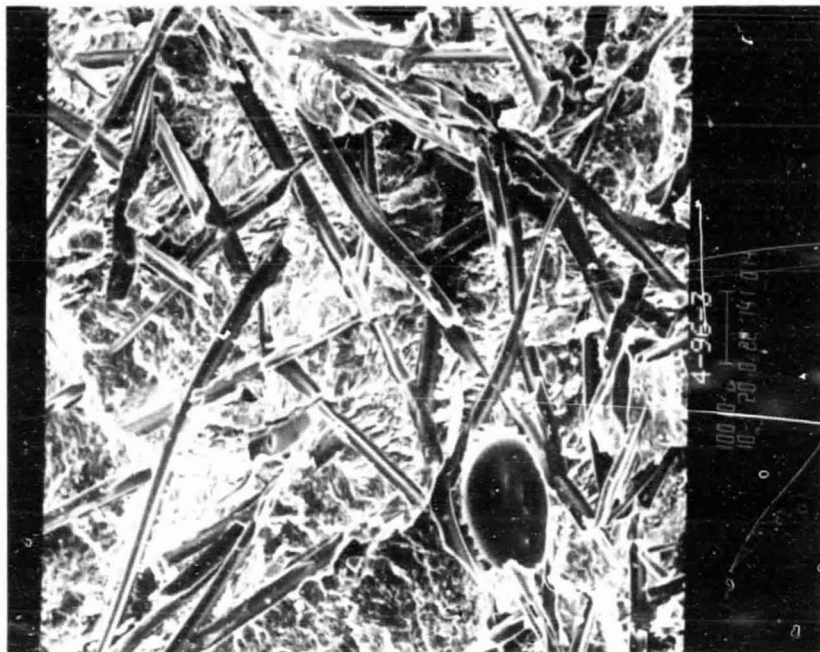


Figure 16. Scanning electron micrograph at 100x showing the knit tricot mat used to control adhesive thickness.

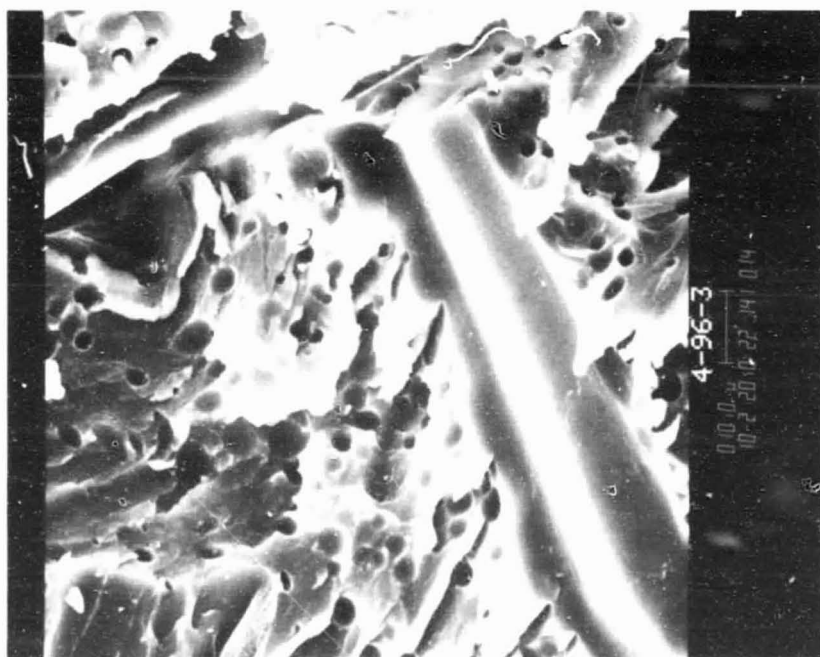


Figure 17. Scanning electron micrograph at 1000x showing small holes in the fractured adhesive surface caused by small particles used to toughen the adhesive.

ORIGINAL PAGE IS
OF POOR QUALITY

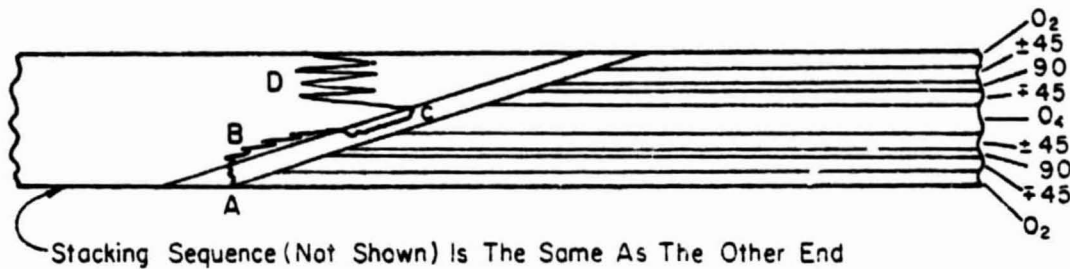


Figure 18. Failure mode of 19, 33 and 52 milliradian scarf joints.

toughen the adhesive.

The 19, 33 and 52 milliradian (1.1, 1.9 and 3.0 degree) scarf joints failed in a different mode. The failure surface, Figure 18, begins at one of the adherend tips and goes through the adhesive at point A. Inside the joint at B many 45 degree and 90 degree adherend fibers are pulled out. Between the inside zero degree plies, which are too strong to pull out, the adhesive breaks. The surface is similar to the regions of adhesive separation in the 110 and 160 milliradian joints. The failure surface then goes through the adherend with considerable delamination and 'brooming' of the remaining plies, Figures 19, 20, and 21.

ORIGINAL PAGE IS
OF POOR QUALITY

27

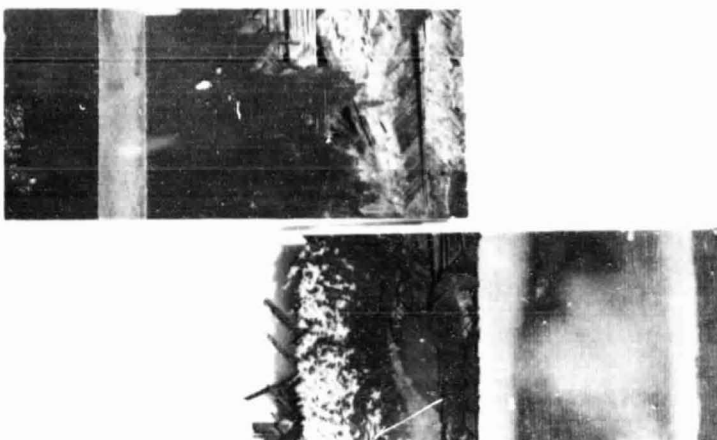


Figure 19. Fracture surface of a 52 milliradian scarf joint, specimen number 3-13-2.

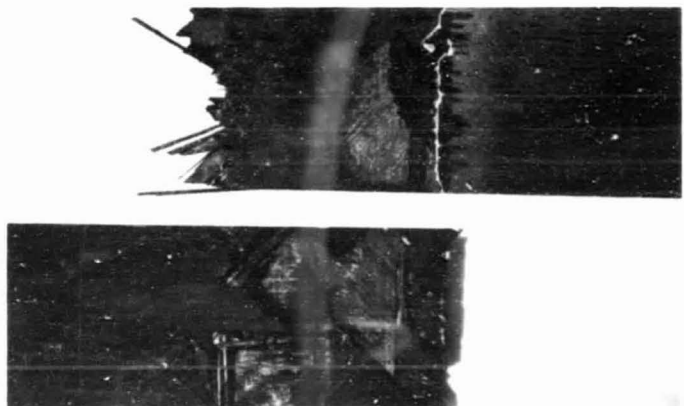


Figure 20. Fracture surface of a 33 milliradian scarf joint, specimen number 3-34-4.

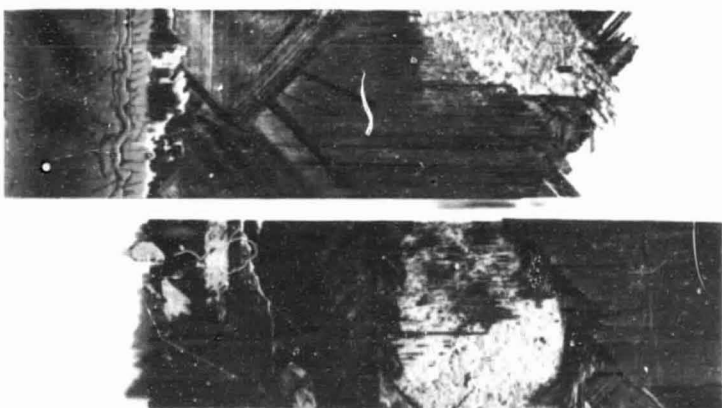


Figure 21. Fracture surface of a 19 milliradian scarf joint, specimen number 3-121-4.

Where the failure begins is important for analysis. Modeling joint strength requires a failure mechanism which depends on calculated conditions at a particular site. In this paper failure is assumed to begin at the end of the bondline in the adhesive. Unfortunately this is difficult to verify because the joints break so quickly. The specimens can be inspected after testing, however, for evidence supporting or contradicting the assumed site of failure initiation.

Supporting the idea that failure begins at the end of the bondline is the observation that every break has one adherend tip intact. This is a reasonable thing to expect for end failure because after the adherend tip separates it would be very unlikely to suffer more damage.

Evidence supporting failure initiation in the adhesive is somewhat less conclusive. Every broken joint has a region where the adherend matrix has broken like in Figure 14. It cannot be determined if failure began in the adhesive at point A in Figure 18 or in the adjacent adherend matrix.

Other Experiments

Three other experiments were made on plain scarf joints. One was grinding scarfs with a hand held rotary bur to demonstrate making the joints with small portable equipment. Another one was reducing stress concentrations by rounding the adherend tips. And the last was

making joints with slightly more overlap.

Because aircraft repairs must often be made directly on the airplane without sophisticated equipment, a simple way of machining the repair is desirable. To evaluate cutting the scarf's without a surface grinder one set of joints was made by cutting them with a hand held pneumatic rotary bur. This simple, easily portable device worked very well.

Fifty two milliradian (3.0 degree) scarf's were wet-cut with a carbide bur. Water removed the dust and also made the individual plies visible. Visibility of the plies helped cut the scarf's uniformly because their interfaces were like the contour lines on a topographical map. The contour of the cut surface was easy to determine by studying the pattern of the ply interfaces. Figure 22 shows the scarfed plies of a machine ground laminate and a hand ground laminate. With care (and some practice) a surprisingly uniform scarf can be cut by hand. It is helpful that a one millimeter deviation in the position of a ply interface (a contour line) corresponds to only 50 microns deviation in thickness for a 50 milliradian (3 degree) scarf. For example the deviation of the contour lines on the right hand side of the unfinished hand ground specimen in Figure 22 are due to the specimen being only 0.3 mm too thick.

The hand ground scarf joint strength averaged 0.80 ± 0.039 GN/m (4570 ± 220 lb/in), Appendix iii. This is significantly lower than the 0.99 GN/m of the machine ground joints. Interestingly, the failure

ORIGINAL PAGE IS
OF POOR QUALITY

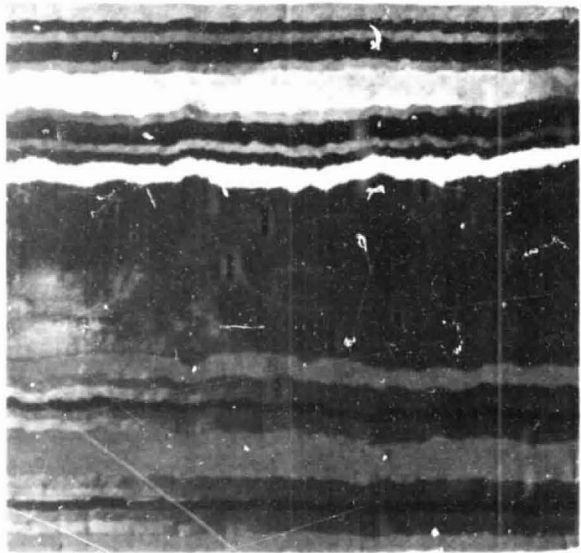
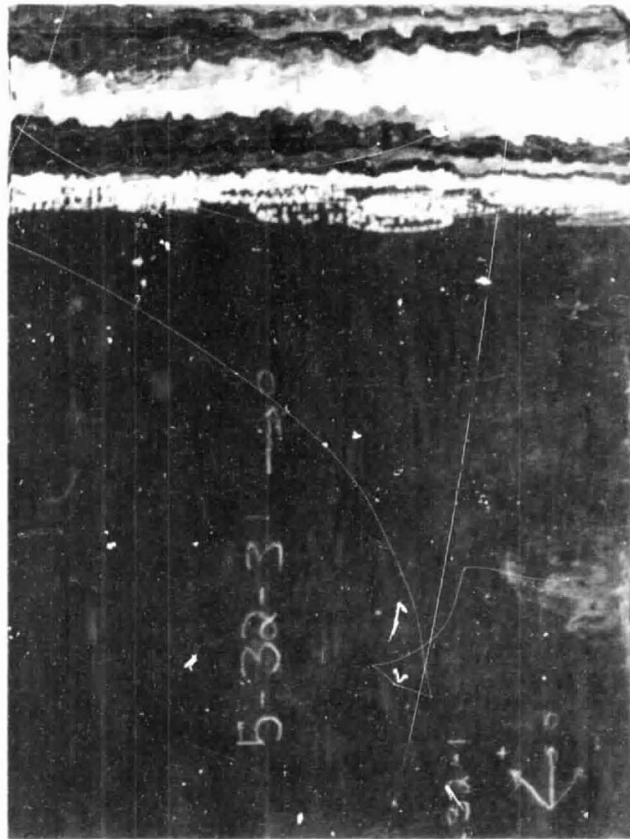


Figure 22. Machine ground (left) and hand ground scarfed laminates.

modes were also very different. The hand ground specimens broke directly through the adhesive with very little adherend damage. In addition, the specimens consistently broke where one of the adherend tips did not have a sharp tip.

This suggests that the shape of the adherend tips is very important, even on a relatively small scale. The tips of these adherends were tapered out to a thickness of about 0.2 millimeters. Analysis also supports the idea, showing that tips tapered to a mere ten microns thick induce significant shear stress concentration.

In a 1971 paper (Ref. 27) A. K. Rao suggested that high stresses predicted at interface corners by wedge stress functions might be alleviated by rounding one wedge tip. The idea is that the nature of the stress concentration depends on the angle between the interface and the free surface. If the interface angle is changed by appropriately curving the interface, stress singularities might be avoided.

A set of scarf joints were made to test this hypothesis. The adherend tips were shaped as shown in Figure 23 by cutting the under surface with a diamond saw and lightly abrading the resulting edge with emory paper. The angle labeled β in Figure 23 was cut at $\pi/6$ radians (30 degrees) to avoid stress singularities according to Rao's calculations. Adhesive film was inserted the entire length of the scarf to make sure the region of the removed tip filled with adhesive.

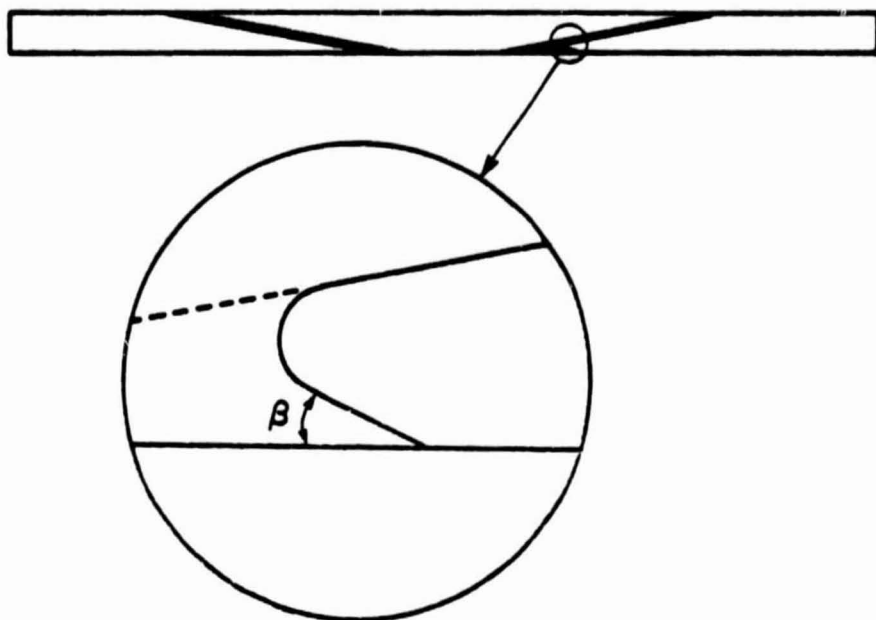


Figure 23. Scarf joint with rounded adherend tips.

The strength of the round-tipped joints, 0.43 ± 0.049 GN/m (2460 \pm 280 lb/in), Appendix iii, was only about 70% that of the sharp-tipped joints. The fracture surfaces were also different. The round-tipped scarf joints had a two millimeter wide band at one end of each break where part of the adherend pulled off. The separation occurred directly across the adhesive from the rounded tip. This separation was similar to the regions on the sharp-tipped joints where a thin layer of matrix and fibers pulled off. The bands did not extend all the way across most of the joints. But the joints were consistently weaker the longer the band.

Clearly any increase in strength from eliminating large tip stresses is outweighed by the detrimental effects of the rounded tips.

The rounded tips reduce joint strength two ways. First, the adhesive area is reduced. Second, the tips cause shear stress concentrations at the ends of the adhesive by the same mechanism as the lap joint described on page 5. That such a small change in tip geometry changes both failure mode and significantly reduces joint strength emphasizes its importance.

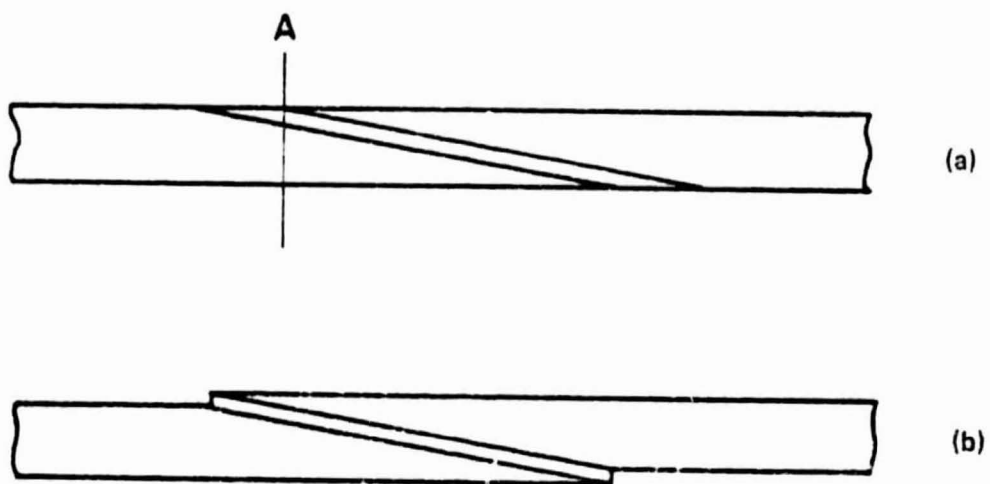


Figure 24. Scarf joint with slightly increased overlap.

Slightly more overlap of the adherends increases joint strength. A set of scarf joints was made as shown in Figure 24(b). This geometry increases adhesive area and reduces the effect of replacing zero degree plies with adhesive as at section A. However, it also protrudes beyond the mold line of the original laminate, which may be a disadvantage for aerodynamic surfaces. These joints averaged 1.63 ± 0.28 GN/m (9300 ± 1600 lb/in) and 1.22 ± 0.10 GN/m (6970 ± 570 lb/in) respectively for 19 and 33 milliradian (1.1 and 3.0 degree) scarf joints, Appendix iii. This is about 20% stronger than the corresponding joints with less

overlap. These 19 milliradian (1.1 degree) scarf joints were the strongest made in this study and attained 74% of the strength of the undamaged laminate.

ORIGINAL PAGE IS
OF POOR QUALITY

ANALYSIS OF SCARF JOINTS WITHOUT DOUBLERS

Several experimental results suggest that the small scale geometry of scarf adherends is important to joint strength. These results include lower than expected strengths for small scarf angle joints and lower strength and different failure modes for scarf joints with rounded tips. It turns out that a scarf adherend which breaks off, before bonding, where it is only a few microns thick causes significant shear stress concentrations in the adhesive. This corresponds to a laminate breaking where it is only as thick as a few reinforcing fibers. Such breakage is not surprising considering the brittleness of typical reinforcing fibers such as carbon and glass.

The mechanism of this stress concentration is the same as for the lap joint described on page 5. The surprising part is that the effect is so pronounced for such a slight deviation from perfect geometry.

To calculate the effect of a broken adherend tip on the adhesive shear stress distribution the mechanism of load transfer between the adherends must be modeled. The analysis used here is similar to those developed by Erdogan and Ratwani (Ref. 16) and by Reddy and Sinha (Ref. 17). The adhesive is deformed, mostly in shear, while transferring the load, Figure 25(a). At the same time the adherends are strained

ORIGINAL PAGE IS
OF POOR QUALITY

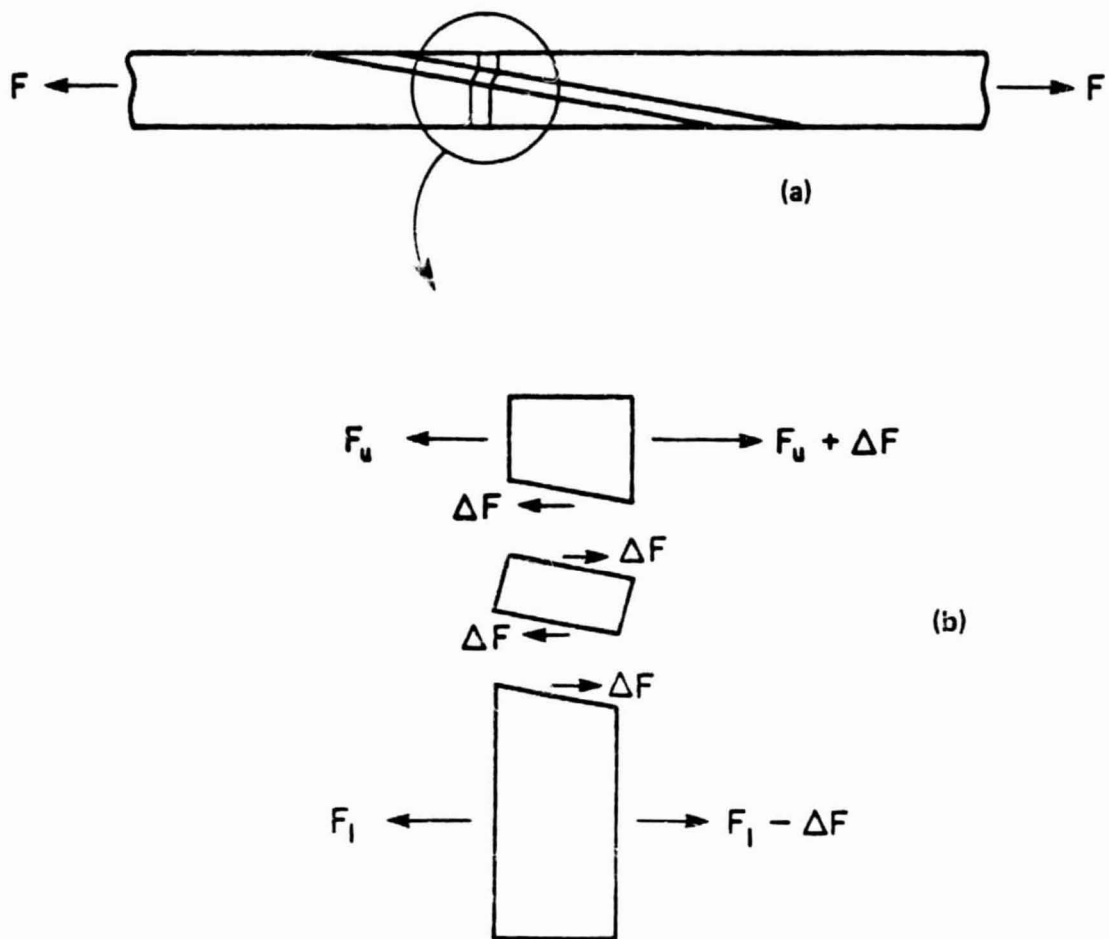


Figure 25. Load transfer between adherends by the adhesive.

horizontally by their loads. The correct combination of adhesive and adherend deformation is defined by the interface condition that stresses and displacements be equal. Since the joint is symmetric only one half of it need be analysed.

Stating these relationships mathematically requires some simplifying assumptions. To model the adhesive deformation assume that its behavior in shear and in tension are independent. Assume also that stresses are constant through the adhesive thickness. It turns out that these assumptions are reasonable away from the ends of the joint. As discussed later, in the section on two dimensional stress distribution, significant variation of stresses occurs through the thickness at the ends of the joint. However, these assumptions allow modeling the most important characteristics of scarf joint behavior. And through the thickness stress variations at the adhesive ends can be dealt with separately.

Assuming the adhesive behaves linearly its strains and stresses are proportional, so the relative displacements are, Figures 26 and 27:

$$\Delta u_1 = \frac{t_{\text{adhes}}}{G_{\text{adhes}}} \tau_{12} \text{ and}$$

$$\Delta u_2 = \frac{t_{\text{adhes}}}{E_{\text{adhes}}} \sigma_{22}.$$

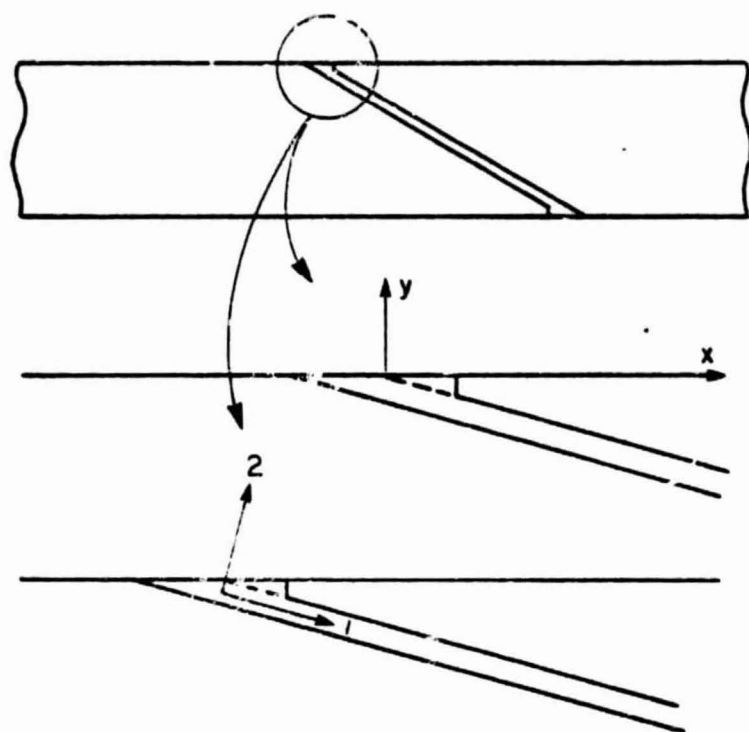


Figure 26. Joint (global) and adhesive coordinate systems.

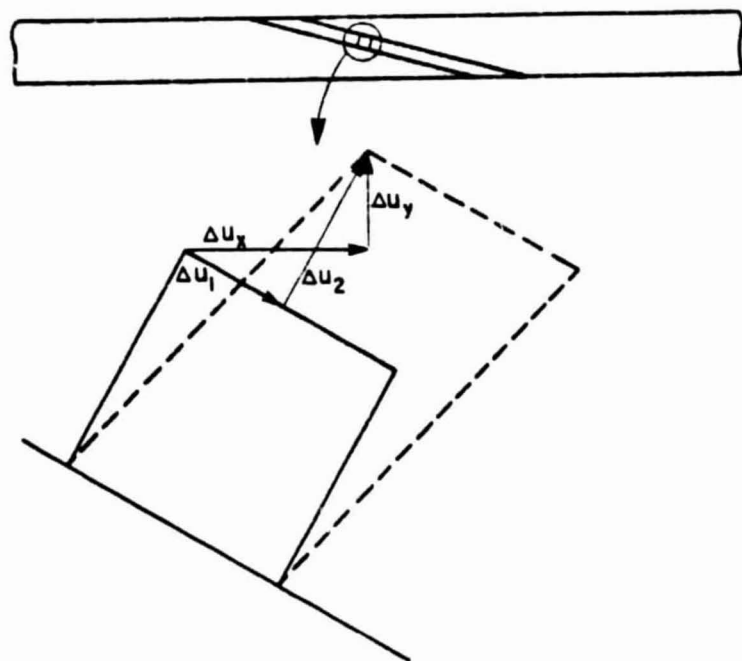


Figure 27. Adhesive displacement (exaggerated) in joint and adhesive coordinate systems.

ORIGINAL PAGE IS
OF POOR QUALITY

In terms of displacements in the x-y coordinate system

$$\tau_{12} = \frac{G_{adhes}}{t_{adhes}} \Delta u_1 = \frac{G_{adhes}}{t_{adhes}} (\Delta u_x \cos \alpha - \Delta u_y \sin \alpha) \quad (1)$$

$$\sigma_{22} = \frac{E_{adhes}}{t_{adhes}} \Delta u_2 = \frac{E_{adhes}}{t_{adhes}} (\Delta u_x \sin \alpha + \Delta u_y \cos \alpha). \quad (2)$$

To model the strain of the adherends assume that they are subject to only normal stresses in the x-direction and that normal stresses in the y-direction, σ_{yy} , are zero. The first assumption requires that loads introduced by the adhesive be distributed very quickly across the adherend by shear. This happens in thin specimens because the load does not have very far to be distributed. But it must be remembered that stresses do not become uniform as quickly in materials which have low shear modulus compared to their extensional modulus (Ref. 42). Fortunately, the composite adherends considered here are thin and the scarf geometry makes them even thinner. The thinness of the adherends also justifies the assumption that normal stresses, σ_{yy} , are zero perpendicular to the loading plane.

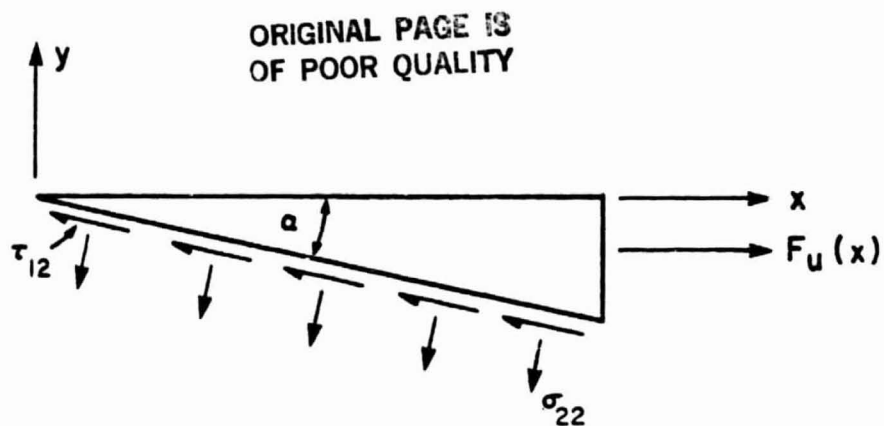


Figure 28. Adherend tip free body diagram.

The adherend strain is a function of the load at the particular cross-section. The load depends on the tractions at the adherend-adhesive interface. Equilibrium of the adherends in the x and y-directions, Figure 28, requires

$$F_u(x) = w \int_0^x \{\tau_{12}(t) \cos \alpha + \sigma_{22}(t) \sin \alpha\} \frac{dt}{\cos \alpha} \quad (3)$$

and

$$\int_0^x \{\tau_{12}(t) \sin \alpha - \sigma_{22}(t) \cos \alpha\} \frac{dt}{\cos \alpha} = 0 \quad (4)$$

with $F_u + F_1 = F_{ext}$, Figure 25.

Since (4) holds for all x it can also be stated as

$$\tau_{12}(t) \sin \alpha = \sigma_{22}(t) \cos \alpha \quad (5)$$

and substituting in (3) gives

$$F_u(x) = w(1 + \tan^2 \alpha) \int_0^x \tau_{12}(t) dt.$$

Differentiating gives,

ORIGINAL PAGE IS
OF POOR QUALITY

$$\frac{dF_u}{dx} = w(1+\tan^2\alpha)\tau_{12}(x). \quad (6)$$

The adherend strain can be calculated once the load is known.

The upper adherend will be analysed first. From Hooke's Law,

$$\epsilon_{xxu} = \frac{\sigma_{xxu}}{E_{xu}} - \frac{\sigma_{yyu}}{E_{yu}}\nu_{yxu} - \frac{\sigma_{zzu}}{E_{zu}}\nu_{zxu}. \quad (7)$$

Since $\sigma_{yy}=0$ by assumption, the middle term is zero. Z-direction normal stress, σ_{zzu} , depends on the Poisson contraction of the specimen. Poisson's ratio varies along the upper adherend because of the changing stacking sequence. At each point the upper adherend will tend to contract an amount usually different from the lower adherend. However, since they are attached by the adhesive they must contract the same amount, at least away from the specimen edges. Therefore,

$$\epsilon_{zz} = \epsilon_{zzu} = -\frac{\sigma_{xavg}}{E_{xlam}}\nu_{xlam}.$$

Now, since

$$\epsilon_{zzu} = \frac{\sigma_{zzu}}{E_{zu}} - \frac{\sigma_{xxu}}{E_{xu}}\nu_{xzu} - \frac{\sigma_{yyu}}{E_{yu}}\nu_{yzu}$$

and the last term is zero, as before,

$$\sigma_{zzu} = E_{zu} \frac{\sigma_{xxu}}{E_{xu}}\nu_{xzu} - E_{zu} \frac{\sigma_{xavg}}{E_{xlam}}\nu_{xlam}.$$

Substituting into (7)

$$\begin{aligned} \epsilon_{xxu} &= \frac{\sigma_{xxu}}{E_{xu}} - \frac{\nu_{zxu}}{E_{zu}} \left(E_{zu} \frac{\sigma_{xxu}}{E_{xu}}\nu_{xzu} - E_{zu} \frac{\sigma_{xavg}}{E_{xlam}}\nu_{xlam} \right) \\ &= \frac{(1-\nu_{xzu}\nu_{zxu})}{E_{xu}} \sigma_{xxu} + \frac{\nu_{xlam}\nu_{zxu}}{E_{xlam}} \sigma_{xavg}. \end{aligned}$$

Since $\sigma_{xxu} = F_u / (t_u w)$ and $\sigma_{xavg} = F_{ext} / (t_{lam} w)$,

$$\epsilon_{xxu} = \frac{(1-\nu_{xz1}\nu_{zx1})}{E_{xz1}} \frac{F_1}{t_1 w} + \frac{\nu_{xz1am}\nu_{zxu}}{E_{xlam}} \frac{F_{ext}}{t_{lam} w}. \quad (8)$$

Similarly, for the lower adherend,

$$\epsilon_{xx1} = \frac{(1-\nu_{xz1}\nu_{zx1})}{E_{xz1}} \frac{F_1}{t_1 w} + \frac{\nu_{xz1am}\nu_{zx1}}{E_{xlam}} \frac{F_{ext}}{t_{lam} w}. \quad (9)$$

To combine these equations substitute (5) into (1) and (2) and solve for τ_{12} in terms of Δu_x :

$$\tau_{12} = \frac{\cos \alpha (1 + \tan^2 \alpha) G_{adhes} E_{adhes}}{(E_{adhes} + G_{adhes} \tan^2 \alpha) t_{adhes}} \Delta u_x.$$

Substituting into (6) gives

$$\frac{dF_u}{dx} = \frac{w \cos \alpha (1 + \tan^2 \alpha)^2 G_{adhes} E_{adhes}}{(E_{adhes} + G_{adhes} \tan^2 \alpha) t_{adhes}} \Delta u_x = w K \Delta u_x.$$

Noting from Figure 27 that $\Delta u_x = u_{xu} - u_{x1}$ and differentiating to express Δu_x in terms of adherend strains gives

$$\frac{d^2 F_u}{dx^2} = w K (\epsilon_{xxu} - \epsilon_{xx1}).$$

ORIGINAL PAGE IS
OF POOR QUALITY

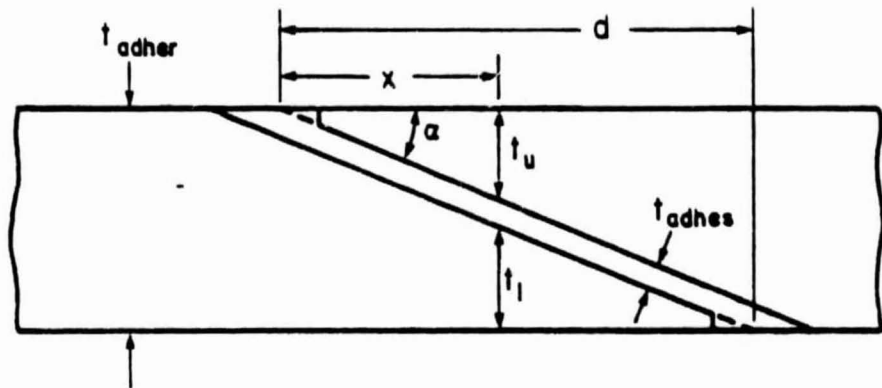


Figure 29. Scarf joint cross-section dimensions.

And finally substituting for the strains from equations (8) and (9), recalling that

$$F_u + F_1 = F_{ext}, \text{ gives}$$

$$\begin{aligned} \frac{d^2 F_u}{dx^2} - K \left[\frac{1 - \nu_{xz u} \nu_{zx u}}{E_{xz u} t_u} + \frac{1 - \nu_{xz l} \nu_{zx l}}{E_{xz l} t_l} \right] F_u \\ = K \left[\frac{\nu_{xz l \text{lam}}}{E_{xz l \text{lam}} t_{\text{lam}}} (\nu_{zx u} - \nu_{zx l}) - \frac{1 - \nu_{xz l} \nu_{zx l}}{E_{xz l} t_l} \right] F_{ext}. \end{aligned} \quad (10)$$

Now, the adherend thicknesses, Figure 29, are

$$t_u = x \tan \alpha \quad \text{and}$$

$$t_l = t_{\text{adher}} - t_{\text{adhes}} / \cos \alpha - x \tan \alpha = (d - x) \tan \alpha$$

where $d = (t_{\text{adher}} - t_{\text{adhes}} / \cos \alpha) / \tan \alpha$ is the length of the joint.

Substituting into (10) gives

$$\begin{aligned} \frac{d^2 F_u}{dx^2} &= K \left[\frac{1-\nu_{xzu} \nu_{zxu}}{E_{xu} x \tan \alpha} + \frac{1-\nu_{xz1} \nu_{zx1}}{E_{x1} (d-x) \tan \alpha} \right] F_u \\ &= K \left[\frac{\nu_{xz1am}}{E_{x1am} t_{1am}} (\nu_{zxu} - \nu_{zx1}) - \frac{1-\nu_{xz1} \nu_{zx1}}{E_{x1} (d-x) \tan \alpha} \right] F_{ext}. \end{aligned} \quad (11)$$

This equation may be written in terms of dimensionless variables by defining $\bar{F} = F_u / F_{ext}$ and $\bar{x} = x/d$. The equation then becomes

$$\begin{aligned} \frac{d^2 \bar{F}}{d \bar{x}^2} &= \frac{Kd}{\tan \alpha} \left[\frac{1-\nu_{xzu} \nu_{zxu}}{E_{xu} \bar{x}} + \frac{1-\nu_{xz1} \nu_{zx1}}{E_{x1} (1-\bar{x})} \right] \bar{F} \\ &= \frac{Kd}{\tan \alpha} \left[\frac{d \nu_{xz1am} (\nu_{zxu} - \nu_{zx1}) \tan \alpha}{E_{x1am} t_{1am}} - \frac{1-\nu_{xz1} \nu_{zx1}}{E_{x1} (1-\bar{x})} \right]. \end{aligned} \quad (12)$$

The boundary conditions for (11) are that $F_u = 0$ at $x = 0$ and $F_u = F_{ext}$ at $x = d$. That is, the upper adherend carries no load at the tip because no load has been transferred to it. And at the other end of the joint, $x = d$, all of the load is carried by the upper adherend. Equivalent boundary conditions for (12) are $\bar{F} = 0$ at $\bar{x} = 0$ and $\bar{F} = 1$ at $\bar{x} = 1$.

SOLUTION OF THE GOVERNING DIFFERENTIAL EQUATION

Equation (12) is a second order inhomogeneous ordinary differential equation with variable coefficients. It has regular singular points at $x=0$ and $x=1$ because of the denominators of the F coefficient. Two techniques will be used to solve it approximately: perturbation methods and series solutions¹. Perturbation methods give a global solution which is patched with the local series solution where the perturbation solution does not work.

Equation (12) can be written as

$$\epsilon^2 \bar{F}'' - Q(\bar{x}) \bar{F} + R(\bar{x}) = 0 \quad (13)$$

where $\epsilon = \sqrt{\tan\alpha/Kd}$,

$$Q(\bar{x}) = \frac{1-\nu_{xzu} \nu_{zxu}}{E_{xu} \bar{x}} + \frac{1-\nu_{xz1} \nu_{zx1}}{E_{x1} (1-\bar{x})} ,$$

$$\text{and } R(\bar{x}) = \frac{1-\nu_{xz1} \nu_{zx1}}{E_{x1} (1-\bar{x})} - \frac{d\nu_{xlam} (\nu_{zxu} - \nu_{zx1}) \tan\alpha}{E_{xlam} t_{lam}} .$$

The complementary equation is $\epsilon^2 \bar{F}'' = Q(\bar{x}) \bar{F}$. Approximate solutions to this type equation are easy to find by the WKB perturbation method when ϵ is small.

1. Both of these techniques are described in Bender and Orszag, Advanced Mathematical Methods for Scientists and Engineers, McGraw Hill Book Company, 1978. The notation used in that text is adopted here.

The idea of the WKB method (Ref. 43), named after Wentzel, Kramers and Brillouin, is to approximate the solution by

$$F \sim A(\bar{x}) \epsilon S(\bar{x})/\delta, \quad \delta \rightarrow 0^+ \quad (14)$$

where δ is the boundary layer thickness. $A(\bar{x})$ is a slowly varying amplitude function. $S(\bar{x})$ is called the phase and can be imaginary. This allows for a solution which is exponential or oscillatory.

It is best to represent this approximation in a different form for deriving asymptotic relations. $A(\bar{x})$ and $S(\bar{x})$ depend explicitly on δ . Expanding them in power series in δ and combining the two series in a single exponential power series gives

$$\bar{F}(\bar{x}) \sim \exp \left[\frac{1}{\delta} \sum_{n=0}^{\infty} \delta^n S_n(\bar{x}) \right], \quad \delta \rightarrow 0^+. \quad (15)$$

Substituting (15) into the complementary equation gives a sequence of equations from which to determine the S_n 's. After substituting, the coefficients of terms of equal powers of ϵ are set equal. It turns out that δ is proportional to ϵ so they may be set equal. The final result for the first two terms is

$$S_0(\bar{x}) = \pm \int^{\bar{x}} \sqrt{Q(t)} dt \quad (16)$$

$$S_1(\bar{x}) = -\frac{1}{4} \ln Q(\bar{x}).$$

This gives for $\bar{F}(\bar{x})$

$$\bar{F}(\bar{x}) \sim B_1 \exp\left[\frac{S_0}{\epsilon} + S_1\right] + B_2 \exp\left[-\frac{S_0}{\epsilon} + S_1\right].$$

The integral for $S_0(\bar{x})$ cannot be solved in closed form.

However, if $Q(\bar{x})$ is written in the form

$$Q(\bar{x}) = \frac{\frac{1-\nu_{xzu}}{E_{xu}} \nu_{zxu} (1-\bar{x}) + \frac{1-\nu_{xzl}}{E_{xl}} \nu_{zxz} \bar{x}}{\bar{x}(1-\bar{x})}$$

the numerator of the integrand can very adequately be represented by a Taylor series. This gives

$$\sqrt{Q(\bar{x})} = \frac{C_0 + C_1 \bar{x} + C_2 \bar{x}^2 + C_3 \bar{x}^3}{\sqrt{\bar{x}(1-\bar{x})}}$$

which can be integrated in closed form.

The solution of the particular equation is very straight forward. Since $R(\bar{x})$ and $Q(\bar{x})$ are both smooth and there are no turning points, i.e. $Q(\bar{x}) \neq 0$ for all \bar{x} , we may simply take the limit $\epsilon \rightarrow 0^+$

$$F(\bar{x}) \sim \frac{R(\bar{x})}{Q(\bar{x})}, \quad \epsilon \rightarrow 0^+.$$

This asymptotic relation is valid for all $0 < \bar{x} < 1$. Finally, the approximate solution of (12) is

$$F(\bar{x}) \sim \frac{R(\bar{x})}{Q(\bar{x})} + B_1 \exp\left[\frac{S_0}{\epsilon} + S_1\right] + B_2 \exp\left[-\frac{S_0}{\epsilon} + S_1\right]. \quad (17)$$

Two conditions must be satisfied for the WKB approximation to hold on an interval (Ref. 44). First, the series $\sum \delta^{n-1} S_n(\bar{x})$ must be an asymptotic series in δ as $\delta \rightarrow 0$ uniformly for all \bar{x} on the

interval. This is equivalent to the quotients $S_{n+1}(\bar{x})/S_n(\bar{x})$ being bounded functions of \bar{x} on the interval. If the series $\sum \delta^{n-1} S_n(\bar{x})$ is uniformly asymptotic in \bar{x} as $\delta \rightarrow 0$, truncating the series before the smallest term, $\delta^N S_{N+1}(\bar{x})$, should give an approximation with uniformly small error throughout the \bar{x} interval.

The second condition is necessary because the WKB series appears in the exponent of (14). For the WKB approximation to hold, the first truncated term $\delta^N S_{N+1}(\bar{x})$ must be small compared to unity.

It turns out that these two conditions are satisfied for the scarf joint equation with small ϵ if the series is truncated after two terms. However, for larger values of ϵ , corresponding to scarf angles of 0.1 radian (six degrees) and more, the WKB approximation does not hold near the scarf tip. In these cases a Frobenius series solution, valid locally, can be used at the scarf tip.

A local solution of (12) can be expanded about the regular singular point $\bar{x}=0$ by the Frobenius method (Ref. 45). First, write the complementary equation corresponding to (12) in the form

$$\bar{F}'' + \frac{q(\bar{x})}{\bar{x}^2} \bar{F} = 0 \quad (18)$$

where

$$q(\bar{x}) = -\frac{K_d}{t \tan \alpha} \bar{x}^2 \left[\frac{1-\nu}{E_{xu} \bar{x}} \frac{\nu}{z_{xu}} + \frac{1-\nu}{E_{x1} (1-\bar{x})} \frac{\nu}{z_{x1}} \right].$$

Note that, although the coefficient of \bar{F} in (12) is singular, $q(\bar{x})$ is analytic. Expanding $q(\bar{x})$ in a Taylor series gives

$$q(\bar{x}) = \sum_{n=0}^{\infty} q_n \bar{x}^n$$

with $q_0=0$

$$\text{and } q_n = -\frac{Kd}{t \tan \alpha} \frac{1-\nu_{xz} \nu_{zx}}{E_{xz}} \quad n=1,2,3,\dots$$

Next, assume a solution in the form of a Frobenius series:

$$\bar{F}(\bar{x}) = \bar{x}^a \sum_{n=0}^{\infty} a_n \bar{x}^n. \quad (19)$$

Substituting into (18) and equating coefficients of \bar{x}^{n+a-2} gives

$$(a^2-a)a_0 = 0 \quad (20)$$

$$\text{and } ((a+n)^2-a-n)a_n = - \sum_{k=0}^{n-1} q_{n-k} a_k.$$

Since $a_0 \neq 0$ by assumption a must be a root of the indicial polynomial, $P(a) = a^2 - a$. Let $a_1 = 1$ and $a_2 = 0$ denote the roots of the indicial polynomial. For $a = a_1$ the recursion relation (20) can be solved for a_n in terms of a_0 for all n :

$$a_n = -\frac{1}{n+n^2} \sum_{k=0}^{n-1} q_{n-k} a_k. \quad (21)$$

This gives one solution to (18) with one arbitrary coefficient, a_0 .

Since $a_1 - a_2$ is an integer, there is, in general (Ref. 53), only one solution in Frobenius form. The solution obtained by using the recursion relation with $a = a_2$ is identical to (21). The second linearly independent solution involves the function $\ln \bar{x}$. It can be found by

differentiating (19) with respect to the indicial exponent, α .

Ignoring the first equation of (20) for a moment to leave α arbitrary, we solve for a_n as a function of α . The resulting Frobenius series is

$$\bar{F}(\bar{x}, \alpha) = \bar{x}^\alpha \sum_{n=0}^{\infty} a_n(\alpha) \bar{x}^n. \quad (22)$$

It is helpful to define the operator

$$L \equiv \frac{d^2}{d\bar{x}^2} + \frac{q(\bar{x})}{\bar{x}^2}.$$

Any solution of (18) satisfies $L\bar{F}(\bar{x})=0$. However, $\bar{F}(\bar{x}, \alpha)$ satisfies

$$L\bar{F}(\bar{x}, \alpha) = a_0 \bar{x}^{\alpha-2} P(\alpha).$$

If we differentiate both sides with respect to α and set $\alpha=a_1$ we get

$$L \left[\frac{\partial}{\partial \alpha} \bar{F}(\bar{x}, \alpha) \Big|_{\alpha=a_1} \right] = a_0 P'(a_1) \bar{x}^{(a_1-2)}. \quad (23)$$

If the right hand side were zero, then $(\partial/\partial \alpha) \bar{F}(\bar{x}, \alpha) \Big|_{\alpha=a_1}$ would be a second solution to (18).

To get around this we can construct another particular solution to the inhomogeneous equation (23) and subtract the particular solution $(\partial/\partial \alpha) \bar{F}(\bar{x}, \alpha) \Big|_{\alpha=a_1}$ from it. This will be a solution to the homogeneous part of (23) which is what we really want.

It turns out that the second particular solution has an ordinary Frobenius expansion,

$$\sum_{n=0}^{\infty} c_n \bar{x}^n.$$

Substituting into (23) and equating coefficients of \bar{x}^{n-2} gives

$$P(0)c_0 = 0$$

$$P(n)c_n + \sum_{k=0}^{n-1} q_{n-k}c_k = 0 \quad n \neq 0, 1$$

$$P(1)c_1 + q_1c_0 = a_0P'(0).$$

Since $P(1)=P(a_1)=0$ the last equation relates a_0 to the coefficient c_0 ,

$$a_0 = \frac{1}{P'(0)}q_1c_0 = q_1c_0. \quad (24)$$

And the middle equation gives

$$c_n = -\frac{1}{P(n)} \sum_{k=0}^{n-1} q_{n-k}c_k = -\frac{1}{n(n-1)} \sum_{k=0}^{n-1} q_{n-k}c_k, \quad n \neq 0, 1. \quad (25)$$

So the second linearly independent solution to (18) is the difference between the two particular solutions:

$$\bar{F}(\bar{x}) = \sum_{n=0}^{\infty} c_n \bar{x}^n - \frac{\partial}{\partial a} \bar{F}(\bar{x}, a) \Big|_{a=a_1}.$$

Differentiating (22) with respect to a gives

$$\frac{\partial}{\partial a} \bar{F}(\bar{x}, a) \Big|_{a=a_1} = \bar{x}^{a_1} \sum_{n=0}^{\infty} \frac{\partial}{\partial a} a_n(a) \Big|_{a=a_1} \bar{x}^n + \bar{F}(\bar{x}, a_1) \ln \bar{x}$$

$$= \sum_{n=0}^{\infty} b_n \bar{x}^{n+1} + \ln \bar{x} \sum_{n=0}^{\infty} a_n \bar{x}^{n+1}$$

$$\text{where } b_n = \frac{\partial}{\partial a} a_n(a) \Big|_{a=a_1}$$

$$= \frac{2n+1}{(n^2+n)^2} \sum_{k=0}^{n-1} q_{n-k} a_k - \frac{1}{n^2+n} \sum_{k=0}^{n-1} q_{n-k} b_k, \quad (26)$$

and $b_0 = 0$.

So the second linearly independent solution of (18) is

$$\bar{F}(\bar{x}) = \sum_{n=0}^{\infty} c_n \bar{x}^n - \sum_{n=0}^{\infty} b_n \bar{x}^{n+1} - \ln \bar{x} \sum_{n=0}^{\infty} a_n \bar{x}^{n+1}. \quad (27)$$

The last step in finding a local solution to (12) is finding a particular solution. The particular equation may be written

$$F'' + \frac{q(\bar{x})}{\bar{x}^2} F = r(\bar{x}) \quad (28)$$

where $r(\bar{x}) = \frac{Kd}{\tan \alpha} \left[\frac{d\nu_{xz1am} (\nu_{zxu} - \nu_{zx1}) \tan \alpha}{E_{x1am} t_{1am}} - \frac{1 - \nu_{xz1} \nu_{zx1}}{E_{x1} (1 - \bar{x})} \right].$

Expanding $r(x)$ in a Taylor series about $x=0$,

$$\begin{aligned} r(\bar{x}) &= \sum_{n=0}^{\infty} r_n \bar{x}^n \\ \text{gives } r_0 &= \frac{Kd}{\tan \alpha} \left[\frac{d\nu_{xz1am} (\nu_{zxu} - \nu_{zx1}) \tan \alpha}{E_{x1am} t_{1am}} - \frac{1 - \nu_{xz1} \nu_{zx1}}{E_{x1}} \right]. \\ \text{and } r_n &= -\frac{Kd}{\tan \alpha} \frac{1 - \nu_{xz1} \nu_{zx1}}{E_{x1}} \quad n = 1, 2, \dots \end{aligned}$$

Assuming a solution of the form

$$\bar{F}^{pt} = \bar{x}^a \sum_{n=0}^{\infty} a_n^{pt} \bar{x}^n$$

and substituting into (28) gives $a = 1, 0$ and

$$a_n^{pt} = \frac{r_{n-1} - \sum_{k=1}^n q_k a_{n-k}^{pt}}{n(n+1)} \quad n = 1, 2, \dots \quad (29)$$

The coefficient a_0^{pt} is arbitrary, so make it zero.

The general solution to (12) is then

$$\bar{F}(\bar{x}) = \sum_{n=0}^{\infty} a_n \bar{x}^{n+1} + \sum_{n=0}^{\infty} c_n \bar{x}^n - \ln \bar{x} \sum_{n=0}^{\infty} a_n \bar{x}^{n+1} - \sum_{n=0}^{\infty} b_n \bar{x}^{n+1} + \sum_{n=0}^{\infty} a_n^{pt} \bar{x}^{n+1} \quad (30)$$

where c_0 and c_1 are the two arbitrary constants,

the a_n 's are determined as in (21) and (24),

the b_n 's are determined as in (26),

the c_n 's are determined as in (25), and

the a_n^{pt} 's are determined as in (29).

The expansions in (30) can be shown to converge (Ref. 46) in a complex disk whose radius is at least as large as the distance to the nearest singularity of $q(\bar{x})$ or $r(\bar{x})$, i.e. at $\bar{x} = 1$.

A series solution is also useful for parts of the joint away from the tip. In these cases the solution is expanded about an ordinary point and Taylor series can be used. The procedure is simple. First, assume a solution of the form

$$\bar{F} = \sum_{n=0}^{\infty} a_n (\bar{x} - \bar{x}_i)^n \quad (31)$$

where \bar{x}_i is the point about which the solution is expanded. For the complementary solution, substitute a Taylor series expansion of the \bar{F} coefficient (this is a different $q(\bar{x})$ than used in the Frobenius series),

$$q(\bar{x}) = \sum_{n=0}^{\infty} q_n (\bar{x} - \bar{x}_i)^n.$$

into the complementary equation $\bar{F}'' - q(\bar{x})\bar{F} = 0$. Note that adherend properties that are functions of position can be accounted for in the expansion of $q(\bar{x})$. The solution coefficients are determined by the recursion relation,

$$a_n = -\frac{1}{n(n-1)} \sum_{k=0}^{n-2} q_k a_{n-k-2} \quad n = 2, 3, 4, \dots \quad (32)$$

For the particular solution assume a solution of the form

$$\bar{F}^{pt} = \sum_{n=0}^{\infty} a_n^{pt} (\bar{x} - \bar{x}_i)^n.$$

Expand $r(\bar{x})$ in a Taylor series about $\bar{x} = \bar{x}_i$ and substitute into the particular equation $\bar{F}'' + q(\bar{x})\bar{F} = r(\bar{x})$. Equating coefficients of equal powers of $(\bar{x} - \bar{x}_i)$ gives a recursion relation for a_n^{pt} ,

$$a_n^{pt} = \frac{r_{n-2} - \sum_{k=0}^{n-2} q_k a_{n-k-2}^{pt}}{n(n-1)} \quad n = 2, 3, \dots \quad (33)$$

Although a_0^{pt} and a_1^{pt} are arbitrary they are not needed for a particular solution. They may be set to zero. The general series solution to (30) expanded about an ordinary point $\bar{x} = \bar{x}_i$ is

$$\bar{F} = \sum_{n=0}^{\infty} (a_n + a_n^{pt}) (\bar{x} - \bar{x}_i)^n \quad (34)$$

This expansion converges (Ref. 47) within a disk whose radius is the distance to the nearest singularity of $q(\bar{x})$ or $r(\bar{x})$, i.e. $\bar{x} = 0$ or $\bar{x} = 1$.

ORIGINAL PAGE IS
OF POOR QUALITY

ADHESIVE STRESSES IN THE SCARF JOINT

In this section the methods developed for solving the scarf joint governing equation (12) are applied to the experimental scarf joints described earlier. Once the load transfer stresses are calculated they are combined with stresses caused by gross extension of the entire joint. This gives actual joint stresses which can be used to predict joint strength.

In calculating the load transfer stresses two practical considerations must be satisfied. First, the mechanical properties of the adherends vary along the joint. And second, the appropriate method of solution, WKB or series, must be used for certain regions of the joint. This requires dividing the joint into five regions, each with its own solution. The boundary conditions of the individual solutions are determined to provide a smooth solution for the entire joint.

As mentioned in the introduction, page 7, the stiffness of the adherends influences the adhesive shear stress. For composites large differences in modulus between adherends are possible. Also, load-direction modulus can vary with position in a scarfed composite adherend. For example, near the adherend tip in Figure 30 the modulus E_{xu} is the modulus of zero degree plies only. Further into the joint, at point A, for example, the average modulus is lower because of

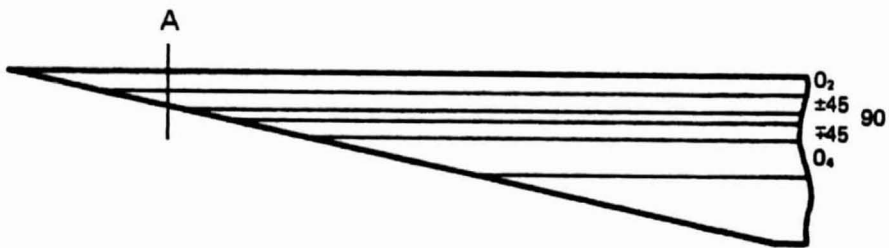


Figure 30. Changing modulus at the adherend tip caused by the stacking sequence.

the 45 degree plies. The properties of the lower adherend also change for the same reason. Figure 31 shows the variation in average modulus, E_x , and Poisson's ratios, ν_{xz} and ν_{zx} , as a function of x for both upper and lower adherends. Properties are shown for only half the joint because the shear stress distribution is symmetrical about the center.

The properties shown in Figure 31 were calculated from laminate theory (Refs. 47,48). For example, the modulus of section A in Figure 30 is that of a [0₂/±45] laminate. The adherends are constrained from bending or shearing by being bonded to each other. So it is assumed in these calculations that $\epsilon_{xz} = k_x = k_z = k_{xz} = 0$, (Ref. 47). In some joint problems the bending and shearing forces are important, but in this case they are small because the adherends are so long and thin. For these conditions

$$E_x = \frac{1}{t} (A_{11} - A_{21}A_{22}),$$

$$\nu_{xz} = A_{21}/A_{22} \quad \text{and}$$

$$\nu_{zx} = A_{12}/A_{11}.$$

ORIGINAL PAGE IS
OF POOR QUALITY

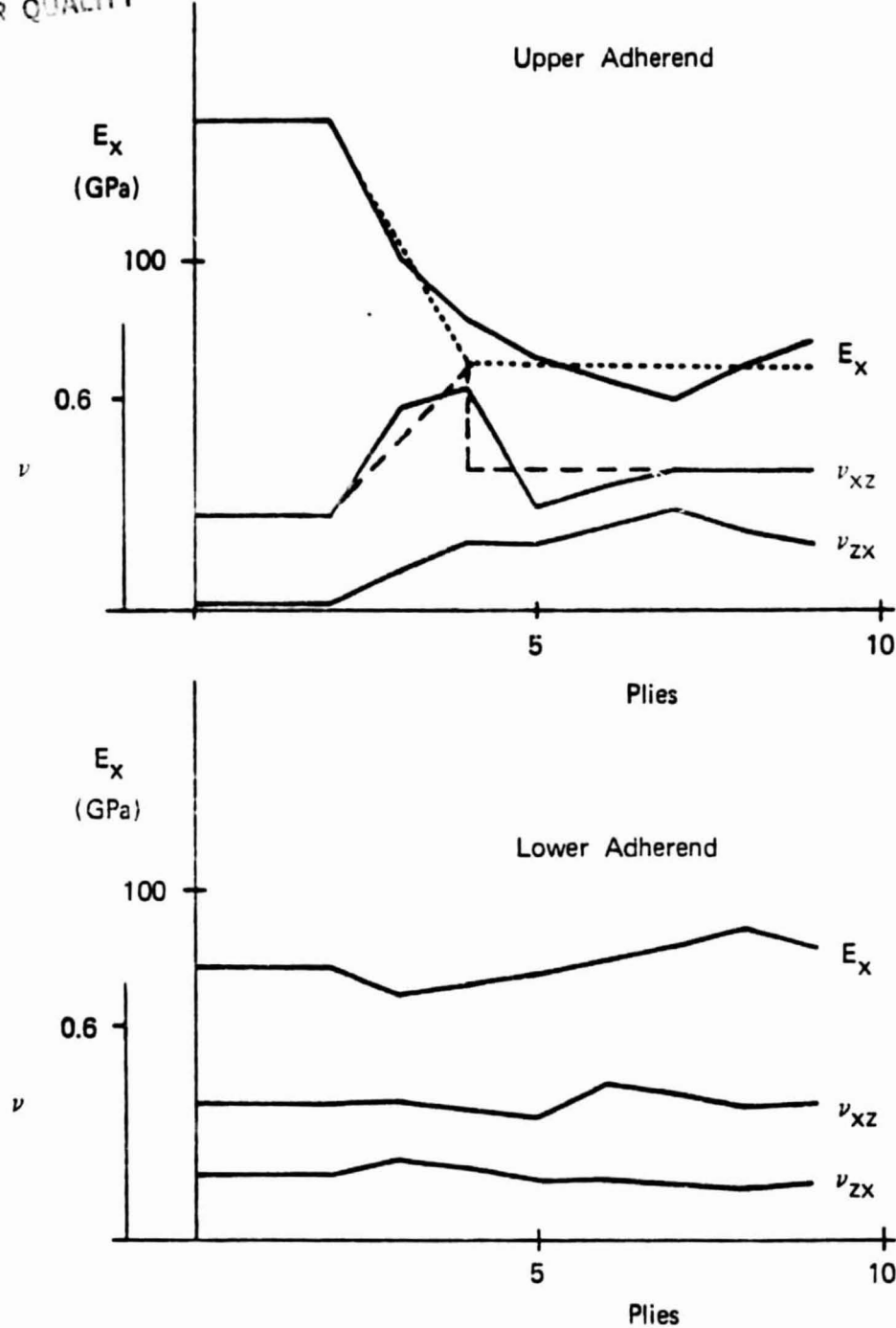


Figure 31. Adherend mechanical properties versus position.

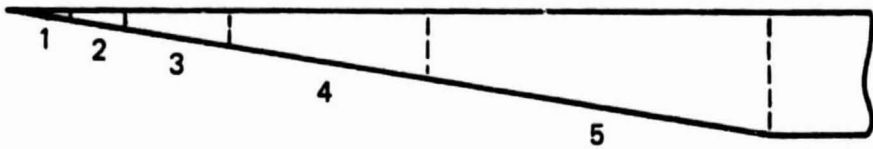


Figure 32. Regions of the scarf joint for solving the governing equation.

For calculating the shear stress distribution adherend properties may be approximated by the dashed lines in Figure 31. This gives an exact representation at the end of the adherend, which is the most important part. Since the lower adherend properties change little they are assumed constant at $E_x = 78.0$ GPa, $\nu_{xz} = 0.4$ and $\nu_{zx} = 0.2$. Properties assumed for the adhesive are $E = 3.45$ GPa and $\nu = 0.3$.

To calculate the shear stress distribution it is easiest to divide the scarf joint into five regions. This division is based on the adherend mechanical properties and the best solution method for each region. Figure 32 shows the five regions. Region one is the sharp tip of the adherend. In the case of an adherend with a broken tip this region has the mechanical properties of the adhesive. For scarf angles of 35 milliradians (two degrees) and less, the adherend load, F , is calculated in the form of a WKB expansion, equation (17). For larger scarf angles a Frobenius series, equation (30), is used.

Region two is the end of the blunt adherend. Region four is

where the upper adherend mechanical properties change linearly from those at the tip to those in the middle, Figure 31. Taylor series expansions, equation (34), are used in both these regions. The series in region two is expanded about the blunt adherend tip to provide a good solution at the most important part of the joint. Because it is so close to the singular point at $\bar{x} = 0$, region two must be relatively small for reasonably quick convergence. Region three simply connects regions two and four with another Taylor series solution. The solutions for regions three and four are expanded about their midpoints and their convergence is rapid.

Region five covers the largest part of the scarf joint, from the end of region four, about $\bar{x} = 0.25$ to the middle of the joint, $\bar{x} = 0.5$. The adherend load is modeled by a WKB approximation in region five.

Adhesive load transfer stresses are calculated in the FORTRAN programs SCARF3 and SCARF4, Appendix iv. SCARF3 uses a Frobenius solution for region one and SCARF4 uses a WKB expansion. Otherwise they are the same. The adhesive stress data are presented as an adhesive stress factor. It is a stress concentration factor which accounts for adherend stiffness and broken adherend tips. The adhesive stress factor equals the adhesive stress in the 1-2 coordinate system divided by the average stress for the entire joint. It is the same for normal and shear stress. The average stress is the stress expected for the ideal scarf joint of Figure 4. Deviation of adhesive stresses from the ideal are apparent by the deviation of the adhesive stress factor from unity.

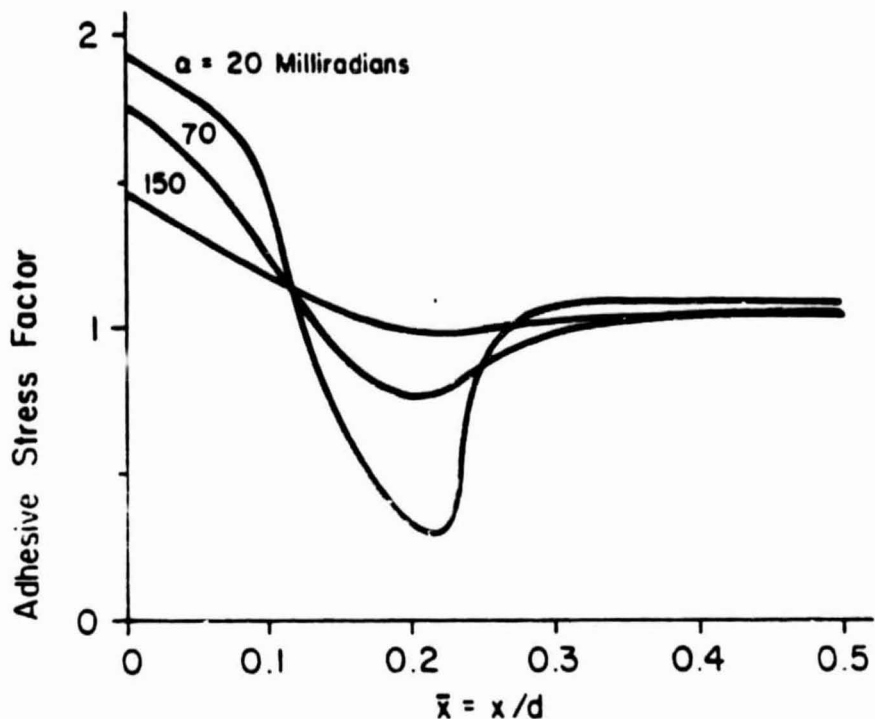


Figure 33. Adhesive stress factor for several scarf joints with sharp tipped adherends.

The adhesive stress factors for sharp tipped adherends of different scarf angles are plotted in Figure 33. All of the deviation from the optimal distribution in Figure 33 is caused by adherend stacking sequences. Because of its modulus the tip region strains less than the adherend to which it is bonded. This tends to induce shear stresses of opposite sign at each end of the high modulus region. At the free end, the tip of the adherend, the adhesive is strained more. On the other end, toward the interior of the joint, the adhesive is strained less. This causes the dip in the curve. The effect is much more pronounced for smaller scarf angles. In fact the interior adhesive stress can even change sign.

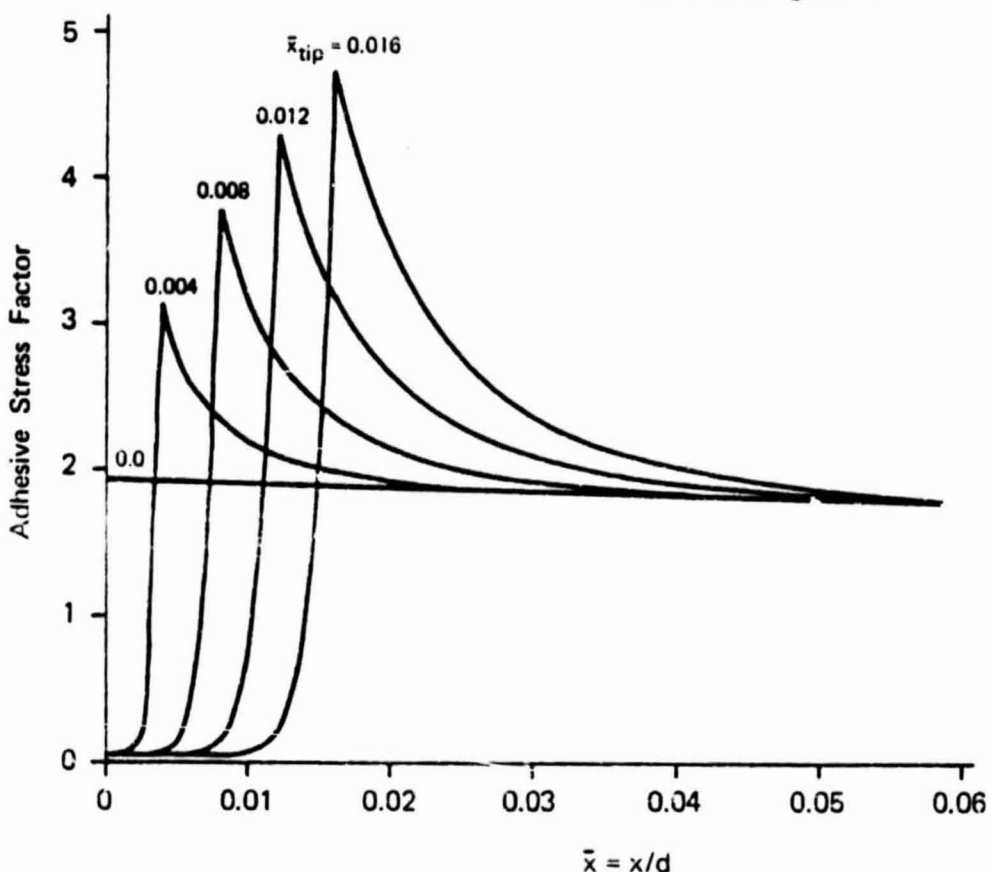


Figure 34. Adhesive stress factors for 20 milliradian scarf joints.

In many cases it may be possible to design adherends to improve or even eliminate such stress concentrations as in Figure 33. However, for repair of laminates the stacking sequence of one adherend is predetermined. The remaining options may not be adequate to allow an optimal joint design.

The stress factors for scarf adherends with broken tips are plotted in Figures 34 through 36. The effect of the broken tips is limited to a small region, a boundary layer, near the end of the adherend, so only that part is shown. The stress for a 20 milliradian

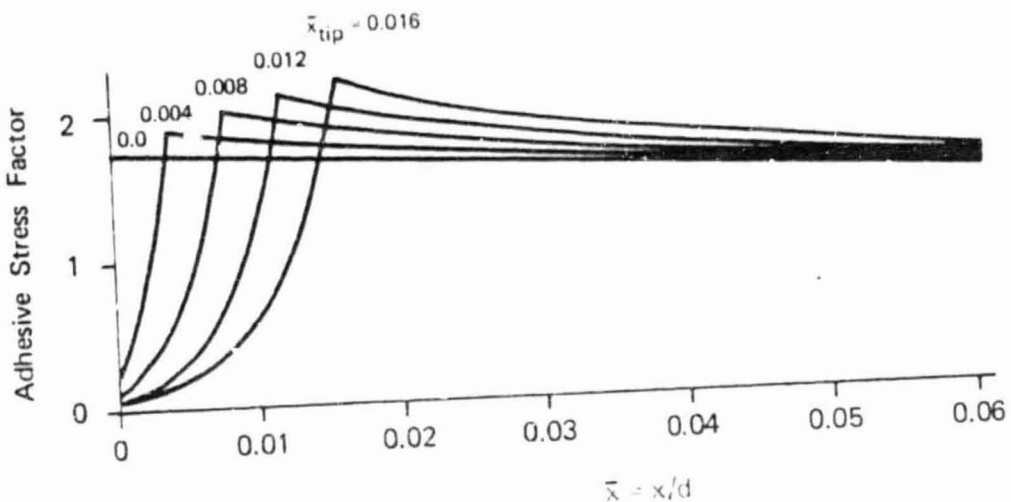


Figure 35. Adhesive stress factors for 70 milliradian scarf joints.

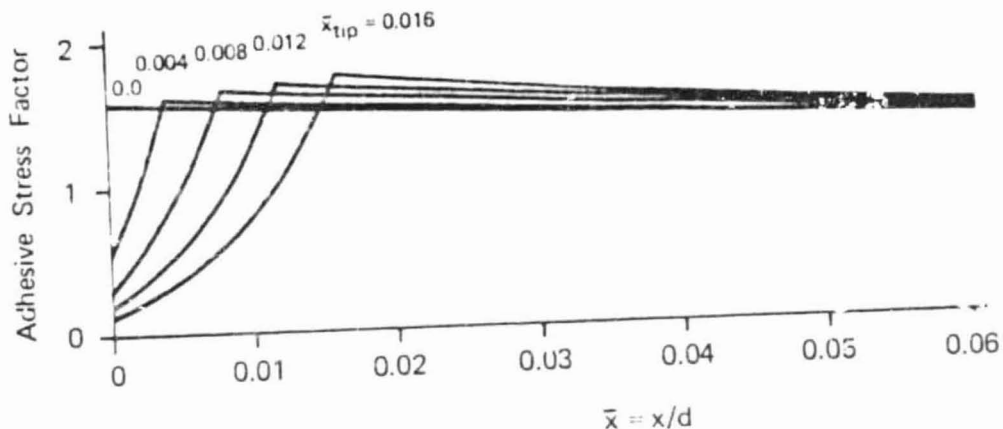


Figure 36. Adhesive stress factors for 110 milliradian scarf joints.

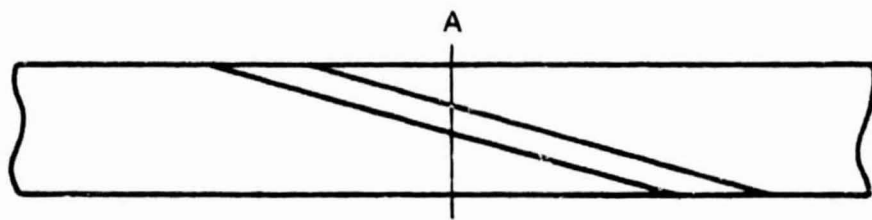


Figure 37. Scarf joint cross-section.

(1.1 degree) composite joint with the tip broken at $\bar{x} = 0.016$ is nearly five times the optimum value, Figure 34. As pointed out earlier, this is equivalent to breaking the tip off where the adherend is only 40 microns (0.0016 inches) thick. Comparison of Figures 34, 35 and 36, which are drawn to the same scale, shows that the effect of broken tips is much more pronounced for joints with smaller scarf angles. In fact, broken tips have practically no effect at all for 110 milliradian joints, as Figure 36 shows. So smaller angle joints are more sensitive to both adherend stiffness and tip breaks.

The adhesive stress factors of Figures 33 through 36 account only for the adhesive stresses required to transfer load between adherends. In addition to those stresses an extensional stress will be induced in the adhesive by extensional strain of the entire joint. The whole joint will strain an amount depending on the load and the section stiffness. The average stiffness of the joint at any section, say A in Figure 37, is approximately that of the laminate away from the joint. This is true because the stacking sequence at A is identical to that of the laminate away from the joint except for a small part where the adhesive is.

Disregarding the load carried by the soft adhesive the entire joint will strain in the load direction by an amount

$$\epsilon_x = \frac{\sigma_{xxlam}}{E_{xxlam}} = \frac{F_{ext}}{\left(t_{adher} - \frac{t_{adhes}}{\cos \alpha}\right) w E_{xxlam}},$$

where the term in parentheses is the load carrying thickness. The stress in the adhesive due to this strain is

$$\sigma_{xx} = E_{adhes} \epsilon_x = \frac{F_{ext}}{w} \frac{E_{adhes}}{\left(t_{adher} - \frac{t_{adhes}}{\cos \alpha}\right) E_{xxlam}}. \quad (35)$$

To superpose the load transfer stresses and the stress due to extension, they must be expressed in the same coordinate system. In the 1-2 coordinate system the stresses due to tension are

$$\sigma_{11extens} = \frac{1}{2} [1 + \cos(-2\alpha)] \sigma_{xx}$$

$$\tau_{12extens} = -\frac{1}{2} \sin(-2\alpha) \sigma_{xx}$$

$$\sigma_{22extens} = \frac{1}{2} [1 + \cos(\pi - 2\alpha)] \sigma_{xx}.$$

Adding these stresses to the load transfer stresses gives the total adhesive stresses

$$\sigma_{11tot} = \frac{1}{2} [1 + \cos(-2\alpha)] \sigma_{xx},$$

$$\tau_{12tot} = -\frac{1}{2} \sin(-2\alpha) \sigma_{xx} + K_{str} \frac{F_{ext} \cos \alpha \sin \alpha}{w t_{adher}},$$

$$\sigma_{22tot} = \frac{1}{2} [1 + \cos(\pi - 2\alpha)] \sigma_{xx} + K_{str} \frac{F_{ext} \cos \alpha \sin \alpha \tan \alpha}{w t_{adher}},$$

ORIGINAL PAGE IS
OF POOR QUALITY

where K_{str} is the stress concentration factor for a particular location in the joint.

Substituting from (35) and setting F_{ext}/w , the applied force resultant, equal to unity gives

$$\sigma_{11tot} = \frac{1}{2}(1+\cos(-2a)) \frac{E_{adhes}}{E_{xlam}} \frac{1}{\left(t_{adher} - \frac{t_{adhes}}{\cos a}\right)}, \quad (36)$$

$$\tau_{12tot} = -\frac{1}{2}\sin(-2a) \frac{E_{adhes}}{E_{xlam}} \frac{1}{\left(t_{adher} - \frac{t_{adhes}}{\cos a}\right)} + K_{str} \frac{\cos a \sin a}{t_{adher}},$$

$$\sigma_{22tot} = \frac{1}{2}(1+\cos(\pi-2a)) \frac{E_{adhes}}{E_{xlam}} \frac{1}{\left(t_{adher} - \frac{t_{adhes}}{\cos a}\right)} + K_{str} \frac{\sin^2 a}{t_{adher}}.$$

These are the adhesive stresses for a unit applied force resultant.

The maximum stresses per unit load are

$$\tau_{max} = R = \sqrt{\sigma_{11tot}^2 + \left(\frac{\sigma_{11tot} - \sigma_{22tot}}{2}\right)^2} \quad \text{and} \quad (37)$$

$$\sigma_{max} = \frac{\sigma_{11tot} + \sigma_{22tot}}{2} + R.$$

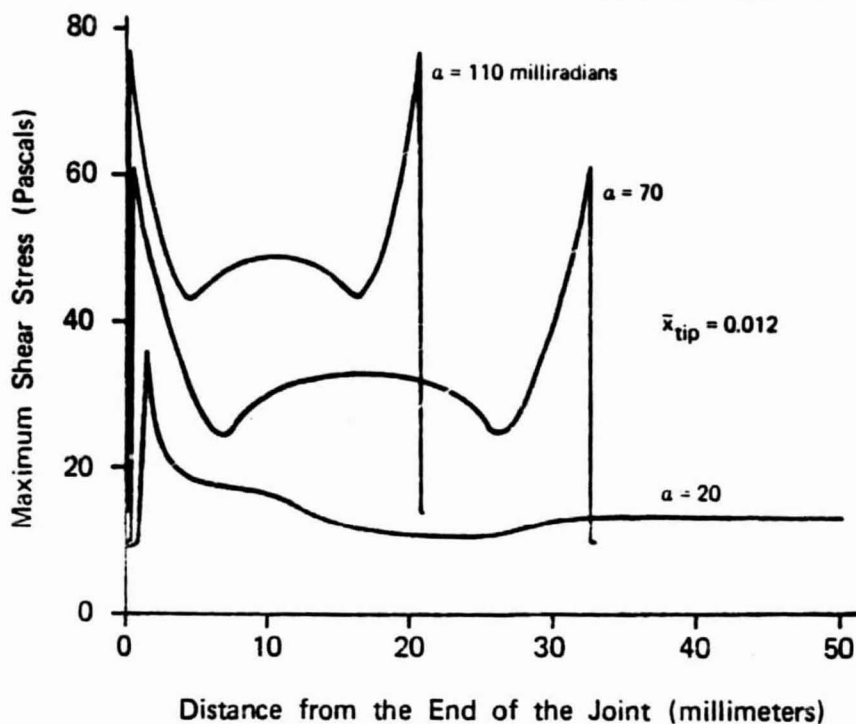


Figure 38. Maximum shear stress distribution for several scarf joints.

They can be calculated for a particular joint once K_{str} is known. The maximum normal and shear stress distributions for unit load are plotted for several scarf joints in Figures 38 and 39. The load is one Newton/meter applied to the laminate and $\bar{x}_{tip} = 0.012$. Only half of the 20 milliradian scarf joint stress distribution is shown because the joint is so long. These plots show the effects of adherend stacking sequence and broken adherend tips in terms of actual joint stresses and dimensions.

These stress distributions demonstrate the lower than expected scarf joint strengths for small scarf angles. In these plots the ideal stress is very nearly the value shown at the middle of each joint. In

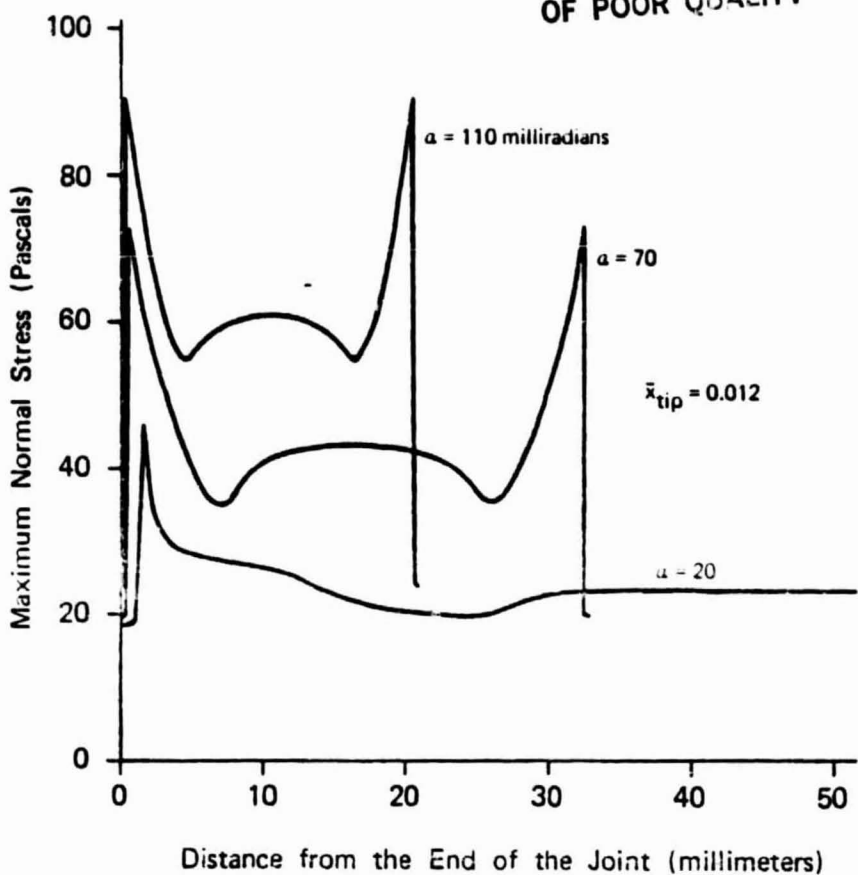


Figure 39. Maximum normal stress distribution for several scarf joints.

Figure 39, for example, the end stress is 50 percent higher than the ideal for the 110 milliradian joint, 70 percent higher for the 70 milliradian joint and 100 percent higher for the 20 milliradian joint. The strength of the joints is therefore decreased much more for the small scarf angle joint.

To translate these calculated stress values into predicted strengths ultimate stresses are needed. They can be calculated from the experimental strength data for the 110 milliradian scarf joints. These data are the most significant because there are many more data values. Also, the effect of broken adherend tips is small for scarf angles

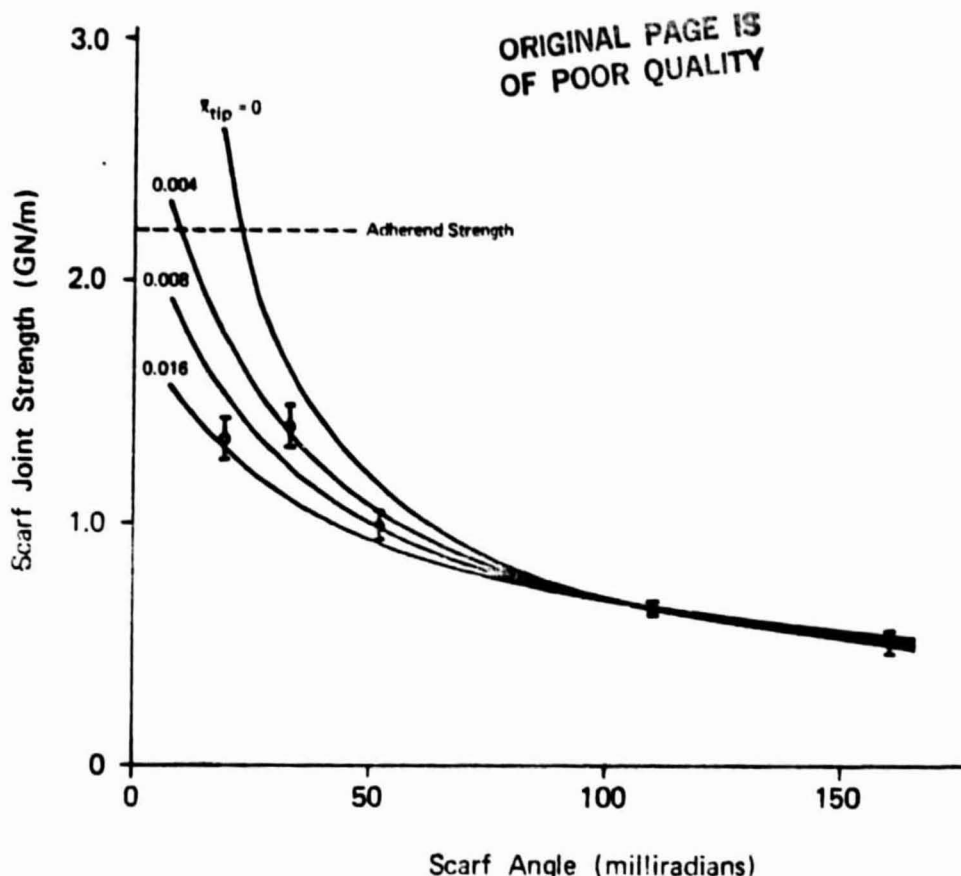


Figure 40. Predicted scarf joint strength based on maximum shear stress.

this large, Figure 36. Accurate knowledge of the amount of tip breakage is therefore much less important. The maximum normal stress is 54.6 to 59.6 GPa, depending on which value of $\bar{\epsilon}_{tip}$ is assumed. And the maximum shear stress is 45.9 to 50.7 GPa.

Predicted strengths are plotted as functions of scarf angle for several values of $\bar{\epsilon}_{tip}$ in Figures 40 and 41. The curves in Figure 40 are based on maximum shear stress and those in Figure 41 are based on maximum normal stress.

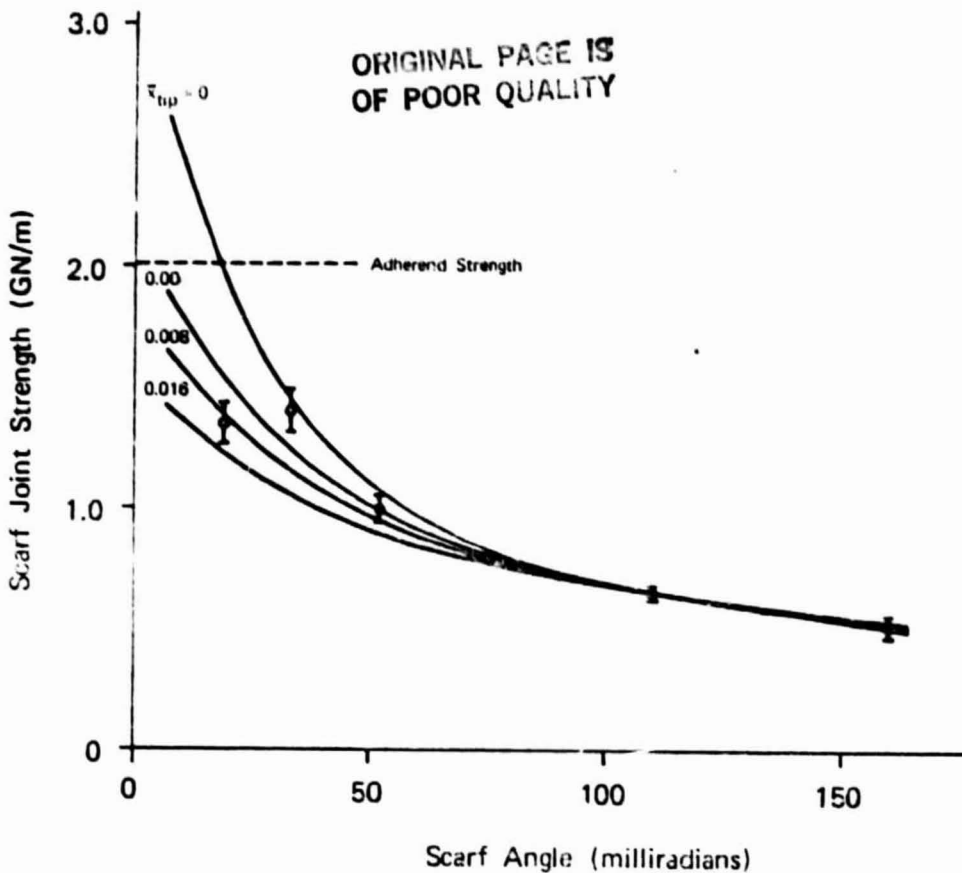


Figure 41. Predicted scarf joint strength based on maximum normal stress.

As the curves show, broken adherend tips can explain the lower than expected experimental scarf joint strengths. For example, the strength predicted for the scarf joint with relatively small breakage of $\bar{x}_{tip} = 0.016$ agrees with the actual strength of the 19 milliradian (1.1 degree) scarf joints.

An article published by Thamm in 1976 (Ref. 7) supports the reduction in strength for adherends which are not perfectly sharp. He studied the effect of partially thinning the adherends of lap joints to reduce the shear stress concentrations. This is the same as scarfing

the adherends. He concludes that the adherends must be completely sharpened to obtain a substantial increase in joint strength. Thamm also points out that even slight damage to the edge of a sharpened adherend can cause a significant decrease in joint strength. His calculations, however, are limited to very short scarf joints, equivalent to about 0.5 radian scarf angle for the joints studied in this paper. Also, for Thamm's joints a relatively sharp adherend has an equivalent $\bar{x}_{tip} = 0.1$. Under these limitations the sensitivity of small angle scarf joints to extremely small bluntness and to adherend tip stiffness is not apparent.

Another paper which supports the results of this one is by Adams and Peppiatt (Ref. 32). They apply the finite element method to a 36 milliradian (2.1 degree) scarf joint with a blunt tip, $\bar{x}_{tip} = 0.1$. This analysis shows a stress boundary layer similar to Thamm's. Again, however, the tip bluntness is much larger than those considered here.

An important question is just how much, if any, are the tips actually broken or left blunt. Since each experimental repair specimen actually had two scarf joints, the unbroken scarfs can be examined for bluntness. Microscopic examination of several joints revealed adherend tips from 10 to 100 microns thick at the end, with most around 30 microns. This is equivalent to \bar{x}_{tip} of 0.012. A micrograph of a typical adherend tip is in Figure 42.

ORIGINAL PAGE IS
OF POOR QUALITY



Figure 42. Cross-section photomicrograph of specimen number 1-21-3. The scarf angle is 110 milliradians and the tip is 50 microns thick.

The predicted strengths in Figures 40 and 41 suggest that a 10 milliradian scarf joint with $\bar{x}_{tip} = 0.004$ might reach the goal strength. It will clearly be very difficult to actually construct such a joint for a practical application. Also, it may be impractical simply because of the size of the joint. A repair of this scarf angle bonding 2.5mm thick laminates would be 460mm (18 in.) wide just for the scarf. Many repair situations may not permit such large repairs. Certainly the strength gained by letting the scarf repair extend above the original moldline, page 33, must also be considered.

As mentioned before, it is possible to build stronger joints when the adherend stacking sequence can be controlled. A simple example is bonding unidirectional laminates. Such adherends would not have stress concentrations caused by the modulus changing along their length, as in Figure 33. They would, however, still be sensitive to broken tips and the goal strength would be higher. The best laminate for bonding would have the stiff plies near the middle with the softer plies on the outside. This, unfortunately, is the worst design if laminate bending stiffness is needed.

ORIGINAL PAGE IS
OF POOR QUALITY

TWO DIMENSIONAL STRESS DISTRIBUTION AT THE ADHESIVE ENDS

The adhesive stresses near the ends of the joint vary through its thickness for two reasons. First, the stress distribution is different on the upper and lower interfaces because one adherend is continuous and the other is not. Second, the sudden change in applied load at the end of the adherend induces significant normal stresses in the adhesive, especially for joints of smaller scarf angles.

The reason that normal stresses are induced inside the adhesive is to satisfy two dimensional equilibrium requirements. The equilibrium equation (Ref. 49,

$$\frac{\partial \tau_{12}}{\partial x_1} \cdot \frac{\partial \sigma_{22}}{\partial x_2} = 0$$

requires that a normal stress gradient in the 2-direction balance the shear stress gradient in the 1-direction. Such a gradient is apparent in Figure 34, for example, where the adhesive stress factor rises rapidly from near zero to a large value where the broken adherend tip is. This argument suggests that there may be significant normal stresses in the adhesive but doesn't indicate their values.

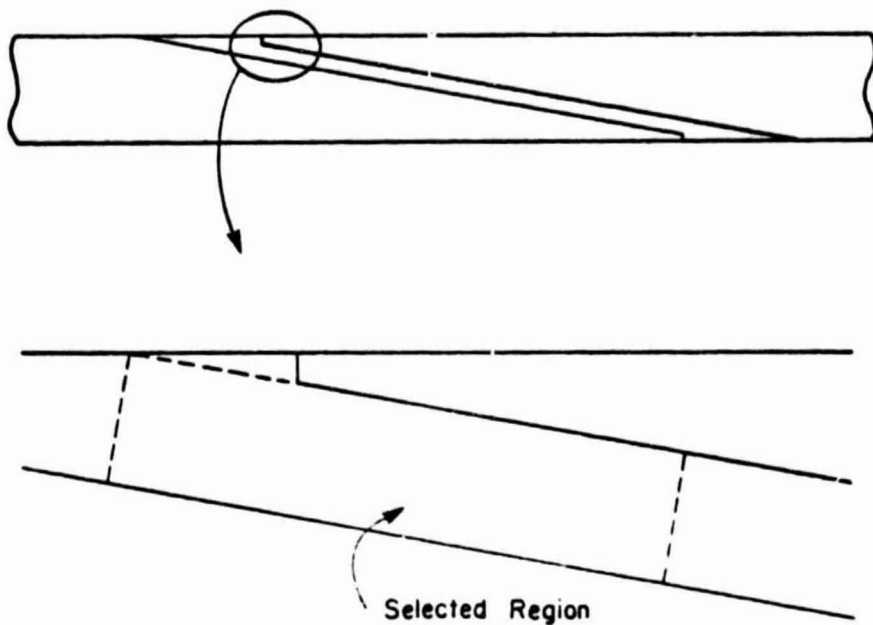


Figure 43. The rectangular region for two dimensional analysis.

The two dimensional stress distribution can be approximated by using stress function solutions for a rectangular region with Fourier series boundary conditions (Ref. 51). The appropriate rectangular region is shown in Figure 43. It extends across the adhesive and far enough to either side of the adherend tip that the stresses are constant through the adhesive thickness.

Approximate boundary conditions can be easily determined from the results of the preceding analysis and from equilibrium requirements for the entire rectangle. On the upper boundary, $x_2 = +t_{\text{adhes}}/2$, of the rectangular region the shear and normal stresses calculated in the previous section apply. That is, shear stress rises quickly from zero on the left to a large value at the adherend tip and then drops more gradually, see Figures 34 through 36. Normal stress is proportional to the shear stress, equation (5). Stresses at the ends of the

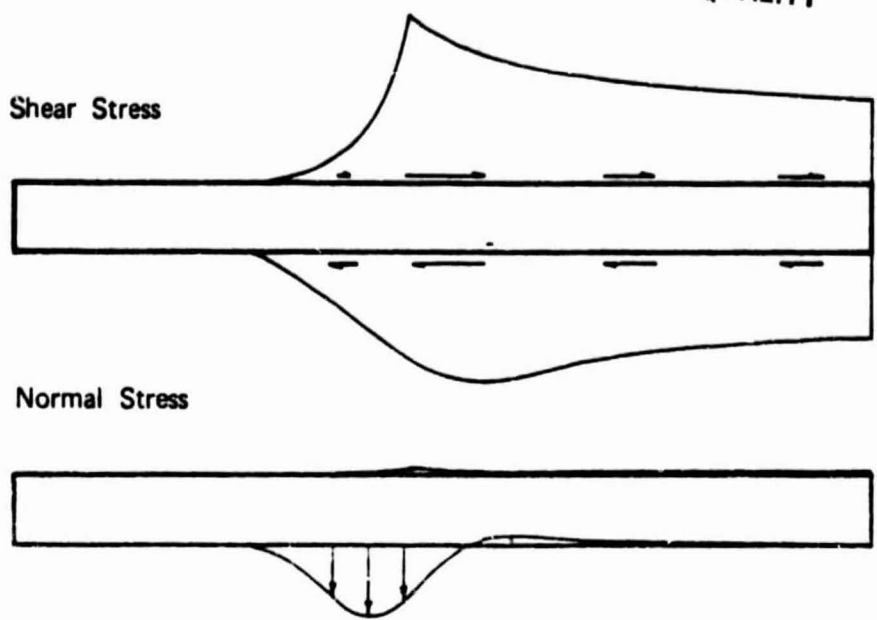


Figure 44. Boundary stresses for the two-dimensional analysis.

rectangular region are assumed constant and equal the stresses at the upper boundary. This is appropriate if the upper boundary and lower boundary stresses are changing slowly.

On the lower boundary, $x_2 = -t_{\text{adhes}}$ / 2, stresses are assumed to change more smoothly than on the upper boundary because there is no discontinuity in the adherend. The stresses must equal the upper boundary stresses at the ends of the rectangular region. In addition, lower boundary stresses must balance the forces on other surfaces to maintain equilibrium of the rectangular region.

Boundary conditions which satisfy these criteria on the upper and lower boundaries for a scarf joint with a scarf angle of 20 milliradians (1.1 degrees) and $\bar{x}_{\text{tip}} = 0.012$ are plotted in Figure 44. The boundary conditions are for a region 3 millimeters long. The normal

stress on the lower boundary, σ_{22} , comprises two components. One maintains vertical equilibrium, including the slowly changing shear stress on the right hand side for all x greater than two millimeters. The other component has zero vertical resultant and balances the moment of all other stresses. It is centered directly under the end of the adherend tip on the upper boundary.

Two stress functions are required to represent these boundary conditions for the rectangular region. One is in terms of sine functions and the other is in terms of cosine functions. The first stress function is (Ref. 50)

$$\phi = \sin\beta x_1 (C_1 \cosh\beta x_2 + C_2 \sinh\beta x_2 + C_3 x_2 \cosh\beta x_2 + C_4 x_2 \sinh\beta x_2),$$

where $\beta = n\pi/L$. The corresponding stresses are

$$\begin{aligned} \sigma_{11} &= \frac{\partial^2 \phi}{\partial x_2^2} = \sin\beta x_1 [C_1 \beta^2 \cosh\beta x_2 + C_2 \beta^2 \sinh\beta x_2 \\ &\quad + C_3 \beta (2 \sinh\beta x_2 + \beta x_2 \cosh\beta x_2) \\ &\quad + C_4 \beta (2 \cosh\beta x_2 + \beta x_2 \sinh\beta x_2)], \\ \sigma_{22} &= \frac{\partial^2 \phi}{\partial x_1^2} = -\beta^2 \sin\beta x_1 (C_1 \cosh\beta x_2 + C_2 \sinh\beta x_2 \\ &\quad + C_3 x_2 \cosh\beta x_2 + C_4 x_2 \sinh\beta x_2), \\ \tau_{12} &= -\frac{\partial^2 \phi}{\partial x_1 \partial x_2} = -\beta \cos\beta x_1 [C_1 \beta \sinh\beta x_2 + C_2 \beta \cosh\beta x_2 \\ &\quad + C_3 (\cosh\beta x_2 + \beta x_2 \sinh\beta x_2) \\ &\quad + C_4 (\sinh\beta x_2 + \beta x_2 \cosh\beta x_2)]. \end{aligned} \tag{38}$$

And the second stress function is

$$\phi = \cos\beta x_1 (C_1 \cosh\beta x_2 + C_2 \sinh\beta x_2 + C_3 x_2 \cosh\beta x_2 + C_4 x_2 \sinh\beta x_2)$$

with the corresponding stresses

$$\begin{aligned} \sigma_{11} &= \frac{\partial^2 \phi}{\partial x_2^2} = \cos\beta x_1 [C_1 \beta^2 \cosh\beta x_2 + C_2 \beta^2 \sinh\beta x_2 \\ &\quad + C_3 \beta (2 \sinh\beta x_2 + \beta x_2 \cosh\beta x_2) \\ &\quad + C_4 \beta (2 \cosh\beta x_2 + \beta x_2 \sinh\beta x_2)] , \end{aligned} \tag{39}$$

$$\begin{aligned} \sigma_{22} &= \frac{\partial^2 \phi}{\partial x_1^2} = -\beta^2 \cos\beta x_1 (C_1 \cosh\beta x_2 + C_2 \sinh\beta x_2 \\ &\quad + C_3 x_2 \cosh\beta x_2 + C_4 x_2 \sinh\beta x_2) , \end{aligned}$$

$$\begin{aligned} \tau_{12} &= -\frac{\partial^2 \phi}{\partial x_1 \partial x_2} = \beta \sin\beta x_1 [C_1 \beta \sinh\beta x_2 + C_2 \beta \cosh\beta x_2 \\ &\quad + C_3 (\cosh\beta x_2 + \beta x_2 \sinh\beta x_2) \\ &\quad + C_4 (\sinh\beta x_2 + \beta x_2 \cosh\beta x_2)] . \end{aligned}$$

The stresses are all in terms of $\sin\beta x_1$ or $\cos\beta x_1$ multiplied by functions of x_2 only. Any boundary conditions on the upper and lower boundaries which can be represented in the form of Fourier series can be used by superposing stress function solutions of this form. The functions of x_2 must equal the Fourier coefficients of the sine or cosine terms at the boundaries.

The boundary conditions of Figure 44 may be represented as

$$\begin{aligned}
 \sigma_{11top} &= \frac{a_{tnor0}}{2} + \sum_{n=1}^{\infty} a_{tnorn} \cos \frac{n\pi x_1}{L}, \\
 \tau_{12top} &= \frac{a_{tshrv0}}{2} + \sum_{n=1}^{\infty} a_{tshrn} \cos \frac{n\pi x_1}{L}, \\
 \sigma_{11bot} &= \frac{a_{bnor0}}{2} + \sum_{n=1}^{\infty} a_{bnorn} \cos \frac{n\pi x_1}{L} \quad \text{and} \\
 \tau_{12bot} &= \frac{a_{bshrv0}}{2} + \sum_{n=1}^{\infty} a_{bshrn} \cos \frac{n\pi x_1}{L}.
 \end{aligned} \tag{40}$$

Using the cosine series has the advantage that the stresses don't change suddenly at the ends of the rectangle.

Once the Fourier coefficients are known they are used to determine the coefficients C_1 through C_4 in equations (38) and (39). For example, for each value of n the coefficients in (38) must be determined so that

$$\sigma_{22} = 0 \text{ and}$$

$$\tau_{12} = a_{tshrn} \cos \beta x_1$$

for $x_2 = +t_{adhes}/2$, and so that

$$\sigma_{22} = 0 \text{ and}$$

$$\tau_{12} = a_{bshrn} \cos \beta x_1$$

for $x_2 = -t_{adhes}/2$. This gives four equations for the unknowns C_1 through C_4 for each value of n in (38). The reason $\sigma_{22} = 0$ for this case is because it is a function of $\sin \beta x_1$ in (38), the Fourier

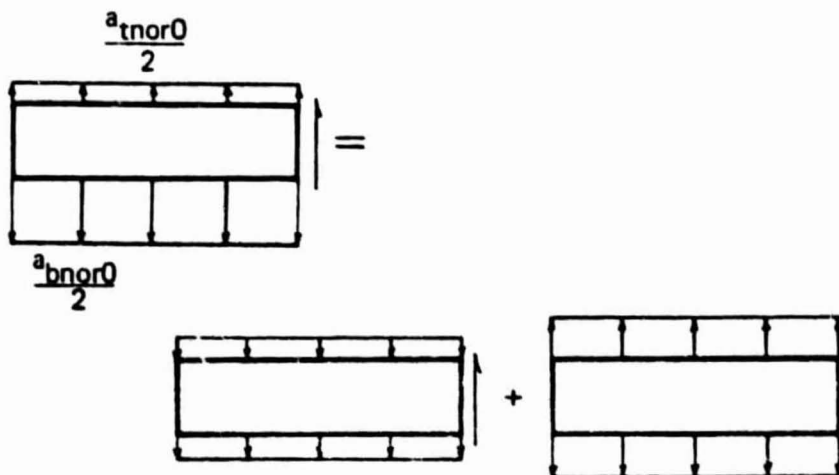


Figure 45. Stress function boundary conditions to impose shear stress on only one end of the rectangular region.

coefficient of which is zero, equation (40). The boundary condition for σ_{zz} is represented by the second stress function, equation (39).

Two additions to this solution are required. The rectangular region has a constant shear stress on the right hand end and no shear stress on the left hand end. Equilibrium can be maintained only by normal stresses applied to the upper and lower boundaries. For equilibrium the coefficients a_{tnor0} and a_{bnor0} are unequal. The application of such a boundary condition requires superposing stress functions with boundary conditions as shown in Figure 45. The resulting

ORIGINAL PAGE IS
OF POOR QUALITY

stress function is

$$\phi = \frac{b_3}{2} x_1^2 x_2 + \frac{a_2}{2} x_1^3 \quad (41)$$

where $b_3 = \frac{a_{tnor0} - a_{bnor0}}{2 t_{adhes}}$

and $a_2 = \frac{a_{tnor0} - b_3 t_{adhes}}{2}$

This stress function is a combination of second and third order polynomial stress functions (Ref. 51). The corresponding stresses are

$$\sigma_{11} = 0,$$

$$\sigma_{22} = b_3 x_2 + a_2$$

$$\tau_{12} = -b_3 x_1.$$

This undesired linear shear stress is eliminated by including a compensating linear term in the boundary condition for τ_{12} .

The second addition to the solution corrects the 1-direction normal stress, σ_{11} . The procedure so far gives a linearly increasing σ_{11} with a parabolic shear stress distribution across the adhesive. Since neither of these stresses has been specified in the boundary conditions their values are not surprising. A linearly increasing σ_{11} through the entire joint is unreasonable, however, and it can be eliminated by superposing one more stress function solution. It has the form

$$\phi = b_3 x_1 x_2 + \frac{d_1}{6} x_2^3 + \frac{d_4}{6} x_1 x_2^3. \quad (42)$$

This stress function is a combination of second, third and fourth order polynomial stress functions (Ref. 52). The coefficients are determined

from the slope of σ_{11} and the values of τ_{12} at the ends of the rectangular region. The corresponding stresses are

$$\sigma_{11} = d_4 x_1 x_2 + d_3 x_2$$

$$\tau_{12} = -\frac{d_4}{2} x_2^2 - b_2$$

$$\sigma_{22} = 0.$$

The stress distributions for a cross section of adhesive calculated by this method are shown in Figure 46. The boundary conditions used are for a 20 milliradian (1.1 degree) scarf joint with the adherend tip broken at $\bar{x} = 0.012$. The adhesive cross section is 3 millimeters long and 0.2 millimeters wide. Note that these dimensions are not to scale in Figure 46 so that through-the-thickness variations can be seen. These stresses are calculated by the FORTRAN program SF3 in Appendix v. Note that the normal and shear stress boundary conditions shown in Figure 44 are satisfied.

The most interesting feature of this stress distribution is the σ_{11} induced by gradients in the other stresses. Although only about 40% as large as the shear stress it is certainly significant. The magnitude of this stress depends on the steepness of the shear stress curve as shown in Figure 34. Since these stress gradients are larger for joints with smaller scarf angles the induced σ_{11} stresses will also be more important for small scarf angles.

An interesting possibility is that such a normal stress might actually cause failure to begin in the adherend rather than the adhesive. Composites are notorious weak in the transverse direction

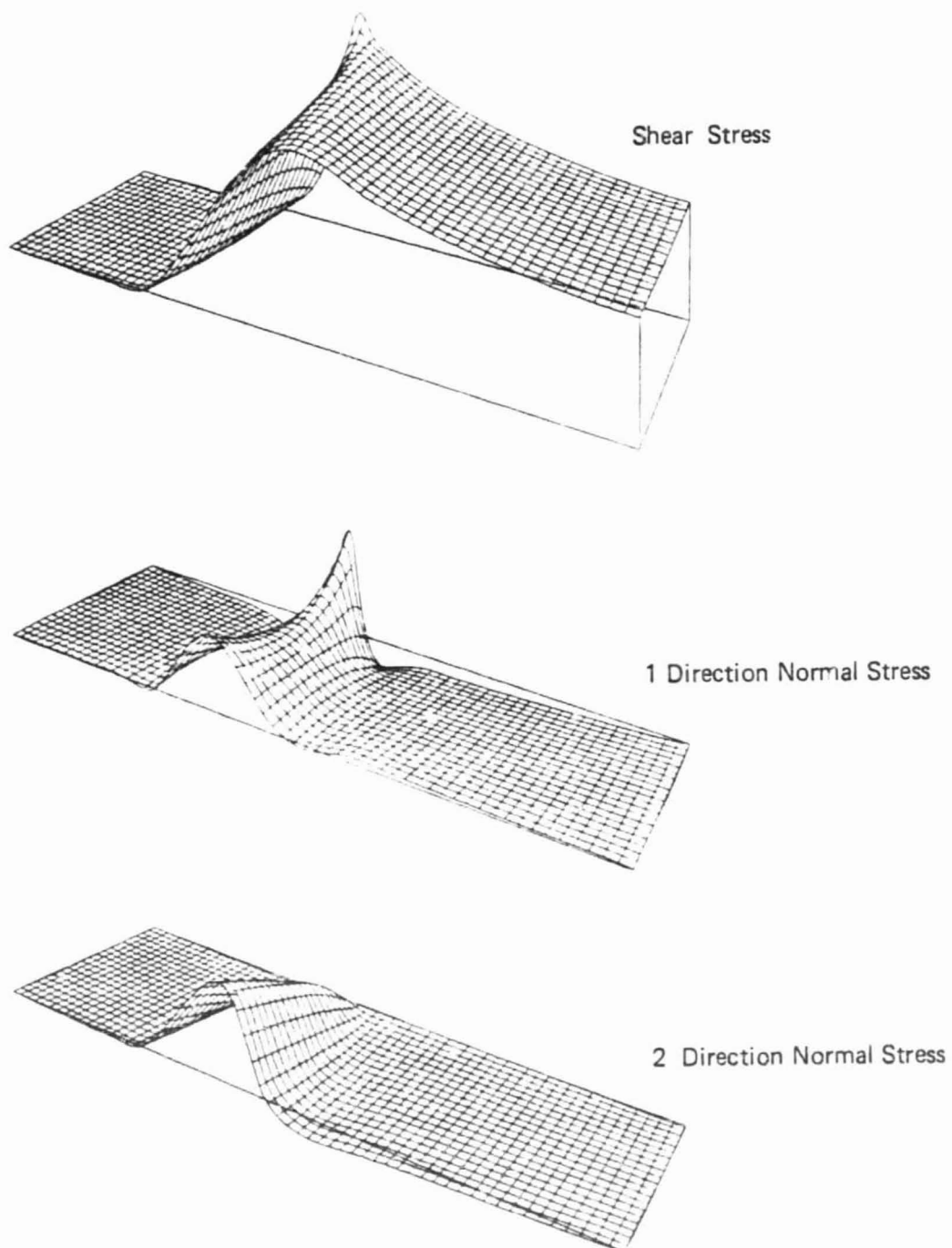


Figure 46. Two-dimensional stress distribution at the end of the scarf joint adhesive.

and experimental evidence of such failure was observed in Figures 14 and 15. Such normal stresses may also be important in the failure process itself where the shear stress changes suddenly at the tip of a shearing mode crack.

The induced stress may explain why strength values in Figures 40 and 41 fall on curves corresponding to different values of \bar{x}_{tip} . The induced normal stress would be expected to lower the joint strength for smaller scarf angles. This is exactly how the prediction curves are off. Joints with scarf angles of 33 and 52 milliradians fall on prediction curves for \bar{x}_{tip} between zero and 0.004 in Figure 41. The strength of the 19 milliradian joint corresponds to \bar{x}_{tip} around 0.01. The data of Figure 40 are similar.

ORIGINAL PAGE IS
OF POOR QUALITY

SCARF JOINTS WITH DOUBLERS

Bonding a doubler over a completed joint is a common way to reinforce it. However, careful design is important because addition of a doubler doesn't necessarily increase joint strength and may actually lower it. Doubler design is complicated by the addition of another adhesive bond which is a potential site of failure initiation. Also, bending induced by the doubler influences the load at which failure will occur in the scarf adhesive.

This section presents experimental data for scarf joints with doublers. Both full-length and multiple short doublers are evaluated. Also, a bending model is suggested with limited experimental verification.

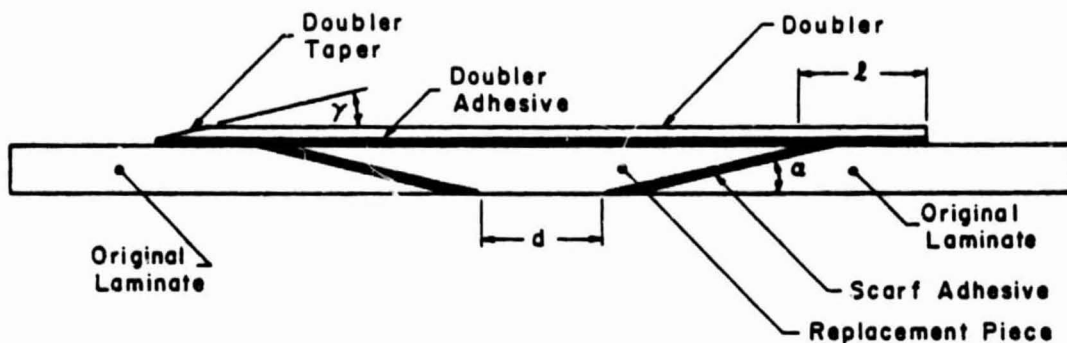


Figure 47. Scarf joint with a full length doubler.

Several 110 milliradian (6.2 degree) scarf joints, as shown in Figure 47, were tested with doublers of Hercules carbon/epoxy and Ti-6Al-4V titanium to measure their tensile strength. The specimen dimensions were $d = 25\text{mm}$, $l = 25\text{ mm}$ and they were nominally 25 mm wide. The stacking sequence of the carbon/epoxy doublers was [90/0/0/90]. The titanium doublers were 0.64 mm (0.025 inches) thick.

Table II

Strength of 110 Milliradian Scarf Joints with Full-Length Doublers

Doubler Geometry	Width (mm)	Ultimate Load (kN)	Ultimate In-Plane Force Resultant (kN/m) (1bf/in)
Untapered Carbon/Epoxy	25.0	15.0	598 3430
Untapered Carbon/Epoxy	25.0	15.4	616 3520
Untapered Carbon/Epoxy	24.4	13.5	553 3160
Tapered (0.10 rad.) C/E	25.0	22.4	893 5120
Tapered (0.10 rad.) C/E	24.8	21.8	878 5020
Tapered (0.05 rad.) C/E	25.4	21.6	850 4860
Tapered (0.05 rad.) C/E	25.5	20.8	816 4660
Tapered (0.05 rad.) C/E	25.4	21.6	850 4860
Tapered (0.05 rad.) C/E	25.2	21.8	865 4940
Untapered Titanium	24.9	10.2	409 2340
Untapered Titanium	25.5	15.2	594 3400
Tapered Titanium	24.9	18.5	742 4240
Tapered Titanium	25.1	18.2	728 4140
Plain Scarf Joint (No Doubler)			648 3700

The strength data are in Table II. They are consistent for all specimen types except for those with untapered titanium doublers. This variation may be caused by sensitivity to flaws at the end of the doubler adhesive aggravated by the very stiff doubler. The data for untapered doublers indicate the importance of proper design for increasing the repair strength. All of these joints have lower strength than the plain scarf joint. The data are limited, however.

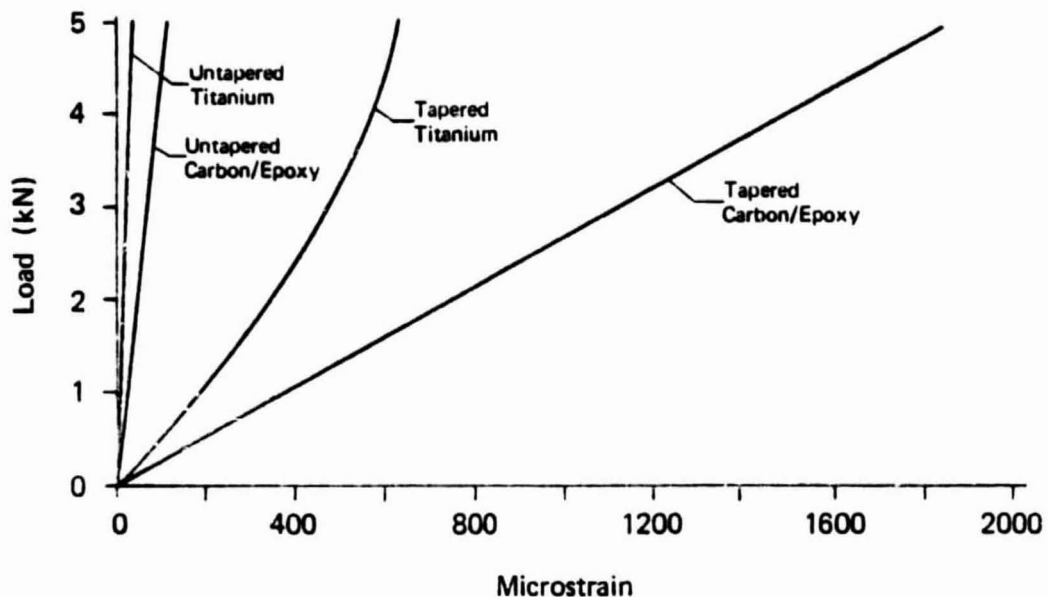
ORIGINAL PAGE IS
OF POOR QUALITY

Figure 48. Strain at the ends of several doublers.

The section stiffness of the end of the doubler is important to joint strength. The strength of specimens with tapered doublers is greater by about half than those with untapered doublers. Strains measured at the doubler ends also show the effect of doubler stiffness. Microstrain versus load for each of the four doubler types is shown in Figure 48. For all cases the stiffer the doubler end, the lower the strength of the joint.

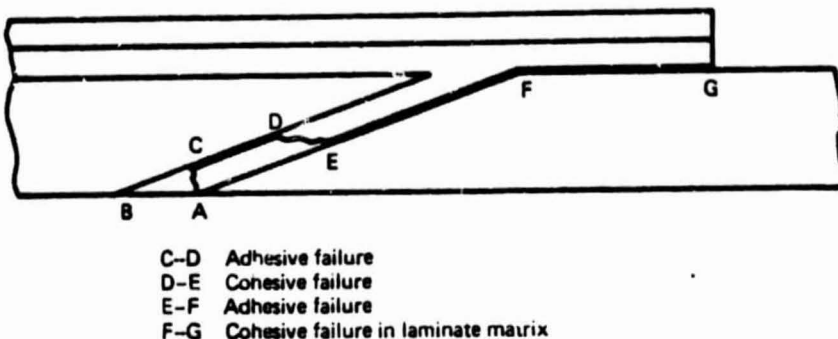


Figure 49. Mixed mode failure.

The specimens with untapered doublers and those with tapered titanium doublers failed in the same mode. In each case the adhesive separated from the 'original laminate' under the doubler and part way along the scarf joint, as shown in Figure 49. At that point there was a 3 mm to 5 mm wide band of cohesively failed adhesive. Here the adhesive failure changed to the 'replacement piece' side of the joint. Also, the failed adhesive surfaces under the doubler were dark, indicating that failure occurred in the matrix. For the tapered titanium doubler specimens the adhesive separated from the doubler near the end, rather than from the laminate. This region extended along roughly half the taper length. In addition, all the carbon/epoxy doublers had interlaminar separation between the zero degree plies and the bottom 90 degree ply. Also the exposed ends of all scarf joints had a strip of adhesive corresponding to ABC in Figure 49. All the scarf joints had pulled-out 45 degree plies, usually two sets near the doubler and one set near an exposed end. Interestingly, the strongest specimens, those with tapered carbon/epoxy doublers, failed in a different mode.

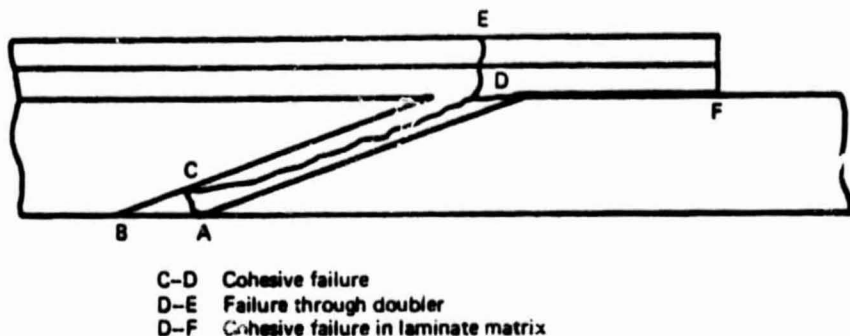


Figure 50. Cohesive failure

The plain scarf joints and those with the tapered carbon/epoxy doublers failed predominantly in cohesion. That is, the adhesive separated from itself, rather than from the adherends. Cohesive failure occurred over the scarf joint surfaces as shown in Figure 50. On one of the carbon/epoxy doubler specimens the doubler adhesive separated from the 'original laminate,' D-F in Figure 50. The separated adhesive surface was dark, like the laminate matrix, indicating that failure actually occurred in a very thin outer layer of the matrix. The other doubler broke in two as shown at E-D in Figure 50.

The two failure modes correspond to the locations where failure began. The cohesive failures, in the plain scarf joints and the joints with tapered carbon/epoxy doublers, began at the end of the scarf adhesive. The other failures began at the end of the doubler. That is why the section stiffness of the doubler ends is so important to joint strength. Tapering the carbon/epoxy doubler relieved the doubler

ORIGINAL PAGE IS
OF POOR QUALITY

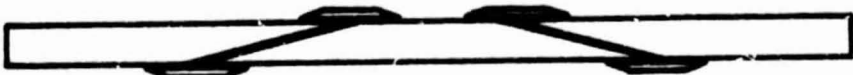


Figure 51. Scarf joint with small tapered doublers.

adhesive stress concentration enough that the scarf adhesive failed first.

The stress concentration in the scarf adhesive may be the cause of fracture through the adhesive at A-C. This path corresponds with the highly stressed region shown by analysis in preceding sections.

It may be possible to lower the stresses associated with bending, and strengthen the joint, by bonding small doublers over the adherend tips. Small doublers are desirable because they may be used in repairs where one side of the laminate is accessible only through the hole being repaired. Also, they induce less bending of the joint than larger doublers.

A series of 52 milliradian (3.0 degree) scarf joint specimens with small tapered doublers, as shown in Figure 51 were tested to evaluate this idea. These doublers were also of carbon/epoxy with [90/0/0/90] stacking sequence, tapered at a 100 milliradian angle by end milling. The two sets of finished doublers were 15 mm and 30 mm from tip to tip. The strength data are in Table III.

ORIGINAL PAGE IS
OF POOR QUALITY

Table III

Strength of Scarf Joints with Short Doublers

Specimen Number	Doubler Length (mm)	Width (mm)	Ultimate Load (kN)	Ultimate In-Plane Force Resultant (kN/m) (lbf/in)
3-43-1	15	23.1	26.8	1160 6510
3-43-2	15	24.4	27.5	1130 6440
3-43-3	15	24.0	24.0	1000 5710
3-43-4	15	24.6	23.0	939 5340
3-103-1	30	25.5	26.5	1040 5930
3-103-2	30	25.6	24.0	939 5350
3-103-3	30	25.6	28.9	1130 6450
3-103-4	30	25.5	26.0	1020 5820
Plain Scarf Joint				990 5650

The strength of the specimens with small doublers average only slightly higher than the plain scarf joints. Although the failure mode is unchanged the failure locations are different. Specimens without doublers failed in the 'replacement piece' of the joint. Specimens with 15 mm doublers failed in the 'original laminate' part of the joint. And specimens with 30 mm doublers failed in the 'replacement piece' of the joint. An exception is the weakest specimen with 30 mm doublers which failed through the 'original laminate.' In general, the doublers were too small to redistribute the joint load adequately. The change of location of the failure is probably due to bending induced by the doublers.

6 - 2

ORIGINAL PAGE IS
OF POOR QUALITY

Joint Bending Model

Since bending is important to joint strength an analytical model is necessary to predict joint strength. It is best to separate the geometrically non-linear bending problem from the linear load transfer problem of the preceding sections. The bending stresses might then be calculated for a series of joint loads and then combined with the corresponding load transfer stresses.

This section proposes a bending model and limited experimental data to verify it. When the repair is loaded its deflection moves the neutral surface, changing the moment distribution of the eccentric load force. The moment at most sections decreases considerably with initial deflection. This is the source of the geometric non-linearity.

The moment distribution and strains for a specimen with joint adhesive layers can be calculated from beam theory, regarding the laminate as an elastic layered beam at each section. All parts of the specimen must satisfy the beam deflection equation:

$$\frac{d^2y}{dx^2} = \frac{F(y+e)}{(EI)}. \quad (43)$$

The effective bending rigidity at any location of an N-layered specimen is calculated from the relation

$$(EI) = \sum_{n=1}^N E_n I_n. \quad (44)$$

ORIGINAL PAGE IS
OF POOR QUALITY

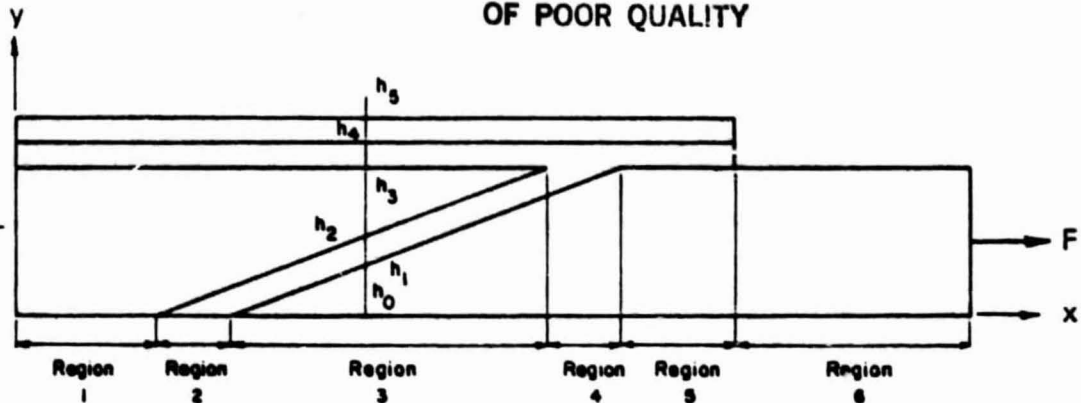


Figure 52. Regions of a scarf joint with a doubler.

This equation accounts for the lower stiffness of the adhesive layer and the associated change in the location of the neutral surface. Figure 52 illustrates the layered beam. For example, in region 3, h_0 to h_1 is the stiff lower layer of the original laminate, h_1 to h_2 is the less stiff adhesive layer, h_2 to h_3 is the replacement piece layer, h_3 to h_4 is the doubler adhesive layer and, finally, h_4 to h_5 is the doubler. This model may be adapted for laminated adherends by treating each lamina as a separate layer as in the FORTRAN program DEFLCOMP in Appendix vi. Linear distribution of bending strain through the section is assumed in all cases.

Equation (43) may be solved by numerical integration, iterating the boundary condition (i.e. the midspan deflection) until the end deflection is zero. When the deflection at a section is known the moment distribution and surface strains can be calculated.

A plot of the surface strains predicted by this model for an aluminum specimen is shown in Figure 53. Inspection of the specimens showed that the adhesive layers of some were tapered, rather than

ORIGINAL PAGE IS
OF POOR QUALITY

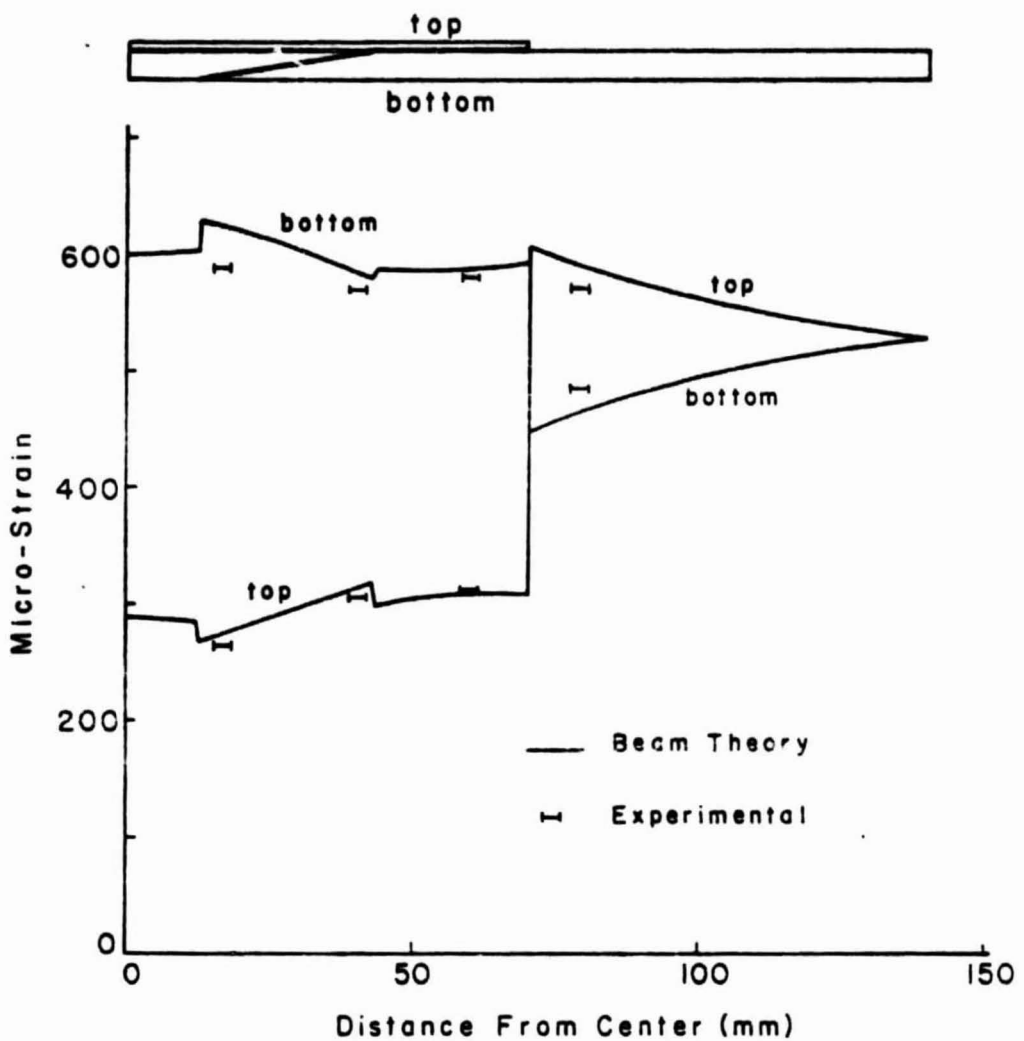


Figure 53. Predicted and experimental surface strains for an aluminum scarf joint with an aluminum doubler.

uniform, and this was accounted for in the deflection model. The experimental strain data in Figure 53 correspond very well with the predicted strains.

The theoretical and experimental surface strains for scarf joint repairs of two carbon/epoxy laminate specimens with carbon/epoxy doublers are shown in Figures 54 and 55. For the specimen represented in Figure 55 strain gages were placed as close as possible to the adhesive on the lower surface. Predicted strains and experimental strains agree very well except for the strain near the adhesive on the bottom surface. This strain is considerably lower than the average predicted strain for the region the strain gage covers. However, this region is a stiff part of an adherend (zero degree plies only) adjacent to the soft adhesive. This is a likely place for the beam theory assumption that plane sections remain plane to not hold. The measured strain would, therefore, be lower than expected. Fortunately, it is precisely this effect that the load transfer model accounts for.

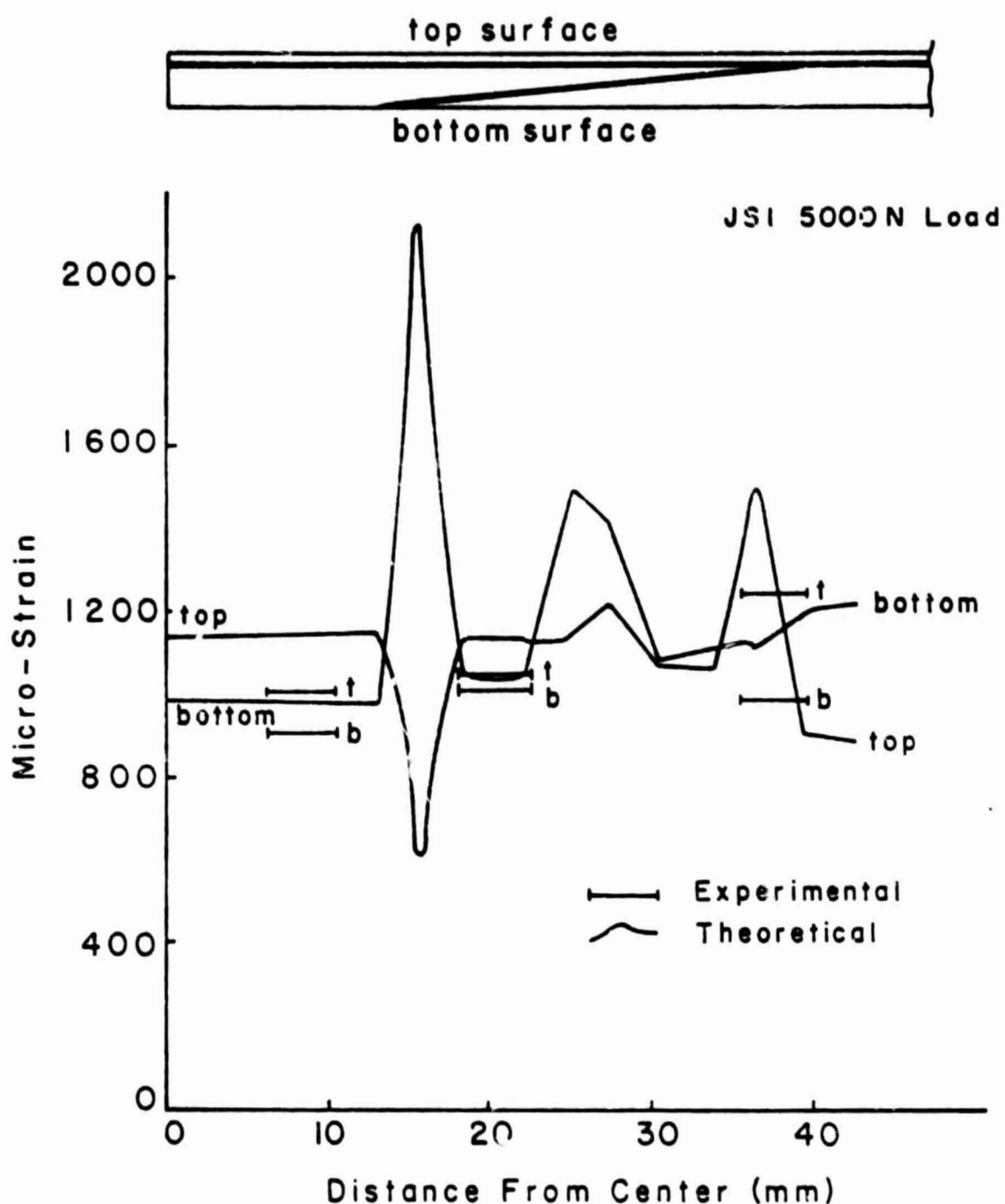


Figure 54. Predicted and experimental surface strains for a carbon/epoxy scarf joint with a carbon/epoxy doubler.

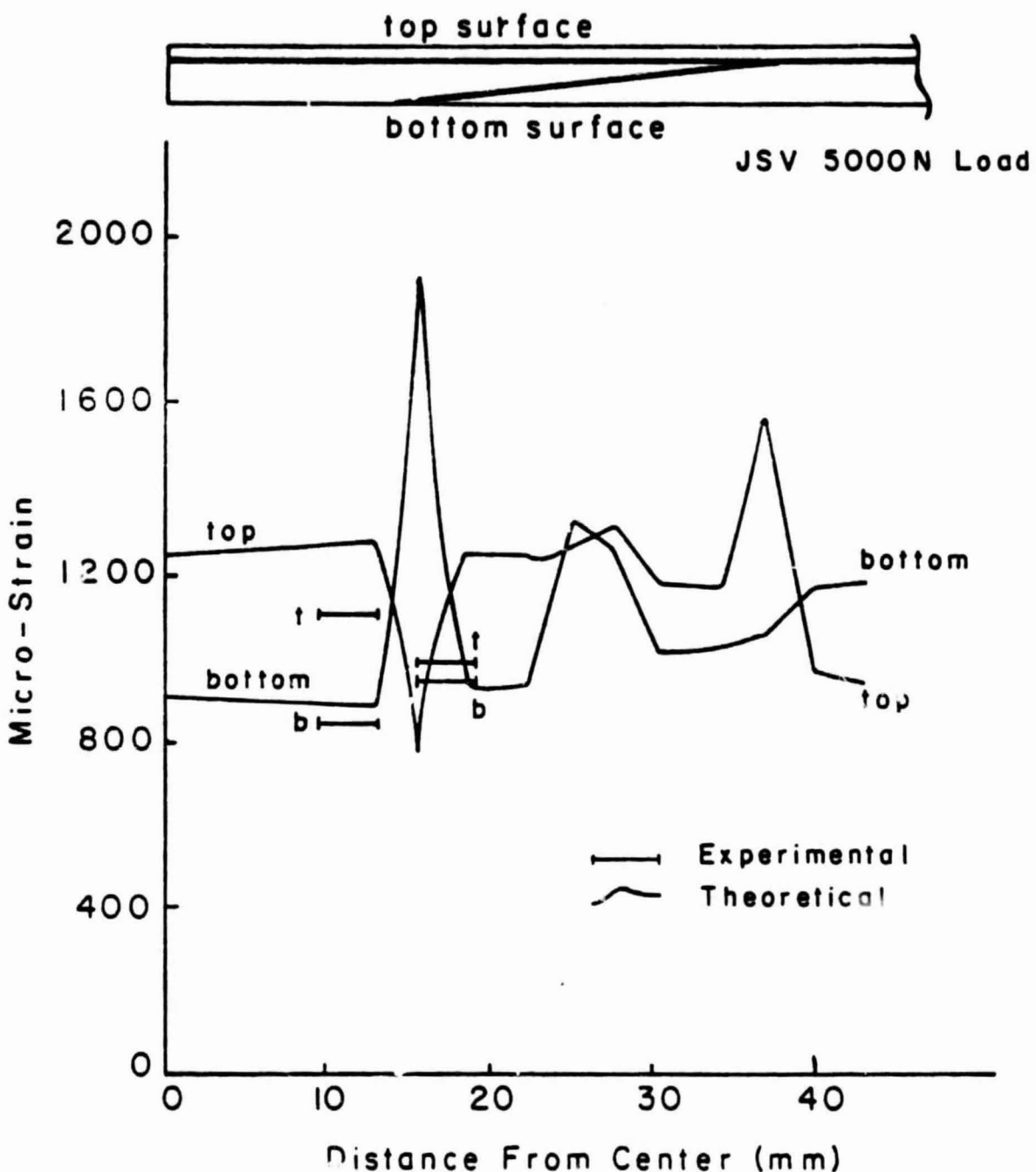
ORIGINAL PAGE IS
OF POOR QUALITY

Figure 55. Predicted and experimental surface strains for a carbon/epoxy scarf joint with a carbon/epoxy doubler.

ORIGINAL PAGE IS
OF POOR QUALITY

REFERENCES

1. V. O. Volkerson, 'Die Nietkraftverteilung in zugbeanspruchten Nietverbindungen mit konstanten Laschenquerschnitten,' Luftfahrtforschung, 1938, pp. 41-47
2. M. Goland and E. Reissner, 'The Stresses in Cemented Joints,' Journal of Applied Mechanics, March 1944
3. T. S. Ramamurthy and A. K. Rao, 'On the Shaping of Bonded Joints for Efficient Load Transfer,' Proceedings of the Sixth Canadian Congress of Applied Mechanics, Vancouver, May 29-June 3, 1977
4. T. S. Ramamurthy and A. K. Rao, 'Shaping of Adherends in Bonded Joints,' Int. J. Mech. Sci., Vol 20, 1978, pp 721-727
5. J. B. Sainsbury-Carter, 'Automated Design of Bonded Joints,' Journal of Engineering for Industry, November 1973, pp. 919-924
6. B. W. Cherry and N. L. Harrison, 'The Optimum Profile for a Lap Joint,' J. Adhesion, Vol. 2, April 1970, pp. 125-128
7. Frigyes Thamm, 'Stress Distribution in Lap Joints with Partially Thinned Adherends,' J. Adhesion, Vol. 7, 1976, pp. 301-309
8. J. L. Lubkin, 'A Theory of Adhesive Scarf Joints,' Journal of Applied Mechanics, June 1957, pp. 255-260
9. L. J. Hart-Smith, 'Adhesive Bonded Single Lap Joints,' NASA CR 112236, Jan 1973
10. L. J. Hart-Smith, 'Adhesive Bonded Double Lap Joints,' NASA CR 112235, Jan 1973
11. L. J. Hart-Smith, 'Adhesive Bonded Scarf and Stepped-Lap Joints,' NASA CR 112237, Jan 1973
12. R. C. Wetherhold and J. R. Vinson, 'An Analytical Model for Bonded Joint Analysis in Composite Structures Including Hygrothermal Effects,' AFOSR-TR-78-1337, June 1978
13. P. K. Sinha and M. N. Reddy, 'Thermal Analysis of Composite Bonded Joints,' Fiber Science and Technology, Vol. 9, 1976

14. W. T. Chen and C. W. Nelson, 'Thermal Stress in Bonded Joints,' IBM J. Res. Develop., Vol. 23, No. 2, March 1979
15. J. R. Vinson and J. R. Zumsteg, 'Analysis of Bonded Joints in Composite Material Structures Including Hygrothermal Effects,' Collected Tech. Papers AIAA/ASME Struct. Struct. Dyn. Mater. Conf. 20th, April 4-6, 1979, pp. 291-302, Paper no. 79-0798
16. F. Erdogan and M. Ratwani, 'Stress Distribution in Bonded Joints,' J. of Composite Materials, Vol 5, July 1971, pp. 378-393
17. M. N. Reddy and P. K. Sinha, 'Stresses in Adhesive Bonded Joints for Composites,' Fiber Science and Technology, Vol. 8, 1975
18. W. J. Renton and J. R. Vinson, 'The Analysis and Design of Composite Material Bonded Joints Under Static and Fatigue Loadings,' AFOSR-TR-73-1627, August 1973
19. W. J. Renton and J. R. Vinson, 'Analysis of Adhesively Bonded Joints Between Panels of Composite Materials,' Journal of Applied Mechanics, March 1977, pp. 101-106
20. I. U. Ojalvo and H. L. Eidinoff, 'Bond Thickness Effects upon Stresses in Single Lap Adhesive Joints,' AIAA Journal, Vol. 16, No. 3, March 1978, pp. 204-211
21. R. D. Adams, S. H. Chambers, P. J. Del Strother and N. A. Peppiatt, 'Rubber Model for Adhesive Lap Joints,' J. Strain Analysis, Vol. 8, No. 1, 1973, pp. 52-57
22. R. D. Adams and N. A. Peppiatt, 'Effect of Poisson's Ratio Strains in Adherends on Stresses of an Idealized Lap Joint,' J. Strain Analysis, Vol. 8, No. 2, 1973, pp. 134-139
23. W. J. Renton and J. K. Vinson, 'Shear Property Measurements of Adhesives in Composite Material Bonded Joints,' Composite Reliability, ASTM STP 580, American Society for Testing and Materials, 1975
24. W. James Renton, 'The Symmetric Lap-Shear Test—What Good Is It?' Experimental Mechanics, Nov. 1976, pg. 409
25. T. R. Guess, R. E. Allred and F. P. Gerstle, Jr., 'Comparison of Lap Shear Test Specimens,' J. of Testing and Evaluation, Vol. 5, No. 2, pp. 84-93
26. J. W. Sawyer and Paul A. Cooper, 'Analytical and Experimental Results for Bonded Single Lap Joints with Preformed Adherends,' AIAA Journal, Vol. 19, No. 11, November 1981, pp. 1443-1451

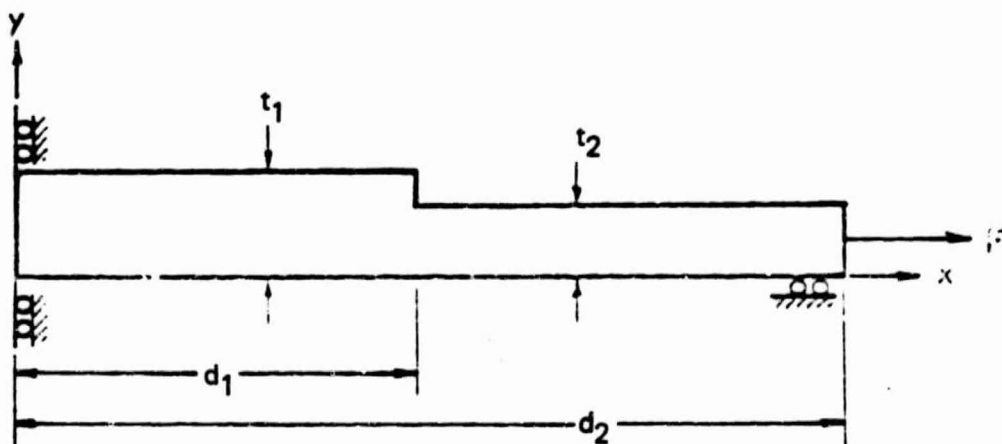
27. A. K. Rao, 'Stress Concentrations and Singularities at Interface Corners,' ZAMM, Vol. 51, 1971, pp. 395-406
28. V. L. Hein and F. Erdogan, 'Stress Singularities in A Two-Material Wedge,' Int. J. of Fracture Mechanics, Vol. 7, No. 3, Sept 1971
29. D. B. Bogy, 'Two Edge-Bonded Elastic Wedges of Different Materials and Wedge Angles Under Surface Tractions,' Journal of Applied Mechanics, June 1971, pp. 377-386
30. T. S. Ramamurthy and A. K. Rao, 'Influence of Adhesive Non-Linearities on the Performance and Optimal Length of Adhesive Bonded Joints,' Mech. Res. Comm., Vol. 5, No. 1, 1978, Pergamon Press
31. R. D. Adams, N. A. Peppiatt and J. Coppendale, 'Prediction of Strength of Joints Between Composite Materials,' Symposium: Jointing in Fiber Reinforced Plastics, Sept 4-5, 1978, Imperial College London, Reprinted by permission of the Institution of Civil Engineers from Fiber Reinforced Materials, ICE London, 1977, pp. 45-55
32. R. D. Adams and N. A. Peppiatt, 'Stress Analysis of Lap Joints in Fibre Reinforced Composite Materials,' Fibre Reinforced Materials: Design and Engineering Applications, Institution of Civil Engineers, London, 1977, Proceedings of the conference held in London, March 23-24, 1977
33. P. Grant, 'Analysis of Adhesive Stresses in Bonded Joints,' Symposium: Jointing in Fiber Reinforced Plastics, Sept 4-5, 1978, Imperial College, London
34. Y. R. Nagaraja and R. S. Alwar, 'Viscoelastic Analysis of an Adhesive-Bonded Plane Lap Joint,' Computers and Structures, Vol 11, pp. 621-627
35. Joyanto K. Sen and Robert M. Jones, 'Stresses in Double-Lap Joints Bonded with a Viscoelastic Adhesive: Part I. Theory and Experimental Corroboration,' AIAA Journal, Vol. 18, No. 10, Oct. 1980
36. Joyanto K. Sen and Robert M. Jones, 'Stresses in Double-Lap Joints Bonded with a Viscoelastic Adhesive: Part II. Parametric Study and Joint Design,' AIAA Journal, Vol. 18, No. 11, pp. 1376-1382
37. F. Delale and F. Erdogan, 'Viscoelastic Analysis of Adhesively Bonded Joints,' Journal of Applied Mechanics, Vol. 48, June 1981, pg. 331
38. Thien Wah, 'Plane Stress Analysis of a Scarf Joint,' Int. J. Solids Structures, Vol. 12, 1976, pp. 491-500

39. M. D. Wright, 'Stress Distribution in Carbon Fibre Reinforced Plastic Joints,' Composites, Jan. 1980, pp. 46-50
40. J. R. Vinson, 'On the State of Technology in Adhesively Bonded Joints in Composite Material Structures,' Emerging Technol. in Aerosp. Struct. Des. Struct. Dyn. and Mater., presented at the Aerospace Conf. Aug. 1980
41. F. L. Matthews, P. F. Kilty and E. W. Godwin, 'A Review of the Strength of Joints in Fibre-Reinforced Plastics, Part 2. Adhesively Bonded Joints,' Composites, Vol 13, Issue 1, January 1982, pp. 29-37
42. Paul E. Sandorff, 'Saint-Venant Effects in an Orthotropic Beam,' J. Composite Materials, vol. 14, July 1980, pp. 199-212
43. Carl M. Bender and Steven A. Orsag, Advanced Mathematical Methods for Scientists and Engineers, McGraw-Hill Book Company, 1978, pg. 484
44. Carl M. Bender and Steven A. Orsag, Advanced Mathematical Methods for Scientists and Engineers, McGraw-Hill Book Company, 1978, pg. 493
45. Carl M. Bender and Steven A. Orsag, Advanced Mathematical Methods for Scientists and Engineers, McGraw-Hill Book Company, 1978, pg. 70
46. Carl M. Bender and Steven A. Orsag, Advanced Mathematical Methods for Scientists and Engineers, McGraw-Hill Book Company, 1978, pgs. 71 and 76
47. Bhagwan D. Agarwal and Lawrence J. Broutman, Analysis and Performance of Fiber Composites, John Wiley and Sons, New York, 1980
48. J. R. Vinson and T. W. Chou, Composite Materials and Their Use in Structures, John Wiley and Sons, New York, 1975
49. S. P. Timoshenko and J. N. Goodier, Theory of Elasticity, Third Edition, McGraw-Hill Book Company, pg 27
50. S. P. Timoshenko and J. N. Goodier, Theory of Elasticity, Third Edition, McGraw-Hill Book Company, pg. 53
51. S. P. Timoshenko and J. N. Goodier, Theory of Elasticity, Third Edition, McGraw-Hill Book Company, pg 35,36
52. S. P. Timoshenko and J. N. Goodier, Theory of Elasticity, Third Edition, McGraw-Hill Book Company, pg. 36,37
53. J. C. Burkill, The Theory of Ordinary Differential Equations, Oliver and Boyd, Edinburgh and London, New York: Interscience Publishers, Inc., 1956

APPENDICES

ORIGINAL PAGE IS
OF POOR QUALITY

Appendix i. BENDING OF A SPECIMEN WITH A THICK SECTION IN THE MIDDLE



Half of a specimen with a thick section in the middle.

This specimen bends along its entire length because the eccentricity of the thicker section and the bending deflection it causes both make the neutral axis eccentric to the load. Only half the specimen requires analysis because it is symmetric.

All sections of the specimen must satisfy the beam deflection equation

$$\frac{d^2y}{dx^2} = \frac{M}{EI}$$

where M is the moment

E is the x -direction elastic modulus and

I is the moment of inertia.

Letting $e = (t_1 - t_2)/2$, the eccentricity of the thicker section when undeflected, the moment along the bar is

$$M = \begin{cases} F(e+y) & \text{for } 0 \leq x \leq d_1 \\ Fy & \text{for } d_1 < x \leq d_2 \end{cases}$$

For $0 \leq x \leq d_1$ then

$$\frac{d^2y}{dx^2} = \frac{F}{E_1 I_1} (e + y)$$

where E_1 and I_1 are the elastic modulus and moment of inertia of the thicker part of the bar. The solution of this differential equation is

$$y = C_1 \sinh \sqrt{\frac{F}{E_1 I_1}} x + C_2 \cosh \sqrt{\frac{F}{E_1 I_1}} x - e.$$

Introducing the boundary conditions $y = y_0$ and $dy/dx = 0$ at $x = 0$ the solution is

$$y = (e + y_0) \cosh \sqrt{\frac{F}{E_1 I_1}} x - e.$$

y_0 must be calculated last because it depends on the deflection of the thinner part of the bar.

For $d_1 < x \leq d_2$ the differential equation is

$$\frac{d^2y}{dx^2} = \frac{F}{E_2 I_2} y$$

where E_2 and I_2 are the elastic modulus and moment of inertia of the thinner part of the bar. Its solution is

$$y = C_3 \sinh \sqrt{\frac{F}{E_2 I_2}} x + C_4 \cosh \sqrt{\frac{F}{E_2 I_2}} x$$

The boundary conditions require that the slope and deflection of both parts of the bar be identical where they meet. Therefore at $x = d_1$

$$y = (e + y_0) \cosh \sqrt{\frac{F}{E_1 I_1}} d_1 - e \text{ and}$$

$$\frac{dy}{dx} = (e + y_0) \sqrt{\frac{F}{E_1 I_1}} \sinh \sqrt{\frac{F}{E_1 I_1}} d_1$$

The two remaining constants of integration are then

$$C_3 = \frac{ACe - \frac{BD}{G}(E-1)e + (AC - \frac{BDE}{G})y_0}{BG - \frac{BD^2}{G}} \text{ and}$$

$$C_4 = \frac{(E-1)e}{G} - \frac{D}{G} \frac{[AC - \frac{BD}{G}(E-1)]e}{BG - \frac{BD^2}{G}} + \left[\frac{E}{G} - \frac{D}{G} \frac{(AC - \frac{BDE}{G})}{BG - \frac{BD^2}{G}} \right] y_0.$$

where

$$A = \sqrt{\frac{F}{E_1 I_1}}, \quad B = \sqrt{\frac{F}{E_2 I_2}},$$

$$C = \sinh \sqrt{\frac{F}{E_1 I_1}} d_1, \quad D = \sinh \sqrt{\frac{F}{E_2 I_2}} d_1, \quad E = \cosh \sqrt{\frac{F}{E_1 I_1}} d_1,$$

$$G = \cosh \sqrt{\frac{F}{E_2 I_2}} d_2, \quad H = \sinh \sqrt{\frac{F}{E_2 I_2}} d_2, \quad I = \cosh \sqrt{\frac{F}{E_2 I_2}} d_2.$$

Using the condition that $y = 0$ at $x = d_2$.

$$y_0 = \frac{-\frac{ACeGH - BD(E-1)eH}{BG^2 - BD^2} - \frac{(E-1)eI}{G} + \frac{DACEGI - BD^2(E-1)eI}{BG^3 - BD^2G}}{\frac{HACG - BDEH}{BG^2 - BD^2} + \frac{EI}{G} - \frac{DAGCI - BDEI}{DG^3 - BD^2G}}.$$

The end slopes of composite specimens are calculated from these relations. At $x = d_2$, the slope is

$$\begin{aligned}\frac{dy}{dx} &= C_3 \sqrt{\frac{F}{E_2 I_2}} \cosh \sqrt{\frac{F}{E_2 I_2}} d_2 + C_4 \sqrt{\frac{F}{E_2 I_2}} \sinh \sqrt{\frac{F}{E_2 I_2}} d_2 \\ &= C_3 BI + C_4 BH\end{aligned}$$

However, section moduli ($E_i I_i$'s) which give bending stiffnesses equivalent to those of the inhomogeneous composite and the composite-doubler must be used. For the thicker section, the section modulus may be calculated by treating the specimen as a layered beam. Note that the difference between bending stiffness and extensional stiffness must be accounted for. The effective properties are

$$E_1 I_1 = 6.37 \text{ Nm}^2 \text{ and}$$

$$E_2 I_2 = 4.64 \text{ Nm}^2 .$$

The end slopes are calculated with the FORTRAN program SLOPE. The program and sample output follow. In SLOPE the coordinates are y , z and l in place of x , y and d .

PRINT SLOPE

```

1000 $RESET FREE
1010 C  CALCULATE THE DEFLECTION AND END SLOPE OF A BEAM WITH STEP
1020 C  CHANGE IN THICKNESS
1030 C  SI UNITS
1040    DOUBLE PRECISION FORCE,E1I1,E2I2,A,B,C,D,E,F,G,H,I,J,K,L
1050    1      Z0,C5,C6,DZDY,L1,L2,ECC,DENOM
1060    FORCE=7000
1070 C  FOR THE COMPOSITE LAYER WITH A DOUBLER:
1080    E1I1=6.37406
1090    E2I2=4.63606
1100    ECC=0.25
1110    A=DSQRT(FORCE/E1I1)
1120    B=DSQRT(FORCE/E2I2)
1130    DO 1 M1=25,75,25
1140    L1=M1
1150    WRITE (6,200) L1
1160    200 FORMAT (/1X/" L1 IS "F4.1/5X" L2"8X" Z0"11X" DZDY")
1170    C=DSINH(A*L1)
1180    D=DSINH(B*L1)
1190    E=DCOSH(A*L1)
1200    F=DCOSH(B*L1)
1210    DO 2 M2=100,200,10
1220    L2=M2
1230    G=DSINH(B*L2)
1240    H=DCOSH(B*L2)
1250    DENOM=B*F-B*D*D/F
1260    I=(A*C-B*D*(E-1.0)*ECC/F)/DENOM
1270    J=(A*C-B*D*E/F)/DENOM
1280    K=(E-1.0)*ECC/F-D*I/F
1290    L=(E-D*J)/F
1300    Z0=-(I*G+K*H)/(J*G+L*H)
1310    C5=I+J*Z0
1320    C6=K+L*Z0
1330    DZDY=B*C5*H+B*C6*G
1340    WRITE (6,201) L2,Z0,DZDY
1350    201 FORMAT(4XF4.0,2X1PE12.5,2XE12.5)
1360    2  CONTINUE
1370    1  CONTINUE
1380    END

```

L1	IS	25.0	L2	Z0	DZDY
100.		-1.33659E-01	100.	-1.33659E-01	3.86394E-04
110.		-1.33794E-01	110.	-1.33794E-01	2.62094E-04
120.		-1.33856E-01	120.	-1.33856E-01	1.77740E-04
130.		-1.33885E-01	130.	-1.33885E-01	1.20522E-04
140.		-1.33898E-01	140.	-1.33898E-01	8.17198E-05
150.		-1.33904E-01	150.	-1.33904E-01	5.54087E-05
160.		-1.33907E-01	160.	-1.33907E-01	3.75686E-05
170.		-1.33908E-01	170.	-1.33908E-01	2.54724E-05
180.		-1.33909E-01	180.	-1.33909E-01	1.72709E-05
190.		-1.33909E-01	190.	-1.33909E-01	1.17100E-05
200.		-1.33909E-01	200.	-1.33909E-01	7.93963E-06
L1	IS	50.0	L2	Z0	DZDY
100.		-1.97752E-01	100.	-1.97752E-01	1.22834E-03
110.		-1.98254E-01	110.	-1.98254E-01	8.33907E-04
120.		-1.98485E-01	120.	-1.98485E-01	5.65739E-04
130.		-1.98591E-01	130.	-1.98591E-01	3.83687E-04
140.		-1.98640E-01	140.	-1.98640E-01	2.60180E-04
150.		-1.98663E-01	150.	-1.98663E-01	1.76417E-04
160.		-1.98673E-01	160.	-1.98673E-01	1.19618E-04
170.		-1.98678E-01	170.	-1.98678E-01	8.11044E-05
180.		-1.98680E-01	180.	-1.98680E-01	5.49908E-05
190.		-1.98681E-01	190.	-1.98681E-01	3.72850E-05
200.		-1.98682E-01	200.	-1.98682E-01	2.52800E-05
L1	IS	75.0	L2	Z0	DZDY
100.		-2.24631E-01	100.	-2.24631E-01	3.31881E-03
110.		-2.26192E-01	110.	-2.26192E-01	2.26518E-03
120.		-2.26917E-01	120.	-2.26917E-01	1.54054E-03
130.		-2.27251E-01	130.	-2.27251E-01	1.04599E-03
140.		-2.27405E-01	140.	-2.27405E-01	7.09665E-04
150.		-2.27476E-01	150.	-2.27476E-01	4.81312E-04
160.		-2.27509E-01	160.	-2.27509E-01	3.26384E-04
170.		-2.27524E-01	170.	-2.27524E-01	2.21309E-04
180.		-2.27531E-01	180.	-2.27531E-01	1.50057E-04
190.		-2.27534E-01	190.	-2.27534E-01	1.01743E-04
200.		-2.27535E-01	200.	-2.27535E-01	6.89842E-05

Appendix ii. METHOD OF MAKING SCARF JOINT SPECIMENS

The experimental specimens were made by bonding beveled laminate panels and cutting them into tensile coupons. The carbon/epoxy panels were of Hercules AS1/3501-6 with a $[0_2/\pm45/90/\pm45/0_2]_S$ stacking sequence. They were vacuum bag cured at 590 kPa (85 psi) and 175° C (350°F) for two hours.

The panels were beveled on a surface grinder while taped to a wedge-shaped block (Figures ii1-ii5). The wedge-shaped block, Figure ii1, holds the panel at the desired scarf angle. Two blocks, with angles of 33 milliradians and 52 milliradians were used. The blocks were made by surface grinding a steel plate about 200 mm x 125 mm x 20 mm (8 in x 5 in x 3/4 in) on one side to provide a flat surface. Milling the plate on the unground side formed the required angle. When beveling the panels the magnetic chuck of the surface grinder holds the plate with the milled side down and the panel taped to the top, Figures ii2 through ii4. A 110 milliradian jig was made for the larger angle scarf joints. The jig and wedges can also be used taped one on top of another for other scarf angles.

The laminate panels were held to the wedge-shaped blocks with double-faced cloth tape made by Permacel. The panel is first aligned with the edge of the plate and then pressed down against the tape by hand, with extra pressure along the edges of the panel. Careful pressure and acetone on the tape are necessary to remove the scarfed panels. The pieces required for five tensile specimens with 52

milliradian scarf angle can be ground in less than one hour.

For bonding, the scarfed pieces were pinned to a 36-ply laminate made of two layers of the same stacking sequence as the panels being bonded. This held them in position while permitting thermal expansion without loading the adhesive. First, one of the 'original laminate' pieces was fastened on the fixture with two 1/8 inch pins. Then, measuring a 0.20 mm (0.008 in) gap between the 'replacement piece' and the pinned panel with a feeler gauge, the 'replacement piece' was drilled and pinned in place. The remaining 'original laminate' was similarly positioned and pinned. The careful spacing between panels controls squeeze-out of the adhesive. The spacing must balance between too little squeeze-out causing a weak joint and too much squeeze-out lifting the replacement piece off the fixture and misaligning it.

After the panels were pinned in place they were taken apart and put together again with American Cyanamid 0.08 psf FM-300M film adhesive in place. For the thermal cure they were vacuum bagged and autoclave cured. The cure cycle was 60 minutes heatup to 175° C, 60 minutes at temperature and 280 kPa (40 psi).

The pre-cured doublers were held in place for bonding with TEMP-ER-TAPE. The panel was bagged without a caul plate so that the bag covered both sides and doublers on both sides could be bonded at once. The doublers were tapered by end milling them while the specimen was held to the 110 milliradian scarf joint jig.

The bonded scarf joint panels were cut into 25 mm wide tensile

specimens with a diamond saw. End tabs were unnecessary. Finally, the specimens were instrumented with strain gages. Micro-Measurements EA-06-125AC-350 strain gages were applied following the manufacturer's recommended procedure.

The specimens were statically loaded to failure in an Instron load frame. Strain gage data were recorded with a Datran II Model 321 strain indicator coupled to a Franklin Electronics data printer.

ORIGINAL PAGE IS
OF POOR QUALITY

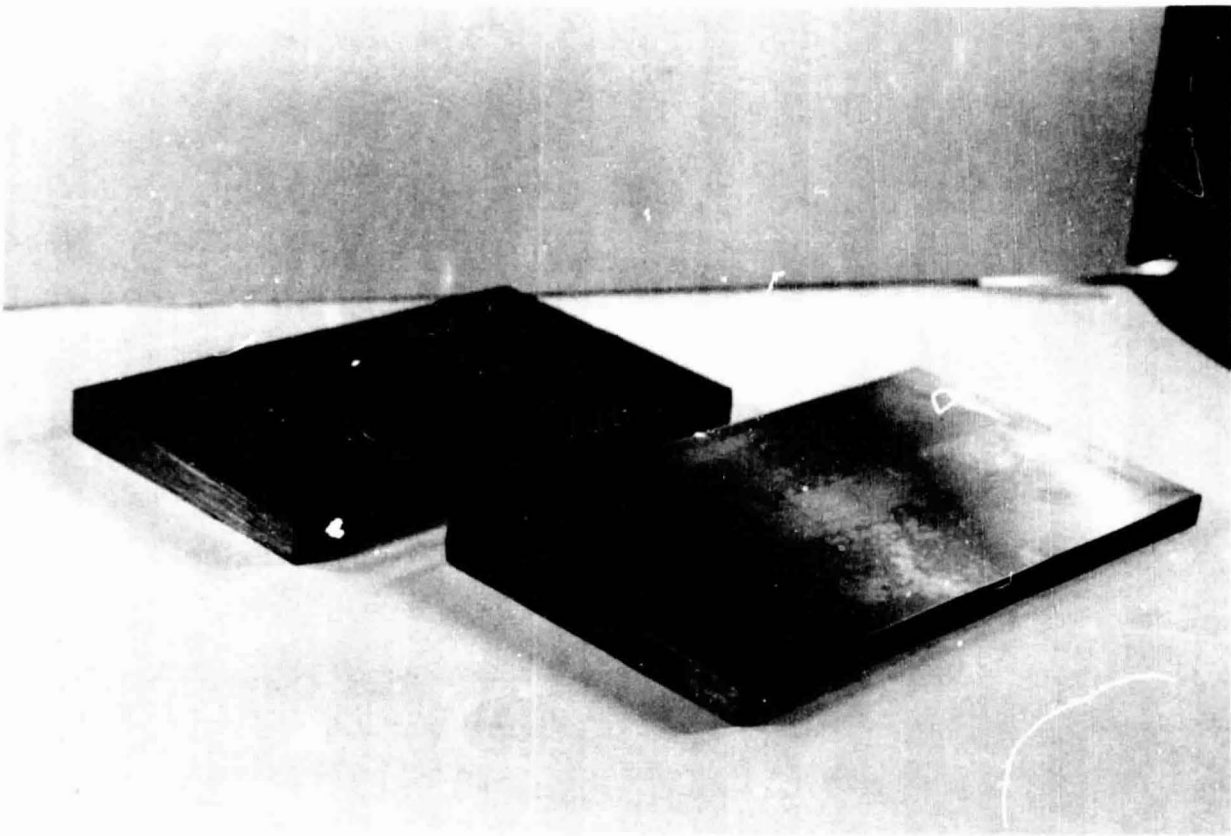


Figure iii. Wedge-shaped steel blocks.

ORIGINAL PAGE IS
OF POOR QUALITY

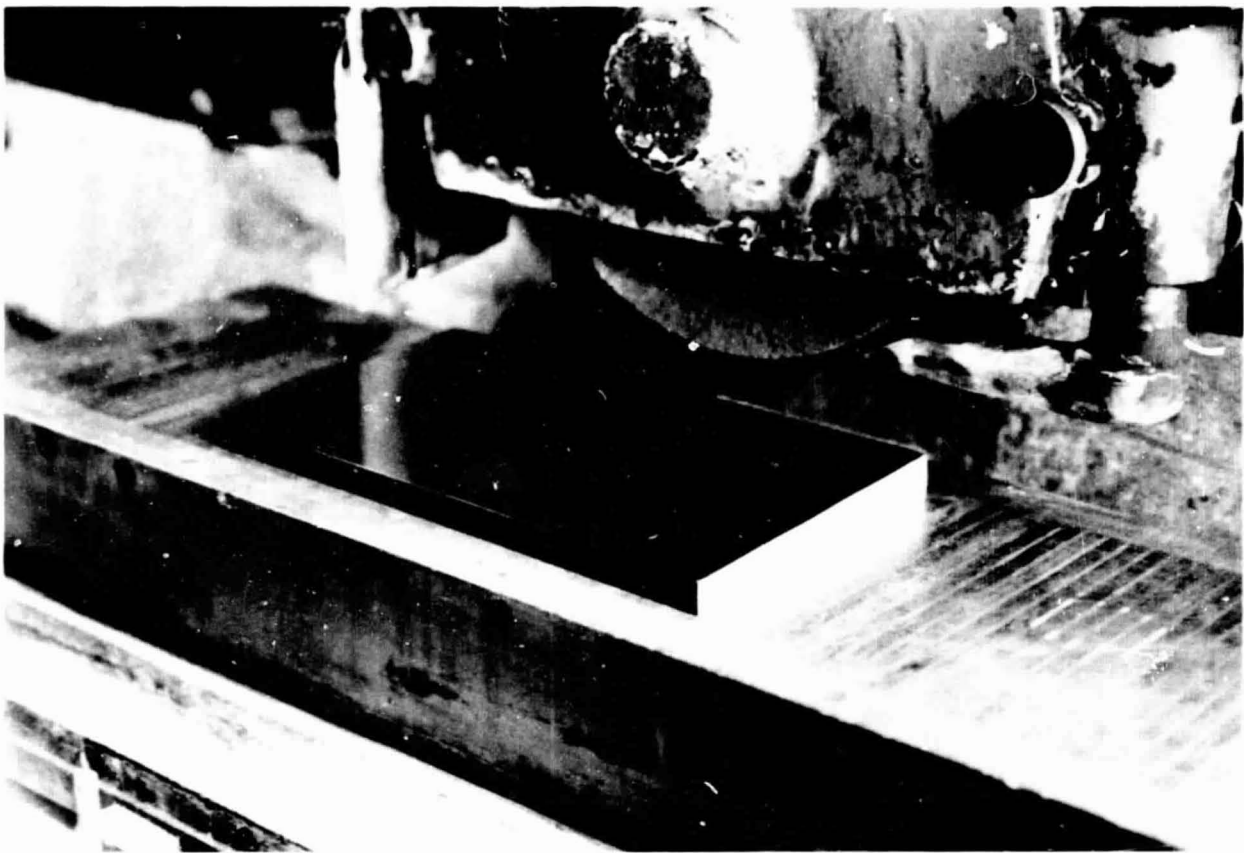


Figure ii2. Wedge-shaped block mounted on the magnetic chuck of a surface grinder.

ORIGINAL PAGE IS
OF POOR
QUALITY

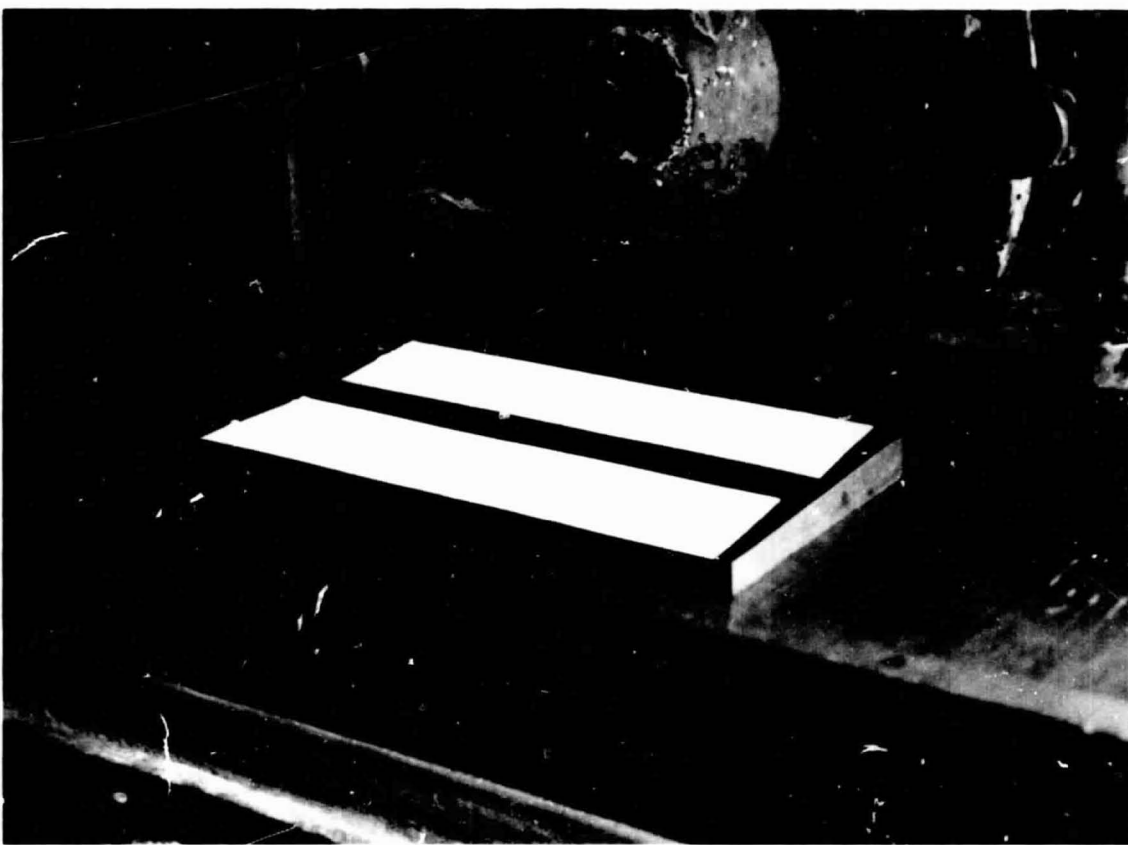


Figure ii3. Double faced adhesive tape applied to the wedge-shaped block.

ORIGINAL PAGE IS
OF POOR QUALITY

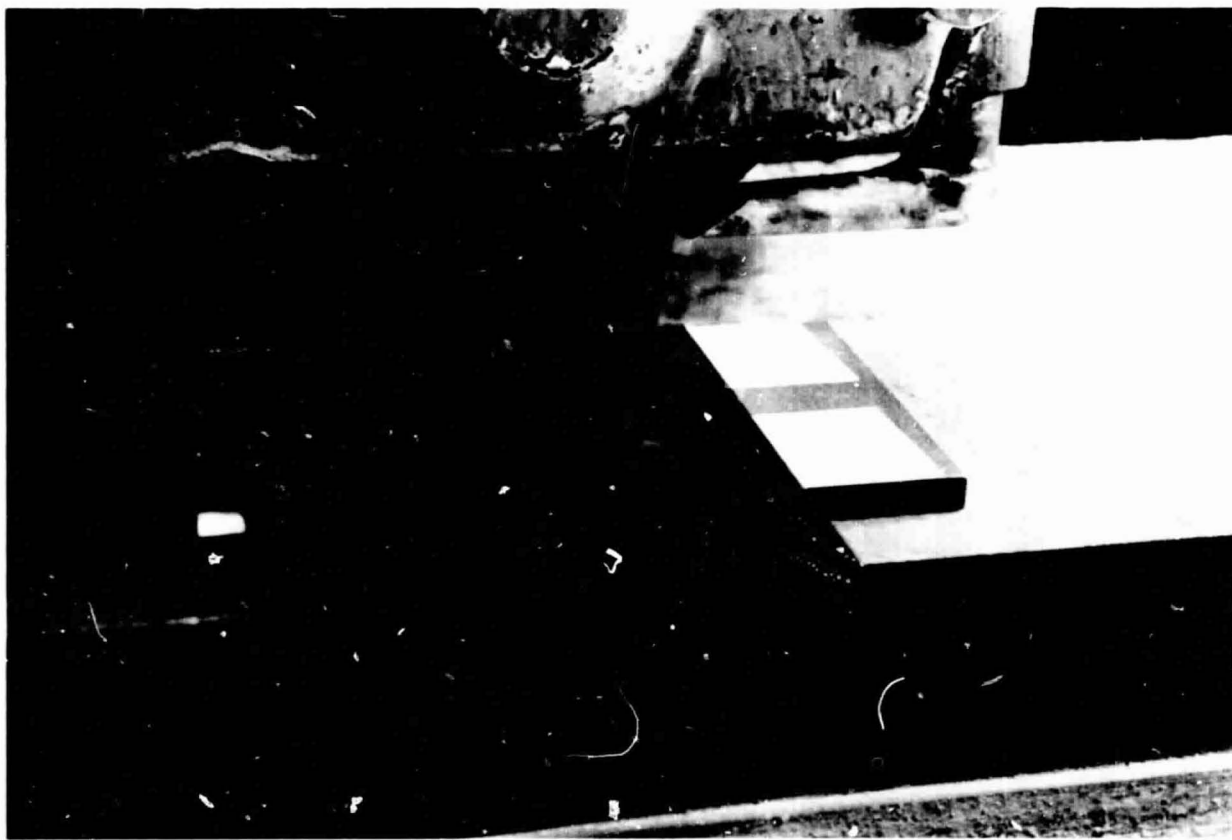


Figure ii4. Laminate stuck squarely to the adhesive tape ready for grinding.

ORIGINAL PAGE IS
OF POOR
QUALITY

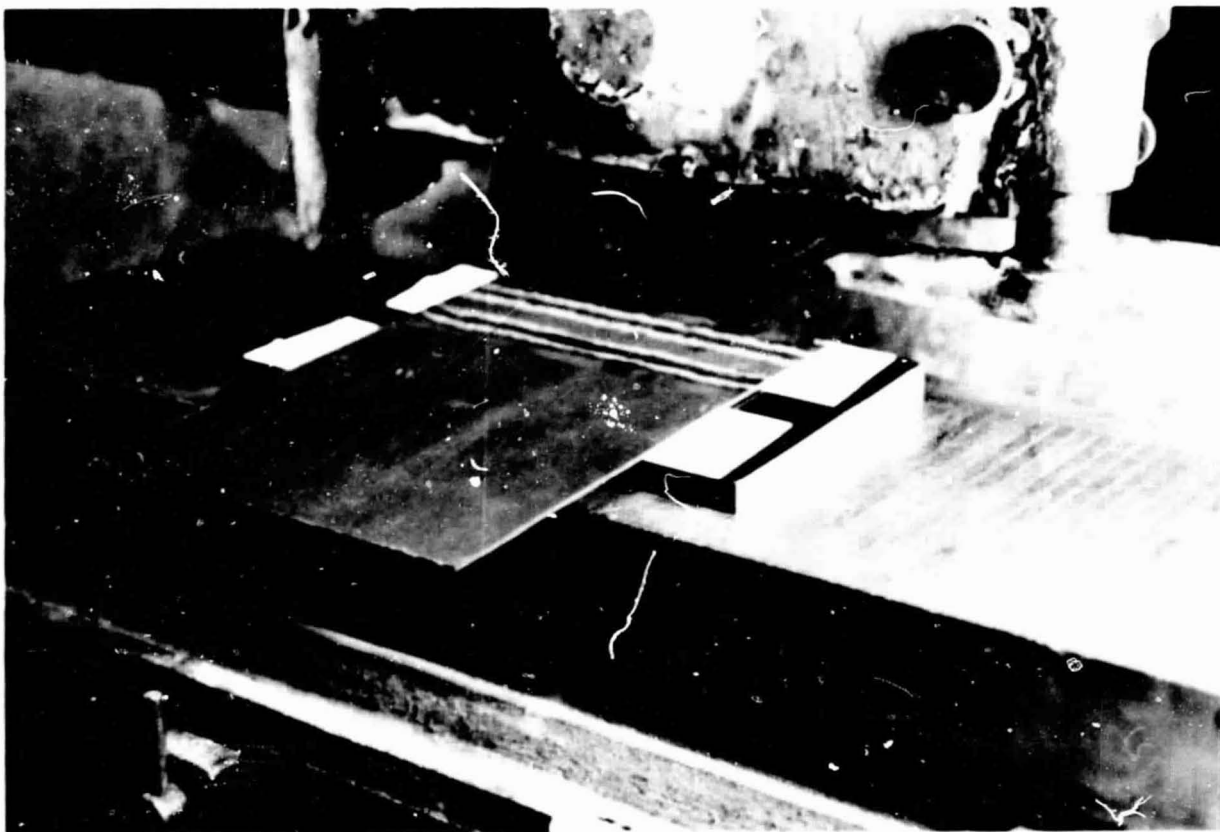


Figure ii5. Ground scarf adherend.

Appendix iii. EXPERIMENTAL DATA

This appendix compiles five sets of scarf joint experimental strength data. These data are for:

- o the 18 ply laminate from which all scarf joints in this study were made,
- o plain (without doublers) scarf joints with five scarf angles,
- o scarf joints which were ground with a hand-held rotary bur,
- o joints with round-tipped adherends and
- o joints with slightly raised replacement pieces.

One datum for the plain scarf joints (3-121-3) was discarded in calculating average values because it falls outside expected bounds based on the other data values. Discarding this datum is supported by Chauvenet's criterion, a statistical basis for testing outlying data points (Ref. J. P. Holman, Experimental Methods for Engineers, Third Edition, McGraw-Hill Book Company, 1973).

The only data not included in this Appendix are in the section on scarf joints with doublers.

ORIGINAL PAGE IS
OF POOR QUALITY

STRENGTH OF ADHEREND LAMINATE

Specimen Number	Width (mm)	Ultimate Load (kN)	Ultimate In-Plane Force Resultant (kN/m)
1304-3-1	19.9	40.9	2060
1304-3-2	24.7	49.0*	--
1304-3-3	20.3	44.3	2180
1304-3-4	21.5	49.3	2290
1304-3-5	22.5	49.0*	--
1304-3-6	18.9	44.8	2370
1304-3-7	21.0	46.7	2220
1304-3-8	19.7	43.7	2220
1304-3-9	18.6	41.3	2220
1304-3-10	20.0	42.0	2100
MEAN			2210
STANDARD DEVIATION			98.4

* Exceeded testing machine capacity because the specimen
was cut too wide.

ORIGINAL PAGE IS
OF POOR QUALITY

STRENGTH OF SCARF JOINTS WITH DIFFERENT SCARF ANGLES

Specimen Number	Scarf Angle (milli- radians)	Width (mm)	Ultimate Load (kN)	Ultimate In-Plane Force Resultant (kN/m) (lbf/in)
3-121-1	19	25.4	33.6	1320 7530
3-121-2	19	25.4	34.3	1350 7700
3-121-3	19	25.5	25.5	1000 5710
3-121-4	19	25.5	31.9	1250 7130
5-11-1	19	25.4	34.4	1350 7700
5-11-2	19	25.4	34.1	1340 7640
5-11-3	19	25.5	38.2	1500 8560
3-34-1	33	24.2	31.9	1320 7530
3-34-2	33	24.2	35.3	1460 8330
3-34-3	33	24.2	34.1	1410 8040
3-34-4	33	24.1	33.6	1400 7990
3-14-2	52	26.0	26.3	1010 5760
3-14-3	52	25.5	25.5	1000 5710
3-14-4	52	25.7	27.2	1060 6050
3-14-5	52	25.8	24.8	961 5480
3-14-6	52	25.8	24.0	930 5310
JS-1	110	25.2	15.4	611 3490
JS-2	110	25.0	15.5	622 3550
JS-3	110	25.1	15.6	622 3550
JS-4	110	25.2	15.7	623 3550
1-21-1	110	25.6	17.2	672 3830
1-21-2	110	25.1	16.9	673 3840
1-21-3	110	25.5	19.0	745 4250
1-21-4	110	25.6	18.1	707 4030
1-21-5	110	25.3	18.3	723 4130
4-96-1	110	26.6	14.7	553 3160
4-96-2	110	25.5	16.3	639 3650
4-96-3	110	27.0	16.9	626 3570
4-96-4	110	26.2	16.1	614 3500
3-136-1	160	25.3	11.8	466 2660
3-136-2	160	25.4	13.3	524 2990
3-136-3	160	25.4	13.4	528 3010
3-136-4	160	25.6	13.3	520 2970

ORIGINAL PAGE IS
OF POOR QUALITY

STRENGTH OF HAND GROUND 52 MILLIRADIAN SCARF JOINTS

Specimen Number	Width (mm)	Ultimate Load (kN)	Ultimate In-Plane Force Resultant (kN/m) (1bf/in)
5-35-1	25.4	21.3	837 4780
5-35-2	25.4	20.4	803 4580
5-35-3	25.4	19.4	764 4360
5-35-4	25.4	19.9	784 4470
5-35-5	25.8	21.1	818 4670

STRENGTH OF 110 MILLIRADIAN SCARF JOINTS
WITH ROUND-TIPPED ADHERENDS

Specimen Number	Width (mm)	Ultimate Load (kN)	Ultimate In-Plane Force Resultant (kN/m) (1bf/in)
1-21-6	25.0	12.0	480 2740
1-21-7	25.1	11.6	463 2640
1-21-8	25.6	10.7	418 2390
1-21-9	25.4	10.8	425 2430
1-21-10	24.9	9.5	381 2180

STRENGTH OF SCARF JOINTS WITH RAISED REPLACEMENT PIECES

Specimen Number	Scarf Angle (milli-radians)	Width (mm)	Ultimate Load (kN)	Ultimate In-Plane Force Resultant (kN/m) (1bf/in)
5-24-1	19	25.4	43.1	1700 9680
5-24-2	19	25.3	46.4	1830 10500
5-24-3	19	25.4	38.5	1520 8650
5-24-4	19	25.5	37.0	1450 8280
5-35-11	52	25.4	28.9	1140 6490
5-35-12	52	25.4	31.9	1260 7170
5-35-13	52	25.4	31.9	1260 7170
5-35-14	52	25.4	30.7	1210 6900
5-35-15	52	26.2	30.7	1170 6690

ORIGINAL PAGE IS
OF POOR QUALITY

Appendix iv. FORTRAN PROGRAMS SCARF3 AND SCARF4

These computer programs calculate the adhesive shear stress distributions. Output data for scarf angles from 10 milliradians to 160 milliradians and tip bluntness values from zero to $x_{tip} = 0.16$ are also included.

121

SCARF3

ORIGINAL PAGE IS
OF POOR QUALITY

```

C THIS PROGRAM CALCULATES THE SHEAR STRESSES IN THE ADHESIVE OF A
C STAFF JOINT. IT USES THE WEINHOLD, FRANKEL-JUS SERIES, AND TAYLOR SERIES
C TO SOLVE FOR ADHEREND LOADS AND ADHESIVE STRESSES.
C THE PROGRAM ALLOWS FOR VARIATION IN THE LOAD-DIRECTION MODULUS OF
C ELASTICITY IN THE ADHERENDS TO MODEL CUFFSITE LAMINATES. IT ALSO
C ACCOUNTS FOR ADHEREND TIP BLUNTNES.
C

C I IS THE REGION NUMBER STARTING AT THE LEFT
C XEARIF(I) IS THE DIMENSIONLESS COORDINATE OF THE INTERFACE BETWEEN REGIONS
C I AND (I+1). IN THIS COORDINATE SYSTEM THE JOINT IS ONE UNIT LONG.
C A1(I,N) J
C A2(I,N) J ARE THE N TH EXPANSION COEFFICIENTS OF THE I TH REGION
C AF1(I,N) J
C XEAI(I) IS THE COORDINATE OF THE EXPANSION POINT IN EACH REGION.
C EXU(I) IS THE MODULUS OF ELASTICITY OF THE UPPER ADHEREND IN GIGA PASCALS
C EXL IS THE MODULUS OF ELASTICITY OF THE LOWER ADHEREND
C
C

C COMMON XEARIF(0:5),EXU(5),EXL,XEAI(5),
C 1 NUXZU(5),NUZXL(5),NUZL,NUZL1,NUZL2,NUZL3,NUZL4,EXLAP,TLAM,NUXZU,FNUXZU,
C 2 C1,AU,A1,NIEFMS,
C 3 CC4KE(5),C14KE(5),C24KE(5),C34KE(5),
C 4 DS,GF,UF,F,S,MP,FFF,EFSIL,SL,SCF,SCFF,S1,S1F,S1PP,
C 5 EU,EL,FEAR,F,FEAT,FFAFFF,E,TALF,KAY,D,
C 6 CFF,TAL12,TAL22
C
C REAL NUXZU,FNUXZG,NUZL1,NUZXL,NUZL3,NUZL4,NUXZU,FNUXZU,FNUXZU,FNUXZU,FNUXZU,
C DOUBLE PRECISION C1(0:20),AU(5,0:20),A1(5,0:20),A1(5,0:20),
C 1 C(0:20),F(0:20),X(5,5),B(5),WAREA(120)
C DIMENSION U1(0:20),C2(0:20),C3(0:20),C4(0:20),G12(0:20),G123(0:20)
C CALL ASSIGN(5,"SYI1.DAT")
C CALL ASSIGN(6,"SYI1U.DAT")
C
C
C READ TS, #1 ALPH, XEARIF, EXU, NUXZU, NUZXL, NUXZL, NUZL, NUXZL
C WRITE (6,*) " ALPH = ", ALPH
C WRITE (6,*) " XEARIF = ", XEARIF(5), XEARIF(4), XEARIF(3), XEARIF(2), XEARIF(1),
C 1 XEARIF(0)
C WRITE (6,*) " EXU ", EXU(1), EXU(2), EXU(3), EXU(4), EXU(5)
C WRITE (6,*) " EXL ", EXL
C WRITE (6,*) " NUZL1 ", NUZL1
C WRITE (6,*) " NUZL2 ", NUZL2
C WRITE (6,*) " NUZL3 ", NUZL3, TALF, TAL22, NUZL, NUZL
C
C
C PI=3.141592654
C TADHES=0.2 ADHESIVE THICKNESS IN MILLIMETERS
C EACHES=3.45 ADHESIVE YOUNG'S MODULUS IN GPa
C GADHES=1.33 ADHESIVE SHEAR MODULUS IN GPa
C TLAM=2.5 ADHEREND THICKNESS IN MILLIMETERS
C EXLAP=77.8 ADHESIVE MODULUS IN GPa
C NULAM=0.391 ADHESIVE POISSON'S RATIO
C
C
C CALCULATE SHEAR STRESSES AS A FUNCTION OF POSITION IN THE JOINT:
C
C *****

C
C
C ALPH,A=ALPH/A/1000.0
C TALF=TAU(ALPH)
C COSALF=CCS(ALPH)
C SINALF=SIN(ALPH)
C D=(TLAM-TADHES)/COSALF
C KAY=CCSALF*(1.0+TALF**2)**2*GADHES*EACHES
C 1 /(TADHES*(EACHES+GADHES*TALF**2))
C EFSIL=SCFT(TALF/(KAY*D))
C

```

```

C   CALCULATE THE COEFFICIENTS FOR REGION ONE. THIS REGION IS THE TIP WHERE
C   THE UPPER ADHEREND TAPERS TO ZERO THICKNESS. THE ADHEREND LOAD IS
C   CALCULATED IN THE FORM OF A FERBERIUS SERIES EXPANSION ABOUT XBAR=0. THE
C   COEFFICIENTS CAN BE CHOSEN TO MODEL THE PERIODICALLY SHARP, STIFF ADHEREND
C   TIP OR THE ADHESIVE WHICH FILLS IN FOR A BROKEN ADHEREND TIP.
C
C   NTIPPS=15
C   FIRST CALCULATE THE C'S AND R'S:
C   Q(0)=0.0
C   Q(1)=KAY*L*(1.0-NU2XL(1)*NU2XL(1))/TALF/EXU(1)
C   Q(2)=-KAY*C*(1.0-NU2XL*NL2XL)/TALF/EXL
C   R(0)=(KAY*L/TALF)*(C*NU2XL*(NU2XL(1)-NL2XL)*TALF/(EXLM+TLAM)
C   1   -(1.0-NU2XL*NU2XL)/EXL)
C   R(1)=Q(2)
C   R(2)=Q(2)
C   DO 10 N=3,NTIPPS
C   Q(N)=Q(2)
C   R(N)=Q(2)
C   CONTINUE
C
C   CALCULATE THE C-ONE'S.
C   C1(0)=0.0
C   C1(1)=1.0
C   DO 11 N=2,NTIPPS
C   C1(N)=0.0
C   DO 12 K=0,N-1
C   C1(N)=C1(N)+C(N-K)*C1(K)
C   12   CONTINUE
C   C1(N)=1.0/(N*(N-1))*C1(N)
C   11   CONTINUE
C
C   CALCULATE THE COEFFICIENTS OF THE PARABOLIC EQUATION, APT(1,N).
C   APT(1,0)=0.0
C   DO 13 N=1,NTIPPS
C   SUM=0.0
C   DO 14 K=1,N
C   SUM=SUM+G(K)*APT(1,N-K)
C   14   CONTINUE
C   APT(1,N)=(K(N-1)-SUM)/(N*(N+1))
C   13   CONTINUE
C
C   CALCULATE THE COEFFICIENTS FOR REGION TWO. THIS REGION BEGINS AT THE END
C   OF AN ADHEREND WITH A BROKEN TIP AND EXTENDS A SHORT DISTANCE TO THE RIGHT.
C   THE ADHEREND LOAD IS CALCULATED IN THE FORM OF A TAYLOR SERIES EXPANSION
C   ABOUT THE PLANE TIP OF THE ADHEREND.
C
C   FIRST CALCULATE THE C'S AND R'S.
C   NT2=13
C   XBAFI(2)=(XEARIF(1)+XEARIF(2))/2.0
C   T1=(-KAY*L/TALF)*(1.0-NU2XL(2)*NU2XL(2))/EXU(2)/(XEARIF(2))
C   T2=(-KAY*L/TALF)*(1.0-NU2XL*NU2XL)/EXL/(1.0-XEARIF(2))
C   DO 20 N=0,NT2
C   Q(N)=(T1+T2)
C   20   CONTINUE
C   T1=-T1/XEARIF(2)
C   T2=T2/(1.0-XEARIF(2))
C   CONTINUE
C   R(0)=(KAY*C/TALF)*(C*NU2XL*(NL2XL(2)+NL2XL)*TALF/(EXLM+TLAM)
C   1   -(1.0-NU2XL*NL2XL)/EXL/(1.0-XEARIF(2)))
C   R(1)=(-KAY*C/TALF)*(1.0-NU2XL*NL2XL)/EXL/(1.0-XEARIF(2))**2
C   DO 23 N=2,NT2
C   R(N)=R(N-1)/(1.0-XEARIF(2))
C   23   CONTINUE
C
C   CHECK THE REGION 2 C'S AND R'S:
C   DELTA=(XBAFI(2)-XBAFI(1))/10.0
C   DO 26 N=0,10
C   GAFFCX=G(0)
C   RAPPCX=R(0)
C   XBAF=XBAFI(1)+N*X*DELTA
C   DO 27 N=1,NT2
C   GAFFCX=GAFFCX+G(N)*(XBAF-XEARIF(2))**N
C   RAPPCX=RAPPCX+R(N)*(XBAF-XEARIF(2))**N
C   27   CONTINUE
C   GEXACT=(-KAY*L/TALF)*((1.0-NU2XL(2)*NU2XL(2))/EXU(2)*XBAF
C   1   +(1.0-NU2XL*NL2XL)/EXL/(1.0-XEARIF(2)))
C   PEXACT=(KAY*L/TALF)*(C*NU2XL*(NL2XL(2)+NL2XL)*TALF/(EXLM+TLAM)
C   1   -(1.0-NU2XL*NL2XL)/EXL/(1.0-XEARIF(2)))
C   WHILE (.6,.8) "R2 QDF CHK1",XEARIF,GEXACT,GAFFCX,PEXACT,PAPPX
C26   CONTINUE

```

```

C CALCULATE THE EXPANSION COEFFICIENTS WITH A(0) AND A(1) FACTORED OUT.
A0(2,0)=1.0
A0(2,1)=0.0
A1(2,0)=0.0
A1(2,1)=1.0
DO 21 K=2,N12
SUM0=0.0
SUM1=0.0
LG 22 K=0,N-2
SUM0=SUM0+G(K)*A0(2,K-K-2)
SUM1=SUM1+G(K)*A1(2,K-K-2)
22 CONTINUE
A0(2,K)=-SUM0/(K*(K-1))
A1(2,K)=-SUM1/(K*(K-1))
21 CONTINUE
C
C CALCULATE THE COEFFICIENTS OF THE PARTICULAR SOLUTION:
AFT(2,0)=0.0
AFT(2,1)=0.0
DO 24 K=2,N12
SUM=0.0
DC 25 K=0,N-2
SUM=SUM+G(K)*AFT(2,K-K-2)
25 CONTINUE
AFT(2,K)=(P(K-2)-SUM)/(K*(K-1))
24 CONTINUE
C
C CALCULATE THE TAILOR SERIES COEFFICIENTS FOR REGION THREE.
C
C FIRST CALCULATE THE C'S AND R'S.
N13=20
X=AY1(3)=(XEAR1(3)+XPAH1F(2))/2.0
T1=(-RAY*C/TALF)*(1.0+KUXZL(3)*KUZXL(3))/EXL(3)/XEAR1(3)
T2=(-RAY*L/TALF)*(1.0+KUXZL*KUZAL)/EXL/(1.0-XEAR1(3))
DC 30 K=0,N13
L(N)=T1+T2
T1=-T1/XEAR1(3)
T2=T2/(1.0-XPAH1(3))
30 CONTINUE
R(0)=(RAY*L/TALF)*(C*ULLAM*(KUZXL(3)+KLZXL)*TALF/(EXLAM*TALM)
      -(1.0+KUXZL*KUZXL)/EXL/(1.0-XEAR1(3)))
R(1)=(RAY*C/TALF)*(1.0+KUXZL*KUZXL)/EXL/(1.0-XEAR1(3))**2
DC 33 K=2,N13
P(N)=R(N-1)/(1.0-XEAR1(3))
33 CONTINUE
C
C CALCULATE THE EXPANSION COEFFICIENTS WITH A(0) AND A(1) FACTORED OUT.
A0(3,0)=1.0
A0(3,1)=0.0
A1(3,0)=0.0
A1(3,1)=1.0
DO 31 K=2,N13
SUM0=0.0
SUM1=0.0
LG 32 K=0,N-2
SUM0=SUM0+G(K)*A0(3,K-K-2)
SUM1=SUM1+G(K)*A1(3,K-K-2)
32 CONTINUE
A0(3,K)=-SUM0/(K*(K-1))
A1(3,K)=-SUM1/(K*(K-1))
31 CONTINUE
C
C CALCULATE THE COEFFICIENTS OF THE PARTICULAR SOLUTION:
AFT(3,0)=0.0
AFT(3,1)=0.0
DO 34 K=2,N13
SUM=0.0
LG 35 K=0,N-2
SUM=SUM+G(K)*AFT(3,K-K-2)
35 CONTINUE
AFT(3,K)=(P(K-2)-SUM)/(K*(K-1))
34 CONTINUE
C

```

```

C CALCULATE THE TAYLOR SERIES SOLUTION COEFFICIENTS FOR REGION FOUR.
C
C CALCULATE THE C'S.
XBAF1(4)=(XBAF1F(3)+XBAF1F(4))/2.0
EXU(4)=(EXU(3)+EXU(5))/2.0
EXUF=(EXU(5)-EXU(3))/(XBAF1F(4)-XBAF1F(3))
Q1(C)=1.0-NUAZUL(4)*KL2XL(4)
G1(1)=NUAZU(4)*NU2XLF-NUUXUF*NUZXU(4)
Q1(2)=2.0*NUAZU(4)*KL2XLF
DC 40 N=3,20
G1(N)=0.0
40 CONTINUE
Q2(C)=1.0/EXU(4)
G3(0)=1.0/XBAF1(4)
G4(0)=(1.0-NUAZL*NU2XL)/EXL/(1.0-XBAF1(4))
DC 41 N=1,20
G2(N)=(-K*EXL/F/EXU(N))*G2(N-1)
Q3(N)=(-K/XBAF1(4))*G3(N-1)
G4(N)=(-K/(1.0-XBAF1(4)))*G4(N-1)
41 CONTINUE
C CALCULATE THE DERIVATIVES OF THE PRODUCT TERMS.
CALL FASCAL (C12,C11,C2)
CALL FASCAL(C12,C12,C3)
C
C CALCULATE THE VALUES OF C
FACT=1.0
G(0)=(-KAY*D/TALF)*(C123(0)+G4(0))
DC 45 N=1,20
FACT=FACT/N
G(N)=(-KAY*D/TALF)*FACT*(C123(N)+G4(N))
45 CONTINUE
C
C CHECK THE FOURIER COEFFICIENTS, G.
D DELTA=(XBAF1F(4)-XBAF1F(3))/10.0
D DC 46 N=0,10
D XBAF1=XBAF1F(3)+N*DELTA
D GAFCX=G(0)
D DC 47 N=1,20
D GAFCX=GAFCX+G(NC)*(XBAF1-XBAF1F(4))**NC
D47 CONTINUE
C EXU(4)+EXUF*(XBAF1-XBAF1F(4))
D GNL1=NUAZU(4)*NUAZUF*(XBAF1-XBAF1F(4))
D GNL2=NUZXU(4)*NUZXLF*(XBAF1-XBAF1F(4))
D GEXACI=(-KAY*D/TALF)*((1.0-GNL1*GNL2)/XBAF1F(4))
D I +(1.0-NUAZL*KL2XL)/EXL/(1.0-XBAF1F(4))
D WRITE (6,*) " REGION 4 C CHECK: ",XBAF1,GEXACI,GAFCX
D46 CONTINUE
C
C CALCULATE THE R'S.
R(0)=(-KAY*D/TALF)*(C*NULAFL*(NUZXU(4)-KL2XL)*TALF/(EXLAM*TALM)
1 -(1.0-NUAZL*KL2XL)/EXL/(1.0-XBAF1F(4)))
R(1)=(-KAY*D/TALF)*(C*NULAFL*NUZXUF*TALF/(EXLAM*TALM)
1 -(1.0-NUAZL*NUZXU(4))/EXL/(1.0-XBAF1F(4))**2)
R(2)=(-KAY*D/TALF)*(1.0-NUAZL*NUZXU(4))/EXL/(1.0-XBAF1F(4))**3
DC 48 N=3,20
R(N)=R(N-1)/(1.0-XBAF1F(4))
48 CONTINUE

```

ORIGINAL PAGE IS
OF POOR QUALITY

```

C   CALCULATE THE EXPANSION COEFFICIENTS WITH A(0) AND A(1) FACTORED OUT.
A0(4,0)=1.0
A0(4,1)=0.0
A1(4,0)=0.0
A1(4,1)=1.0
DO 49 N=2,20
SUMC=0.0
SUM1=0.0
DC 30 N=0,N=2
SUM0=SUM0+G(N)*A0(4,N-F-2)
SUM1=SUM1+G(N)*A1(4,N-F-2)
50  CONTINUE
AN(4,N)=SUM0/(N*(N-1))
A1(4,N)=SUM1/(N*(N-1))
49  CONTINUE
C
C   CALCULATE THE COEFFICIENTS OF THE PARTICULAR SOLUTION:
A0(4,0)=0.0
A0(4,1)=0.0
DO 51 N=2,20
SUM=0.0
DC 52 N=0,N=2
SUM=SUM+G(N)*A0(4,N-F-2)
52  CONTINUE
A0(4,N)=(F(N-2)-SUM)/(N*(N-1))
51  CONTINUE
C
C   CALCULATE THE COEFFICIENTS FOR THE SOLUTIONS FOR REGION FIVE.
C
C   CALCULATE THE POLYNOMIAL COEFFICIENTS (C'S) FROM THE TAYLOR'S SERIES
C   EXPANSION OF THE NUMERATOR OF THE S-ZERO INTEGRALS.
I=5
XEAR1(I)=(XEAR1(I)+XEAR1(I-1))/2.0
CNU=(1.0-NLXZU(5)*NLZU(5))*(1.0-XEAR1(I))/EXL(5)
1      +(1.0-NLXZL*NLZU(5))*XEAR1(I)/EXL
CNLXPF=(1.0-NLXZU(5)*NLZU(5))/EXL(5)+(1.0-NLXZL*NLZU(5))/EXL
FES=RT(CNU*1)
FF=1.5/SQRT(CNU*1)*NLXPF
FFF=0.25/(CNLXPF*SQRT(CNLXPF))+CNLXPF*0.2
FFFF=3.0/(8.0*CNLXPF*2*SQRT(CNLXPF))*CNLXPF*0.3
AC=FF
A1=FF
A2=FF/2.0
A3=FF/6.0
C1=AC-A1-A2=AC-XEAR1(I)+A2*AC*2*XEAR1(I)**2-A3*AC*3*XEAR1(I)**3
C1=AC-A1-A2=2.0*AC*2*XEAR1(I)**2+3.0*AC*3*XEAR1(I)**3
C2=AC-A2=3.0*AC*3*XEAR1(I)
C3=AC-A3=AC

C
C   CHECK VALIDITY OF FOURIER SERIES APPROXIMATION TO THE NUMERATOR OF S0(I).
C   SELECT VALUES OF XEAR AND CALCULATE EXACT AND APPROXIMATED VALUES.
I=5
DO 30 N=0,10
XEAR=XEAR1(I)+0.1*N*(XEAR1(I)-XEAR1(I-1))
30  AFFF=C1+AC(I)*C1*F(I)*XEAR+C2*AC(I)*XEAR**2+C3*AC(I)*XEAR**3
EXACT=SQRT((1.0-NLXZL*NLZU(5))*(1.0-XEAR)/EXL(5))
1      +(1.0-NLXZL*NLZU(5))/EXL*XEAR
30  WRITE (6,*) "N=I", I, XEAR, EXACT, EXACT, AFFF
CONTINUE

```

C NEW CALCULATE THE SOLUTION COEFFICIENTS FROM THE BOUNDARY CONDITIONS:

C FEAR=0 AT XEAR=0
C FBAR(LEFT HAND SIDE)=FEAR(RHS) AND
C FEARF(LHS)=FBAF(RHS) AT EACH REGION INTERFACE
C FEAR=0.5 AT XEAR=0.5

C

DO 70 h=1,9

b(h)=0.0

DO 70 h=1,9

A(h,h1)=0.0

70

CONTINUE

DO 71 h=0,NTERMS

A(1,1)=A(1,1)+C1(h)*XBARIF(1)**h

A(1,2)=A(1,2)-A0(2,h)*(XEARIF(1)-XEAR1(2))**h

A(1,3)=A(1,3)-A1(2,h)*(XEARIF(1)-XEAR1(2))**h

B(1)=B(1)-APT(1,h)*XEARIF(1)**(h+1)+FI(2,h)*(XBARIF(1)-XBAR1(2))**h

A(2,1)=A(2,1)+C1(h)*XEARIF(1)**(h-1)

A(2,2)=A(2,2)-A0(2,h)*(XBARIF(1)-XBAR1(2))**(h-1)

A(2,3)=A(2,3)-A1(2,h)*(XBARIF(1)-XBAR1(2))**(h-1)

B(2)=B(2)-(h+1)*APT(1,h)*XBARIF(1)**h

1 +h*APT(2,h)*(XEARIF(1)-XEAR1(2))**(h-1)

A(3,2)=A(3,2)+A0(2,h)*(XEARIF(2)-XEAR1(2))**h

A(3,3)=A(3,3)+A1(2,h)*(XEARIF(2)-XEAR1(2))**h

A(3,4)=A(3,4)-A0(3,h)*(XEARIF(2)-XEAR1(3))**h

A(3,5)=A(3,5)-A1(3,h)*(XEARIF(2)-XEAR1(3))**h

B(3)=B(3)-APT(2,h)*(XEARIF(2)-XEAR1(2))**h

1 +APT(3,h)*(XEARIF(2)-XEAR1(3))**h

A(4,2)=A(4,2)+h*A0(2,h)*(XEARIF(2)-XEAR1(2))**h

A(4,3)=A(4,3)+h*A1(2,h)*(XEARIF(2)-XEAR1(2))**h

A(4,4)=A(4,4)-h*A0(3,h)*(XEARIF(2)-XEAR1(3))**h

A(4,5)=A(4,5)-h*A1(3,h)*(XEARIF(2)-XEAR1(3))**h

B(4)=B(4)-h*APT(2,h)*(XEARIF(2)-XEAR1(2))**h

1 +h*APT(3,h)*(XEARIF(2)-XEAR1(3))**h

A(5,4)=A(5,4)+A0(3,h)*(XEARIF(3)-XEAR1(3))**h

A(5,5)=A(5,5)+A1(3,h)*(XEARIF(3)-XEAR1(3))**h

A(5,6)=A(5,6)-A0(4,h)*(XEARIF(3)-XEAR1(4))**h

A(5,7)=A(5,7)-A1(4,h)*(XEARIF(3)-XEAR1(4))**h

B(5)=B(5)-APT(3,h)*(XEARIF(3)-XEAR1(2))**h

1 +APT(4,h)*(XEARIF(3)-XEAR1(4))**h

A(6,4)=A(6,4)+h*A0(3,h)*(XEARIF(3)-XEAR1(3))**h

A(6,5)=A(6,5)+h*A1(3,h)*(XEARIF(3)-XEAR1(3))**h

A(6,6)=A(6,6)-h*A0(4,h)*(XEARIF(3)-XEAR1(4))**h

A(6,7)=A(6,7)-h*A1(4,h)*(XEARIF(3)-XEAR1(4))**h

B(6)=B(6)-h*APT(3,h)*(XEARIF(3)-XEAR1(2))**h

1 +h*APT(4,h)*(XEARIF(3)-XEAR1(4))**h

A(7,6)=A(7,6)+A0(4,h)*(XEARIF(4)-XEAR1(4))**h

A(7,7)=A(7,7)+A1(4,h)*(XEARIF(4)-XEAR1(4))**h

B(7)=B(7)-APT(4,h)*(XEARIF(4)-XEAR1(3))**h

A(6,6)=A(6,6)+h*A0(4,h)*(XEARIF(4)-XEAR1(4))**h

A(6,7)=A(6,7)+h*A1(4,h)*(XEARIF(4)-XEAR1(4))**h

B(6)=B(6)-h*APT(4,h)*(XEARIF(4)-XEAR1(3))**h

71

CONTINUE

CALL ESS(5,XEARIF(4))

A(7,6)=EXF(+SC/EFSIL+S1)

A(7,5)=EXF(-SC/EFSIL+S1)

B(7)=B(7)+RE/G8

A(6,8)=-(+50F/EFSIL+51F)*EXF(+SC/EFSIL+S1)

A(6,9)=-(+50F/EFSIL+51F)*EXF(-SC/EFSIL+S1)

B(8)=B(8)+(-GS*RE-RS*CF)/GS**2

CALL ESS(5,XEARIF(5))

A(9,6)=EXF(+SC/EFSIL+S1)

A(9,9)=EXF(-SC/EFSIL+S1)

B(9)=0.5-RS/G8

C

C SOLVE THE SYSTEM OF ALGEBRAIC EQUATIONS

#=1

h=9

IA=9

IDGT#6

CALL LEI12F(A,4,N,IA,B,IEGT,MAHEA,IEF)

IF(IEF .EQ. 129) WRITE(6,*) ' THE MATRIX IS ALGEBRAICALLY SINGULAR'

IF(IEF .EQ. 34) WRITE(6,*) ' THE ACCURACY TEST FAILED'

IF(IEF .EQ. 131) WRITE(6,*) ' ITERATIVE IMPROVEMENT NOT EFFECTIVE'

D

WRITE(6,*) ' IEGT= ',IEGT

D

WRITE(6,*) ' B=MAATRIX: ', B

ORIGINAL PAGE IS
OF POOR QUALITY

```

C
2 1=2
GNU1=NLXZU(2)
GNU2=NLZAU(2)
EU=EXU(2)
GO TO 21
2=3
GNU1=NLXZU(3)
GNU2=NLZAU(3)
EU=EXU(3)
GO TO 21
4 1=4
GNU1=NLXZU(4)+NUZUFP(XEAR+XBAR(4))
GNU2=NLZAU(4)+NLZAU(4)*(XEAR-XEAR(4))
EU=EXU(3)+(XEAR-XEAR(3))*(EXU(5)-EXU(3))/(XEAR(4)-XEAR(3))
CONTINUE
C FOR REGION 2 OR 3 OR 4.
FBARF=(E(2*1-2)*A0(1,0)+E(2*1-1)*A1(1,0)+APT(1,0))
1 +(E(2*1-2)*A0(1,1)+E(2*1-1)*A1(1,1)+APT(1,1))*(XEAR-XEAR(1))
2 +(E(2*1-2)*A0(1,2)+E(2*1-1)*A1(1,2)+APT(1,2))*(XEAR-XEAR(1))*2
FBARF=(B(2*1-2)+1.0*A0(1,1)+E(2*1-1)*0.0*A1(1,1)+1.0*APT(1,1))
1 +(E(2*1-2)*2.0*(1,2)+E(2*1-1)*2.0*A1(1,2)+2.0*APT(1,2))
2 *(XEAR-XEAR(1))
FEARIF=E(2*1-2)*2.0*A0(1,2)+E(2*1-1)*2.0*A1(1,2)+2.0*APT(1,2)
DO 20 N=3,20
FEARF=FEARF+(E(2*1-2)*A0(1,N)+E(2*1-1)*A1(1,N)+APT(1,N))
1 +(XEAR-XEAR(1))*N
FEARF=FEARF+(E(2*1-2)*N*A0(1,N)+E(2*1-1)*N*A1(1,N)+N*APT(1,N))
1 *(XEAR-XEAR(1))*N*(N-1)
FEARFF=FEARFF+(E(2*1-2)*N*(N-1)*A0(1,N)+E(2*1-1)*N*(N-1)*A1(1,N)
1 +N*(N-1)*APT(1,N))*(XEAR-XEAR(1))*N*(N-2)
20 CONTINUE
GO TO 100
C
C
C FOR REGION 5.
5 1=5
GNU1=NLXZU(1)
GNU2=NLZAU(1)
EU=EXU(1)
CALL ESS(I,XEAR)
FEARF=S/CS+F(2*1-2)*EAF(+SC/EPSS1+S1)+E(2*1-1)*EXP(-S0/EPSS1+S1)
FEARF=(CS*F1+S*LF)/CS*2*(2*1-2)*(+SCF/EPSS1+S1)*EXP(+S0/EPSS1+S1)
1 +E(2*1-1)*(-S0F/EPSS1+S1)*EXP(-S0/EPSS1+S1)
FEARFF=(CS*(CS*FF-FS0UFF)-2.0*LF*(CS*FF-FE*CF))/CS**3
1 +E(2*1-2)*(+SCF/EPSS1+S1)**2*EXP(+S0/EPSS1+S1)
2 +E(2*1-2)*(+SCF/EPSS1+S1)*EXP(+S0/EPSS1+S1)
3 +E(2*1-1)*(-SCF/EPSS1+S1)*EXP(-S0/EPSS1+S1)
4 +E(2*1-1)*(-SCF/EPSS1+S1)*EXP(-S0/EPSS1+S1)
C
100 CONTINUE
C CALCULATE THE ERROR IN THE 2ND ORDER CCE
C CALCULATE VALUES OF EACH TERM OF THE EQUATION:
TERM1=FEARFF
TERM2=KAY*D/TALF3*(1.0-GNU1*GNU2)/EC/XEAR
1 +(1.0-NUX2L*NL2AL)/EXL/(1.0-XEAR)*FEAR
TERM3=[KAY*D/TALF)*(E*NL2AL*(GNL2-NL2AL)*TALF/(EXLAP*LN)
1 -(1.0-NUX2L*NL2AL)/EXL/(1.0-XEAR))
PTG=PTX(ABS(TERM1),RES(TERM2),ABS(TERM3))
CHM=abs(TERM1+TERM2+TERM3)/PTG
C
101 GO TO 102
CONTINUE
CHM=0.0
102 CONTINUE
C
C CALCULATE THE ADHESIVE SHEAR AND NORMAL STIFFNESSES FOR UNIT LOAD AND UNIT WIDTH
TAU12=FBARF/(1.0*TALF**2)
TAU22=TAU12*TALF
RETURN
END

```

131

SCARF4

```

C THIS PROGRAM CALCULATES THE SHEAR STRESSES IN THE ADHESIVE OF A
C SCAFF JOINT. IT USES AKE METHODS, TAYLOR SERIES, AND TAYLOR SERIES
C TO SOLVE FOR ADHEREND LENGTHS AND ADHESIVE STRESSES.
C THE PROGRAM ALLOWS FOR VARIATION IN THE LOAD-CONNECTION MODULUS OF
C ELASTICITY IN THE ADHERENDS TO MODEL COMPOSITE LAMINATES. IT ALSO
C ACCOUNTS FOR ADHEREND TIP BLUNTNES.
C

C I IS THE REGION NUMBER STARTING AT THE LEFT
C XBARIF(I) IS THE DIMENSIONLESS COORDINATE OF THE INTERFACE BETWEEN REGIONS
C I AND (I+1). IN THIS COORDINATE SYSTEM THE JOINT IS ONE UNIT LENGTH.
C A1(I,N) )
C A2(I,N) ) ARE THE N TH EXPANSION COEFFICIENTS OF THE I TH REGION
C AFT(I,N) )
C XBAK(I) IS THE COORDINATE OF THE EXPANSION POINT IN EACH REGION.
C EXU(I) IS THE MODULUS OF ELASTICITY OF THE UPPER ADHEREND IN GIGA PASCALS
C EXL IS THE MODULUS OF ELASTICITY OF THE LOWER ADHEREND
C
C

COMMON XBARIF(0:5),EXU(5),EXL,XBAK(5),
1 NUXZL(5),NUZXL(5),NUZXL,NUZL,ALLEN,EXALM,EXALN,NUZUP,NUZUF,
2 C1,AFT,AU,A1,ATLHMS,
3 CLAE(5),C1AE(5),C2AE(5),C3AE(5),
4 UZUF,UF,PF,FF,FCIL,SC,SCF,UF,SI,SIFF,SIFF,
5 EL,EL,FEAR,FEARFF,FEARFF,F,TALF,KAY,L,
6 CHN,TAU12,TAU22
REAL NUXZD,NUZAU,NUZXL,NUZAL,ALXZUF,ALZXF,KAY,INT0,INT1,INT2,INT3
DOUBLE PRECISION C1(0:5),AFT(5,0:20),AU(5,0:20),A1(5,0:20),
1 C(0:20),F(0:20),A(0:10),E(0:10),KRAKEA(150)
DIMENSION G1(0:20),G2(0:20),G3(0:20),G4(0:20),G12(0:20),G123(0:20)
CALL ASSISTS,"STICK.DAT")
CALL ASSINC(6,"STICK.LAT")

C
C
READ (5,*),ALPHA,XBARIF,EXU,NUXZL,NUZXL,NUZUF,NUZUP,EXL,NUZXL,NUZXL
WRITE (6,*), "ALPHA IS", ALPHA
WRITE (6,*), "XBARIF1", XBARIF(0), XBARIF(1), XBARIF(2), XBARIF(3),
1 XBARIF(4), XBARIF(5)
WRITE (6,*), "EXU", EXU(1), EXU(2), EXU(3), EXU(4), EXU(5)
WRITE (6,*), "EXL", EXL
WRITE (6,*), "NUZAU", NUZAU
WRITE (6,*), "NUZAL", NUZAL
WRITE (6,*), "NUZUF", NUZUF
C
C
F1=3.141592e54
TACHES=0.7 TACHES= THICKNESS IN MILLIMETERS
EACHES=3.45 EACHES= YOUNG'S MODULUS IN GPa
GACHES=1.73 GACHES= SHEAR MODULUS IN GPa
TALF=2.5 TALF= LENGTH IN MILLIMETERS
EXLAF=77.9 EXLAF= STAPLE MODULUS IN GPa
KULAF=0.391 KULAF= STAPLE POISSON'S RATIO
C
C
C CALCULATE SHEAR STRESSES AS A FUNCTION OF POSITION IN THE JOINT
C
C
C
C
ALPHALPHA/1000.0
TALF=TAU12(ALPHA)
COSALF=CLS(ALPHA)
SINALF=SIN(ALPHA)
D=(TALF-TACHES/CCSALF)/TALF
KAY=CCSALF*((1.0+TALF**2)**2*GACHES*EACHES
1 /(TALF*(EALHES+GACHES*TALF**2)))
EFSTI=SDRT(TALF/(KAY**2))

```

```

C   CALCULATE THE COEFFICIENTS FOR REGION ONE. THIS REGION IS THE TIP WHERE
C   THE LOWER ADHEREND TAPES TO ZERO THICKNESS. THE ADHEREND LOAD IS
C   CALCULATED BY A PRE APPROXIMATION. THE COEFFICIENTS CAN BE CHOSEN TO MODEL
C   THE PERFECTLY SHARP, STIFF ADHEREND TIP OR THE ADHESIVE WHICH FILLS IN
C   FOR THE BROKEN ADHEREND TIP.
C
C   CALCULATE THE POLYNOMIAL COEFFICIENTS (C'S) FROM THE TAYLOR'S SERIES
C   EXPANSION OF THE NUMERATOR OF THE S-ZONE INTEGRALS.
I=1
  XEAR1(I)=(XEAR1F(I)+XEAR1F(I-1))/2.0
  GRUM=(1.0-NUX2U(I)*AL2XL(I))*(1.0-XEAR1(I))/EXU(I)
  1           +(1.0-NUX2I*NU2XL)*XEAR1(I)/EXL
  GRUMF=(1.0-NUX2U(I)*NU2AU(I))/EXU(I)+(1.0-NUX2L*NU2XL)/EXL
  F=SQRT(GRUM)
  FPP0.5/SQRT(GRUM)*GRUMF
  FPP1=0.25/(GRUM*SQRT(GRUM))*GRUMF**2
  FPP2=3.0/(6.0*GRUM**2*SQRT(GRUM))*GRUMF**3
  A0RE=FF
  A1RE=FPP
  A2RE=FPP/2.0
  A3RE=FPP/6.0
  C0RE=XEAR1(I)+A1RE*XEAR1(I)+A2RE*XEAR1(I)**2+A3RE*XEAR1(I)**3
  C1RE=(I-1)*A1RE+2.0*A2RE*XEAR1(I)+3.0*A3RE*XEAR1(I)**2
  C2RE=(I-2)*A2RE+3.0*A3RE*XEAR1(I)
  C3RE=(I-3)*A3RE
C
C
C   CHECK VALIDITY OF FLUHIER SERIES APPROXIMATION TO THE NUMERATOR OF SQRT(Q).
C   SELECT VALUES OF XEAR AND CALCULATE EXACT AND APPROXIMATED VALUES.
I=1
  LC 10 R=0.10
  XEAR=XEAR1F(I-1)+0.1*R*(XEAR1F(I)-XEAR1F(I-1))
  APPFCX=C0*RF(I)+(I-1)*XEAR+C1*RF(I)*XEAR+C2*RF(I)*XEAR**2+C3*RF(I)*XEAR**3
  EXACT=SQRT((1.0-NUX2L(I)*NU2XL(I))*(1.0-XEAR)/EXL(I))
  1           +(1.0-NUX2L*NU2XL)/EXL*XEAR)
  WRITE (6,*) 'RKE1:', I, XEAR, EXU(I), EXL, EXACT, APPFCX
  D10  CONTINUE
C
C   CALCULATE THE COEFFICIENTS FOR REGION TWO. THIS REGION BEGINS AT THE END
C   OF AN ADHEREND WITH A SHARP TIP AND EXTENDS A SHORT DISTANCE TO THE RIGHT.
C   THE ADHEREND LOAD IS CALCULATED IN THE FORM OF A TAYLOR SERIES EXPANSION
C   AROUND THE SHARP TIP OF THE ADHEREND.
C
C   FIRST CALCULATE THE C'S AND R'S.
  NT2=13
  XEAR1(2)=(XEAR1F(1)+XEAR1F(2))/2.0
  T1=(-RAY*C/TALF)*(1.0-NUX2U(2)*NU2XL(2))/EXU(2)/(XEAR1(2))
  T2=(-RAY*C/TALF)*(1.0-NUX2L*NU2XL)/EXL/(1.0-XEAR1(2))
  LC 20 R=0,NT2
  0(N)=T1+T2
  T1=T1/XEAR1(2)
  T2=T2/(1.0-XEAR1(2))
  D20  CONTINUE
  F(0)=(-RAY*C/TALF)*(C*NULAM*(NU2XL(2)*AL2XL)*TALF/(EXLAM*TALM))
  1           -(1.0-NUX2L*NU2XL)/EXL/(1.0-XEAR1(2))
  R(1)=(-RAY*C/TALF)*(1.0-NUX2L*NU2XL)/EXL/(1.0-XEAR1(2))**2
  DO 23 N=2,NT2
  R(N)=F(N-1)/(1.0-XEAR1(2))
  D23  CONTINUE
C
C
C   CHECK THE REGION 2 C'S AND R'S:
  DELTAS=(XEAR1F(2)-XEAR1F(1))/10.0
  DO 26 R=0,10
  GAFFCX=6.0
  FAF=CF=0.0
  XEAR=XEAR1F(I)+X*DELTAS
  D27  N=1,NT2
  GAFFCX=GAFFCX+R(N)*(XEAR-XEAR1(2))**N
  FAF=CF=GAFFCX+R(N)*(XEAR-XEAR1(2))**N
  CONTINUE
  GEXACT=(-RAY*C/TALF)*((1.0-NUX2U(2)*AL2XL(2))/EXL(2)/XEAR
  1           +(1.0-NUX2L*AL2XL)/EXL/(1.0-XEAR))
  PEXACT=(RAY*C/TALF)*(C*NULAM*(NU2XL(2)*AL2XL)*TALF/(EXLAM*TALM))
  1           +(1.0-NUX2L*NU2XL)/EXL/(1.0-XEAR))
  WRITE (6,*) 'F2 C&R CKE:', XEAR, GEXACT, GAFFCX, PEXACT, PAPROX
  D26  CONTINUE

```

ORIGINAL PAGE IS
OF POOR QUALITY

```

C   CALCULATE THE EXPANSION COEFFICIENTS WITH A(0) AND A(1) FACTORED OUT.
A0(2,0)=1.0
DO 21 K=2,N12
SUM0=0.0
SUM1=0.0
DO 22 K=0,N-2
SUM=SUM+G(K)*A0(2,K-K-2)
SUM1=SUM1+G(K)*A1(2,K-K-2)
22 CONTINUE
A0(2,N)=SUM0/(N*(N-1))
A1(2,N)=-SUM1/(N*(N-1))
23 CONTINUE
C
C   CALCULATE THE COEFFICIENTS OF THE PARTICULAR SOLUTION:
AFT(2,0)=0.0
AFT(2,1)=0.0
DO 24 K=2,N12
SUM=0.0
DO 25 K=0,N-2
SUM=SUM+G(K)*AFT(2,K-K-2)
25 CONTINUE
AFT(2,N)=(R(N-2)-SUM)/(N*(N-1))
24 CONTINUE
C
C   CALCULATE THE TAYLOR SERIES COEFFICIENTS FOR REGION THREE.
C
C   FIRST CALCULATE THE C's AND R's.
N13=20
XBAF1(3)=XEAFF1(3)+XEAFF1(2))/2.0
T1=(-RAY*E/IALF)*(1.0-NUX2L(3)*NL2XL(3))/EXU(3)/XEAH1(3)
T2=(-RAY*E/IALF)*(1.0-NUX2L*NU2XL)/EXL/(1.0-XEAH1(3))
DC 31 N=0,N13
R(N)=(T1+T2)
T1=T1/XAFT1(3)
30 CONTINUE
R(0)=(RAY*E/IALF)*(EXLAM4*IALM4*(NU2XL(3)-NL2XL)*IALF/(EXLAM4*IALM4
1 -(1.0-PLX2L*NU2XL)/EXL/(1.0-XEAH1(3)))
R(1)=(-RAY*E/IALF)*(1.0-NUX2L*NL2XL)/EXL/(1.0-XEAH1(3))*2
DC 33 N=2,N13
R(N)=R(N-1)/(1.0-XEAH1(3))
33 CONTINUE
C
C   CALCULATE THE EXPANSION COEFFICIENTS WITH A(0) AND A(1) FACTORED OUT.
A0(3,0)=1.0
A0(3,1)=0.0
A1(3,0)=0.0
A1(3,1)=1.0
DO 31 K=2,N13
SUM0=0.0
SUM1=0.0
DO 32 K=0,N-2
SUM=SUM+G(K)*A0(3,K-K-2)
SUM1=SUM1+G(K)*A1(3,K-K-2)
32 CONTINUE
A0(3,N)=SUM0/(N*(N-1))
A1(3,N)=-SUM1/(N*(N-1))
31 CONTINUE
C
C   CALCULATE THE COEFFICIENTS OF THE PARTICULAR SOLUTION:
AFT(3,0)=0.0
AFT(3,1)=0.0
DO 34 K=2,N13
SUM=0.0
DO 35 K=0,N-2
SUM=SUM+G(K)*AFT(3,K-K-2)
35 CONTINUE
AFT(3,N)=(R(N-2)-SUM)/(N*(N-1))
34 CONTINUE
C

```

ORIGINAL PAGE IS
OF POOR QUALITY.

C CALCULATE THE TAYLOR SERIES SOLUTION COEFFICIENTS FOR REGION FOUR.

C CALCULATE THE C'S.

XEAR1(4)=(XPA1IF(3)+XEAR1F(4))/2.0
EXU(4)=(EXL(3)+EXU(5))/2.0
EXUF=(EXU(5)-EXU(3))/(XEAR1F(4)-XEAR1F(3))
Q1(0)=1.0-NUXZL(4)*NUZXU(4)
Q1(1)=NUXZL(4)*NUZXU(4)-NUZUF*NUZXU(4)
Q1(2)=2.0*NUXZL*NUZXU
D1=45 N=3,20
Q1(-)=0.0

40 CONTINUE

Q2(0)=1.0/EXU(4)
Q3(0)=1.0/XEAR1(4)
Q4(0)=(1.0-NUXZL*NUZXU)/EXL/(1.0-XEAR1(4))
D1=45 N=1,20
Q2(-)=(-K*EXUF/EXU(4))*C2(N-1)
Q3(-)=(-K/XEAR1(4))*C3(N-1)
Q4(-)=(1/(1.0-XEAR1(4)))*C4(N-1)

41 CONTINUE

C CALCULATE THE DE-1/2 INTEGERS OF THE PRODUCT TERMS.

CALC PASCAL (12, Q1, Q2)
CALC PASCAL (Q123, Q12, Q3)

C CALCULATE THE VALUES OF C

FACT1=1.0
C(0)=(-RAY*D/TALF)*(Q123(0)+Q4(0))
D1=45 N=1,20
FACT2=FACT1/N
C(N)=(-RAY*D/TALF)*FACT2*(Q123(N)+Q4(N))

45 CONTINUE

C CHECK THE FOURIER COEFFICIENTS, G.

DELTA=(XEAR1F(4)-XEAR1F(3))/10.0
IC 46 N=0,10
XBAF=XEAR1F(5)+N*DELTA
GAF=1
D1=47 N=1,20
GAF1=X=GAFGX+G(NG)*(XBAF-XEAR1(4))**NG

D47 CONTINUE

E=EXL(4)+EXUF*(XEARF-XEAR1(4))
GR1=NUXZL(4)*NUZUF*(XEARF-XEAR1(4))
GR2=NUZXU(4)*NUZUF*(XEARF-XEAR1(4))
GFA=CT=(-RAY*D/TALF)*(1.0-GR1*GR2)/XBAF/EL
D 1 +(1.0-NUZUF*NUZXU)/EXL/(1.0-XEARF))

D WRITE (6,*) ' REGION 4 & CHECK: ',XFAF,GEXACT,GAF,GRX

D46 CONTINUE

C CALCULATE THE R'S.

R(0)=(RAY*D/TALF)*(1.0-GR1*GR2)/XBAF/EL
1 -(1.0-NUXZL*NUZXU)/EXL/(1.0-XEAR1(4))
R(1)=(RAY*D/TALF)*(1.0-GR1*GR2)/XBAF/EL
1 -(1.0-NUXZL*NUZXU)/EXL/(1.0-XEAR1(4))**2
R(2)=(-RAY*D/TALF)*(1.0-NUXZL*NUZXU)/EXL/(1.0-XEAR1(4))**3
D1=46 N=3,20
R(N)=R(N-1)*7(1.0-XEAR1(4))

48 CONTINUE

ORIGINAL PAGE IS
OF POOR QUALITY

```

C CALCULATE THE EXPANSION COEFFICIENTS WITH A(0) AND A(1) FACTORED OUT.
A0(4,0)=1.0
A0(4,1)=0.0
A1(4,0)=0.0
A1(4,1)=1.0
DO 49 K=2,20
SUM0=0.0
SUM1=0.0
DO 50 K=0,N=2
SUM0=SUM0+G(K)*A0(4,K-K-2)
SUM1=SUM1+G(K)*A1(4,K-K-2)
49 CONTINUE
A0(4,N)=SUM0/(N*(N-1))
A1(4,N)=SUM1/(N*(N-1))
49 CONTINUE
C CALCULATE THE COEFFICIENTS OF THE PARTICULAR EQUATION:
AFT(4,0)=C0
AFT(4,1)=0.0
10 S1 K=2,20
SU=C0
10 S2 K=0,N=2
SUM=SUM+G(K)*AFT(4,K-K-2)
52 CONTINUE
AFT(4,N)=(N*(N-2)+SU)/(N*(N-1))
51 CONTINUE
C
C CALCULATE THE COEFFICIENTS FOR THE SOLUTIONS FOR REGION FIVE.
C CALCULATE THE POLYNOMIAL COEFFICIENTS (C'S) FROM THE TAYLOR'S SERIES
C EXPANSION OF THE NUMERATOR OF THE S-ZERO INTEGRALS.
105
XPAF(I)=(XPAF(I)+XPAF(I-1))/2.0
GRUM=(1.0-NLXZL(I)*NLXZL(I))*(1.0-XPAF(I))/EXU(I)
106
GRUM=(1.0-NLXZL(I)*NLXZL(I))/EXU(I)+(1.0-NLXZL(I))/EXL
GRUM=(1.0-NLXZL(I)*NLXZL(I))/EXU(I)+(1.0-NLXZL(I))/EXL
E=SGRT(GRUM)
FF=0.5/SQRT(GRUM)*GRUM
FFF=0.25/(GRUM*SGRT(GRUM))*GRUM**2
FFF=3.0/(8.0*GRUM**2*SGRT(GRUM))*GRUM**3
A1=FFF
A1=FFF
A2=FFF/2.0
A3=FFF/6.0
CUMF(I)=A0*FFF-A1*FF*XPAF(I)+A2*FF**2*XPAF(I)**2-A3*FF**3*XPAF(I)**3
C1=FFF(I)*A1+FFF*(1.0-NLXZL(I)*NLXZL(I))+3.0*A3*FFF*XPAF(I)**2
C2=FFF(I)*A2+FFF*(1.0-NLXZL(I)*NLXZL(I))
C3=FFF(I)*A3*FFF
C
C CHECK VALIDITY OF FOURIER SERIES APPROXIMATION TO THE NUMERATOR OF SGRT(G).
C SELECT VALUES OF XPAF AND CALCULATE EXACT AND APPROXIMATED VALUES.
10 DC 36 K=0,10
10 XPAF=XPAF(I-1)+0.1*N*(XPAF(I)-XPAF(I-1))
10 APP=CA0*AE(I)+C1*AE(I)*XPAF+C2*AE(I)*XPAF**2+C3*APP(I)*XPAF**3
10 EXACT=SGRT((1.0-NLXZL(I)*NLXZL(I))*(1.0-XPAF)/EXL(I))
10 I = (1.0-NLXZL(I)*NLXZL(I))/EXL*XPAF
C WRITE (6,*) ' NLXZL', 1,XPAF,EXU(I),EXL,EXACT,APP,EX
106 CONTINUE

```

```

C  NOW CALCULATE THE SOLUTION COEFFICIENTS FOR THE BOUNDARY CONDITIONS:
C  FEAR(LEFT HAND SIDE)=FEAR(RHS) AND
C  FEARP(LHS)=FEARP(RHS)                                AT EACH REGION INTERFACE
C  FEAR=0.5 AT XBAR=0.5
C
C
C  DG 70 N=1,10
C  B(N)=0.0
C  DG 70 N=1,10
C  A(1,N)=0.0
70  CONTINUE
DO 71  b=0,20
A(2,3)=A(2,3)-A0(2,N)*(XEAF1(1)-XEAF1(2))**N
A(2,4)=A(2,4)-A1(2,N)*(XEAF1(1)-XEAF1(2))**N
b(2)=P(2)+AF1(2,N)*(XEAF1(1)-XEAF1(2))**N
A(3,3)=A(3,3)-N*A0(2,N)*(XEAF1(1)-XEAF1(2))**N
A(3,4)=A(3,4)-N*A1(2,N)*(XEAF1(1)-XEAF1(2))**N
b(3)=P(3)+N*AF1(2,N)*(XEAF1(1)-XEAF1(2))**N
A(4,3)=A(4,3)+A0(2,N)*(XEAF1(2)-XEAF1(3))**N
A(4,4)=A(4,4)+A1(2,N)*(XEAF1(2)-XEAF1(3))**N
A(4,5)=A(4,5)-A0(3,N)*(XEAF1(2)-XEAF1(3))**N
A(4,6)=A(4,6)-A1(3,N)*(XEAF1(2)-XEAF1(3))**N
B(4)=B(4)-AF1(2,N)*(XEAF1(2)-XEAF1(3))**N
1      +AF1(3,N)*(XEAF1(2)-XEAF1(3))**N
A(5,3)=A(5,3)+N*A0(2,N)*(XEAF1(2)-XEAF1(3))**N
A(5,4)=A(5,4)+N*A1(2,N)*(XEAF1(2)-XEAF1(3))**N
A(5,5)=A(5,5)-N*A0(3,N)*(XEAF1(2)-XEAF1(3))**N
A(5,6)=A(5,6)-N*A1(3,N)*(XEAF1(2)-XEAF1(3))**N
b(5)=P(5)-N*AF1(2,N)*(XEAF1(2)-XEAF1(3))**N
1      +N*AF1(3,N)*(XEAF1(2)-XEAF1(3))**N
A(6,5)=A(6,5)+A0(3,N)*(XEAF1(3)-XEAF1(4))**N
A(6,6)=A(6,6)+A1(3,N)*(XEAF1(3)-XEAF1(4))**N
A(6,7)=A(6,7)-A0(4,N)*(XEAF1(3)-XEAF1(4))**N
A(6,8)=A(6,8)-A1(4,N)*(XEAF1(3)-XEAF1(4))**N
b(6)=b(6)-AF1(3,N)*(XEAF1(3)-XEAF1(4))**N
1      +AF1(4,N)*(XEAF1(3)-XEAF1(4))**N
A(7,5)=A(7,5)+N*A0(3,N)*(XEAF1(3)-XEAF1(4))**N
A(7,6)=A(7,6)+N*A1(3,N)*(XEAF1(3)-XEAF1(4))**N
A(7,7)=A(7,7)-N*A0(4,N)*(XEAF1(3)-XEAF1(4))**N
A(7,8)=A(7,8)-N*A1(4,N)*(XEAF1(3)-XEAF1(4))**N
b(7)=B(7)-N*AF1(3,N)*(XEAF1(3)-XEAF1(4))**N
1      +N*AF1(4,N)*(XEAF1(3)-XEAF1(4))**N
A(8,7)=A(8,7)+A0(4,N)*(XEAF1(4)-XEAF1(5))**N
A(8,8)=A(8,8)+A1(4,N)*(XEAF1(4)-XEAF1(5))**N
B(8)=B(8)-AF1(4,N)*(XEAF1(4)-XEAF1(5))**N
A(9,7)=A(9,7)+N*A0(4,N)*(XEAF1(4)-XEAF1(5))**N
A(9,8)=A(9,8)+N*A1(4,N)*(XEAF1(4)-XEAF1(5))**N
B(9)=B(9)-N*AF1(4,N)*(XEAF1(4)-XEAF1(5))**N
71  CONTINUE
CALL ESS(1,1,GE=0B)
A(1,1)=EXP(+50/EFSIL+S1)
A(1,2)=EXP(-50/EFSIL+S1)
B(1)=0.0
CALL ESS(1,XEARIF(1))
A(2,1)=EXP(+50/EFSIL+S1)
A(2,2)=EXP(-50/EFSIL+S1)
B(2)=B(2)-RS70S
A(3,1)=+(50/EFSIL+S1)*EXP(+50/EFSIL+S1)
A(3,2)=-(50/EFSIL+S1)*EXP(-50/EFSIL+S1)
b(3)=B(3)-(GE*H-RS*GP)/GS**2
CALL ESS(3,XEARIF(4))
A(4,9)=EXP(+50/EFSIL+S1)
A(4,10)=EXP(-50/EFSIL+S1)
B(4)=B(4)+GS/GS
A(5,9)=-(50/EFSIL+S1)*EXP(+50/EFSIL+S1)
A(5,10)=-(50/EFSIL+S1)*EXP(-50/EFSIL+S1)
B(5)=B(5)-RS*GP/GS**2
CALL ESS(5,XEARIF(5))
A(6,9)=EXP(+50/EFSIL+S1)
A(6,10)=EXP(-50/EFSIL+S1)
B(6)=B(6)+GS/GS
A(7,9)=-(50/EFSIL+S1)*EXP(+50/EFSIL+S1)
A(7,10)=-(50/EFSIL+S1)*EXP(-50/EFSIL+S1)
B(7)=B(7)-RS*GP/GS**2
CALL ESS(7,XEARIF(7))
A(8,9)=EXP(+50/EFSIL+S1)
A(8,10)=EXP(-50/EFSIL+S1)
B(8)=B(8)+GS/GS
A(9,9)=-(50/EFSIL+S1)*EXP(+50/EFSIL+S1)
A(9,10)=-(50/EFSIL+S1)*EXP(-50/EFSIL+S1)
B(9)=B(9)-RS*GP/GS**2
CALL ESS(9,XEARIF(9))
A(10,9)=EXP(+50/EFSIL+S1)
A(10,10)=EXP(-50/EFSIL+S1)
B(10)=B(10)+GS/GS

```

ORIGINAL PAGE IS
OF POOR QUALITY

```

C  SOLVE THE SYSTEM OF ALGEBRAIC EQUATIONS
  N=1
  N=10
  I=0
  I=10
  I=0
  CALL LEC12F(A,N,N,1A,B,1LG1,1KAREA,1ER)
  IF(IER .EQ. 129) WRITE(6,*) ' THE MATRIX IS ALGEBRAICALLY SINGULAR'
  IF(IER .EQ. 34) WRITE(6,*) ' THE ACCURACY TEST FAILED'
  IF(IER .EQ. 131) WRITE(6,*) ' ITERATIVE IMPROVEMENT NOT EFFECTIVE'
  D  WRITE (6,*) ' IER= ',IER
  D  WRITE (6,*) ' I=0',1LG1
  D  WRITE (6,*) ' N=KAREA ', b
C  SELECT POSITIONS ALONG THE JOIN1 AND CALCULATE STRESSES, ETC.
C
  WRITE (6,102) ALPHA=1000.0,L,EPSIL  !WRITE THE DATA HEADING
102  F04=AT ('T77/15,'IPE PROGRAM IS SCAPP4',/
  1  15,'SCAPP ANGLE IS ',F5.1,' MILLIACRANS./'
  1  15,'JC1 LENGTH IS ',F5.1,' MILLIMETERS'
  2  15,'EPSILON IS ',F5.4/
  3  15,'ADHERENT MELLUS',T42'ADHESIVE'
  4  15,'X',T15,'XAN',143,'STRESS',153,' CHA ',164'FBAR',
  4  172'FAPP',183'FEAPP'
  5  17,'MILLI',151,'LEFFF',133,'LCRFR',143,'FACTOR'
  6  17,'METERS',127,'GFA',134,'GFA'//)
C
C  SELECT X VALUES NEAR THE END OF THE JOIN1.
  DO 72 NX=0,16
  XPAF=NX*0.001
  IF (NX .EQ. 0) XBAR=C.0004
  X=XBAR*D
  CALL FCPCE(XBAR)
  STRFAC=TAU12*TLAM/(C*CCSALF*SINALF)
  WRITE (6,101) X,XPAF,EL,FL,SIFAC,CHA,FEAR,FEAPP,FBARPP
101  F04=AT (6,101) X,XBAR,EL,FL,SIFAC,CHA,FEAR,FEAPP,FBARPP
  72  CONTINUE
C  SELECT XBAR VALUES FOR THE REST OF THE JOIN1
  DO 73 NX=18,30,2
  XBAR=NX*0.001
  X=XBAR*D
  CALL FCPCE(XBAR)
  STRFAC=TAU12*TLAM/(C*CCSALF*SINALF)
  WRITE (6,101) X,XBAR,EL,FL,SIFAC,CHA,FEAR,FEAPP,FBARPP
  73  CONTINUE
  DO 74 NX=4,50,2
  XBAR=NX*0.01
  X=XBAR*D
  CALL FCPCE(XBAR)
  STRFAC=TAU12*TLAM/(C*CCSALF*SINALF)
  WRITE (6,101) X,XBAR,EL,FL,SIFAC,CHA,FEAR,FEAPP,FBARPP
  74  CONTINUE
  END
C
C
  SUBROUTINE PASCAL (CCUT,GIN1,GIN2)
  DIMENSION CCUT(0:20),GIN1(0:20),GIN2(0:20),FAS(20),PSTCR(20)
  DO 1 N=1,20
  PAS(N)=1.0
  1  CONTINUE
  GOUT(0)=GIN1(0)*GIN2(0)
  GOUT(1)=GIN1(0)*GIN2(1)+GIN1(1)*GIN2(0)
  DO 2 N=2,20
  DO 3 N=1,20
  PSTCR(N)=FAS(N)
  3  CONTINUE
  DO 4 N=2,NC
  PASTR)=PSTCR(N)+PSTCR(N-1)
  4  CONTINUE
  DO 2 N=0,NC
  GOUT(N)=GOUT(N)+FAS(N+1)*GIN1(N)*GIN2(N-N)
  2  CONTINUE
  RETURN
  END

```

```

FUNCTION ESZERC(I,XBAR)
C THIS FUNCTION CALCULATES THE VALUE OF THE SZERO INTEGRAL FOR A GIVEN REGION
C AND POSITION
COMMON XEARIF(0:5),EXU(5),EXL,XEARIF(5),
1  NUZUL(5),NUZXL(5),NUZL,NUZXL,NULAM,EXLAM,TLAM,NUZXUP,NUZXUF,
2  C1,AFT,A0,A1,NIEPMS,
3  C0=KB(5),C1=KB(5),C2=KB(5),C3=KB(5),
4  GS,GF,GPP,RS,RF,FFF,EPSSIL,SO,SOF,S0PP,S1,S1F,S1PP,
5  EU,EL,FEAR,FEARF,FEARFP,B,TALF,RAY,E,
6  CHK,IAU12,IAL22
REAL NUZXU,NUZUL,NUZXL,NULAM,NUZXUF,NUZXUP,RAY,INT0,INT1,INT2,INT3
DOUBLE PRECISION C1(0:20),AFT(5,0:20),A0(5,0:20),A1(5,0:20),
1  A1(0:20),R(0:20),A(10,10),B(10),KAREA(150)
INT0=ASIN(XEAR-XBAR-1.0)
INT1=SQRT(XEAR-XBAR**2)+0.5*ASIN(2.0*XBAR-1.0)
INT2=(-XEAR/2.0-0.75)*SQRT(XEAR-XBAR**2)+0.375*ASIN(2.0*XBAR-1.0)
INT3=(-XEAR**2/3.0-0.5*XBAR/12.0-0.625)*SQRT(XBAR-XBAR**2)
I = 0.3125*ASIN(2.0*XBAR-1.0)
ESZERC=C0=KB(1)*INT0+C1=KB(1)*INT1+C2=KB(1)*INT2+C3=KB(1)*INT3
RETURN
END
C
C SUBROUTINE ESS(I,XEAR)
C THIS SUBPROGRAM CALCULATES THE VALUES OF S=ZEP0, S=CNE, CS, RS AND THEIR
C DERIVATIVES FOR A GIVEN POSITION.
COMMON XEARIF(0:5),EXU(5),EXL,XEARIF(5),
1  NUZUL(5),NUZXL(5),NUZL,NUZXL,NULAM,EXLAM,TLAM,NUZXUF,NUZXLF,
2  C1,AFT,A0,A1,NIEPMS,
3  C0=KB(5),C1=KB(5),C2=KB(5),C3=KB(5),
4  GS,GF,GPP,RS,RF,FFF,EPSSIL,SO,SOF,S0PP,S1,S1F,S1PP,
5  EU,EL,FEAR,FEARF,FEARFP,E,TALF,RAY,L,
6  CHK,IAU12,IAL22
REAL NUZXU,NUZUL,NUZXL,NULAM,NUZXUF,NUZXUP,RAY,INT0,INT1,INT2,INT3
DOUBLE PRECISION C1(0:20),AFT(5,0:20),A0(5,0:20),A1(5,0:20),
1  A1(0:20),R(0:20),A(10,10),B(10),KAREA(150)
C
C CALCULATE SO, SOF, S0PP, S1, S1F AND S1PP
SO=ESIFRC(I,XBAR)-ESIFRC(I,XEARIF(I-1))
T1=(1.0-NUZUL(I))*NUZUL(I)/EXU(I)
T2=(1.0-NUZXL(I))*NUZXL(I)/EXL
US=T1/XEAR+T2/(1.0-XEAR)
LP=T1/XEAR**2+T2/(1.0-XEAR)**2
GFF=Z.0*T1/XEAR**3+Z.0*T2/(1.0-XBAR)**3
SOF=SQRT(GS)
S0PP=GP/(2.0*SQRT(GS))
S1=-0.25*LCG(GS)
S1F=GF/(4.0*GS)
S1PP=(GF**2-GS*JPF)/(4.0*GS**2)
C CALCULATE R AND ITS DERIVATIVES
RS=T2/(1.0-XBAR)-C*NUZUL*(NUZXU(I)-NUZXL)*TALF/(EXLAM*TLAM)
RF=T2/(1.0-XEAR)**2
RPP=2.0*T2/(1.0-XBAR)**3
RETURN
END
C
C SUBROUTINE FCPCE(XEAR)
C THIS SUBROUTINE CALCULATES FCPA, ITS DERIVATIVES, ADHESIVE
C FCPAL AND SHEAR STRESSES, AND CHECKS THE EQUATION.
COMMON XEARIF(0:5),EXU(5),EXL,XEARIF(5),
1  NUZUL(5),NUZXL(5),NUZL,NUZXL,NULAM,EXLAM,TLAM,NUZXUP,NUZXUF,
2  C1,AFT,A0,A1,NIEPMS,
3  C0=KB(5),C1=KB(5),C2=KB(5),C3=KB(5),
4  GS,GF,GPP,RS,RF,FFF,EPSSIL,SO,SOF,S0PP,S1,S1F,S1PP,
5  EU,EL,FEAR,FEARF,FEARFP,E,TALF,RAY,L,
6  CHK,IAU12,IAL22
REAL NUZXU,NUZUL,NUZXL,NUZL,NUZXL,NUZUF,NUZXUP,RAY,INT0,INT1,INT2,INT3
DOUBLE PRECISION C1(0:20),AFT(5,0:20),A0(5,0:20),A1(5,0:20),
1  A1(0:20),R(0:20),A(10,10),B(10),KAREA(150)
C
C DETERMINE WHICH REGION.
IF(XEAR .GE. XEARIF(0)) .AND. XEAR .LE. XEARIF(1)) GO TO 1
IF(XEAR .GE. XEARIF(1)) .AND. XEAR .LE. XEARIF(2)) GO TO 2
IF(XEAR .GE. XEARIF(2)) .AND. XEAR .LE. XEARIF(3)) GO TO 3
IF(XEAR .GE. XEARIF(3)) .AND. XEAR .LE. XEARIF(4)) GO TO 4
IF(XBAR .GE. XEARIF(4)) .AND. XBAR .LE. XEARIF(5)) GO TO 5
WRITE(6,*) ' ERROR IN REGION SELECTION.'
RETURN

```

```

2      I=2
      GRU1=NUXZU(2)
      GRU2=NU2ZU(2)
      EU=EXU(2)
      EL=EXL
      GO TO 21
3      I=3
      GRU1=NUXZU(3)
      GRU2=NU2ZU(3)
      EU=EXU(3)
      EL=EXL
      GO TO 21
4      I=4
      GRU1=NUXZU(4)+NUXZU*(XBAR-XBAR1(4))
      GRU2=NU2ZU(4)+NU2ZU*(XBAR-XBAR1(4))
      EU=EXU(3)*(XBAR-XBAR1(3))+(EXU(5)-EXU(3))/(XBAR1(4)-XBAR1(3))
      EL=EXL
21    CONTINUE
C    FCR REGION 2 CR 4.
      FBAH=(B(2*I-1)*AO(1,0)+B(2*I)*AI(1,0)+APT(1,0))
      1   +(B(2*I-1)*AO(1,1)+B(2*I)*AI(1,1)+APT(1,1))* (XBAR-XBAR1(I))
      2   +(B(2*I-1)*AO(1,2)+B(2*I)*AI(1,2)+APT(1,2))* (XBAR-XBAR1(I))*2
      FBAHF=(B(2*I-1)*1.0*AO(1,1)+B(2*I)*1.0*AI(1,1)+1.0*APT(1,1))
      1   +(B(2*I-1)*2.0*AO(1,2)+B(2*I)*2.0*AI(1,2)+2.0*APT(1,2))
      2   *(XBAR-XBAR1(I))
      FBAH1=(B(2*I-1)*2.0*AO(1,2)+B(2*I)*2.0*AI(1,2)+2.0*APT(1,2))
      GO TO 1=3,20
      FBAHF=FBAH+(B(2*I-1)*AO(1,N)+B(2*I)*AI(1,N)+APT(1,N))
      1   *(XBAR-XBAR1(I))*N
      FBAHF=FBAHF+(B(2*I-1)*AO(1,N)+B(2*I)*N*AI(1,N)+N*APT(1,N))
      1   *(XBAR-XBAR1(I))*N*(N-1)
      FBAHF=FBAHF+(B(2*I-1)*N*(N-1)*AO(1,N)+B(2*I)*N*(N-1)*AI(1,N)
      1   +N*(N-1)*APT(1,N))*(XBAR-XBAR1(I))*2*(N-2)
20    CONTINUE
      GO TO 100
C
C    FCR REGION 1 CR REGION 5.
1      I=1
      GO TO 10
5      I=5
10    CONTINUE
      GRU1=NUXZU(1)
      GRU2=NU2ZU(1)
      EU=EXU(1)
      EL=EXL
      CALL ESS(1,XBAR)
      FPAF=RS/LS+(2*I-1)*EXF(+SO/EPSIL+S1)+B(2*I)*FAP(+SO/EPSIL+S1)
      FBAHF=(US*RF+RS*LP)/GS#2+B(2*I-1)*(+SCF/EFSIL+S1F)*EXP(+SO/EFSIL+S1)
      1   +B(2*I)*(-SCF/EFSIL+S1F)*EXP(-SO/EFSIL+S1)
      FBAHF=(GS*(GS*FFF-FS*GFF)-2.0*GP*(GS*RF+RS*LP))/GS#3
      1   +B(2*I-1)*(+SCF/EFSIL+S1F)*2*EXF(+SO/EFSIL+S1)
      2   +B(2*I-1)*(-SCF/EFSIL+S1F)*EXF(-SO/EFSIL+S1)
      3   +B(2*I)*(-SCF/EFSIL+S1F)*2*EXF(-SO/EFSIL+S1)
      4   +B(2*I)*(-SCF/EFSIL+S1F)*EXF(-SC/EFSIL+S1)
C
C100   CONTINUE
C    CALCULATE THE ERICH IN THE 2ND ORDER LDE
C    CALCULATE VALUES OF EACH TERM OF THE EQUATION:
      TER1=FFAFFF
      TERM2=(-KAY*E/TALF)*((1.0-GRU1*GRU2)/EL/XBAR
      1   +(1.0-NUXZL*NU2ZL)/EL/(1.0-XBAR))*FRAF
      TERM3=(KAY*E/TALF)*((GRU2-GRU1)*TALF/(EXAM+EL))
      1   -(1.0-NUAZL*NU2ZL)/EL/(1.0-XBAR))
      BIG=AES(TEP#1),AES(TEP#2),AES(TEP#3)
      CHR=AES(1EP#1+TERM2-TERM3)/BIG
C
      GO TO 102
101   CONTINUE
      CHR=0.0
102   CONTINUE
C
C    CALCULATE THE ADHESIVE SHEAR AND NORMAL STRESSES FOR UNIT LOAD AND UNIT #IETH
      TAU12=FAHF/(1.0+TALF**2)
      TAU22=TAU12*TALF
      RETURN
      END

```

ORIGINAL PAGE IS
OF POOR QUALITY.

THE PROGRAM IS SCARF4
SCARF ANGLE IS 10.0 MILLIRADIANS.
JOINT LENGTH IS 230.0 MILLIMETERS
EPSILON IS 0.0026

A PILLOW PETERS	XBAR	UPPER GPA	LOWER GPA	ADHESIVE STRESS FACTOR	CHK	FBAR		FBARPF
						FBAR	FBARF	
0.1	0.000	146.0	76.0	1.6310	1.3E-03	0.00071	1.77652	-2.58837
0.2	0.001	146.0	76.0	1.5263	1.3E-03	0.00178	1.77496	-2.59323
0.3	0.002	146.0	76.0	1.5265	1.3E-03	0.00355	1.77236	-2.59023
0.7	0.003	146.0	76.0	1.5237	1.3E-03	0.00532	1.76976	-2.60633
0.9	0.004	146.0	76.0	1.5208	1.3E-03	0.00709	1.76715	-2.61919
1.1	0.005	146.0	76.0	1.5189	1.3E-03	0.00886	1.76452	-2.63722
1.3	0.006	146.0	76.0	1.5151	1.3E-03	0.01062	1.76187	-2.66259
1.6	0.007	146.0	76.0	1.5122	1.3E-03	0.01238	1.75919	-2.69657
1.8	0.008	146.0	76.0	1.5092	1.3E-03	0.01414	1.75647	-2.74242
2.1	0.009	146.0	76.0	1.5062	1.3E-03	0.01589	1.75370	-2.80142
2.3	0.010	146.0	76.0	1.5031	1.3E-03	0.01764	1.75067	-2.87710
2.5	0.011	146.0	76.0	1.5000	1.3E-03	0.01939	1.74754	-2.97320
2.8	0.012	146.0	76.0	1.4967	1.3E-03	0.02114	1.74451	-3.09408
3.0	0.013	146.0	76.0	1.4932	1.3E-03	0.02288	1.74174	-3.24453
3.2	0.014	146.0	76.0	1.4896	1.3E-03	0.02462	1.73841	-3.43174
3.4	0.015	146.0	76.0	1.4857	1.3E-03	0.02636	1.73467	-3.66212
3.7	0.016	146.0	76.0	1.4816	1.3E-03	0.02809	1.73107	-3.94440
4.1	0.018	146.0	76.0	1.4779	1.0E-01	0.03155	1.72764	-1.92110
4.6	0.020	146.0	76.0	1.4734	6.2E-06	0.03500	1.72353	-2.16258
5.1	0.022	146.0	76.0	1.4695	6.2E-06	0.03645	1.71906	-2.29552
5.5	0.024	146.0	76.0	1.4653	6.0E-01	0.04168	1.71436	-2.37422
6.0	0.026	146.0	76.0	1.4652	6.2E-06	0.04530	1.70956	-2.42670
6.4	0.028	146.0	76.0	1.4626	6.2E-06	0.04872	1.70468	-2.46877
6.9	0.030	146.0	76.0	1.4675	1.4E-05	0.05212	1.65970	-2.28831
7.2	0.040	146.0	76.0	1.5220	2.5E-06	0.06900	1.67624	-2.36519
13.6	0.060	146.0	76.0	1.5777	1.2E-07	0.10206	1.62900	-2.36557
18.4	0.080	146.0	76.0	1.7116	1.2E-07	0.13412	1.57481	-3.43240
23.0	0.100	146.0	76.0	1.5634	1.1E-07	0.16457	1.43829	-13.63151
27.8	0.120	135.0	76.0	1.0047	3.5E-06	0.18652	0.92430	-19.63409
32.2	0.140	123.5	76.0	0.7332	3.3E-07	0.20417	0.67451	-8.76921
36.7	0.160	112.7	76.0	0.5646	0.0E-01	0.21605	0.51945	-7.16951
41.4	0.180	101.5	76.0	0.4110	0.0E-01	0.22503	0.37611	-7.14614
46.0	0.200	90.4	76.0	0.2415	1.1E-06	0.23109	0.22221	-8.99615
50.6	0.220	79.2	76.0	-0.4439	6.6E-06	0.23326	-0.04038	-20.71537
55.2	0.240	78.0	76.0	0.8917	4.0E-06	0.24199	0.82040	17.96552
59.8	0.260	78.0	76.0	1.6601	1.0E-06	0.26043	0.97526	2.44056
64.4	0.280	78.0	76.0	1.0834	5.9E-07	0.28021	0.89666	0.34835
69.0	0.300	78.0	76.0	1.0867	6.7E-07	0.30019	0.99976	0.05079
73.7	0.320	78.0	78.0	1.0872	6.3E-07	0.32019	1.00022	0.00646
78.2	0.340	78.0	76.0	1.0672	1.1E-07	0.34019	1.00026	-0.00041
82.7	0.360	78.0	78.0	1.0972	8.1E-07	0.36020	1.00024	-0.00152
87.4	0.380	78.0	76.0	1.0672	5.1E-07	0.38020	1.00020	-0.00174
92.0	0.400	78.0	78.0	1.0871	9.7E-07	0.40021	1.00017	-0.00203
96.6	0.420	78.0	76.0	1.0871	6.3E-07	0.42021	1.00012	-0.00346
101.2	0.440	78.0	78.0	1.0869	9.3E-07	0.44021	0.99955	-0.01125
105.8	0.460	78.0	78.0	1.0864	3.7E-07	0.46021	0.99945	-0.05377
110.4	0.480	78.0	78.0	1.0834	4.9E-07	0.48018	0.98665	-0.26513
115.0	0.500	78.0	78.0	1.0672	4.1E-07	0.50000	0.98179	-1.54474

ORIGINAL PAGE IS
OF POOR QUALITY

THE PROGRAM IS SCARF4
SCAFF ANGLE IS 30.0 MILLIPACIANS.
JOINT LENGTH IS 230.0 MILLIMETERS
EPSILON IS 0.0026

WILLI PETERS	X	XBAR	ADHERENCE MODULUS		ADHESIVE SHEAR TENSILE	CHK	FBAR	FSARP	FBARPF
			UPPER GPA	LOWER GPA					
0.1	0.000	3.5	78.0	0.0467	4.9E-05	0.00002	0.04300	0.60716	
0.2	0.001	3.5	78.0	0.0466	4.9E-05	0.00004	0.04307	0.20124	
0.3	0.002	3.5	78.0	0.0462	3.1E-05	0.00009	0.04611	13.35519	
0.4	0.003	3.5	78.0	0.0457	3.4E-04	0.00017	0.19840	555.66537	
0.5	0.004	3.5	78.0	0.0453	1.0E-03	0.00151	0.37577	0.000000000	
0.6	0.005	140.0	78.0	0.0453	8.4E-04	0.00520	3.27836	-782.61426	
0.7	0.006	140.0	78.0	0.0453	3.4E-05	0.00023	2.68866	-436.54926	
0.8	0.007	140.0	78.0	0.0450	6.3E-07	0.01074	2.35063	-257.98886	
0.9	0.008	140.0	78.0	0.0450	1.3E-07	0.01298	2.14639	-159.74861	
1.0	0.009	140.0	78.0	0.0450	2.1936	6.3E-06	0.01506	2.01757	-102.82752
1.1	0.010	140.0	78.0	0.0450	1.1014	1.3E-07	0.01703	1.93331	-66.46134
1.2	0.011	140.0	78.0	0.0450	2.0356	1.3E-07	0.01893	1.87639	-47.01169
1.3	0.012	140.0	78.0	0.0450	1.5655	1.2E-07	0.02079	1.83674	-33.25847
1.4	0.013	140.0	78.0	0.0450	1.9656	1.9E-05	0.02261	1.80631	-24.22284
1.5	0.014	140.0	78.0	0.0450	1.9426	2.8E-04	0.02441	1.76744	-17.70464
1.6	0.015	140.0	78.0	0.0450	1.9275	1.2E-03	0.02619	1.77362	-11.55745
1.7	0.016	140.0	78.0	0.0450	1.9165	7.6E-04	0.02795	1.76313	-9.50963
1.8	0.016	140.0	78.0	0.0450	1.8991	2.9E-04	0.03146	1.74716	-6.70246
1.9	0.020	140.0	78.0	0.0450	1.8885	1.1E-04	0.03495	1.73556	-5.02962
2.0	0.022	140.0	78.0	0.0450	1.8766	4.1E-05	0.03841	1.72662	-4.01854
2.1	0.024	140.0	78.0	0.0450	1.8687	1.6E-05	0.04185	1.71924	-3.41137
2.2	0.026	140.0	78.0	0.0450	1.8616	6.6E-06	0.04520	1.71282	-3.04050
2.3	0.028	140.0	78.0	0.0450	1.8554	3.4E-06	0.04870	1.70656	-2.81068
2.4	0.030	140.0	78.0	0.0450	1.8495	2.0E-06	0.05211	1.70152	-2.6e546
2.5	0.040	140.0	78.0	0.0450	1.8223	2.4E-07	0.06900	1.67645	-2.41272
2.6	0.046	140.0	78.0	0.0450	1.7707	6.0E-06	0.10205	1.62901	-2.36124
2.7	0.080	140.0	78.0	0.0450	1.7117	2.5E-07	0.13412	1.57450	-3.33356
2.8	0.106	140.0	78.0	0.0450	1.5633	4.4E-06	0.16457	1.43820	-13.3476
2.9	0.120	135.0	78.0	0.0447	3.2E-04	0.18851	0.92436	-19.63964	
3.0	0.140	123.5	78.0	0.7332	3.3E-07	0.20417	0.67452	-8.76566	
3.1	0.160	112.7	78.0	0.5846	1.1E-07	0.21605	0.51945	-7.16955	
3.2	0.180	101.9	78.0	0.4110	1.1E-07	0.22503	0.37811	-7.14615	
3.3	0.200	90.4	78.0	0.2418	1.1E-06	0.23109	0.22221	-5.95615	
3.4	0.220	79.2	78.0	-0.0435	6.7E-06	0.23328	-0.04036	-20.71537	
3.5	0.240	78.0	78.0	0.8917	4.0E-06	0.24199	0.82040	17.96552	
3.6	0.260	78.0	78.0	1.0601	1.0E-06	0.26043	0.97526	2.44086	
3.7	0.280	78.0	78.0	1.0834	9.9E-07	0.28021	0.99668	0.34835	
3.8	0.300	78.0	78.0	1.6867	6.7E-07	0.30019	0.99976	0.05079	
3.9	0.320	78.0	78.0	1.0872	6.5E-07	0.32019	-1.00022	-0.00846	
4.0	0.340	78.0	78.0	1.0872	6.1E-07	0.34019	1.00026	-0.00041	
4.1	0.360	78.0	78.0	1.0872	6.1E-07	0.36020	1.00024	-0.00152	
4.2	0.380	78.0	78.0	1.0872	5.1E-07	0.38020	1.00020	-0.00174	
4.3	0.400	78.0	78.0	1.0871	5.7E-07	0.40021	1.00017	-0.00203	
4.4	0.420	78.0	78.0	1.0871	6.3E-07	0.42021	1.00012	-0.00346	
4.5	0.440	78.0	78.0	1.0869	9.3E-07	0.44021	0.99995	-0.01125	
4.6	0.460	78.0	78.0	1.0864	3.7E-07	0.46021	0.99945	-0.05377	
4.7	0.480	78.0	78.0	1.0834	4.9E-07	0.48018	0.99869	-0.28513	
4.8	0.500	78.0	78.0	1.0672	4.1E-07	0.50000	0.98175	-1.54474	

ORIGINAL PAGE IS
OF POOR QUALITY

THE PROGRAM IS SCARF
SCARF ANGLE IS 10.0 MILLIRADIANS.
JOINT LENGTH IS 230.0 MILLIPETERS
EPSILON IS 0.0026

X PILLI PETERS	XEAR	ADHEREND MODULUS		ADHESIVE STRESS FACTOR	CHK	TBAR	TBARF	TBARPF
		UPPER GPA	LOWER GPA					
0.2	0.001	3.5	78.0	0.0468	5.0E-05	0.00004	0.04305	0.08583
0.3	0.002	3.5	78.0	0.0469	4.9E-05	0.00009	0.04314	0.08663
0.7	0.003	3.5	78.0	0.0470	5.0E-05	0.00013	0.04323	0.10936
0.9	0.004	3.5	78.0	0.0473	4.9E-05	0.00017	0.04345	0.64577
1.1	0.005	3.5	78.0	0.0509	4.5E-05	0.00022	0.04660	9.50219
1.4	0.006	3.5	78.0	0.1004	5.7E-06	0.00026	0.09237	124.77630
1.6	0.007	3.5	78.0	0.6655	2.6E-04	0.00054	0.612311344.79362	
1.7	0.008	3.5	78.0	6.1316	5.0E-04	0.00280	3.641208888888888	
2.1	0.010	140.0	78.0	4.7e51	1.7E-06	0.00777	4.36758-955.76544	
2.3	0.010	140.0	78.0	3.6872	6.3E-05	0.01173	3.57623-654.46014	
2.5	0.011	140.0	78.0	3.3005	1.3E-07	0.01501	3.03646-441.16e37	
2.8	0.012	140.0	78.0	2.9006	6.2E-06	0.01786	2.66870-304.09946	
3.0	0.013	140.0	78.0	2.6227	1.9E-07	0.02039	2.41276-213.88971	
3.2	0.014	140.0	78.0	2.4251	6.0E-04	0.02271	2.23110-153.35611	
3.4	0.015	140.0	78.0	2.2223	8.7E-07	0.02487	2.09968-112.06466	
3.7	0.016	140.0	78.0	2.1769	2.9E-05	0.02692	2.00275-63.50463	
4.1	0.016	140.0	78.0	2.0599	3.1E-03	0.03091	1.85512-42.03741	
4.6	0.020	140.0	78.0	1.9866	1.2E-03	0.03452	1.82781-26.57125	
5.1	0.022	140.0	78.0	1.5400	4.5E-04	0.03813	1.78476-17.25856	
5.5	0.024	140.0	78.0	1.3091	1.6E-04	0.04167	1.75635-11.62626	
6.0	0.026	140.0	78.0	1.6676	5.0E-05	0.04516	1.73660-6.16501	
6.4	0.028	140.0	78.0	1.6725	1.9E-05	0.04862	1.72269-6.08467	
6.9	0.030	140.0	78.0	1.6606	5.9E-06	0.05206	1.71154-4.77206	
9.2	0.040	140.0	78.0	1.6240	0.0E-01	0.06890	1.67808-2.69156	
13.6	0.080	140.0	78.0	1.7706	1.2E-07	0.10205	1.62968-2.39655	
18.4	0.080	140.0	78.0	1.7119	1.2E-07	0.13413	1.57494-3.41775	
23.0	0.100	140.0	78.0	1.5646	1.7E-05	0.16458	1.43945-13.53054	
27.6	0.120	135.0	78.0	1.0038	3.5E-06	0.18852	0.92345-19.54156	
32.2	0.140	123.5	78.0	0.7331	3.3E-07	0.20417	0.67441-6.77845	
36.6	0.160	112.7	78.0	0.5646	1.1E-07	0.21605	0.51944-7.16616	
41.4	0.180	101.5	78.0	0.4110	0.0E-01	0.22503	0.37811-7.14556	
46.0	0.200	90.4	78.0	0.2415	7.1E-06	0.23109	0.22221-8.99613	
50.6	0.220	79.2	78.0	-0.0439	6.5E-06	0.23326	-0.04036-20.71536	
55.2	0.240	78.0	78.0	0.6917	4.0E-06	0.24199	0.02040-17.96552	
59.6	0.260	78.0	78.0	1.0001	1.0E-06	0.26043	0.97526-2.44056	
64.4	0.280	78.0	78.0	1.0034	5.9E-07	0.28021	0.99666-0.34635	
69.0	0.300	78.0	78.0	1.0667	6.7E-07	0.30019	0.99976-0.05076	
73.6	0.320	78.0	78.0	1.0972	6.5E-07	0.32019	-1.00022-0.00646	
78.2	0.340	78.0	78.0	1.0872	8.1E-07	0.34019	1.00026-0.00041	
82.8	0.360	78.0	78.0	1.0872	6.1E-07	0.36020	1.00024-0.00152	
87.4	0.380	78.0	78.0	1.0872	5.1E-07	0.38020	1.00020-0.00174	
92.0	0.400	78.0	78.0	1.0871	5.7E-07	0.40021	1.00017-0.00263	
96.6	0.420	78.0	78.0	1.0871	6.3E-07	0.42021	1.00012-0.00346	
101.2	0.440	78.0	78.0	1.0869	5.3E-07	0.44021	0.99999-0.01125	
105.8	0.460	78.0	78.0	1.0864	3.7E-07	0.46021	0.99945-0.05377	
110.4	0.480	78.0	78.0	1.0834	4.9E-07	0.48018	0.99665-0.28513	
115.0	0.500	78.0	78.0	1.0672	4.1E-07	0.50000	0.98176-1.54474	

ORIGINAL PAGE IS
OF POOR QUALITY

THE PROGRAM IS SCARFF
SCARF ANGLE IS 10.0 MILLIRADIANS.
JOINT LENGTH IS 230.0 MILLIMETERS
EFFSLCH IS 0.0026

X PILLI PETERS	XPAR	ADHEREND MODULUS UPPER GPA	ADHEREND MODULUS LOWER GPA	ADHESIVE STRESS FACTOR	CNA	FBAR	FBARF	FBARFF
-0.2	0.001	3.5	78.0	0.0469	5.0E-05	0.00004	0.04305	0.08583
0.5	0.002	3.5	78.0	0.0469	4.9E-05	0.00009	0.04314	0.06668
0.7	0.003	3.5	78.0	0.0470	5.0E-05	0.00013	0.04322	0.06634
0.9	0.004	3.5	78.0	0.0471	5.0E-05	0.00017	0.04331	0.06661
1.1	0.005	3.5	78.0	0.0472	5.0E-05	0.00022	0.04340	0.06667
1.4	0.006	3.5	78.0	0.0473	5.0E-05	0.00026	0.04350	0.12750
1.6	0.007	3.5	78.0	0.0476	5.0E-05	0.00030	0.04380	0.63107
1.9	0.008	3.5	78.0	0.0459	4.8E-05	0.00035	0.04592	5.09667
2.1	0.009	3.5	78.0	0.0467	3.7E-05	0.00040	0.06317	40.67653
2.3	0.010	3.5	78.0	0.0452	2.4E-05	0.00051	0.19249	254.94241
2.5	0.011	3.5	78.0	1.1E66	2.0E-04	0.00101	1.075131951.50183	
4.0	0.012	140.0	78.0	7.1E67	1.3E-04	0.00406	6.613520000000000	
3.0	0.013	140.0	78.0	5.74E5	1.4E-05	0.00998	5.288550000000000	
3.2	0.014	140.0	78.0	4.733E6	8.3E-07	0.01477	4.35564-763.94614	
3.4	0.015	140.0	78.0	4.008E6	1.2E-07	0.01871	3.68737-564.83075	
3.7	0.016	140.0	78.0	3.481E6	1.2E-07	0.02221	3.20335-412.15226	
4.1	0.018	140.0	78.0	2.805E3	6.2E-06	0.02793	2.58482-227.12849	
4.6	0.020	140.0	78.0	2.431E6	0.0E-01	0.03272	2.23708-130.33032	
5.1	0.022	140.0	78.0	2.211E2	8.0E-07	0.03698	2.03428-77.62260	
5.5	0.024	140.0	78.0	2.077E3	1.2E-03	0.04091	1.91149-45.45552	
6.0	0.026	140.0	78.0	1.597E3	4.3E-04	0.04466	1.83765-29.64336	
6.4	0.028	140.0	78.0	1.544E3	1.5E-04	0.04821	1.78896-19.80902	
6.9	0.030	140.0	78.0	1.908E3	4.6E-05	0.05182	1.75556-13.64430	
9.2	0.047	140.0	78.0	1.831E3	1.2E-06	0.06695	1.66478-3.87340	
-13.9	0.060	140.0	78.0	1.771E0	0.0E-01	0.10205	1.62935-2.44115	
18.4	0.060	140.0	78.0	1.711E0	0.0E-01	0.13412	1.57464-3.43354	
23.0	0.100	140.0	78.0	1.563E0	4.6E-07	0.16457	1.43842-13.61732	
27.6	0.120	135.0	78.0	1.004E0	3.7E-07	0.18852	0.92420-19.62265	
32.2	0.140	123.9	78.0	0.733E2	3.3E-07	0.20417	0.67450-6.78750	
36.6	0.160	112.7	78.0	0.584E2	1.1E-07	0.21605	0.51945-7.1e934	
-71.4	0.180	101.5	78.0	0.411E0	1.1E-07	0.22503	0.37811-7.14612	
46.0	0.200	90.4	78.0	0.242E1	1.2E-06	0.23109	0.22221-8.99815	
50.6	0.220	79.2	78.0	-0.0435	6.6E-06	0.23326	-0.04038-20.71537	
55.2	0.240	78.0	78.0	0.651E1	4.0E-06	0.24199	0.82046-17.90552	
59.8	0.260	78.0	78.0	1.06E1	1.0E-06	0.26043	0.97526-2.64056	
64.4	0.280	78.0	78.0	1.083E4	5.9E-07	0.28021	0.95666-0.34835	
-29.0	0.300	78.0	78.0	1.08E7	6.7E-17	0.30019	0.99978-0.05079	
73.0	0.320	78.0	78.0	1.087E2	6.5E-17	0.32019	1.00022-0.00646	
78.2	0.340	78.0	78.0	1.087E2	6.1E-07	0.34019	1.00026-0.00041	
82.6	0.360	78.0	78.0	1.087E2	6.1E-07	0.36020	1.00024-0.00151	
87.4	0.380	78.0	78.0	1.087E2	5.1E-07	0.38020	1.00020-0.00174	
92.0	0.400	78.0	78.0	1.087E1	5.7E-07	0.40021	1.00017-0.00203	
-30.6	0.420	78.0	78.0	1.087E1	6.3E-07	0.42021	1.00012-0.00346	
101.2	0.440	78.0	78.0	1.0869	5.3E-07	0.44021	0.99995-0.01125	
105.0	0.460	78.0	78.0	1.0864	3.7E-07	0.46021	0.99945-0.05377	
110.4	0.480	78.0	78.0	1.0834	4.9E-07	0.48018	0.99865-0.28513	
115.0	0.500	78.0	78.0	1.0672	4.1E-07	0.50000	0.98179-1.54474	

ORIGINAL PAGE IS
OF POOR QUALITY

THE PROGRAM IS SCARF4
SCAFF ANGLE IS 10.0 MILLIRADIANS.
JOINT LENGTH IS 230.0 MILLIMETERS
EF&ILCA IS 0.0026

X PILLI PETERS	XBAR	ADHEREND MODULUS		ADHESIVE STRESS FACTOR	CIR	TBAR	TBARF	TBARFF
		UPPER GPA	LOWER GPA					
-0.2	0.001	3.5	78.0	0.0468	5.0E-05	0.00004	-7.04305	0.00583
0.5	0.002	3.5	78.0	0.0469	4.9E-05	0.00009	0.04316	0.00638
0.7	0.003	3.5	78.0	0.0470	5.0E-05	0.00013	0.04322	0.00633
0.9	0.004	3.5	78.0	0.0471	5.0E-05	0.00017	0.04321	0.00638
1.1	0.005	3.5	78.0	0.0472	5.0E-05	0.00022	0.04339	0.00663
1.4	0.006	3.5	78.0	0.0473	5.0E-05	0.00026	0.04348	0.00715
1.6	0.007	3.5	78.0	0.0474	5.0E-05	0.00030	0.04357	0.00666
1.8	0.008	3.5	78.0	0.0475	5.0E-05	0.00035	0.04366	0.00627
2.1	0.009	3.5	78.0	0.0476	5.0E-05	0.00039	0.04377	0.14201
2.3	0.011	3.5	78.0	0.0479	5.0E-05	0.00043	0.04403	0.48160
2.5	0.011	3.5	78.0	0.0481	5.0E-05	0.00048	0.04530	2.69263
2.7	0.012	3.5	78.0	0.0484	4.7E-05	0.00053	0.05276	15.96238
3.0	0.013	3.5	78.0	0.0483	3.0E-05	0.00059	0.08593	90.41363
3.2	0.014	3.5	78.0	0.0487	3.2E-05	0.00078	0.33096	461.84454
3.4	0.015	3.5	78.0	0.0492	1.6E-04	0.00156	1.539372427	90415
3.7	0.016	3.5	78.0	0.0495	2.9E-04	0.00530	7.432530000000000	
4.1	0.018	140.0	78.0	0.4663	1.3E-06	0.01755	5.04735-673.36121	
4.6	0.020	140.0	78.0	0.4383	0.0E-01	0.02619	3.71520-497.64243	
5.1	0.022	140.0	78.0	0.2007	1.2E-07	0.03278	2.94467-292.83075	
5.5	0.024	140.0	78.0	2.7013	0.0E-01	0.03817	2.48521-177.29023	
6.0	0.026	140.0	78.0	2.3983	0.0E-01	0.04284	2.20363-110.16035	
6.4	0.028	140.0	78.0	2.2028	9.2E-07	0.04705	2.02660-70.21026	
6.9	0.030	140.0	78.0	2.0788	3.7E-04	0.05096	1.91250-44.94953	
7.2	0.040	140.0	78.0	1.6574	3.0E-06	0.06880	1.70476-8.09463	
13.4	0.060	140.0	78.0	1.7721	7.4E-07	0.10205	1.63035-2.56643	
16.4	0.080	140.0	78.0	1.7119	3.5E-07	0.13412	1.57490-3.44311	
23.0	0.100	140.0	78.0	1.5634	3.4E-07	0.16457	1.43036-13.62633	
27.8	0.120	135.0	78.0	1.0046	3.5E-06	0.18652	0.92425-19.62662	
32.2	0.140	123.9	78.0	0.7332	4.5E-07	0.20417	0.747450-8.76659	
38.4	0.160	112.7	78.0	0.5646	1.1E-07	0.21605	0.51945-7.16543	
41.4	0.180	101.5	78.0	0.4110	0.0E-01	0.22503	0.37811-7.14613	
46.4	0.200	90.4	78.0	0.2315	1.2E-06	0.23109	0.22221-8.99615	
50.6	0.220	79.2	78.0	-0.0439	6.0E-06	0.23328	-0.04038-20.71537	
55.2	0.240	78.0	78.0	0.8917	4.0E-06	0.24195	0.82040-17.96552	
59.4	0.260	78.0	78.0	1.0601	1.0E-06	0.26043	0.97526-2.44058	
64.4	0.280	78.0	78.0	1.0834	5.0E-07	0.28021	0.95666-0.34635	
79.0	0.300	78.0	78.0	1.0887	8.7E-07	0.30019	0.99978-0.05079	
73.8	0.320	78.0	78.0	1.0872	6.5E-07	0.32019	1.00022-0.00646	
78.2	0.340	78.0	78.0	1.0877	8.1E-07	0.34019	1.00026-0.00041	
82.4	0.360	78.0	78.0	1.0872	6.1E-07	0.36020	1.00024-0.00152	
87.4	0.380	78.0	78.0	1.0872	5.1E-07	0.38020	1.00026-0.00174	
92.0	0.400	78.0	78.0	1.0671	5.7E-07	0.40021	1.00017-0.00203	
96.6	0.420	78.0	78.0	1.0871	6.3E-07	0.42021	1.00012-0.00346	
101.2	0.440	78.0	78.0	1.0869	5.3E-07	0.44021	0.99995-0.01125	
105.8	0.460	78.0	78.0	1.0884	3.7E-07	0.46021	0.99945-0.01177	
110.4	0.480	78.0	78.0	1.0634	4.9E-07	0.48018	0.98669-0.23513	
115.0	0.500	78.0	78.0	1.0672	4.1E-07	0.50000	0.98179-1.54474	

ORIGINAL PAGE IS
OF POOR QUALITY

THE PROGRAM IS SCARF4
SCARF ANGLE IS 20.0 MILLIRADIANS.
JACKET LENGTH IS 115.0 MILLIMETERS
EPSILON IS 0.0051

X PILLOW PETERS	XBAR	ADHEREND MODULUS		ADHESIVE STRENGTH FACTOR	CHK	FBAR	FBARF	FBARFF
		UPPER GPA	LOWER GPA					
0.0	0.000	140.0	78.0	1.5252	3.3E-03	0.00071	1.77481	-2.16448
0.1	0.001	140.0	78.0	1.5275	4.6E-03	0.00177	1.77329	-2.73221
0.2	0.002	140.0	78.0	1.5244	5.0E-03	0.00355	1.77046	-2.89760
0.3	0.003	140.0	78.0	1.5212	5.0E-03	0.00532	1.76752	-2.97167
0.4	0.004	140.0	78.0	1.5180	5.1E-03	0.00708	1.76452	-3.03247
0.5	0.005	140.0	78.0	1.5147	5.1E-03	0.00884	1.76145	-3.09148
0.6	0.006	140.0	78.0	1.5113	5.1E-03	0.01060	1.75833	-3.15339
0.7	0.007	140.0	78.0	1.5076	5.1E-03	0.01236	1.75515	-3.21972
0.8	0.008	140.0	78.0	1.5043	5.1E-03	0.01411	1.75185	-3.29127
0.9	0.009	140.0	78.0	1.5011	5.1E-03	0.01586	1.74856	-3.36578
1.0	0.010	140.0	78.0	1.4979	5.1E-03	0.01761	1.74515	-3.45263
1.1	0.011	140.0	78.0	1.4931	5.0E-03	0.01935	1.74165	-3.54403
1.2	0.012	140.0	78.0	1.4882	5.0E-03	0.02109	1.73806	-3.64267
1.3	0.013	140.0	78.0	1.4832	5.0E-03	0.02283	1.73436	-3.74969
1.4	0.014	140.0	78.0	1.4781	5.0E-03	0.02456	1.73056	-3.86556
1.5	0.015	140.0	78.0	1.4726	5.0E-03	0.02629	1.72663	-3.99072
1.6	0.016	140.0	78.0	1.4674	5.0E-03	0.02802	1.72257	-4.12577
1.7	0.018	140.0	78.0	1.4624	1.2E-07	0.03146	1.71852	-4.19375
1.8	0.020	140.0	78.0	1.4564	0.0E-01	0.03489	1.71487	-4.21053
1.9	0.022	140.0	78.0	1.4503	1.2E-07	0.03832	1.71055	-4.21705
2.0	0.024	140.0	78.0	1.4444	6.2E-08	0.04173	1.70603	-4.30356
2.1	0.026	140.0	78.0	1.4383	1.2E-07	0.04514	1.70135	-4.37142
2.2	0.028	140.0	78.0	1.4324	1.2E-07	0.04854	1.69655	-4.42774
2.3	0.030	140.0	78.0	1.4266	1.2E-07	0.05193	1.69164	-4.42626
2.4	0.040	140.0	78.0	1.4112	6.1E-06	0.06872	1.66626	-4.644674
2.5	0.060	140.0	78.0	1.3745	6.0E-06	0.10147	1.60622	-3.51e37
2.6	0.080	140.0	78.0	1.3458	1.2E-07	0.13276	1.51414	-6.15445
2.7	0.100	140.0	78.0	1.4452	1.1E-07	0.16144	1.32956	-13.49064
2.8	0.120	135.0	78.0	1.4544	2.3E-07	0.18456	0.97001	-16.18037
2.9	0.140	123.0	78.0	0.780E	1.1E-07	0.20124	0.71832	-10.01244
3.0	0.160	112.7	78.0	0.5933	1.1E-07	0.21380	0.54586	-7.54829
3.1	0.180	101.5	78.0	0.4456	0.0E-01	0.22331	0.41015	-6.05016
3.2	0.200	90.4	78.0	0.3349	1.1E-07	0.23042	0.30808	-3.86611
3.3	0.220	79.2	78.0	0.3006	1.1E-07	0.23609	0.27651	1.68039
3.4	0.240	78.0	78.0	0.7715	4.5E-05	0.24611	0.70981	14.58764
3.5	0.260	78.0	78.0	0.5700	1.7E-05	0.26243	0.89235	5.27113
3.6	0.280	78.0	78.0	1.042E	7.6E-06	0.28106	0.95919	1.96009
3.7	0.300	78.0	78.0	1.0695	4.4E-06	0.30053	0.96429	0.74657
3.8	0.320	78.0	78.0	1.0804	3.1E-06	0.32033	0.99393	-0.28978
3.9	0.340	78.0	78.0	1.0645	2.6E-06	0.34025	0.99765	0.11366
4.0	0.360	78.0	78.0	1.0801	2.6E-06	0.36022	0.99916	0.04399
4.1	0.380	78.0	78.0	1.0667	2.4E-06	0.38021	0.99971	0.01501
4.2	0.400	78.0	78.0	1.0868	2.4E-06	0.40021	0.99986	0.00061
4.3	0.420	78.0	78.0	1.0867	2.2E-06	0.42020	0.99975	-0.01147
4.4	0.440	78.0	78.0	1.0863	2.1E-06	0.44020	0.99935	-0.03079
4.5	0.460	78.0	78.0	1.0852	2.0E-06	0.46017	0.99636	-0.07210
4.6	0.480	78.0	78.0	1.0826	1.8E-06	0.48012	0.99612	-0.16680
4.7	0.500	78.0	78.0	1.0771	1.4E-06	0.50000	0.99089	-0.36720

ORIGINAL PAGE IS
OF POOR QUALITY

THE PROGRAM IS SCARF4
SCARF ANGLE IS 20.0 MILLIRADIANS.
SCANT LENGTH IS 773.0 MILLIMETERS
EPSILON IS 0.0051

X PILLI PETERS	XBAR	ADHEREND MODULUS		ADHESIVE STRESS FACTCR	CNR	FBAR	FBARP	FBARPF
		UPPER	LOWER					
0.0	0.000	3.5	78.0	0.0477	2.4E-04	0.00002	0.04392	3.99022
0.1	0.001	3.5	78.0	0.0546	0.8E-04	0.00005	0.05028	20.96873
0.2	0.002	3.5	78.0	0.1367	2.5E-03	0.00012	0.12974	174.19014
0.3	0.003	3.5	78.0	0.4521	4.2E-03	0.00042	0.39991	970.54122
0.4	0.004	3.5	78.0	1.1164	4.2E-03	0.00188	2.868854297.62158	
0.5	0.005	140.0	78.0	2.8092	2.3E-04	0.00460	2.58076-233.17758	
0.7	0.006	140.0	78.0	2.5936	9.3E-05	0.00708	2.38604-102.05951	
0.9	0.007	140.0	78.0	2.4434	6.3E-05	0.00939	2.24753-117.44633	
1.1	0.008	140.0	78.0	2.3329	1.3E-07	0.01158	2.14620-87.91658	
1.3	0.009	140.0	78.0	2.2490	6.3E-08	0.01369	2.06907-67.54741	
1.1	0.010	140.0	78.0	2.1635	0.0E-01	0.01573	2.00917-53.02659	
1.3	0.011	140.0	78.0	2.1132	2.5E-07	0.01771	1.96172-42.46482	
1.4	0.012	140.0	78.0	2.0918	1.9E-07	0.01965	1.92347-34.48019	
1.5	0.013	140.0	78.0	2.0587	4.2E-08	0.02156	1.89217-28.40777	
1.6	0.014	140.0	78.0	2.0265	8.1E-08	0.02344	1.86621-23.69037	
1.7	0.015	140.0	78.0	2.0090	1.8E-03	0.02530	1.84455-19.11616	
1.8	0.016	140.0	78.0	1.9957	1.1E-03	0.02713	1.82677-16.52913	
2.1	0.018	140.0	78.0	1.9522	4.4E-04	0.03075	1.79787-12.61511	
2.3	0.020	140.0	78.0	1.9266	1.7E-04	0.03433	1.77551-9.60511	
2.5	0.022	140.0	78.0	1.9106	8.1E-05	0.03786	1.75771-8.00360	
2.8	0.024	140.0	78.0	1.8947	2.2E-05	0.04136	1.74313-6.65141	
3.0	0.026	140.0	78.0	1.8814	8.8E-06	0.04483	1.73086-5.67757	
3.2	0.028	140.0	78.0	1.8659	2.2E-06	0.04826	1.72025-4.96830	
3.4	0.030	140.0	78.0	1.8557	3.7E-07	0.05172	1.71086-4.44746	
4.6	0.040	140.0	78.0	1.7151	1.9E-07	0.06863	1.67352-3.30727	
6.9	0.060	140.0	78.0	1.7475	6.0E-08	0.10165	1.60764-3.62116	
9.2	0.080	140.0	78.0	1.7462	2.3E-07	0.13276	1.51452-6.17576	
11.5	0.100	140.0	78.0	1.6954	1.4E-06	0.16164	1.32975-13.49252	
13.8	0.120	135.0	78.0	1.6543	1.1E-07	0.18456	0.96997-16.17823	
16.1	0.140	123.5	78.0	0.7908	0.0E-01	0.20124	0.71831-10.01172	
18.4	0.160	112.7	78.0	0.1933	1.1E-07	0.21380	0.54586-7.54644	
20.7	0.180	101.5	78.0	0.4458	0.0E-01	0.22331	0.41015-6.05049	
23.0	0.200	90.4	78.0	0.3349	0.0E-01	0.23042	0.30808-3.88646	
25.3	0.220	79.2	78.0	0.3006	0.0E-01	0.23609	0.27651-1.68040	
27.6	0.240	78.0	78.0	0.7715	4.5E-05	0.24611	0.70961-14.58745	
29.9	0.260	78.0	78.0	0.9700	1.7E-05	0.26243	0.89239-5.27113	
32.2	0.280	78.0	78.0	1.4426	7.6E-06	0.28106	0.95919-1.96049	
34.5	0.300	78.0	78.0	1.6999	4.4E-06	0.30053	0.98426-0.74657	
36.8	0.320	78.0	78.0	1.6004	3.1E-06	0.32033	0.99353-0.4978	
39.1	0.340	78.0	78.0	1.0045	2.8E-06	0.34025	0.99769-0.31388	
41.4	0.360	78.0	78.0	1.0861	2.6E-06	0.36022	0.99916-0.04359	
43.7	0.380	78.0	78.0	1.0867	2.4E-06	0.38021	0.99971-0.01501	
46.0	0.400	78.0	78.0	1.0868	2.4E-06	0.40021	0.99986-0.00061	
48.3	0.420	78.0	78.0	1.0867	2.2E-06	0.42020	0.99975-0.01147	
50.6	0.440	78.0	78.0	1.0863	2.1E-06	0.44020	0.99935-0.03079	
52.9	0.460	78.0	78.0	1.0862	2.0E-06	0.46017	0.99939-0.07210	
55.2	0.480	78.0	78.0	1.0828	1.8E-06	0.48012	0.99612-0.16680	
57.5	0.500	78.0	78.0	1.0771	1.4E-06	0.50000	0.99089-0.38720	

ORIGINAL PAGE IS
OF POOR QUALITY

THE PROGRAM IS SCARF4
 SCARF ANGLE IS 20.0 MILLIRADIANS.
 JOINT LENGTH IS 115.0 MILLIMETERS
 EPSILON IS 0.0051

P ILLI PETERS	ADHESIVE STRENGTH MPA GPA	ADHEREND MODULUS UPPER LOWER GPA GPA		ADHESIVE STRESS FACTOR	TMA	TEAR	TEAR	SCARF
		ADHESIVE MODULUS UPPER GPA	ADHESIVE MODULUS LOWER GPA					
0.1	0.001	3.5	76.0	0.6469	1.9E-04	0.00004	0.04310	0.24374
0.2	0.002	3.5	76.0	0.6476	1.7E-04	0.00009	0.04376	0.40278
0.3	0.003	3.5	76.0	0.6516	9.2E-05	0.00013	0.04743	7.42546
0.5	0.004	3.5	76.0	0.6703	1.4E-04	0.00019	0.06466	32.58732
0.6	0.005	3.5	76.0	0.1452	6.7E-04	0.00028	0.13356	123.37754
0.7	0.006	3.5	76.0	0.4096	1.4E-03	0.00051	0.37682	417.60861
0.8	0.007	3.5	76.0	1.2576	1.9E-03	0.00120	1.15056	1294.61409
0.9	0.008	3.5	76.0	3.7764	2.1E-03	0.00332	3.47426	3740.07642
1.0	0.009	140.0	76.0	3.4224	2.5E-07	0.00682	3.14552	-264.19317
1.1	0.010	140.0	76.0	3.1495	6.3E-06	0.00964	2.85749	-221.25923
1.3	0.011	140.0	76.0	2.5353	1.9E-07	0.01244	2.70041	-175.20128
1.4	0.012	140.0	76.0	2.7644	1.2E-07	0.01505	2.54323	-140.75156
1.5	0.013	140.0	76.0	2.6263	1.2E-07	0.01753	2.41818	-114.50777
1.6	0.014	140.0	76.0	2.9134	6.2E-08	0.01989	2.31225	-94.20003
1.7	0.015	140.0	76.0	2.4200	6.2E-06	0.02216	2.22632	-76.27164
1.8	0.016	140.0	76.0	2.3420	4.2E-06	0.02435	2.15461	-65.62873
2.1	0.018	140.0	76.0	2.2244	2.0E-03	0.02855	2.04645	-46.17466
2.3	0.020	140.0	76.0	2.1375	7.7E-04	0.03256	1.96649	-34.40141
2.5	0.022	140.0	76.0	2.0720	2.5E-04	0.03643	1.50622	-26.25926
2.8	0.024	140.0	76.0	2.0217	1.0E-04	0.04019	1.85989	-20.35633
3.0	0.026	140.0	76.0	1.5622	3.5E-05	0.04387	1.82356	-16.15712
3.2	0.028	140.0	76.0	1.5506	1.1E-05	0.04749	1.79451	-13.05087
3.4	0.030	140.0	76.0	1.5246	3.6E-06	0.05105	1.77062	-10.74666
4.6	0.040	140.0	76.0	1.8437	1.1E-07	0.06835	1.69617	-5.36235
6.9	0.060	140.0	76.0	1.7523	6.0E-06	0.10139	1.61206	-3.54865
9.2	0.080	140.0	76.0	1.6475	0.6E-01	0.13274	1.51568	-6.24417
11.5	0.100	140.0	76.0	1.4459	4.6E-06	0.16144	1.33025	-13.50366
13.8	0.120	135.0	76.0	1.0543	1.1E-07	0.18456	0.96953	-16.17556
16.1	0.140	123.9	76.0	0.7804	0.6E-01	0.20124	0.71629	-10.01057
18.4	0.160	112.7	76.0	0.5533	1.1E-07	0.21380	0.54565	-7.54776
20.7	0.180	101.5	76.0	0.4456	1.1E-07	0.22331	0.41014	-6.05000
23.0	0.200	90.4	76.0	0.3349	1.1E-07	0.23042	0.30866	-3.86604
25.3	0.220	79.2	76.0	0.3006	0.6E-01	0.23609	0.27651	1.66042
27.6	0.240	78.0	76.0	0.7715	4.5E-05	0.24611	0.70981	14.58765
29.9	0.260	76.0	76.0	0.5700	1.7E-05	0.26243	0.86239	5.27113
32.2	0.280	75.0	76.0	1.0426	7.6E-06	0.28106	0.95919	1.96009
34.5	0.300	75.0	76.0	1.0699	4.4E-06	0.30053	0.98429	0.74657
36.8	0.320	75.0	76.0	1.0904	3.1E-06	0.32033	0.99393	0.28978
39.1	0.340	75.0	76.0	1.0845	2.8E-06	0.34025	0.99769	0.11366
41.4	0.360	75.0	76.0	1.0961	2.6E-06	0.36022	0.99916	0.04399
43.7	0.380	75.0	76.0	1.0867	2.4E-06	0.38021	0.99971	0.01501
46.0	0.400	75.0	76.0	1.0868	2.4E-06	0.40021	0.99986	0.00061
48.3	0.420	75.0	76.0	1.0867	2.2E-06	0.42020	0.99975	-0.01147
50.6	0.440	75.0	76.0	1.0863	2.1E-06	0.44020	0.99935	-0.03079
52.9	0.460	75.0	76.0	1.0652	2.0E-06	0.46017	0.99836	-0.07210
55.2	0.480	75.0	76.0	1.0828	1.8E-06	0.48012	0.99612	-0.16660
57.5	0.500	75.0	76.0	1.0771	1.4E-06	0.50000	0.99069	-0.36720

ORIGINAL PAGE IS
OF POOR QUALITY

THE PROGRAM IS SCARF4
SCARF ANGLE IS 20.0 MILLIRADIANS.
JOINT LENGTH IS 115.0 MILLIMETERS
EPSILON IS 0.0051

X	YEAR	ADHEREND MODULUS	ADHESIVE	THK	TBAR	TWRF	TBARPF
PILLI	PETERS	UPPER GPA	LOWER GPA	STRESS FACTOR			
0.1	0.001	3.5	76.0	0.6468	2.0E-04	0.00004	0.04305
0.2	0.002	3.5	76.0	0.6469	2.0E-04	0.00009	0.04315
0.3	0.003	3.5	76.0	0.6471	2.0E-04	0.00013	0.04332
0.5	0.004	3.5	76.0	0.6476	1.9E-04	0.00017	0.04378
0.6	0.005	3.5	76.0	0.6494	1.7E-04	0.00022	0.04540
0.7	0.006	3.5	76.0	0.6553	1.3E-04	0.00026	0.05091
0.8	0.007	3.5	76.0	0.6743	2.3E-05	0.00032	0.06839
0.9	0.008	3.5	76.0	0.1306	2.0E-04	0.00041	0.12012
1.0	0.009	3.5	76.0	0.2672	5.7E-04	0.00059	0.26425
1.1	0.010	3.5	76.0	0.7014	9.0E-04	0.00102	0.64526
1.3	0.011	3.5	76.0	1.7478	1.3E-03	0.00207	1.607981461.05725
1.4	0.012	140.0	76.0	4.2896	1.4E-05	0.00468	3.94636-360.37347
1.5	0.013	140.0	76.0	3.9169	1.3E-06	0.00845	3.60352-306.46376
1.6	0.014	140.0	76.0	3.6131	6.2E-08	0.01191	3.32402-252.83270
1.7	0.015	140.0	76.0	3.3630	1.2E-07	0.01512	3.05388-209.16422
1.8	0.016	140.0	76.0	3.1552	1.9E-07	0.01811	2.9027C-174.48779
2.1	0.018	140.0	76.0	2.8344	6.2E-08	0.02360	2.60762-124.11b6
2.3	0.020	140.0	76.0	2.6034	6.2E-08	0.02860	2.39513-90.54773
2.5	0.022	140.0	76.0	2.4332	0.0E-01	0.03322	2.23846-67.50934
2.6	0.024	140.0	76.0	2.3050	5.2E-04	0.03758	2.12056-50.99434
3.0	0.026	140.0	76.0	2.2073	2.0E-04	0.04172	2.03064-39.52653
3.2	0.028	140.0	76.0	2.1309	7.1E-05	0.04571	1.96043-31.05666
3.4	0.030	140.0	76.0	2.0705	2.5E-05	0.04957	1.90482-24.81536
4.4	0.040	140.0	76.0	1.8967	1.0E-07	0.06771	1.74678-9.95650
6.9	0.060	140.0	76.0	1.7630	1.6E-07	0.10124	1.62195-4.6656
9.2	0.080	140.0	76.0	1.6501	1.2E-07	0.13270	1.51809-6.40917
11.5	0.100	140.0	76.0	1.4465	4.6E-07	0.16142	1.35074-13.55633
13.4	0.120	135.0	76.0	1.0548	1.0E-07	0.18455	0.97036-16.19901
16.1	0.140	123.9	76.0	0.7605	0.0E-01	0.20124	0.71844-10.01664
19.4	0.14	112.7	76.0	0.5934	1.1E-07	0.21380	0.54591-7.56045
20.7	0.	101.5	76.0	0.4456	0.0E-01	0.22331	0.41016-6.05655
23.0	0.200	90.4	76.0	0.3349	0.0E-01	0.23042	0.30806-3.86639
25.3	0.220	79.2	76.0	0.3006	1.1E-07	0.23609	0.27651-1.66029
27.6	0.240	78.0	76.0	0.2715	4.5E-05	0.24611	0.70981-14.56760
29.9	0.260	76.0	76.0	0.5700	1.7E-05	0.26243	0.89235-5.27111
32.2	0.280	76.0	76.0	1.0426	7.6E-06	0.28106	0.95919-1.96008
34.5	0.300	76.0	76.0	1.6695	4.4E-06	0.30053	0.98425-0.74657
36.8	0.320	76.0	76.0	1.0804	3.1E-06	0.32033	0.99393-0.28977
39.1	0.340	76.0	76.0	1.0445	2.0E-06	0.34025	0.99769-0.11366
41.4	0.360	76.0	76.0	1.0861	2.6E-06	0.36022	0.99916-0.04359
43.7	0.380	76.0	76.0	1.0867	2.4E-06	0.38021	0.99971-0.01501
46.0	0.400	76.0	76.0	1.0866	2.4E-06	0.40021	0.99986-0.00061
48.3	0.420	76.0	76.0	1.0867	2.2E-06	0.42020	0.99975-0.01147
50.6	0.440	76.0	76.0	1.0863	2.1E-06	0.44020	0.99935-0.03079
52.9	0.460	76.0	76.0	1.0852	2.0E-06	0.46017	0.99836-0.07210
55.2	0.480	76.0	76.0	1.0826	1.8E-06	0.48012	0.99612-0.16660
57.5	0.500	76.0	76.0	1.0771	1.4E-06	0.50000	0.99089-0.38720

ORIGINAL PAGE IS
OF POOR QUALITY

THE PROGRAM IS SCRF4
SCRF ANGLE IS 20.0 MILLIPACIANS.
JETTY LENGTH IS 115.0 MILLIMETERS
EPSILON IS 0.0051

A PIELI METERS	T-SBAR	ADHEREND MODULUS		ADHESIVE STRESS FACTCR	T-CR	T-SBAR	T-SBARF	T-SARFF
		UPPER GPA	LOWER GPA					
0.1	0.001	3.5	78.0	0.0466	2.0E-04	0.00004	0.04305	0.08597
0.2	0.002	3.5	78.0	0.0469	2.0E-04	0.00009	0.04314	0.08723
0.3	0.003	3.5	78.0	0.0470	2.0E-04	0.00013	0.04323	0.09278
0.5	0.004	3.5	78.0	0.0471	2.0E-04	0.00017	0.04333	0.11515
0.6	0.005	3.5	78.0	0.0473	2.0E-04	0.00022	0.04347	0.19520
0.7	0.006	3.5	78.0	0.0476	2.0E-04	0.00026	0.04377	0.45417
0.8	0.007	3.5	78.0	0.0484	1.9E-04	0.00030	0.04455	1.22536
0.9	0.008	3.5	78.0	0.0507	1.8E-04	0.00035	0.04667	3.37469
1.0	0.009	3.5	78.0	0.0570	1.6E-04	0.00040	0.05244	9.04190
1.1	0.010	3.5	78.0	0.0734	9.7E-05	0.00046	0.06755	23.29253
1.3	0.011	3.5	78.0	0.1146	1.9E-05	0.00054	0.10560	57.70120
1.4	0.012	3.5	78.0	0.2151	2.2E-04	0.00069	0.19750	137.87431
1.5	0.013	3.5	78.0	0.4564	4.8E-04	0.00098	0.41433	318.90079
1.6	0.014	3.5	78.0	0.9894	7.5E-04	0.00160	0.90655	716.30767
1.7	0.015	3.5	78.0	2.1650	9.2E-04	0.00299	1.995491566.95063	
1.8	0.016	3.5	78.0	4.7231	1.0E-03	0.00601	4.345213346.53156	
2.1	0.018	140.0	78.0	4.0154	6.2E-06	0.01401	3.69408-273.37915	
2.3	0.020	140.0	78.0	3.5076	0.0E-01	0.02091	3.22697-198.57476	
2.5	0.022	140.0	78.0	3.1351	1.2E-07	0.02700	2.86427-147.23039	
2.8	0.024	140.0	78.0	2.8565	1.2E-07	0.03290	2.82796-111.12056	
3.0	0.026	140.0	78.0	2.6446	6.2E-08	0.03755	2.43303-85.19917	
3.2	0.028	140.0	78.0	2.4611	6.2E-08	0.04226	2.28253-66.26652	
3.4	0.030	140.0	78.0	2.3530	9.9E-05	0.04671	2.16474-52.10176	
4.5	0.040	140.0	78.0	2.0054	1.8E-07	0.06649	1.8445E-18.66816	
6.9	0.060	140.0	78.0	1.7639	1.8E-07	0.10095	1.64112-6.11077	
9.2	0.080	140.0	78.0	1.5553	1.2E-07	0.13262	1.52288-6.72130	
11.5	0.100	140.0	78.0	1.4460	1.1E-07	0.16135	1.33212-13.63670	
13.8	0.120	135.0	78.0	1.0553	1.1E-07	0.18454	0.97084-16.22519	
16.1	0.140	123.5	78.0	0.7811	0.0E-01	0.20123	0.71861-10.02736	
18.4	0.160	112.7	78.0	0.5935	0.0E-01	0.21380	0.54597-7.55346	
20.7	0.180	101.5	78.0	0.4459	1.1E-07	0.22331	0.41016-6.05264	
23.0	0.200	90.4	78.0	0.3349	1.1E-07	0.23042	0.30809-3.88679	
25.3	0.220	79.2	78.0	0.3066	0.0E-01	0.23609	0.27651-1.66014	
27.6	0.240	78.0	78.0	0.7716	6.5E-05	0.24611	0.70901-14.58755	
29.9	0.260	78.0	78.0	0.5700	1.7E-05	0.26243	0.89239-5.2719	
32.2	0.280	78.0	78.0	1.0426	7.4E-06	0.28106	0.9.915-1.96068	
34.5	0.300	78.0	78.0	1.0699	4.4E-06	0.30053	0.9.429-0.74657	
36.8	0.320	78.0	78.0	1.0804	3.7E-06	0.32033	0.9.939-0.28977	
39.1	0.340	78.0	78.0	1.0845	2.0E-06	0.34025	0.9.9769-0.11366	
41.4	0.360	78.0	78.0	1.0861	2.6E-06	0.36022	0.9.9916-0.04359	
43.7	0.380	78.0	78.0	1.0867	2.4E-06	0.38021	0.9.9971-0.01561	
46.0	0.400	78.0	78.0	1.0866	2.6E-06	0.40021	0.9.9986-0.00061	
48.3	0.420	78.0	78.0	1.0867	2.2E-06	0.42020	0.9.9975-0.01147	
50.6	0.440	78.0	78.0	1.0863	2.1E-06	0.44020	0.9.9935-0.03079	
52.9	0.460	78.0	78.0	1.0852	2.0E-06	0.46017	0.9.983E-0.07210	
55.2	0.480	78.0	78.0	1.082F	1.8E-06	0.48012	0.9.5612-0.16680	
57.5	0.500	78.0	78.0	1.0771	1.4E-06	0.50000	0.9.9089-0.36720	

ORIGINAL PAGE IS
OF POOR QUALITY

THE PROGRAM IS SCARF3
SCARF ANGLE IS 40.0 MILLIRADIANS.
JOINT LENGTH IS 57.5 MILLIMETERS
EPSILON IS 0.0102

X MILLI- PETERS	XBAR	ADHEREND PROFILES		ADHESIVE STRESS FACTOR	CHR	FBAR	FBARF	FBARFF
		UPPER GPA	LOWER GPA					
0.0	0.000	140.0	78.0	1.8860	0.0E-01	0.00000	1.73497	-2.89507
0.1	0.001	140.0	78.0	1.8826	1.3E-07	0.00173	1.7320e	-2.91060
0.1	0.002	140.0	78.0	1.8796	6.3E-08	0.00346	1.72914	-2.92705
0.2	0.003	140.0	78.0	1.8764	0.0E-01	0.00519	1.72621	-2.94364
0.2	0.004	140.0	78.0	1.8732	6.3E-08	0.00692	1.72326	-2.96117
0.3	0.005	140.0	78.0	1.8700	1.3E-07	0.00864	1.72025	-2.97905
0.3	0.006	140.0	78.0	1.8666	1.9E-07	0.01036	1.71730	-2.95752
0.4	0.007	140.0	78.0	1.8635	0.0E-01	0.01207	1.71429	-3.01e5t
0.5	0.008	140.0	78.0	1.8602	1.9E-07	0.01379	1.7112t	-3.03e5t
0.5	0.009	140.0	78.0	1.8569	6.3E-08	0.01550	1.70822	-3.05e4t
0.6	0.010	140.0	78.0	1.8536	6.3E-08	0.01720	1.70515	-3.07719
0.6	0.011	140.0	78.0	1.8504	1.3E-07	0.01891	1.70206	-3.0967t
0.7	0.012	140.0	78.0	1.8466	6.2E-08	0.02061	1.69955	-3.12051
0.7	0.013	140.0	78.0	1.8434	1.2E-07	0.02230	1.69562	-3.14371
0.8	0.014	140.0	78.0	1.8400	0.0E-01	0.02400	1.89267	-3.16716
0.4	0.015	140.0	78.0	1.8365	6.2E-08	0.02569	1.69495	-3.19133
0.6	0.016	140.0	78.0	1.8330	0.0E-01	0.02738	1.68628	-3.21618
1.0	0.018	140.0	78.0	1.8260	0.0E-01	0.03074	1.67960	-3.26605
1.1	0.020	140.0	78.0	1.8166	6.2E-08	0.03410	1.67321	-3.32252
1.3	0.022	140.0	78.0	1.8115	0.0E-01	0.03744	1.66891	-3.38050
1.4	0.024	140.0	78.0	1.8041	1.2E-07	0.04076	1.65968	-3.44213
1.5	0.026	140.0	78.0	1.7966	6.2E-08	0.04407	1.65273	-3.50674
1.6	0.028	140.0	78.0	1.7886	6.1E-08	0.04737	1.64565	-3.57467
1.7	0.030	140.0	78.0	1.7816	0.0E-01	0.05066	1.63843	-3.633t1
2.3	0.040	140.0	78.0	1.7354	6.1E-08	0.06685	1.60009	-4.05181
3.4	0.060	140.0	78.0	1.6351	1.2E-07	0.09797	1.50790	-5.26411
4.6	0.080	140.0	78.0	1.5555	0.0E-01	0.12697	1.39495	-7.17405
5.7	0.100	140.0	78.0	1.3157	0.0E-01	0.15305	1.21405	-10.12455
6.9	0.120	135.0	78.0	1.0726	0.0E-01	0.17509	0.96677	-10.78662
8.0	0.140	123.9	78.0	0.6651	0.0E-01	0.19286	0.79951	-6.49428
9.2	0.160	112.7	78.0	0.7145	0.0E-01	0.20738	0.65917	-5.98509
10.3	0.180	101.5	78.0	0.6689	0.0E-01	0.21950	0.56111	-3.67461
11.5	0.200	90.4	78.0	0.5523	0.0E-01	0.23010	0.30808	-1.17067
12.5	0.220	79.2	78.0	0.5663	1.0E-07	0.24027	0.52276	2.97741
13.8	0.240	78.0	78.0	0.7639	3.9E-04	0.25252	0.70272	7.54267
14.9	0.260	78.0	78.0	0.6510	2.0E-04	0.26785	0.81970	4.44515
16.1	0.280	78.0	78.0	0.5666	1.1E-04	0.28500	0.88919	2.66376
17.2	0.300	78.0	78.0	1.0121	6.0E-05	0.30323	0.93111	1.61054
19.4	0.320	78.0	78.0	1.6400	4.3E-05	0.32213	0.95672	0.99532
19.5	0.340	78.0	78.0	1.5572	2.9E-05	0.34144	0.97254	0.61709
20.7	0.360	78.0	78.0	1.6679	2.1E-05	0.36099	0.98237	0.38357
21.6	0.380	78.0	78.0	1.6745	1.6E-05	0.38071	0.98647	0.23756
23.0	0.400	78.0	78.0	1.6786	1.3E-05	0.40052	0.99221	0.14305
24.1	0.420	78.0	78.0	1.6805	1.1E-05	0.42039	0.99440	0.07905
25.3	0.440	78.0	78.0	1.6821	9.4E-06	0.44029	0.99545	0.03153
26.4	0.460	78.0	78.0	1.6824	8.1E-06	0.46020	0.99572	-0.00617
27.6	0.480	78.0	78.0	1.6816	7.1E-06	0.48011	0.99516	-0.04675
28.7	0.500	78.0	78.0	1.6802	5.6E-06	0.50000	0.99371	-0.09787

ORIGINAL PAGE IS
OF POOR QUALITY

THE PROGRAM IS SCARF3
SCARF ANGLE IS 40.0 MILLIRADIANS.
JOINT LENGTH IS 57.5 MILLIMETERS
EPSILON IS 0.0102

X PILLE PETERS	XBAR	ADHEREND MODULUS		ADHESIVE STRESS FACTOR	CHK	FBAR	FBEAR	FBAPP
		UPPER GPA	LOWER GPA					
0.0	0.000	78.0	78.0	0.6711	0.0E+01	0.00000	0.08937	56.53333
0.1	0.001	3.5	78.0	0.1640	0.4E+00	0.00011	0.16924	164.6e127
0.1	0.002	3.5	78.0	0.4694	0.0E+01	0.00039	0.43180	384.28769
0.2	0.003	3.5	78.0	1.08	3.4E+07	0.00107	1.00070	793.79102
0.2	0.004	3.5	78.0	2.3075	2.8E+07	0.00257	2.122791515.57153	
0.3	0.005	140.0	78.0	2.2352	1.9E+07	0.00466	2.05625	-57.47762
0.3	0.006	140.0	78.0	2.1800	1.3E+07	0.00669	2.00548	-44.92574
0.4	0.007	140.0	78.0	2.1361	0.6E+01	0.00868	1.98508	-36.37762
0.5	0.008	140.0	78.0	2.1001	6.3E+06	0.01063	1.93192	-30.25660
0.5	0.009	140.0	78.0	2.0698	1.3E+07	0.01254	1.90406	-25.65377
0.6	0.010	140.0	78.0	2.0501	1.1E+02	0.01442	1.86555	-20.94215
0.6	0.011	140.0	78.0	2.0266	6.9E+03	0.01629	1.86617	-16.67460
0.7	0.012	140.0	78.0	2.0054	4.3E+03	0.01815	1.84646	-16.76656
0.7	0.013	140.0	78.0	1.9920	2.7E+03	0.01990	1.83254	-15.15550
0.8	0.014	140.0	78.0	1.9763	1.7E+03	0.02182	1.81808	-13.78953
0.9	0.015	140.0	78.0	1.9620	1.0E+03	0.02363	1.80465	-12.62710
0.9	0.016	140.0	78.0	1.9488	6.3E+04	0.02543	1.79277	-11.63327
1.0	0.018	140.0	78.0	1.9253	2.3E+04	0.02699	1.77117	-10.64661
1.1	0.020	140.0	78.0	1.9048	8.4E+03	0.03251	1.75232	-8.86028
1.3	0.022	140.0	78.0	1.8866	2.9E+05	0.03600	1.73554	-7.96265
1.4	0.024	140.0	78.0	1.8701	9.8E+06	0.03946	1.72033	-7.27574
1.5	0.026	140.0	78.0	1.8548	3.0E+06	0.04268	1.70633	-6.74575
1.6	0.028	140.0	78.0	1.8406	1.1E+06	0.04626	1.69327	-6.33454
1.7	0.030	140.0	78.0	1.8272	3.1E+07	0.04966	1.66053	-6.01819
2.3	0.040	140.0	78.0	1.7669	1.2E+07	0.06616	1.62542	-5.27052
3.4	0.060	140.0	78.0	1.6557	1.2E+07	0.09764	1.51855	-5.66464
4.6	0.080	140.0	78.0	1.5109	0.0E+01	0.12678	1.36957	-7.35677
5.7	0.100	140.0	78.0	1.3223	9.0E+06	0.15294	1.21643	-10.21963
6.9	0.120	135.0	78.0	1.0747	1.1E+07	0.17502	0.98867	-10.83665
8.0	0.140	123.5	78.0	0.6703	0.0E+01	0.19262	0.80063	-8.12360
9.2	0.160	112.7	78.0	0.7173	1.1E+07	0.20736	0.65983	-6.00264
10.3	0.180	101.5	78.0	0.6053	1.1E+07	0.21949	0.56051	-3.88463
11.5	0.200	90.4	78.0	0.5526	0.0E+01	0.23009	0.50833	-1.17650
12.6	0.220	79.2	78.0	0.5684	1.0E+07	0.24026	0.52263	2.91373
13.6	0.240	78.0	78.0	0.7640	3.5E+04	0.25252	0.70280	7.54042
14.9	0.260	78.0	78.0	0.6911	2.0E+04	0.26765	0.81975	4.44362
16.1	0.280	78.0	78.0	0.9666	1.7E+04	0.28499	0.88922	2.86296
17.2	0.300	78.0	78.0	1.0122	6.8E+05	0.30323	0.93113	1.61846
18.4	0.320	78.0	78.0	1.0400	4.3E+05	0.32213	0.95674	0.99562
19.5	0.340	78.0	78.0	1.0572	2.9E+05	0.34144	0.97255	0.61650
20.7	0.360	78.0	78.0	1.0779	2.1E+05	0.36099	0.98237	0.38385
21.8	0.380	78.0	78.0	1.0745	1.6E+05	0.38071	0.98847	0.23746
23.0	0.400	78.0	78.0	1.0786	1.3E+05	0.40052	0.99221	0.14300
24.1	0.420	78.0	78.0	1.0805	1.0E+05	0.42039	0.99440	0.0796
25.3	0.440	78.0	78.0	1.0821	9.4E+06	0.44029	0.99549	0.03151
26.4	0.460	78.0	78.0	1.0824	8.1E+06	0.46020	0.99572	-0.00869
27.6	0.480	78.0	78.0	1.0818	7.1E+06	0.48011	0.99516	-0.04875
28.7	0.500	78.0	78.0	1.0802	5.8E+06	0.50000	0.99371	-0.09787

ORIGINAL PAGE IS
OF POOR QUALITY

THE PROGRAM IS SCARF3
SCARF ANGLE IS 30.0 MILLIRADIANS.
JILIT LENGTH IS 57.5 MILLIMETERS
EPSILON IS 0.0102

PILLI PETERS	XBAR	ADHEREND MODULUS		ADHESIVE STRENGTH FACTOR	CHK	FBAR	FBARP	FBARPF
		UPPER GPA	LOWER GPA					
0.0	0.000	3.5	78.0	0.0491	0.0E-01	0.00000	0.04317	5.57772
0.1	0.001	3.5	78.0	0.0602	6.1E-08	0.00005	0.05536	16.11747
0.1	0.002	3.5	78.0	0.0880	0.0E-01	0.00012	0.08098	37.46630
0.2	0.003	3.5	78.0	0.1463	4.9E-07	0.00022	0.13641	77.30623
0.2	0.004	3.5	78.0	0.2670	3.0E-08	0.00041	0.24566	147.53252
0.3	0.005	3.5	78.0	0.4664	6.7E-07	0.00074	0.44750	266.10955
0.3	0.006	3.5	78.0	0.6726	9.7E-07	0.00135	0.80274	459.67726
0.4	0.007	3.5	78.0	1.0265	6.6E-07	0.00243	1.40460	767.06024
0.5	0.008	3.5	78.0	2.6114	5.1E-07	0.00429	2.393141244.03430	
0.5	0.009	140.0	78.0	2.5171	5.4E-06	0.00664	2.31560	-70.92562
0.6	0.010	140.0	78.0	2.4461	3.8E-07	0.00892	2.25021	-60.26572
0.6	0.011	140.0	78.0	2.3652	6.2E-08	0.01115	2.19426	-51.93351
0.7	0.012	140.0	78.0	2.3325	0.0E-01	0.01332	2.14579	-45.25072
0.7	0.013	140.0	78.0	2.2484	0.0E-01	0.01544	2.10335	-39.81758
0.8	0.014	140.0	78.0	2.2456	0.0E-01	0.01752	2.06584	-35.34023
0.9	0.015	140.0	78.0	2.2093	6.2E-08	0.01957	2.03242	-31.60752
0.9	0.016	140.0	78.0	2.1767	6.2E-06	0.02159	2.00243	-28.46420
1.0	0.016	140.0	78.0	2.1205	1.2E-07	0.02554	1.95071	-23.50767
1.1	0.020	140.0	78.0	2.0745	4.9E-04	0.02940	1.90838	-19.75856
1.3	0.022	140.0	78.0	2.0346	1.9E-04	0.03316	1.87174	-16.99500
1.4	0.024	140.0	78.0	2.0001	7.2E-05	0.03689	1.83999	-14.84121
1.5	0.025	140.0	78.0	1.5656	2.6E-05	0.04054	1.81206	-13.14277
1.6	0.026	140.0	78.0	1.5427	9.1E-06	0.04414	1.78719	-11.78963
1.7	0.030	140.0	78.0	1.5163	3.0E-06	0.04769	1.76474	-10.70236
2.3	0.040	140.0	78.0	1.6213	1.2E-07	0.06486	1.67547	-7.66336
3.4	0.060	140.0	78.0	1.5735	1.2E-07	0.09698	1.53965	-6.50337
4.5	0.080	140.0	78.0	1.5224	2.3E-07	0.12643	1.40051	-7.65977
5.7	0.100	140.0	78.0	1.3286	1.1E-07	0.15274	1.22227	-10.37418
6.9	0.120	135.0	78.0	1.0776	0.0E-01	0.17491	0.99154	-10.91743
6.0	0.140	123.5	78.0	0.6721	1.1E-07	0.19275	0.80230	-8.16771
9.2	0.160	112.7	78.0	0.7163	0.0E-01	0.20732	0.66063	-6.02755
10.3	0.160	101.5	78.0	0.6100	1.1E-07	0.21946	0.56112	-3.89951
11.5	0.200	90.4	78.0	0.5530	0.0E-01	0.23007	0.50869	-1.16556
12.6	0.220	79.2	78.0	0.5667	0.0E-01	0.24025	0.52315	2.96620
13.8	0.240	78.0	78.0	0.7641	3.5E-04	0.25251	0.70294	7.53703
14.9	0.260	76.0	78.0	0.6612	2.0E-04	0.26784	0.81984	4.44162
16.1	0.280	78.0	78.0	0.9667	1.1E-04	0.28499	0.88927	-2.66179
17.2	0.300	76.0	78.0	1.0122	6.0E-05	0.30323	0.93116	1.61773
18.4	0.320	76.0	78.0	1.0400	4.3E-05	0.32213	0.95676	0.99457
19.5	0.340	78.0	78.0	1.0572	2.9E-05	0.34144	0.97256	0.61662
20.7	0.360	78.0	78.0	1.0679	2.1E-05	0.36099	0.98238	0.38366
21.8	0.380	78.0	78.0	1.0745	1.6E-05	0.38071	0.98848	0.23737
23.0	0.400	78.0	78.0	1.0706	1.3E-05	0.40052	0.99222	0.14263
24.1	0.420	78.0	78.0	1.0809	1.1E-05	0.42039	0.99440	0.07961
25.3	0.440	78.0	78.0	1.0821	9.6E-06	0.44029	0.99549	0.03166
26.4	0.460	78.0	78.0	1.0824	8.1E-06	0.46020	0.99572	-0.00810
27.5	0.480	78.0	78.0	1.0818	7.1E-06	0.48011	0.99516	-0.04876
28.7	0.500	78.0	78.0	1.0802	5.8E-06	0.50000	0.96371	-0.09187

ORIGINAL PAGE IS
OF POOR QUALITY

THE PROGRAM IS SCARF3
SCARF ANGLE IS 40.0 MILLIRADIANS.
DUCT LENGTH IS 97.5 MILLIMETERS
EPSILON IS 0.0102

X PILLI METERS	XBAR PETERS	ADHERED MODULUS		ADHESIVE STRESS FACTCP	CMA	YBAR	YBARP	YBARPF
		UPPER GPA	LOWER GPA					
0.0	0.000	3.5	78.0	0.6471	0.0E-01	0.00000	0.04335	0.96720
0.1	0.001	3.5	78.0	0.6490	0.0E-01	0.00004	0.04505	2.65921
0.1	0.002	3.5	78.0	0.6535	6.7E-08	0.00009	0.04924	6.08610
0.2	0.003	3.5	78.0	0.6633	8.3E-07	0.00014	0.05821	12.48130
0.2	0.004	3.5	78.0	0.6824	4.6E-07	0.00021	0.07582	23.75320
0.3	0.005	3.5	78.0	0.1177	6.5E-07	0.00030	0.10829	42.78616
0.3	0.006	3.5	78.0	0.1793	3.2E-06	0.00043	0.16536	73.85552
0.4	0.007	3.5	78.0	0.2849	1.9E-06	0.00064	0.26206	123.15385
0.5	0.008	3.5	78.0	0.4574	4.3E-06	0.00098	0.42080	199.75169
0.5	0.009	3.5	78.0	0.7335	1.5E-05	0.00152	0.67481	316.22400
0.6	0.010	3.5	78.0	1.1657	5.8E-05	0.00236	1.07240	450.39600
0.6	0.011	3.5	78.0	1.5254	1.6E-04	0.00373	1.68295	746.92456
0.7	0.012	140.0	78.0	2.8315	7.2E-05	0.00585	2.60404	-88.40742
0.7	0.013	140.0	78.0	2.7416	1.6E-05	0.00841	2.82213	-77.36451
0.8	0.014	140.0	78.0	2.6626	3.0E-06	0.01089	2.44943	-66.29160
0.9	0.015	140.0	78.0	2.5526	4.4E-07	0.01331	2.78504	-60.70456
0.9	0.016	140.0	78.0	2.4332	6.2E-08	0.01567	2.32762	-54.31115
1.0	0.018	140.0	78.0	2.4237	6.2E-08	0.02022	2.22962	-44.21575
1.1	0.020	140.0	78.0	2.33e1	6.2E-06	0.02460	2.14905	-36.70403
1.3	0.022	140.0	78.0	2.2626	1.2E-07	0.02882	2.08161	-30.97960
1.4	0.024	140.0	78.0	2.2005	6.2E-08	0.03293	2.02420	-26.53168
1.5	0.026	140.0	78.0	2.1487	6.2E-08	0.03693	1.97487	-23.01958
1.6	0.026	140.0	78.0	2.0999	1.3E-06	0.04063	1.93174	-20.21026
1.7	0.030	140.0	78.0	2.0586	1.8E-05	0.04466	1.89375	-17.91523
2.3	0.040	140.0	78.0	1.5050	6.1E-06	0.06263	1.75247	-11.35060
3.4	0.060	140.0	78.0	1.7055	6.0E-08	0.09597	1.57261	-7.76547
4.5	0.060	140.0	78.0	1.5396	1.2E-07	0.12560	1.41650	-6.23030
5.7	0.100	140.0	78.0	1.3379	2.3E-07	0.15243	1.23082	-10.62456
6.9	0.120	135.0	78.0	1.6630	0.0E-01	0.17472	0.99629	-11.04765
8.0	0.140	123.5	78.0	0.8751	1.1E-07	0.19265	0.80506	-8.24081
9.2	0.160	112.7	78.0	0.7201	0.0E-01	0.20725	0.66248	-6.06962
10.3	0.180	101.9	78.0	0.6110	0.0E-01	0.21942	0.56211	-3.92469
11.5	0.200	90.4	78.0	0.5536	1.1E-07	0.23005	0.50930	-1.20058
12.6	0.220	79.2	78.0	0.5851	1.0E-07	0.26024	0.52352	2.95904
13.8	0.240	78.0	78.0	0.7644	3.5E-04	0.25250	0.70316	7.53141
14.9	0.260	78.0	78.0	0.8913	2.0E-04	0.26784	0.81997	4.43851
16.1	0.280	76.0	78.0	0.5668	1.1E-04	0.28499	0.86935	2.65980
17.2	0.300	78.0	78.0	1.0123	6.2E-05	0.30323	0.93121	1.61652
18.4	0.320	78.0	78.0	1.0401	4.3E-05	0.32213	0.95679	0.99383
19.5	0.340	78.0	78.0	1.3972	2.9E-03	0.34144	0.97258	0.81616
20.7	0.360	78.0	78.0	1.6679	2.1E-05	0.36099	0.98239	0.38339
21.8	0.380	78.0	78.0	1.6705	1.6E-05	0.38071	0.98049	0.23719
23.0	0.400	78.0	78.0	1.6706	1.3E-05	0.40052	0.99222	0.14281
24.1	0.420	78.0	78.0	1.6809	1.1E-05	0.42039	0.99440	0.07894
25.3	0.440	78.0	78.0	1.6821	9.4E-06	0.44029	0.99549	0.03164
26.4	0.460	78.0	78.0	1.6824	8.1E-06	0.46020	0.99572	0.00813
27.6	0.480	78.0	78.0	1.6816	7.1E-06	0.48011	0.99516	-0.04877
28.7	0.500	78.0	78.0	1.6802	3.8E-06	0.50000	0.99372	-0.09787

ORIGINAL PAGE IS
OF POOR QUALITY

THE PROGRAM IS SCARP3
SCARP ANGLE IS 40.0 MILLIRADIANS.
SCARP LENGTH IS 97.8 MILLIMETERS
EPSILON IS 0.0102

PILLI PETERS	T KBAR	ADHEREND MODULUS		ADHESIVE STRESS FACTOR	CHK	T KBAR	T KARP	T KARPFF
		UPPER	LOWER					
		GPA	GPA					
0.0	0.000	3.5	70.0	0.6468	0.0E+01	0.00000	0.04307	0.27265
0.1	0.001	3.5	70.0	0.6473	0.0E+01	0.00004	0.04350	0.63152
0.1	0.002	3.5	70.0	0.6483	0.0E+01	0.00009	0.04446	1.38615
0.2	0.003	3.5	70.0	0.6505	4.1E-07	0.00013	0.04643	2.71405
0.2	0.004	3.5	70.0	0.6546	6.7E-06	0.00018	0.05023	5.10379
0.3	0.005	3.5	70.0	0.6622	0.0E+01	0.00023	0.05710	9.13880
0.3	0.006	3.5	70.0	0.6784	3.4E-06	0.00030	0.06935	15.72577
0.4	0.007	3.5	70.0	0.6977	1.1E-06	0.00038	0.08992	26.18502
0.5	0.008	3.5	70.0	0.1344	6.5E-06	0.00048	0.12364	42.41411
0.5	0.009	3.5	70.0	0.1630	3.6E-05	0.00053	0.17735	67.10052
0.6	0.010	3.5	70.0	0.2647	1.6E-04	0.00085	0.26166	104.00056
0.6	0.011	3.5	70.0	0.4254	5.1E-04	0.00117	0.39133	158.29265
0.7	0.012	3.5	70.0	0.6377	1.3E-03	0.00165	0.56660	237.01466
0.7	0.013	3.5	70.0	0.9529	3.0E-03	0.00237	0.87689	349.52145
0.8	0.014	3.5	70.0	1.4141	6.3E-03	0.00345	1.30092	501.97937
0.9	0.015	3.5	70.0	2.0794	1.2E-02	0.00504	1.91280	727.39235
0.9	0.016	3.5	70.0	3.0247	2.1E-02	0.00736	2.782521026.50745	
1.0	0.018	140.0	70.0	2.8476	0.0E+01	0.01276	2.61988	-73.25926
1.1	0.020	140.0	70.0	2.7030	0.0E+01	0.01786	2.46656	-60.38070
1.3	0.022	140.0	70.0	2.5828	6.2E-08	0.02272	2.37605	-50.55466
1.4	0.024	140.0	70.0	2.4816	8.2E-08	0.02737	2.28269	-42.90667
1.5	0.026	140.0	70.0	2.3951	9.2E-08	0.03186	2.20335	-36.86034
1.6	0.028	140.0	70.0	2.3204	6.1E-08	0.03619	2.13465	-32.06971
1.7	0.030	140.0	70.0	2.2554	3.1E-05	0.04040	2.07484	-28.05173
2.3	0.040	140.0	70.0	2.0225	0.0E+01	0.05998	1.86054	-16.52763
3.4	0.060	140.0	70.0	1.7554	1.2E-07	0.09455	1.81850	-9.54750
4.6	0.080	140.0	70.0	1.5641	0.0E+01	0.12511	1.43867	-6.97946
5.7	0.100	140.0	70.0	1.3595	1.1E-07	0.15199	1.24272	-10.97985
6.9	0.120	135.0	70.0	1.0903	1.1E-07	0.17446	1.00304	-11.23279
7.0	0.140	123.9	70.0	0.8794	1.1E-07	0.19249	0.80903	-8.34474
9.2	0.160	112.7	70.0	0.7227	0.0E+01	0.20715	0.64484	-6.12951
10.3	0.180	101.2	70.0	0.6126	2.2E-07	0.21937	0.56353	-3.96021
11.5	0.200	90.4	70.0	0.5546	1.1E-07	0.23001	0.51016	-1.22233
12.6	0.220	79.2	70.0	0.5697	1.0E-07	0.24022	0.52405	2.94601
13.8	0.240	78.0	70.0	0.7647	3.5E-04	0.25249	0.70347	7.52363
14.9	0.260	78.0	70.0	0.6915	2.0E-04	0.26783	0.82016	4.43381
16.1	0.280	78.0	70.0	0.5665	1.1E-04	0.28498	0.88947	2.65666
17.2	0.300	78.0	70.0	0.4123	6.8E-05	0.30323	0.93120	1.61480
18.4	0.320	78.0	70.0	0.3401	4.3E-05	0.32213	0.95683	0.99277
19.5	0.340	78.0	70.0	0.2573	2.9E-05	0.34143	0.97261	0.81520
20.7	0.360	78.0	70.0	0.1676	2.1E-05	0.36099	0.98241	0.38257
21.8	0.380	78.0	70.0	0.0745	1.0E-05	0.38071	0.98850	0.23693
23.0	0.400	78.0	70.0	0.0766	1.3E-05	0.40052	0.99223	0.14265
24.1	0.420	78.0	70.0	0.0810	1.1E-05	0.42039	0.99441	0.07884
25.3	0.440	78.0	70.0	0.0821	9.4E-06	0.44029	0.99546	0.03177
26.4	0.460	78.0	70.0	0.0824	8.1E-06	0.46020	0.99573	0.00816
27.6	0.480	78.0	70.0	0.0816	7.0E-06	0.48011	0.99516	0.04679
28.7	0.500	78.0	70.0	0.0802	5.8E-06	0.50000	0.98372	0.09787

ORIGINAL PAGE IS
OF POOR QUALITY

THE PROGRAM IS SCARF3
SCARF ANGLE IS 70.0 MILLIRADIANS.
JOINT LENGTH IS 22.0 MILLIMETERS
EPSILON IS 0.0179

X PETERS	XBAR	ADHEREND MODULUS		ADHESIVE STRESS FACTOR	CHK	FBAR	FBAPP	FBARPF
		UPPER GPA	LOWER GPA					
0.0	0.000	140.0	78.0	1.7610	0.0E+01	0.00000	1.81982	-3.50546
0.0	0.001	140.0	78.0	1.7572	0.0E+01	0.00162	1.61630	-3.52167
0.1	0.002	140.0	78.0	1.7534	0.0E+01	0.00323	1.61277	-3.53067
0.1	0.003	140.0	78.0	1.7495	1.0E-07	0.00484	1.60923	-3.53467
0.1	0.004	140.0	78.0	1.7457	0.6E-06	0.00645	1.60566	-3.57149
0.2	0.005	140.0	78.0	1.7418	0.6E-08	0.00805	1.60208	-3.56881
0.2	0.006	140.0	78.0	1.7379	0.0E+01	0.00966	1.59845	-3.60575
0.2	0.007	140.0	78.0	1.7339	9.6E-06	0.01125	1.59487	-3.62320
0.3	0.008	140.0	78.0	1.7300	9.6E-06	0.01284	1.59124	-3.64067
0.3	0.009	140.0	78.0	1.7261	1.0E-07	0.01443	1.56755	-3.65875
0.3	0.010	140.0	78.0	1.7220	2.0E-07	0.01602	1.56392	-3.67686
0.4	0.011	140.0	78.0	1.7180	9.6E-06	0.01760	1.56024	-3.69510
0.4	0.012	140.0	78.0	1.7140	9.5E-06	0.01918	1.57653	-3.71375
0.4	0.013	140.0	78.0	1.7099	9.5E-06	0.02076	1.57281	-3.73254
0.5	0.014	140.0	78.0	1.7059	0.0E+01	0.02233	1.36907	-3.75136
0.5	0.015	140.0	78.0	1.7018	0.0E+01	0.02389	1.56530	-3.77060
0.5	0.016	140.0	78.0	1.6977	0.0E+01	0.02546	1.56182	-3.79026
0.6	0.018	140.0	78.0	1.6936	9.5E-06	0.02697	1.55390	-3.82957
0.7	0.020	140.0	78.0	1.6890	9.5E-06	0.03167	1.54620	-3.87062
0.7	0.022	140.0	78.0	1.6726	9.5E-06	0.03476	1.53642	-3.91225
0.8	0.024	140.0	78.0	1.6640	9.4E-06	0.03783	1.53085	-3.95486
0.9	0.026	140.0	78.0	1.6594	9.4E-06	0.04088	1.52260	-3.99685
0.9	0.028	140.0	78.0	1.6466	9.4E-06	0.04392	1.51456	-4.04326
1.0	0.030	140.0	78.0	1.6376	0.0E+01	0.04694	1.50643	-4.06401
1.1	0.040	140.0	78.0	1.5621	0.0E+01	0.06179	1.46436	-4.32925
2.0	0.060	140.0	78.0	1.4918	0.0E+01	0.09018	1.37216	-4.91257
2.8	0.080	140.0	78.0	1.3774	1.0E-07	0.11659	1.26651	-5.64176
3.3	0.100	140.0	78.0	1.2452	0.6E-06	0.14075	1.14533	-6.54900
3.9	0.120	135.0	78.0	1.0966	0.6E-06	0.16229	1.00865	-6.50746
4.6	0.140	123.5	78.0	0.5697	0.5E-06	0.18125	0.89155	-5.16184
5.2	0.160	112.7	78.0	0.8711	0.4E-06	0.19814	0.80122	-3.86618
5.9	0.180	101.9	78.0	0.6814	0.3E-06	0.21340	0.73716	-2.46973
6.6	0.200	90.4	78.0	0.7644	0.2E-06	0.22783	0.70333	-0.83654
7.2	0.220	79.2	78.0	0.7085	2.0E-07	0.24186	0.70664	1.29116
7.9	0.240	70.0	78.0	0.8446	1.4E-03	0.25680	0.77716	3.24724
8.5	0.260	70.0	78.0	0.9093	9.5E-04	0.27281	0.83270	2.35900
9.2	0.280	70.0	78.0	0.8694	6.6E-04	0.28989	0.87325	1.73200
9.8	0.300	70.0	78.0	0.5619	6.6E-04	0.30767	0.90315	1.26246
10.9	0.320	70.0	78.0	1.0660	3.3E-04	0.32390	0.72536	-0.75545
11.2	0.340	70.0	78.0	1.0241	2.4E-04	0.34464	0.94194	0.71421
11.9	0.360	70.0	78.0	1.0375	1.7E-04	0.36361	0.93433	0.53364
12.5	0.380	70.0	78.0	1.0476	1.3E-04	0.38280	0.96357	0.35626
13.7	0.400	70.0	78.0	1.0590	9.8E-05	0.40216	0.97035	0.25965
13.8	0.420	70.0	78.0	1.0663	7.4E-05	0.42160	0.97530	0.20476
14.9	0.440	70.0	78.0	1.0646	3.9E-05	0.44116	0.97888	0.13452
15.1	0.460	70.0	78.0	1.0673	4.1E-05	0.46074	0.98077	0.07479
15.7	0.480	70.0	78.0	1.0673	2.9E-05	0.48037	0.98171	0.02011
16.4	0.500	70.0	78.0	1.0672	1.0E-05	0.50000	0.98156	-0.03251

ORIGINAL PAGE IS
OF POOR QUALITY

THE PROGRAM IS SCARF3
SCARF ANGLE IS 70.0 MILLIRADIANS.
JOINT LENGTH IS 32.0 MILLIMETERS
EPSILON IS 0.0179

X PILLE PETERS	XBAR	ADHEREND MODULUS		ADHESIVE STRESS TACR	CNR	FBAR	FSCRF	FBARFS
		UPPER GPA	LOWER GPA					
0.0	0.000	3.5	78.0	0.2700	0.0E+01	0.00000	0.24908	170.02386
0.0	0.001	3.5	78.0	0.4974	0.0E+00	0.00035	0.49782	250.48146
0.1	0.002	3.5	78.0	0.8239	0.8E+00	0.00095	0.78787	384.56912
0.1	0.003	3.5	78.0	1.2788	6.6E+00	0.00190	1.17624	487.43695
0.1	0.004	3.5	78.0	1.8944	5.1E+00	0.00335	1.74430	659.01227
0.2	0.005	140.0	78.0	1.8700	0.0E+01	0.00500	1.72354	-16.91134
0.2	0.006	140.0	78.0	1.8591	0.0E+01	0.00680	1.71002	-14.28782
0.2	0.007	140.0	78.0	1.8446	0.0E+01	0.00850	1.69670	-12.45212
0.3	0.008	140.0	78.0	1.8319	0.0E+01	0.01019	1.68495	-11.10417
0.3	0.009	140.0	78.0	1.8204	9.6E+00	0.01187	1.67435	-10.07791
0.3	0.010	140.0	78.0	1.8112	6.7E+00	0.01354	1.66591	-9.00747
0.4	0.011	140.0	78.0	1.8017	4.2E+00	0.01520	1.65718	-8.46254
0.4	0.012	140.0	78.0	1.7927	2.6E+00	0.01685	1.64895	-7.99953
0.4	0.013	140.0	78.0	1.7842	1.6E+00	0.01850	1.64116	-7.66344
0.5	0.014	140.0	78.0	1.7762	1.0E+00	0.02014	1.63373	-7.26385
0.5	0.015	140.0	78.0	1.7684	6.2E+00	0.02177	1.62661	-6.97162
0.5	0.016	140.0	78.0	1.7610	3.8E+00	0.02339	1.61977	-6.71860
0.6	0.018	140.0	78.0	1.7469	1.4E+00	0.02662	1.60677	-6.30731
0.7	0.020	140.0	78.0	1.7335	5.1E+00	0.02982	1.59448	-5.99423
0.7	0.022	140.0	78.0	1.7267	1.0E+00	0.03299	1.58274	-5.75364
0.8	0.024	140.0	78.0	1.7004	5.9E+00	0.03615	1.57143	-5.56553
0.9	0.026	140.0	78.0	1.6865	1.9E+00	0.03924	1.56045	-5.42021
0.9	0.028	140.0	78.0	1.6848	5.6E+00	0.04239	1.54973	-5.30662
1.0	0.030	140.0	78.0	1.6734	2.8E+00	0.04548	1.53921	-5.21912
1.3	0.040	140.0	78.0	1.6180	1.9E+00	0.06062	1.48824	-5.02967
2.0	0.060	140.0	78.0	1.5072	9.1E+00	0.08937	1.36636	-5.24425
2.0	0.080	140.0	78.0	1.3674	0.0E+01	0.11601	1.27611	-5.82639
3.3	0.100	140.0	78.0	1.2526	5.7E+00	0.14032	1.18163	-6.66153
3.9	0.120	139.0	78.0	1.1017	0.0E+01	0.16197	1.01336	-6.58177
4.6	0.140	123.5	78.0	0.5735	1.7E+00	0.16101	0.89539	-5.23376
5.2	0.160	112.7	78.0	0.6738	9.6E+00	0.19795	0.90376	-5.92345
5.9	0.180	101.5	78.0	0.8035	0.0E+01	0.21334	0.73906	-5.51719
6.6	0.200	90.4	78.0	0.7662	8.2E+00	0.22772	0.76475	-5.89740
7.2	0.220	79.2	78.0	0.7656	7.9E+00	0.24178	0.70791	1.27566
7.9	0.240	78.0	78.0	0.8458	1.4E+00	0.25662	0.77796	3.23574
8.5	0.260	78.0	78.0	0.8059	9.5E+00	0.27276	0.83329	2.39057
9.2	0.280	78.0	78.0	0.9499	9.5E+00	0.28983	0.87371	-1.72580
9.8	0.300	78.0	78.0	0.9023	4.6E+00	0.30764	0.90350	1.27767
10.5	0.320	78.0	78.0	1.0603	3.3E+00	0.32594	0.92563	0.95202
11.2	0.340	78.0	78.0	1.0243	2.4E+00	0.34463	0.94215	0.71164
11.8	0.360	78.0	78.0	1.0377	1.7E+00	0.36360	0.96480	0.53171
12.5	0.380	78.0	78.0	1.0477	1.3E+00	0.38279	0.98370	0.39481
13.1	0.400	78.0	78.0	1.0391	9.7E+00	0.40223	0.97049	0.28857
13.6	0.420	78.0	78.0	1.0604	7.4E+00	0.42159	0.97936	0.20400
14.4	0.440	78.0	78.0	1.0641	5.3E+00	0.44114	0.97875	0.13437
15.1	0.460	78.0	78.0	1.0663	4.1E+00	0.46074	0.98063	0.07445
15.7	0.480	78.0	78.0	1.0674	2.9E+00	0.48036	0.98177	0.01954
16.4	0.500	78.0	78.0	1.0672	1.0E+00	0.50000	0.98164	-0.03251

ORIGINAL PAGE IS
OF POOR QUALITY

THE PROGRAM IS SCANF3
BEDRF ANGLE IS 70.0 MILLIRADIANS.
JOINT LENGTH IS 32.0 MILLIMETERS
EPSILON IS 0.0179

X WILEY PETERS	XBAR	ADHEREND MODULUS		ADHESIVE STRESS FACTCR	CNE	PBAR	PBARD	PBARDP
		UPPER GPA	LOWER GPA					
0.0	0.000	78.0	78.0	0.1108	0.0E+01	0.00000	0.10192	88.63881
0.0	0.001	3.5	78.0	0.1786	7.1E-08	0.00013	0.16194	71.62068
0.1	0.002	3.5	78.0	0.2690	8.4E-08	0.00033	0.24742	101.36580
0.1	0.003	3.5	78.0	0.3990	2.3E-08	0.00084	0.36701	139.32670
0.1	0.004	3.5	78.0	0.5785	1.2E-07	0.00171	0.52037	187.20476
0.2	0.005	3.5	78.0	0.8104	1.0E-07	0.00380	0.74538	246.98168
0.2	0.006	3.5	78.0	1.1177	2.1E-08	0.00259	1.02806	320.95746
0.2	0.007	3.4	78.0	1.5144	2.8E-07	0.01089	1.35292	411.79932
0.3	0.008	3.5	78.0	2.0203	6.1E-06	0.00541	1.85831	522.56411
0.3	0.009	140.0	78.0	1.9953	2.9E-08	0.00726	1.83526	21.64555
0.3	0.010	140.0	78.0	1.9730	9.6E-06	0.00908	1.81481	19.35177
0.4	0.011	140.0	78.0	1.9530	9.6E-08	0.01089	1.79641	17.50922
0.4	0.012	180.0	78.0	1.9348	1.9E-07	0.01288	1.77968	16.06183
0.4	0.013	140.0	78.0	1.9181	9.5E-08	0.01445	1.76432	14.74975
0.5	0.014	140.0	78.0	1.9027	9.5E-08	0.01621	1.75011	13.68635
0.5	0.015	140.0	78.0	1.8863	9.5E-08	0.01795	1.73687	12.80039
0.5	0.016	140.0	78.0	1.8746	9.5E-08	0.01968	1.72447	12.03115
0.6	0.018	140.0	78.0	1.8501	9.5E-08	0.02311	1.70171	10.78465
0.7	0.020	140.0	78.0	1.8279	2.8E-04	0.02649	1.688130	9.80911
0.7	0.022	140.0	78.0	1.8074	2.1E-04	0.02983	1.66246	9.06329
0.8	0.024	140.0	78.0	1.7884	4.1E-05	0.03314	1.64495	8.66496
0.8	0.026	140.0	78.0	1.7705	1.5E-05	0.03641	1.62852	7.97974
0.8	0.028	140.0	78.0	1.7536	3.0E-06	0.03965	1.61257	7.50271
1.0	0.030	140.0	78.0	1.7375	1.8E-06	0.04286	1.59814	7.28545
1.3	0.040	140.0	78.0	1.6647	9.3E-08	0.05850	1.531110	6.28357
2.0	0.060	140.0	78.0	1.5351	0.0E+01	0.06792	1.41195	5.83748
2.6	0.080	140.0	78.0	1.4056	9.4E-08	0.11498	1.29283	6.15504
3.3	0.100	140.0	78.0	1.2646	8.8E-06	0.13956	1.16322	6.06046
3.9	0.120	135.0	78.0	1.1116	1.7E-07	0.16141	1.02158	6.71215
4.6	0.140	123.5	78.0	0.9800	1.7E-07	0.18059	0.90141	5.32522
5.2	0.160	212.7	78.0	0.8787	0.0E+01	0.19758	0.80823	3.98939
5.9	0.180	101.5	78.0	0.8071	0.0E+01	0.21310	0.74241	2.56538
6.6	0.200	99.4	78.0	0.7689	0.0E+01	0.22754	0.70726	0.89331
7.2	0.220	79.2	78.0	0.7717	7.9E-08	0.24166	0.70979	1.24647
7.9	0.240	78.0	78.0	0.8473	1.4E-03	0.29652	0.77938	3.21938
8.5	0.260	78.0	78.0	0.9071	9.4E-04	0.27268	0.83434	2.33577
9.2	0.280	78.0	78.0	0.9307	0.9E-04	0.29979	0.87430	1.71393
9.8	0.300	78.0	78.0	0.9829	0.6E-04	0.30759	0.90411	1.26961
10.5	0.320	78.0	78.0	1.0088	0.2E-04	0.32991	0.92010	0.96601
11.2	0.340	78.0	78.0	1.0247	2.4E-04	0.34460	0.94251	0.70713
11.8	0.360	78.0	78.0	1.0380	1.7E-04	0.36358	0.95470	0.52832
12.5	0.380	78.0	78.0	1.0460	1.3E-04	0.38277	0.55393	0.39227
13.1	0.400	78.0	78.0	1.0593	9.7E-05	0.40222	0.57067	0.28669
13.8	0.420	78.0	78.0	1.0606	7.3E-05	0.42159	0.57554	0.20264
14.4	0.440	78.0	78.0	1.0642	5.9E-05	0.44213	0.57880	0.13342
15.1	0.460	78.0	78.0	1.0685	4.1E-05	0.46073	0.58094	0.07385
15.7	0.480	78.0	78.0	1.0675	2.9E-05	0.48036	0.58187	0.01965
16.4	0.500	78.0	78.0	1.0673	1.8E-05	0.50000	0.58174	0.03291

ORIGINAL PAGE IS
OF POOR QUALITY

THE PROGRAM IS SCARF3
SCARF ANGLE IS 70.0 MILLIRADIANS.
UNIT LENGTH IS 22.8 MILLIMETERS
EPSILON IS 0.0179

PILLI PETERS	XBAR	ADHEREND MODULUS UPPER LOWER	ADHESIVE STRESS FACTCP	CMA	XBAR		YBAR	
					GPB	GPB	GPB	GPB
0.0	0.000	3.8	78.0	0.6764	0.0E+01	0.03000	0.86476	17.98083
0.0	0.001	3.8	78.0	0.6944	0.0E+01	0.00000	0.08679	26.45079
0.1	0.002	3.8	78.0	0.61266	9.2E-08	0.00010	0.11849	37.41387
0.1	0.003	3.8	78.0	0.1768	8.4E-08	0.00032	0.15262	51.40489
0.1	0.004	3.8	78.0	0.2419	1.1E-07	0.00091	0.22282	69.05045
0.2	0.005	3.8	78.0	0.3285	1.8E-07	0.00077	0.30210	91.08180
0.2	0.006	3.8	78.0	0.4419	2.0E-07	0.00112	0.46642	118.346C9
0.2	0.007	3.8	78.0	0.5981	1.0E-07	0.00159	0.54095	151.82655
0.3	0.008	3.8	78.0	0.774e	1.5E-07	0.00221	0.71252	192.65710
0.3	0.009	3.8	78.0	1.0102	1.9E-07	0.00303	0.92914	212.14374
0.3	0.010	3.8	78.0	1.3045	1.7E-07	0.00409	1.20020	301.78638
0.4	0.011	3.8	78.0	1.6707	2.5E-07	0.00545	1.53667	373.3C360
0.4	0.012	140.0	78.0	2.1216	3.5E-08	0.00719	1.95141	-26.36821
0.4	0.013	170.0	78.0	2.0942	7.8E-08	0.00913	1.92624	-24.04443
0.5	0.014	140.0	78.0	2.0691	1.4E-08	0.01104	1.90320	-22.08555
0.5	0.015	140.0	78.0	2.0461	9.3E-08	0.01294	1.88197	-20.41740
0.5	0.016	140.0	78.0	2.0247	9.3E-08	0.01481	1.86225	-18.98231
0.6	0.018	140.0	78.0	1.9860	1.9E-07	0.01890	1.82676	-16.65034
0.7	0.020	140.0	78.0	1.9519	9.5E-08	0.02212	1.79534	-14.84856
0.7	0.022	140.0	78.0	1.9212	1.9E-07	0.02568	1.76712	-13.42539
0.8	0.024	140.0	78.0	1.8933	9.4E-08	0.02919	1.74145	-12.28110
0.9	0.026	140.0	78.0	1.8676	1.9E-07	0.03295	1.71785	-11.34767
0.9	0.028	140.0	78.0	1.8438	5.6E-07	0.03606	1.69595	-10.57747
1.0	0.030	140.0	78.0	1.8216	9.3E-07	0.03943	1.67549	-9.92951
1.3	0.040	140.0	78.0	1.7259	0.0E+01	0.05573	1.56750	-7.93073
2.0	0.060	140.0	78.0	1.5715	4.1E-08	0.08602	1.44890	-6.61689
2.6	0.080	140.0	78.0	1.4253	8.4E-09	0.11362	1.31471	-6.50736
3.2	0.100	140.0	78.0	1.2811	1.0E-01	0.13857	1.17833	-7.12259
3.9	0.120	135.0	78.0	1.1224	8.0E-01	0.16067	1.03242	-6.86431
4.5	0.140	123.0	78.0	0.5686	0.3E-01	0.18004	0.90936	-5.44558
5.2	0.160	112.7	78.0	0.8691	0.0E+01	0.19723	0.81413	-4.07621
5.9	0.180	101.2	78.0	0.6119	0.3E-00	0.21279	0.74682	-2.63900
6.6	0.200	96.4	78.0	0.7725	0.0E-01	0.22731	0.71056	-0.94072
7.2	0.220	79.2	78.0	0.7744	7.9E-08	0.24146	0.71227	1.21257
7.6	0.240	78.0	78.0	0.6453	1.4E-03	0.25530	0.78120	3.15881
8.5	0.260	78.0	78.0	0.5086	9.3E-04	0.27150	0.63573	2.31624
9.2	0.280	76.0	78.0	0.9519	6.6E-04	0.28971	0.87955	1.70058
9.7	0.300	76.0	78.0	0.9330	4.3E-04	0.30753	0.90491	1.25916
10.5	0.320	76.0	78.0	1.0075	3.2E-04	0.32586	0.92671	0.938C6
11.2	0.340	76.0	78.0	1.0292	2.3E-04	0.34496	0.94299	-0.70117
11.8	0.360	76.0	78.0	1.0384	1.7E-04	0.36355	0.95516	0.52385
12.5	0.380	76.0	78.0	1.0483	1.3E-04	0.38275	0.96423	-0.10062
13.1	0.400	76.0	78.0	1.0586	9.3E-05	0.40210	0.97051	0.28420
13.8	0.420	76.0	78.0	1.0685	7.3E-05	0.42157	0.97574	0.20063
14.4	0.440	76.0	78.0	1.0644	5.3E-05	0.44112	0.97905	0.13217
15.2	0.460	76.0	78.0	1.0606	4.1E-05	0.46073	0.98109	0.073C6
15.7	0.480	76.0	78.0	1.0676	2.9E-05	0.48036	0.98200	0.01927
16.4	0.500	76.0	78.0	1.0675	1.8E-05	0.50000	0.98467	-0.03251

ORIGINAL PAGE IS
OF POOR QUALITY

THE PROGRAM IS SCARF3
SCARF ANGLE IS 70.0 MILLIRADIANS.
JOINT LENGTH IS 32.8 MILLIMETERS
EPSILON IS 0.0179

X MILLI- METERS	TBARF	ADHEREND MODULUS		ADHESIVE SISSES FACTCF	CHK	TBAR	TBARF	TBARFF
		UPPER GPA	LOWER GPA					
0.0	0.000	3.5	78.0	0.0568	0.0E-01	0.00000	0.05227	7.67462
0.0	0.001	3.5	78.0	0.0670	0.0E-01	0.00006	0.06166	11.26703
0.1	0.002	3.5	78.0	0.0817	0.0E-01	0.00012	0.07515	15.91627
0.1	0.003	3.5	78.0	0.1021	1.3E-07	0.00021	0.09382	21.84973
0.1	0.004	3.5	78.0	0.1298	5.9E-06	0.00031	0.11937	29.33313
0.2	0.005	3.5	78.0	0.1666	1.5E-07	0.00045	0.15320	38.67621
0.2	0.006	3.5	78.0	0.2147	2.2E-07	0.00062	0.19746	50.23873
0.2	0.007	3.5	78.0	0.2768	2.7E-07	0.00085	0.25456	64.43727
0.3	0.008	3.5	78.0	0.3559	2.3E-07	0.00114	0.32737	61.75284
0.3	0.009	3.5	78.0	0.4558	0.0E-01	0.00151	0.41925	102.73927
0.3	0.010	3.5	78.0	0.5605	2.6E-07	0.00199	0.53425	126.03270
0.4	0.011	3.5	78.0	0.7361	1.4E-07	0.00259	0.67703	156.36152
0.4	0.012	3.5	78.0	0.9273	4.0E-07	0.00335	0.85257	194.56021
0.4	0.013	3.5	78.0	1.1616	1.4E-06	0.00431	1.06642	237.57766
0.5	0.014	3.5	78.0	1.4466	1.3E-07	0.00550	1.33075	268.49716
0.5	0.015	3.5	78.0	1.7922	3.1E-07	0.00699	1.64846	346.54742
0.5	0.016	3.5	78.0	2.2085	7.5E-06	0.00862	2.03135	419.12323
0.6	0.016	140.0	78.0	2.1526	0.0E-01	0.01283	1.98014	-23.05686
0.7	0.020	140.0	78.0	2.1041	9.5E-06	0.01675	1.93530	-21.01941
0.7	0.022	140.0	78.0	2.6610	9.5E-06	0.02058	1.05567	-18.77266
0.8	0.024	140.0	78.0	2.0222	9.4E-08	0.02433	1.06000	-16.96150
0.9	0.026	140.0	78.0	1.9870	0.0E-01	0.02802	1.82761	-15.47902
0.9	0.028	140.0	78.0	1.9547	1.9E-07	0.03164	1.79751	-14.25049
1.0	0.030	140.0	78.0	1.9245	1.5E-05	0.03521	1.77049	-13.21378
1.3	0.040	140.0	78.0	1.8012	0.0E-01	0.05232	1.65671	-9.95512
2.0	0.065	140.0	78.0	1.6183	0.0E-01	0.08368	1.48671	-7.57452
2.5	0.080	140.0	78.0	1.4585	0.0E-01	0.11195	1.34157	-7.11652
3.3	0.100	140.0	78.0	1.3012	0.0E-01	0.13734	1.19688	-7.44501
3.9	0.140	135.0	78.0	1.1369	8.6E-06	0.15976	1.04576	-7.05614
4.6	0.140	123.5	78.0	0.9593	8.5E-06	0.17936	0.91914	-5.55457
5.2	0.160	112.7	78.0	0.8930	8.4E-06	0.19672	0.82138	-4.16303
5.9	0.180	101.5	78.0	0.8178	0.0E-01	0.21240	0.75224	-2.70729
6.6	0.210	90.4	78.0	0.7769	8.2E-06	0.22702	0.71463	-0.95905
7.2	0.220	79.2	78.0	0.7777	7.9E-08	0.24124	0.71532	1.16639
7.4	0.240	76.0	78.0	0.6516	1.4E-03	0.25621	0.76347	3.15544
8.5	0.260	78.0	78.0	0.9104	9.3E-04	0.27245	0.83743	2.29721
9.2	0.280	76.0	78.0	0.6533	6.4E-04	0.28961	0.87664	1.66252
9.5	0.300	78.0	78.0	0.9649	4.9E-04	0.30746	0.90585	1.24607
10.5	0.320	76.0	76.0	1.0063	3.2E-04	0.32580	0.92747	0.92829
11.2	0.340	78.0	78.0	1.0258	2.3E-04	0.34092	0.94353	0.99384
11.6	0.360	78.0	78.0	1.0389	1.7E-04	0.36352	0.95562	0.51834
12.5	0.380	78.0	78.0	1.6487	1.3E-04	0.39272	0.98459	0.38479
13.1	0.400	78.0	78.0	1.0559	9.6E-05	0.40208	0.97121	0.28114
13.8	0.420	78.0	78.0	1.0611	7.3E-05	0.42156	0.97598	0.19861
14.4	0.440	78.0	78.0	1.0646	5.5E-05	0.44111	0.97925	0.13062
15.1	0.460	78.0	78.0	1.0666	4.0E-05	0.48072	0.98127	0.07205
15.7	0.480	76.0	76.0	1.0676	2.8E-05	0.48036	0.98217	0.01660
16.4	0.500	78.0	78.0	1.0676	1.8E-05	0.50000	0.98203	-0.03251

ORIGINAL PAGE IS
OF POOR QUALITY

THE PROGRAM IS SCARF3
SCARF ANGLE IS 110.0 MILLIRADIANS.
JOINT LENGTH IS 20.6 MILLIPETERS
EPSILON IS 0.0281

X PETERS	XBAR PETERS	ADHEREND MODULUS		ADHESIVE STRESS FACTOR	CHI	FBAR	FBAR ²	FBARPF
		UPPER GPA	LOWER GPA					
0.0	0.000	140.0	76.0	1.5748	0.0E-01	0.00000	1.44807	-2.97363
0.0	0.001	140.0	78.0	1.5716	0.0E-01	0.00145	1.44509	-2.98036
0.0	0.002	140.0	78.0	1.5683	0.0E-01	0.00289	1.44211	-2.98715
0.1	0.003	140.0	76.0	1.5651	1.2E-07	0.00433	1.43912	-2.99359
0.1	0.004	140.0	78.0	1.5618	0.0E-01	0.00577	1.43612	-3.00067
0.1	0.005	140.0	76.0	1.5586	1.2E-07	0.00720	1.43312	-3.00762
0.1	0.006	140.0	78.0	1.5553	1.2E-07	0.00863	1.43010	-3.01461
0.1	0.007	140.0	76.0	1.5520	0.0E-01	0.0100e	1.42709	-3.02166
0.2	0.008	140.0	78.0	1.5487	0.0E-01	0.01145	1.42406	-3.02856
0.2	0.009	140.0	76.0	1.5454	1.2E-07	0.01291	1.42103	-3.03512
0.2	0.010	140.0	78.0	1.5421	0.0E-01	0.01433	1.41799	-3.04332
0.2	0.011	140.0	78.0	1.5388	0.0E-01	0.01575	1.41494	-3.05059
0.2	0.012	140.0	78.0	1.5355	1.2E-07	0.01716	1.41185	-3.05751
0.3	0.013	140.0	78.0	1.5321	0.0E-01	0.01857	1.40883	-3.06526
0.3	0.014	140.0	78.0	1.5288	1.2E-07	0.01998	1.40576	-3.07271
0.3	0.015	140.0	78.0	1.5255	0.0E-01	0.02138	1.40268	-3.06020
0.3	0.016	140.0	78.0	1.5221	1.2E-07	0.02278	1.39960	-3.08774
0.4	0.018	140.0	78.0	1.5184	1.2E-07	0.02558	1.39341	-3.10259
0.4	0.020	140.0	78.0	1.5066	1.2E-07	0.02836	1.36718	-3.11647
0.5	0.022	140.0	78.0	1.5018	0.0E-01	0.03113	1.36053	-3.13419
0.5	0.024	140.0	78.0	1.4950	1.2E-07	0.03388	1.37465	-3.15013
0.5	0.026	140.0	78.0	1.4661	1.2E-07	0.03662	1.36833	-3.16632
0.6	0.028	140.0	78.0	1.4612	0.0E-01	0.03935	1.36198	-3.18275
0.6	0.030	140.0	78.0	1.4743	1.2E-07	0.04207	1.35560	-3.19656
0.6	0.040	140.0	78.0	1.4350	1.1E-07	0.05547	1.32320	-3.26421
1.2	0.060	140.0	78.0	1.3655	1.1E-07	0.08126	1.25563	-3.47810
1.7	0.090	140.0	78.0	1.2675	1.1E-07	0.10566	1.18388	-3.70187
2.1	0.100	140.0	78.0	1.2043	0.0E-01	0.12856	1.10733	-3.95938
2.5	0.120	135.0	78.0	1.1171	1.1E-07	0.14993	1.02722	-3.81144
2.9	0.140	123.9	76.0	1.0417	0.0E-01	0.16975	0.95766	-3.12334
3.3	0.160	112.7	78.0	0.9815	1.0E-07	0.18833	0.90246	-2.40935
3.7	0.180	101.5	76.0	0.9374	0.0E-01	0.20595	0.86151	-1.63104
4.2	0.200	90.4	78.0	0.9113	0.0E-01	0.22292	0.83797	-0.73635
4.6	0.220	79.2	78.0	0.9066	9.0E-08	0.23960	0.833e1	0.34111
5.0	0.240	78.0	78.0	0.9347	3.4E-03	0.25652	0.85944	1.26341
5.4	0.260	78.0	78.0	0.9553	2.5E-03	0.27394	0.88205	1.01217
5.8	0.280	78.0	78.0	0.9791	1.9E-03	0.29177	0.90025	0.815e5
6.2	0.300	78.0	78.0	0.9951	1.4E-03	0.30993	0.91495	0.65969
6.7	0.320	78.0	78.0	1.0000	1.1E-03	0.32055	0.92688	-0.53417
7.1	0.340	78.0	76.0	1.0185	8.5E-04	0.34699	0.93651	0.43170
7.5	0.360	76.0	78.0	1.0269	6.5E-04	0.36560	0.94427	0.34661
7.9	0.380	78.0	78.0	1.0337	5.0E-04	0.38475	0.95047	0.27534
8.3	0.400	78.0	76.0	1.0390	3.9E-04	0.40381	0.95535	0.21408
8.7	0.420	76.0	78.0	1.0430	2.9E-04	0.42296	0.95906	0.16049
9.2	0.440	78.0	78.0	1.0460	2.2E-04	0.44217	0.96180	0.11250
9.6	0.460	78.0	78.0	1.0480	1.5E-04	0.46142	0.96361	0.06636
10.0	0.480	78.0	78.0	1.0490	9.4E-05	0.48071	0.96456	0.02661
10.4	0.500	76.0	78.0	1.0491	4.3E-05	0.50000	0.96466	-0.01417

ORIGINAL PAGE IS
OF POOR QUALITY

THE PROGRAM IS SCARF3
SCAFF ANGLE IS 110.0 MILLIRADIANS.
JOINT LENGTH IS 20.8 MILLIMETERS
EPSILON IS 0.0281

X MILLI PETERS	YEAR UPPER GPA	ADHEREND MODULUS GPA	ADHESIVE STRENGTH FACTOR	CHA	FEAR		FEARF	FBARPF
					LCBAR GPA	FEAR		
0.0	0.000	3.5	78.0	0.5936	0.0E+01	0.00000	0.54582	168.48077
0.0	0.001	3.5	78.0	0.7928	9.0E-06	0.00063	0.72895	198.32019
0.0	0.002	3.5	78.0	1.0262	5.0E-06	0.00147	0.94361	231.56670
0.1	0.003	3.5	78.0	1.2976	3.4E-05	0.00253	1.19337	268.57858
0.1	0.004	3.5	78.0	1.6116	6.2E-06	0.00367	1.46211	309.60333
0.1	0.005	140.0	78.0	1.6644	0.0E+01	0.00535	1.47529	-6.38652
0.1	0.006	140.0	78.0	1.5976	2.4E-07	0.00682	1.46923	-5.77373
0.1	0.007	140.0	78.0	1.5415	0.0E+01	0.00829	1.46369	-5.34123
0.2	0.008	140.0	78.0	1.5662	0.0E+01	0.00975	1.45881	-5.02120
0.2	0.009	140.0	78.0	1.5805	0.0E+01	0.01120	1.45362	-4.77585
0.2	0.010	140.0	78.0	1.5781	3.6E-03	0.01265	1.44522	-4.51900
0.2	0.011	140.0	78.0	1.5712	2.4E-03	0.01410	1.44477	-4.38640
0.2	0.012	140.0	78.0	1.5655	1.5E-03	0.01554	1.44044	-4.27316
0.3	0.013	140.0	78.0	1.5819	9.1E-04	0.01696	1.43621	-4.17614
0.3	0.014	140.0	78.0	1.5574	5.6E-04	0.01842	1.43268	-4.09265
0.3	0.015	140.0	78.0	1.5530	3.5E-04	0.01985	1.42802	-4.02055
0.3	0.016	140.0	78.0	1.5467	2.1E-04	0.02127	1.42464	-3.95607
0.4	0.018	140.0	78.0	1.5442	7.9E-05	0.02411	1.41623	-3.85636
0.4	0.020	140.0	78.0	1.5319	2.9E-05	0.02694	1.40859	-3.77662
0.5	0.022	140.0	78.0	1.5237	1.0E-05	0.02975	1.40110	-3.71670
0.5	0.024	140.0	78.0	1.5157	3.1E-06	0.03254	1.39371	-3.67226
0.5	0.026	140.0	78.0	1.5076	9.3E-07	0.03532	1.36646	-3.63631
0.6	0.028	140.0	78.0	1.4999	2.3E-07	0.03809	1.37916	-3.60657
0.6	0.030	140.0	78.0	1.4521	0.0E+01	0.04084	1.37196	-3.56743
0.8	0.040	140.0	78.0	1.4533	0.0E+01	0.05438	1.33637	-3.54646
1.2	0.061	140.0	78.0	1.3756	1.1E-07	0.08039	1.26491	-3.62236
1.7	0.080	140.0	78.0	1.2951	1.1E-07	0.10496	1.19086	-3.79307
2.1	0.100	140.0	78.0	1.2102	3.2E-06	0.12600	1.11280	-4.02174
2.5	0.120	135.0	78.0	1.1220	1.1E-07	0.14944	1.03166	-3.85720
2.9	0.140	123.9	78.0	1.0457	0.0E+01	0.16935	0.96151	-3.15908
3.3	0.160	112.7	78.0	0.9647	1.0E-07	0.18800	0.90547	-2.43754
3.7	0.180	101.5	78.0	0.9401	1.0E-07	0.20567	0.66441	-1.65426
4.2	0.200	90.4	78.0	0.9136	0.0E+01	0.22268	0.84005	-0.75754
4.6	0.220	79.2	78.0	0.9065	9.0E-06	0.23940	0.83533	0.32500
5.0	0.240	78.0	78.0	0.9362	3.4E-03	0.25635	0.86087	1.25050
5.4	0.260	76.0	78.0	0.9606	2.5E-03	0.27380	0.86329	1.00162
5.8	0.280	76.0	78.0	0.9802	1.9E-03	0.29105	0.90131	-0.80730
6.2	0.300	78.0	78.0	0.9960	1.4E-03	0.30963	0.91565	0.65253
6.7	0.320	78.0	78.0	1.0088	1.1E-03	0.32827	0.92762	-0.52866
7.1	0.340	78.0	78.0	1.0192	8.4E-04	0.34692	0.93715	0.42725
7.5	0.360	78.0	78.0	1.0275	6.5E-04	0.36574	0.94463	0.34321
7.9	0.380	78.0	78.0	1.0342	5.0E-04	0.38470	0.95097	0.27247
8.3	0.400	78.0	78.0	1.0395	3.9E-04	0.40377	0.95580	0.21182
8.7	0.420	78.0	78.0	1.0435	2.9E-04	0.42293	0.95949	0.15877
9.2	0.440	78.0	78.0	1.0444	2.1E-04	0.44215	0.96218	0.11126
9.6	0.460	78.0	78.0	1.0483	1.5E-04	0.46141	0.96397	0.06757
10.0	0.480	78.0	78.0	1.0494	9.4E-05	0.48070	0.96490	0.02622
10.4	0.500	78.0	78.0	1.0495	4.3E-05	0.50000	0.96502	-0.01417

ORIGINAL PAGE IS
OF POOR QUALITY

THE PROGRAM IS SCARF3
SCARF ANGLE IS 110.0 MILLIRADIANS.
JCINT LENGTH IS 20.8 MILLIMETERS
TFEILCN IS 0.0281

X PILLY PETERS	XBAR	YOUNG'S MODULUS		ADHESIVE STRESS FACTOR	CHK	FBAR	FBARF	FBARFF
		UPPER GPA	LOWER GPA					
0.0	0.000	3.5	78.0	0.3108	0.0E-01	0.00000	-0.28582	01.36806
0.0	0.001	3.5	78.0	0.4070	3.5E-08	0.00033	0.37426	95.77120
0.0	0.002	3.5	78.0	0.5197	7.6E-06	0.00075	0.47792	111.82954
0.1	0.003	3.5	78.0	0.6509	9.9E-06	0.00129	0.59852	129.68430
0.1	0.004	3.5	78.0	0.8025	1.2E-07	0.00196	0.73793	149.46624
0.1	0.005	3.5	78.0	0.9576	3.1E-06	0.00277	0.89819	171.39636
0.1	0.006	3.5	78.0	1.1176	2.1E-07	0.00376	1.06149	195.58630
0.1	0.007	3.5	78.0	1.4031	0.0E-01	0.00494	1.29016	222.23943
0.2	0.008	3.5	78.0	1.6605	7.5E-06	0.00635	1.52665	251.54945
0.2	0.009	140.0	78.0	1.9512	1.7E-06	0.00787	1.51833	-0.16530
0.2	0.010	140.0	78.0	1.6427	1.2E-07	0.00939	1.51047	-7.56027
0.2	0.011	140.0	78.0	1.6347	1.2E-07	0.01089	1.50313	-7.10650
0.2	0.012	140.0	78.0	1.6272	1.2E-07	0.01239	1.49623	-6.71565
0.3	0.013	140.0	78.0	1.6201	0.0E-01	0.01389	1.46966	-6.36689
0.3	0.014	140.0	78.0	1.6133	0.0E-01	0.01537	1.48343	-6.11178
0.3	0.015	140.0	78.0	1.6066	0.0E-01	0.01685	1.47744	-5.87438
0.3	0.016	140.0	78.0	1.6005	0.0E-01	0.01833	1.47167	-5.66913
0.4	0.018	140.0	78.0	1.5965	0.0E-01	0.02126	1.46069	-5.33329
0.4	0.020	140.0	78.0	1.5773	1.7E-04	0.02417	1.45033	-5.06604
0.5	0.022	140.0	78.0	1.5665	6.5E-05	0.02706	1.44041	-4.85972
0.5	0.024	140.0	78.0	1.5461	2.5E-05	0.02993	1.43067	-4.69231
0.6	0.027	140.0	78.0	1.5441	8.7E-06	0.03279	1.42162	-4.55501
0.6	0.028	140.0	78.0	1.5363	3.0E-06	0.03562	1.41263	-4.44140
0.6	0.030	140.0	78.0	1.5267	1.0E-06	0.03844	1.40364	-4.34672
0.6	0.040	140.0	78.0	1.4613	0.0E-01	0.05226	1.36203	-4.05669
1.2	0.050	140.0	78.0	1.3953	1.1E-07	0.07871	1.28301	-3.90268
1.7	0.080	140.0	78.0	1.3059	0.0E-01	0.10359	1.20451	-3.97033
2.1	0.100	140.0	78.0	1.2219	0.0E-01	0.12667	1.12353	-4.14236
2.5	0.120	135.0	78.0	1.1314	0.0E-01	0.14851	1.04031	-3.94576
2.9	0.140	123.5	78.0	1.0534	0.0E-01	0.16857	0.96656	-3.22625
3.3	0.160	112.7	78.0	0.9911	0.0E-01	0.18734	0.91130	-2.49319
3.7	0.180	101.5	78.0	0.9453	0.0E-01	0.20512	0.86924	-1.65920
4.2	0.200	90.4	78.0	0.9179	0.0E-01	0.22223	0.84406	-0.79467
4.6	0.220	79.2	78.0	0.9121	9.8E-06	0.23902	0.83867	0.29363
5.0	0.240	78.0	78.0	0.9392	3.3E-03	0.25603	0.86365	1.22553
5.4	0.260	76.0	78.0	0.9631	2.5E-03	0.27353	0.86562	0.96179
6.2	0.280	76.0	78.0	0.9823	1.8E-03	0.29142	-0.90327	-0.79114
6.2	0.300	76.0	78.0	0.9978	1.4E-03	0.30964	0.91753	0.63963
6.7	0.320	76.0	78.0	1.0104	1.1E-03	0.32811	0.92906	-0.51805
7.1	0.340	76.0	78.0	1.0205	8.2E-04	0.34679	0.93840	0.41863
7.5	0.360	76.0	78.0	1.0287	6.4E-04	0.36563	0.94592	0.33626
7.9	0.380	76.0	78.0	1.0353	4.9E-04	0.38461	0.95193	0.26651
8.3	0.400	76.0	78.0	1.0404	3.8E-04	0.40370	-0.95666	0.20745
8.7	0.420	76.0	78.0	1.0443	2.9E-04	0.42287	0.96026	0.15544
9.2	0.440	76.0	78.0	1.0472	2.1E-04	0.44211	0.96292	0.10885
9.6	0.460	76.0	78.0	1.0491	1.5E-04	0.46138	0.96466	0.06601
10.0	0.480	76.0	78.0	1.0501	9.3E-05	0.48069	0.96557	0.02545
10.4	0.500	76.0	78.0	1.0502	4.3E-05	0.50000	0.96569	-0.01417

ORIGINAL PAGE IS
OF POOR QUALITY

THE PROGRAM IS SCARF3
SCARF ANGLE IS 110.0 MILLIRADIANS.
JOINT LENGTH IS 20.0 MILLIMETERS
EPSILON IS 0.0281

X PILLI PETERS	XBAR GPA	ADHEREND NOCULUS		ADHESIVE STRESE FACIL	CHK	FBAR	FBARF	FBARFF
		UPPER GPA	LOWER GPA					
0.0	0.000	3.5	78.0	0.1922	0.0E-01	0.00000	0.17672	44.81250
0.0	0.001	3.5	78.0	0.2452	1.1E-07	0.00020	0.22542	52.73851
0.0	0.002	3.5	78.0	0.3072	8.8E-08	0.00045	0.28250	61.57452
-0.1	-0.003	3.5	78.0	0.3794	7.8E-08	0.00077	0.34890	71.39982
0.1	0.004	3.5	78.0	0.4429	4.9E-06	0.00115	0.42565	82.29619
0.1	0.005	3.5	78.0	0.5069	1.8E-06	0.00162	0.51388	94.35267
0.1	0.006	3.5	78.0	0.5706	1.6E-06	0.00219	0.61478	107.6635
0.1	0.007	3.5	78.0	0.7935	5.6E-08	0.00286	0.72966	122.32963
0.2	0.016	3.5	78.0	0.5352	3.1E-08	0.00365	0.85992	136.45816
0.2	0.019	3.5	78.0	1.0553	4.5E-08	0.00458	1.00710	156.16327
0.2	0.010	3.5	78.0	1.2755	1.1E-07	0.00567	1.17262	175.56642
0.2	0.011	3.5	78.0	1.4778	6.8E-08	0.00694	1.35884	196.79677
0.2	0.012	140.0	78.0	1.7042	2.0E-05	0.00840	1.56706	-9.78265
0.3	0.013	140.0	78.0	1.6935	4.5E-06	0.00996	1.55759	-9.17572
0.3	0.014	140.0	78.0	1.6942	8.2E-07	0.01151	1.54866	-8.65959
0.3	0.015	140.0	78.0	1.6791	1.2E-07	0.01306	1.34025	-8.21720
0.3	0.016	140.0	78.0	1.6663	1.2E-07	0.01459	1.53223	-7.63347
0.4	0.018	140.0	78.0	1.6500	1.2E-07	0.01764	1.31722	-7.20313
0.4	0.020	140.0	78.0	1.6349	0.0E-01	0.02066	1.50333	-6.70966
0.5	0.022	140.0	78.0	1.6266	1.2E-07	0.02366	1.45932	-6.31337
0.5	0.024	140.0	78.0	1.6074	0.0E-01	0.02662	1.47802	-5.99051
-0.5	-0.026	140.0	78.0	1.5947	1.2E-07	0.02957	1.46632	-5.72441
0.6	0.026	140.0	78.0	1.5825	4.6E-07	0.03249	1.45510	-5.50156
0.6	0.030	140.0	78.0	1.5707	5.4E-06	0.03539	1.44429	-5.31035
0.7	0.040	140.0	78.0	1.51e7	0.0E-01	0.04958	1.39459	-4.70432
1.2	0.080	140.0	78.0	1.4203	0.0E-01	0.07657	1.30598	-4.25853
1.7	0.080	140.0	78.0	1.3226	1.1E-07	0.10165	1.22162	-4.19478
-2.1	-0.100	140.0	78.0	1.2367	1.1E-07	0.12544	1.13712	-4.29567
2.5	0.120	135.0	78.0	1.1433	1.1E-07	0.14732	1.05128	-4.05829
2.4	0.140	123.9	78.0	1.0631	0.0E-01	0.16758	0.97756	-3.31614
3.3	0.160	112.7	78.0	0.5951	0.0E-01	0.18652	0.91871	-2.56340
3.7	0.180	101.5	78.0	0.9520	0.0E-01	0.20443	0.87538	-1.75630
4.2	0.200	90.4	78.0	0.5235	1.0E-07	0.22165	0.84917	-0.84166
-0.6	-0.220	79.2	78.0	0.9167	9.8E-08	0.23853	0.74291	0.25422
5.0	0.240	78.0	78.0	0.5431	3.2E-03	0.25562	0.86716	1.15379
5.4	0.260	78.0	78.0	0.9664	2.4E-03	0.27318	0.88858	0.95634
5.6	0.280	78.0	78.0	0.9851	1.6E-03	0.29113	0.90577	0.77060
6.2	0.300	78.0	78.0	1.0002	1.4E-03	0.30939	0.91966	0.62319
6.7	0.320	78.0	78.0	1.0124	1.0E-03	0.32790	0.93085	0.50454
-7.1	-0.340	78.0	78.0	1.0223	8.0E-04	0.34661	0.93998	-0.40768
7.5	0.360	78.0	78.0	1.0302	6.2E-04	0.36549	0.94731	0.32742
7.9	0.380	78.0	78.0	1.0366	4.8E-04	0.38450	0.95316	0.25984
8.3	0.400	78.0	78.0	1.0416	3.7E-04	0.40361	0.95777	0.20150
8.7	0.420	78.0	78.0	1.0454	2.8E-04	0.42280	0.96129	0.15120
9.1	0.440	78.0	78.0	1.0482	2.1E-04	0.44205	0.96385	0.10579
-9.5	-0.460	78.0	78.0	1.0501	1.3E-04	0.46135	0.96554	0.06402
10.0	0.460	78.0	78.0	1.0510	9.2E-05	0.46067	0.96643	0.02447
10.4	0.500	78.0	78.0	1.0511	4.3E-05	0.50000	0.96653	-0.01417

ORIGINAL PAGE IS
OF POOR QUALITY

THE PROGRAM IS SCARF3
SCARF ANGLE IS 110.0 MILLIRADIANS.
JOINT LENGTH IS 20.0 MILLIMETERS
EPSILON IS 0.0281

X PILLI PETERS	XBAR	ADHEREND MODULUS		ADHESIVE STRESS FACTOR	THK	FBAR	FBARP	FBARPF
		UPPER GPA	LOWER GPA					
0.0	0.000	3.5	78.0	0.1333	0.0E-01	0.00000	0.12261	26.68618
0.0	0.001	3.5	78.0	0.1649	0.3E-08	0.00014	0.15161	31.39976
0.0	0.002	3.5	78.0	0.2018	1.9E-06	0.00030	0.16559	36.65500
0.1	0.003	3.5	78.0	0.2448	5.0E-08	0.00051	0.22312	42.49812
0.1	0.004	3.5	78.0	0.2945	1.5E-06	0.00076	0.27080	48.97645
0.1	0.005	3.5	78.0	0.3516	8.1E-08	0.00105	0.32331	56.14865
0.1	0.006	3.5	78.0	0.4169	2.4E-06	0.00141	0.38335	64.06459
0.1	0.007	3.5	78.0	0.4812	8.7E-08	0.00182	0.45171	72.76724
0.2	0.008	3.5	78.0	0.5755	4.9E-06	0.00231	0.52921	82.37921
0.2	0.009	3.5	78.0	0.6708	7.1E-06	0.00285	0.61676	92.90861
0.2	0.010	3.5	78.0	0.7760	2.4E-06	0.00355	0.71537	104.44825
0.2	0.011	3.5	78.0	0.8983	5.1E-08	0.00432	0.82603	117.07436
0.2	0.012	3.5	78.0	1.0331	1.0E-07	0.00521	0.94951	133.86879
0.3	0.013	3.5	78.0	1.1834	8.3E-06	0.00622	1.08819	145.91824
0.3	0.014	3.5	78.0	1.3599	1.0E-07	0.00739	1.24219	162.31479
0.3	0.015	3.5	78.0	1.5570	2.0E-08	0.00871	1.41330	180.15616
0.3	0.016	3.5	78.0	1.7433	1.3E-07	0.01022	1.60302	199.54556
0.4	0.018	140.0	78.0	1.7219	0.0E-01	0.01341	1.58330	-9.39154
0.4	0.020	140.0	78.0	1.7023	0.0E-01	0.01656	1.56531	-6.62551
0.5	0.022	140.0	78.0	1.6843	0.0E-01	0.01967	1.54870	-8.01022
0.5	0.024	140.0	78.0	1.6674	1.2E-07	0.02275	1.53320	-7.50715
0.5	0.026	140.0	78.0	1.6515	1.2E-07	0.02580	1.51961	-7.08976
0.6	0.026	140.0	78.0	1.6365	0.0E-01	0.02883	1.50480	-6.73921
0.6	0.030	140.0	78.0	1.6222	8.2E-06	0.03182	1.49163	-6.43835
0.6	0.040	140.0	78.0	1.5581	1.1E-07	0.04644	1.43269	-5.46240
1.2	0.060	140.0	78.0	1.4455	0.0E-01	0.07407	1.33285	-4.67506
1.7	0.080	140.0	78.0	1.3506	1.1E-07	0.09961	1.24207	-4.45764
2.1	0.100	140.0	78.0	1.2539	1.1E-07	0.12376	1.15362	-4.47516
2.5	0.120	135.0	78.0	1.1573	1.1E-07	0.14592	1.06413	-4.1904
2.9	0.140	123.9	78.0	1.0746	1.0E-07	0.16642	0.98807	-3.41904
3.3	0.160	112.7	78.0	1.0066	1.0E-07	0.18555	0.92738	-2.64560
3.7	0.180	101.5	78.0	0.9598	0.0E-01	0.20362	0.88257	-1.82316
4.2	0.200	90.4	78.0	0.9300	1.0E-07	0.22097	0.85514	-0.89711
4.6	0.220	79.2	78.0	0.9221	0.0E-01	0.23796	0.84787	0.20765
5.0	0.240	76.0	78.0	0.9476	3.2E-03	0.25514	0.87130	1.15663
5.4	0.260	76.0	78.0	0.9701	2.3E-03	0.27278	0.89204	0.92654
5.6	0.280	76.0	78.0	0.9882	1.7E-03	0.29079	0.90870	0.74656
6.2	0.300	76.0	78.0	1.0029	1.3E-03	0.30911	0.92215	0.60371
6.7	0.320	76.0	78.0	1.0147	1.0E-03	0.32766	0.93303	0.48673
7.1	0.340	76.0	78.0	1.0243	7.0E-04	0.34641	0.94104	0.39465
7.5	0.360	76.0	78.0	1.0320	6.0E-04	0.36532	0.94853	0.31707
7.9	0.380	76.0	78.0	1.0382	4.7E-04	0.38436	0.95460	0.25156
8.3	0.400	76.0	78.0	1.0430	3.6E-04	0.40350	0.95906	0.19540
8.7	0.420	76.0	78.0	1.0467	2.7E-04	0.42272	0.96246	0.14625
9.2	0.440	76.0	78.0	1.0494	2.0E-04	0.44199	0.96494	0.10221
9.6	0.460	76.0	78.0	1.0512	1.4E-04	0.46131	0.96658	0.06170
10.0	0.480	76.0	78.0	1.0521	9.0E-05	0.48065	0.96742	0.02332
10.4	0.500	76.0	78.0	1.0522	4.3E-05	0.50000	0.96751	-0.01417

ORIGINAL PAGE IS
OF POOR QUALITY

THE PROGRAM IS SCARF3
SCARF ANGLE IS 180.0 MILLITRADIANS.
JOINT LENGTH IS 18.2 MILLIMETERS
EPSILON IS 0.0002

Z	XBAR	ADHESIVE MODULUS	ADHESIVE STRESS	CHK	FBAR	FBARF	FBARFF	
PILLE METERS		UPPER GPA	LOWER GPA	FACTOR				
0.0	0.000	140.0	70.0	1.4307	0.0E+01	0.00000	1.32226	-2.21864
0.0	0.001	140.0	70.0	1.4302	1.1E-07	0.00132	1.32004	-2.22165
0.0	0.002	140.0	70.0	1.4300	1.1E-07	0.00264	1.31781	-2.22447
0.0	0.003	140.0	70.0	1.4314	0.0E+01	0.00396	1.31556	-2.22732
0.1	0.004	140.0	70.0	1.4250	2.2E-07	0.00527	1.31336	-2.23010
0.1	0.005	140.0	70.0	1.4265	0.0E+01	0.00658	1.31113	-2.23306
0.1	0.006	140.0	70.0	1.4241	2.2E-07	0.00789	1.30865	-2.23556
0.1	0.007	140.0	70.0	1.4217	1.1E-07	0.00920	1.30666	-2.23867
0.1	0.008	140.0	70.0	1.4152	1.1E-07	0.01051	1.30442	-2.24160
0.1	0.009	140.0	70.0	1.4168	1.1E-07	0.01181	1.30217	-2.24475
0.2	0.010	140.0	70.0	1.4144	0.0E+01	0.01311	1.29953	-2.24772
0.2	0.011	140.0	70.0	1.4119	1.1E-07	0.01441	1.29766	-2.25071
0.2	0.012	140.0	70.0	1.4055	0.0E+01	0.01571	1.29542	-2.25371
0.2	0.013	140.0	70.0	1.4070	1.1E-07	0.01700	1.29317	-2.25674
0.2	0.014	140.0	70.0	1.4046	0.0E+01	0.01829	1.29091	-2.25970
0.2	0.015	140.0	70.0	1.4021	1.1E-07	0.01958	1.28867	-2.26264
0.2	0.016	140.0	70.0	1.3956	1.1E-07	0.02087	1.28626	-2.26552
0.3	0.018	140.0	70.0	1.3947	1.1E-07	0.02344	1.28165	-2.27213
0.3	0.020	140.0	70.0	1.3857	0.0E+01	0.02600	1.27730	-2.27642
0.3	0.022	140.0	70.0	1.3648	0.0E+01	0.02855	1.27273	-2.28479
0.4	0.024	140.0	70.0	1.3798	0.0E+01	0.03109	1.2681	-2.29123
0.4	0.026	140.0	70.0	1.3748	0.0E+01	0.03362	1.26357	-2.29775
0.4	0.028	140.0	70.0	1.3659	0.0E+01	0.03614	1.25897	-2.30434
0.5	0.030	140.0	70.0	1.3648	0.0E+01	0.03866	1.25435	-2.30956
0.6	0.040	140.0	70.0	1.3295	1.1E-07	0.05108	1.23106	-2.34413
0.6	0.060	140.0	70.0	1.2872	1.0E-07	0.07523	1.16346	-2.41944
1.2	0.080	140.0	70.0	1.2341	1.0E-07	0.09881	1.13424	-2.50441
1.5	0.100	140.0	70.0	1.1786	0.0E+01	0.12059	1.08322	-2.55941
1.8	0.120	135.0	70.0	1.1220	9.8E-08	0.14173	1.03120	-2.47655
2.1	0.140	123.9	70.0	1.0726	0.0E+01	0.16189	0.98576	-2.0e317
2.4	0.160	112.7	70.0	1.0324	0.0E+01	0.18122	0.94663	-1.62678
2.7	0.180	101.5	70.0	1.0023	1.9E-07	0.19990	0.92096	-1.1e957
3.0	0.200	90.4	70.0	0.9828	9.4E-08	0.21812	0.90325	-0.60906
3.3	0.220	79.2	70.0	0.9563	1.8E-07	0.23611	0.89727	0.03105
3.6	0.240	78.0	70.0	0.9801	3.3E-03	0.25415	0.90816	0.55522
4.0	0.260	78.0	70.0	0.9992	4.2E-03	0.27242	0.91832	0.46409
4.3	0.280	78.0	70.0	1.0084	3.3E-03	0.29088	0.92683	0.38869
4.6	0.300	78.0	70.0	1.0162	2.6E-03	0.30949	0.93354	0.32661
4.9	0.320	78.0	70.0	1.0227	2.0E-03	0.32823	0.93993	0.27273
5.2	0.340	78.0	70.0	1.0281	1.6E-03	0.34708	0.94492	0.22666
5.5	0.360	78.0	70.0	1.0326	1.3E-03	0.36602	0.94905	0.18716
5.8	0.380	78.0	70.0	1.0363	9.8E-04	0.38503	0.95243	0.15200
6.1	0.400	78.0	70.0	1.0392	7.7E-04	0.40412	0.95515	0.12048
6.4	0.420	78.0	70.0	1.0415	5.9E-04	0.42324	0.95727	0.09175
6.7	0.440	78.0	70.0	1.0432	4.2E-04	0.44240	0.95904	0.06859
7.0	0.460	78.0	70.0	1.0444	3.0E-04	0.46159	0.95985	0.03960
7.3	0.480	78.0	70.0	1.0450	1.9E-04	0.48079	0.96044	0.01561
7.6	0.500	78.0	70.0	1.0451	8.1E-05	0.50000	0.96051	-0.0e618

ORIGINAL PAGE 19
OF POOR QUALITY

THE PROGRAM IS SCARF3
SCARF ANGLE IS 150.0 MILLIRADIANS.
JCINT LENGTH IS 15.2 MILLIMETERS
EPSILON IS 0.0382

X PILLI PETERS	XBAR GPA	ADHEREND MODULUS		ADHESIVE STRESS FACTOR	CHK	FBAR	FBARF	FBARFF
		UPPER GPA	LOWER GPA					
-0.0	0.000	3.5	78.0	0.7987	0.0E-01	0.00000	0.73407	125.04313
0.0	0.001	3.5	78.0	0.8410	6.9E-08	0.00080	0.86486	136.69954
0.0	0.002	3.5	78.0	1.0964	1.4E-07	0.00173	1.00771	149.07153
0.0	0.003	3.5	78.0	1.2657	2.2E-07	0.00282	1.16327	162.15064
0.1	0.004	3.5	78.0	1.4496	1.1E-07	0.00406	1.33235	176.05117
0.1	0.005	140.0	78.0	1.4496	0.0E-01	0.00540	1.32881	-3.40103
0.1	0.006	140.0	78.0	1.4422	1.1E-07	0.00672	1.32551	-3.19662
0.1	0.007	140.0	78.0	1.4364	1.1E-07	0.00805	1.32239	-3.05245
0.1	0.008	140.0	78.0	1.4355	0.0E-01	0.00937	1.31940	-2.94540
0.1	0.009	140.0	78.0	1.4324	1.1E-07	0.01069	1.31649	-2.86316
0.2	0.010	140.0	78.0	1.4254	2.3E-03	0.01200	1.31375	-2.77646
0.2	0.011	140.0	78.0	1.4264	1.4E-03	0.01331	1.31100	-2.73100
0.2	0.012	140.0	78.0	1.4235	9.0E-04	0.01462	1.30829	-2.65366
0.2	0.013	140.0	78.0	1.4205	5.6E-04	0.01593	1.30561	-2.66055
0.2	0.014	140.0	78.0	1.4177	3.9E-04	0.01723	1.30297	-2.63260
0.2	0.015	140.0	78.0	1.4148	2.1E-04	0.01853	1.30034	-2.60846
0.2	0.016	140.0	78.0	1.4120	1.3E-04	0.01983	1.25775	-2.56742
0.3	0.018	140.0	78.0	1.4064	4.9E-05	0.02242	1.29261	-2.55314
0.3	0.020	140.0	78.0	1.4009	1.8E-05	0.02500	1.28753	-2.52657
0.3	0.022	140.0	78.0	1.3554	6.0E-06	0.02757	1.28250	-2.50667
0.4	0.024	140.0	78.0	1.3900	2.2E-06	0.03013	1.27750	-2.49136
0.4	0.026	140.0	78.0	1.3646	1.4E-07	0.03268	1.27253	-2.47942
0.4	0.028	140.0	78.0	1.3792	1.1E-07	0.03522	1.26758	-2.47031
0.5	0.030	140.0	78.0	1.3738	1.1E-07	0.03775	1.26265	-2.46346
0.6	0.040	140.0	78.0	1.3471	1.1E-07	0.05026	1.23810	-2.45160
0.6	0.050	140.0	78.0	1.2935	1.0E-07	0.07453	1.16683	-2.46276
1.2	0.080	140.0	78.0	1.2386	0.0E-01	0.09780	1.13857	-2.54667
1.5	0.100	140.0	78.0	1.1625	1.9E-07	0.12006	1.06664	-2.62986
1.6	0.120	135.0	78.0	1.1254	2.0E-07	0.14127	1.03431	-2.50004
2.1	0.140	123.9	78.0	1.0755	9.7E-06	0.16148	0.98846	-2.08243
2.4	0.160	112.7	78.0	1.0349	9.6E-08	0.18086	0.95116	-1.64251
2.7	0.180	101.5	78.0	1.0043	9.5E-07	0.19959	0.92301	-1.16372
3.0	0.200	90.4	78.0	0.9847	9.4E-06	0.21785	0.90503	-0.62057
3.3	0.220	79.2	78.0	0.9779	9.2E-06	0.23567	0.89882	0.02062
3.6	0.240	78.0	78.0	0.9856	5.4E-03	0.25395	0.90952	0.54651
4.0	0.260	78.0	78.0	1.0005	4.2E-03	0.27224	0.91954	0.45714
4.3	0.280	78.0	78.0	1.0096	3.2E-03	0.29072	0.92791	-0.38305
4.6	0.300	78.0	78.0	1.0172	2.5E-03	0.30935	0.93494	0.32110
4.9	0.320	78.0	78.0	1.0236	2.0E-03	0.32811	0.94082	-0.26661
5.2	0.340	78.0	78.0	1.0290	1.6E-03	0.34697	0.94573	0.22354
5.5	0.360	78.0	78.0	1.0334	1.2E-03	0.36593	0.94980	0.18431
5.6	0.380	78.0	78.0	1.0370	9.7E-04	0.38496	0.95313	0.14967
6.1	0.400	78.0	78.0	1.0400	7.6E-04	0.40403	0.95381	0.11861
6.4	0.420	78.0	78.0	1.0422	5.8E-04	0.42319	0.95790	0.09029
6.7	0.440	78.0	78.0	1.0439	4.3E-04	0.44236	0.95944	0.06403
7.0	0.460	78.0	78.0	1.0450	3.0E-04	0.46156	0.96047	0.03920
7.3	0.480	78.0	78.0	1.0456	1.8E-04	0.48078	0.96101	0.01527
7.6	0.500	78.0	78.0	1.0457	8.1E-05	0.50000	0.96108	-0.00628

ORIGINAL PAGE IS
OF POOR QUALITY

THE PROGRAM IS SCARF3
SCARF ANGLE IS 130.0 MILLIRADIANS.
JOINT LENGTH IS 15.2 MILLIMETERS
EPSILON IS 0.0382

X	XBAR	ADHEREND MODULUS		ADHESIVE	CMK	FBAR	FBARF	FBARFF
PILLE METERS		UPPER	LOWER	SIMPL TACIF				
		GPA	GPA					
0.0	0.000	3.5	78.0	0.9117	0.0E+01	0.00000	0.47034	77.32561
0.0	0.001	3.5	78.0	0.9998	5.7E+08	0.00051	0.55123	84.53104
0.0	0.002	3.5	78.0	0.9955	7.2E+08	0.00110	0.63955	92.17826
0.0	0.003	3.5	78.0	0.9005	5.7E+08	0.00179	0.73574	100.28756
0.1	0.004	3.5	78.0	0.5143	1.1E+07	0.00258	0.84028	106.67951
0.1	0.005	3.5	78.0	1.0376	2.3E+07	0.00346	0.95367	117.97761
0.1	0.006	3.5	78.0	1.1712	5.3E+08	0.00449	1.07641	127.60138
0.1	0.007	3.5	78.0	1.2155	7.5E+08	0.00563	1.20901	137.77637
0.1	0.008	3.5	78.0	1.4712	9.5E+08	0.00691	1.35216	146.52612
0.1	0.009	140.0	78.0	1.4665	9.8E+07	0.00826	1.34763	-4.19564
0.2	0.010	140.0	78.0	1.4620	1.1E+07	0.00961	1.34375	-3.98447
0.2	0.011	140.0	78.0	1.4578	1.1E+07	0.01095	1.33985	-3.81260
0.2	0.012	140.0	78.0	1.4537	0.0E+01	0.01229	1.33611	-3.67066
0.2	0.013	140.0	78.0	1.4498	1.1E+07	0.01362	1.33250	-3.55173
0.2	0.014	140.0	78.0	1.4460	0.0E+01	0.01495	1.32900	-3.45048
0.2	0.015	140.0	78.0	1.4423	0.0E+01	0.01628	1.32560	-3.36352
0.2	0.016	140.0	78.0	1.4387	1.1E+07	0.01760	1.32227	-3.28814
0.3	0.016	140.0	78.0	1.4317	1.1E+07	0.02024	1.31583	-3.16433
0.3	0.020	140.0	78.0	1.4249	1.1E+04	0.02287	1.30961	-3.06476
0.3	0.022	140.0	78.0	1.4163	4.3E+05	0.02548	1.30358	-2.98792
0.4	0.024	140.0	78.0	1.4119	1.6E+05	0.02808	1.29765	-2.92527
0.4	0.026	140.0	78.0	1.4056	5.9E+06	0.03067	1.29165	-2.67365
0.4	0.028	140.0	78.0	1.3954	2.0E+06	0.03325	1.28615	-2.83072
0.5	0.030	140.0	78.0	1.3933	7.5E+07	0.03561	1.28053	-2.75476
0.6	0.040	140.0	78.0	1.3635	1.1E+07	0.04848	1.25321	-2.66251
0.9	0.060	140.0	78.0	1.3061	2.1E+07	0.07302	1.20042	-2.01857
1.2	0.060	140.0	78.0	1.2490	0.0E+01	0.09650	1.14754	-2.63756
1.5	0.100	140.0	78.0	1.1510	0.0E+01	0.11693	1.09466	-2.66523
1.8	0.120	135.0	78.0	1.1326	2.0E+07	0.14028	1.04098	-2.55052
2.1	0.140	123.9	78.0	1.0617	9.7E+06	0.16062	0.99422	-2.12382
2.4	0.160	112.7	78.0	1.0403	0.0E+01	0.18011	0.95615	-1.67756
2.7	0.160	101.5	78.0	1.0090	9.5E+06	0.19893	0.92736	-1.15325
3.0	0.200	90.4	78.0	0.9866	0.0E+01	0.21727	0.90884	-0.64650
3.3	0.220	79.2	78.0	0.9816	9.2E+06	0.23536	0.90215	-0.06176
3.6	0.240	78.0	78.0	0.9928	5.3E+03	0.25350	0.91246	0.52907
4.0	0.260	78.0	78.0	1.0033	4.0E+03	0.27185	0.92215	0.44220
4.5	0.280	78.0	78.0	1.0121	3.1E+03	0.29037	0.93023	0.37051
4.6	0.300	78.0	78.0	1.0195	2.4E+03	0.30905	0.93704	0.31056
4.9	0.320	78.0	78.0	1.0257	1.9E+03	0.32785	0.94273	0.25976
5.2	0.340	78.0	78.0	1.0309	1.5E+03	0.34675	0.94748	0.21615
5.5	0.360	78.0	78.0	1.0352	1.2E+03	0.36574	0.95142	0.17816
5.8	0.380	78.0	78.0	1.0387	9.4E+02	0.38480	0.95464	0.14465
6.1	0.400	78.0	78.0	1.0415	7.4E+02	0.40392	0.95723	0.11456
6.4	0.420	78.0	78.0	1.0437	5.6E+02	0.42309	0.95924	0.08717
6.7	0.440	78.0	78.0	1.0453	4.2E+02	0.44229	0.96073	0.06174
7.0	0.460	78.0	78.0	1.0464	2.9E+02	0.46151	0.96172	0.03770
7.3	0.480	78.0	78.0	1.0469	1.8E+02	0.48075	0.96224	0.01453
7.6	0.500	78.0	78.0	1.0470	8.1E+01	0.50000	0.96230	-0.00826

ORIGINAL PAGE IS
OF POOR QUALITY

THE PROGRAM IS SCARF3
SCARF ANGLE IS 150.0 MILLIRADIANS.
JOINT LENGTH IS 15.2 MILLIMETERS
Epsilon IS 0.0362

X PILLI PETERS	XBAR	ADHEREND MODULUS		ADHESIVE STRENGTH FACTCR	CHK	XBAR	XBARF	XBARFF
		UPPER GPA	LOWER GPA					
0.0	0.000	3.5	70.0	0.3561	0.0E-01	0.00000	0.32733	51.45129
0.1	0.001	3.5	70.0	0.4147	9.7E-06	0.00035	0.38116	56.24300
0.0	0.002	3.5	70.0	0.4786	4.8E-08	0.00076	0.43992	61.32853
0.0	0.003	3.5	70.0	0.5483	1.9E-08	0.00124	0.50372	66.72131
0.1	0.004	3.5	70.0	0.6239	2.6E-07	0.00177	0.57347	72.43532
0.1	0.005	3.5	70.0	0.7060	1.5E-07	0.00238	0.64850	78.46459
0.1	0.006	3.5	70.0	0.7945	7.7E-06	0.00307	0.73055	84.68530
0.1	0.007	3.5	70.0	0.6905	1.1E-07	0.00385	0.81879	91.65177
0.1	0.008	3.5	70.0	0.5944	2.1E-07	0.00471	0.91398	98.80046
0.1	0.009	3.5	70.0	1.1080	2.1E-06	7.00568	1.01552	106.34803
0.2	0.010	3.5	70.0	1.2240	1.6E-07	0.00675	1.12662	114.31171
0.2	0.011	3.5	70.0	1.3545	2.7E-07	0.00793	1.24529	122.70932
0.2	0.012	140.0	70.0	1.4932	1.4E-05	0.00924	1.37239	-4.93226
0.2	0.013	140.0	70.0	1.4860	2.8E-06	0.01061	1.36757	-4.70446
0.2	0.014	140.0	70.0	1.4830	4.3E-07	0.01198	1.36297	-4.51040
0.2	0.015	140.0	70.0	1.4781	1.1E-07	0.01334	1.35854	-4.34329
0.2	0.016	140.0	70.0	1.4735	1.1E-07	0.01469	1.35427	-4.19804
0.3	0.018	140.0	70.0	1.4646	1.1E-07	0.01740	1.34613	-3.95846
0.3	0.020	140.0	70.0	1.4552	0.0E-01	0.02008	1.33841	-3.76962
0.3	0.022	140.0	70.0	1.4462	1.1E-07	0.02275	1.33103	-3.61753
0.4	0.024	140.0	70.0	1.4405	0.0E-01	0.02540	1.32392	-3.49251
0.4	0.026	140.0	70.0	1.4330	1.1E-07	0.02804	1.31704	-3.38933
0.4	0.028	140.0	70.0	1.4257	2.1E-07	0.03067	1.31035	-3.30224
0.5	0.030	140.0	70.0	1.4180	3.6E-06	0.03329	1.30362	-3.22656
0.6	0.040	140.0	70.0	1.3850	0.0E-01	0.04617	1.27291	-2.96441
0.9	0.060	140.0	70.0	1.3225	0.0E-01	0.07105	1.21551	-2.75561
1.2	0.080	140.0	70.0	1.2623	1.0E-07	0.09480	1.16014	-2.75606
1.5	0.100	140.0	70.0	1.2021	0.0E-01	0.11745	1.10485	-2.78049
1.8	0.120	135.0	70.0	1.1421	0.0E-01	0.13099	1.04967	-2.61633
2.1	0.140	123.9	70.0	1.0655	1.9E-07	0.15949	1.00172	-2.17779
2.4	0.160	112.7	70.0	1.0474	0.0E-01	0.17912	0.96267	-1.72276
2.7	0.180	101.5	70.0	1.0152	0.0E-01	0.19806	0.93305	-1.23176
3.0	0.200	90.4	70.0	0.9942	9.4E-06	0.21651	0.91381	-0.67981
3.3	0.220	79.2	70.0	0.9883	1.8E-07	0.23469	0.90650	-0.03100
3.6	0.240	78.0	70.0	0.9670	5.0E-03	0.23291	0.91629	0.50560
4.0	0.260	78.0	70.0	1.0070	3.9E-03	0.27133	0.92555	0.42272
4.3	0.260	78.0	70.0	1.0155	3.0E-03	0.28992	0.93330	0.35416
4.6	0.300	78.0	70.0	1.0225	2.3E-03	0.30866	0.93975	0.29682
4.9	0.340	78.0	70.0	1.0264	1.8E-03	0.32751	0.94523	0.24823
5.2	0.340	78.0	70.0	1.0334	1.5E-03	0.34688	0.94977	0.20691
5.5	0.360	78.0	70.0	1.0375	1.2E-03	0.36549	0.95353	0.17016
5.8	0.380	78.0	70.0	1.0400	9.1E-04	0.38460	0.95860	0.13810
6.1	0.400	78.0	70.0	1.0435	7.1E-04	0.40375	0.95907	0.10933
6.4	0.420	78.0	70.0	1.0496	5.4E-04	0.42296	0.96099	0.08310
6.7	0.440	78.0	70.0	1.0471	4.0E-04	0.44219	0.96241	0.05677
7.0	0.460	78.0	70.0	1.0482	2.8E-04	0.46185	0.96335	0.03575
7.3	0.480	78.0	70.0	1.0467	1.8E-04	0.48072	0.96384	0.01356
7.6	0.500	78.0	70.0	1.0467	8.1E-05	0.50000	0.96390	-0.00826

ORIGINAL PAGE IS
OF POOR QUALITY

THE PROGRAM IS SCARF3
SCARF ANGLE IS 150.0 MILLIRADIANS.
SCARF LENGTH IS 19.2 MILLIMETERS
EPSILON IS 0.0302

X MILLI METERS	XBAR MILLI METERS	ADHEREND MODULUS		ADHESIVE STRESS FACTOR	CHK	FBAR	FBARF	FBARFF
		UPPER GPA	LOWER GPA					
0.0	0.000	3.5	78.0	0.2626	0.0E-01	0.00000	0.24138	35.96040
0.0	0.001	3.5	78.0	0.3035	5.1E-08	0.00026	0.27894	39.24142
0.0	0.002	3.5	78.0	0.3481	9.4E-09	0.00056	0.31994	42.78730
0.0	0.003	3.5	78.0	0.3967	1.1E-07	0.00090	0.36459	46.94742
0.1	0.004	3.5	78.0	0.4455	2.2E-07	0.00129	0.41310	50.53150
0.1	0.005	3.5	78.0	0.5067	1.5E-07	0.00173	0.46573	54.74962
0.1	0.006	3.5	78.0	0.5667	1.0E-07	0.00222	0.52269	59.21222
0.1	0.007	3.5	78.0	0.6357	1.0E-07	0.00278	0.58424	63.93012
0.1	0.008	3.5	78.0	0.7075	6.2E-09	0.00334	0.650E3	68.91451
0.1	0.009	3.5	78.0	0.7857	1.0E-07	0.00408	0.72216	74.17702
0.4	0.010	3.5	78.0	0.8654	5.4E-08	0.00484	0.79509	79.72965
0.2	0.011	3.5	78.0	0.9553	5.1E-08	0.00561	0.86172	85.564E5
0.2	0.012	3.5	78.0	1.0556	1.5E-07	0.00640	0.97036	91.75546
0.2	0.013	3.5	78.0	1.1551	1.0E-07	0.00722	1.06534	98.25461
0.2	0.014	3.5	78.0	1.2597	1.1E-07	0.00874	1.16698	105.09671
0.2	0.015	3.5	78.0	1.3879	1.3E-07	0.00996	1.27585	112.29539
0.2	0.016	3.5	78.0	1.5142	1.0E-07	0.01129	1.36170	119.66560
0.3	0.016	140.0	78.0	1.5932	0.0E-01	0.01406	1.38156	-4.688C7
0.3	0.020	140.0	78.0	1.4926	0.0E-01	0.01682	1.37209	-4.591E6
0.3	0.022	140.0	78.0	1.4832	1.1E-07	0.01955	1.36316	-4.35222
0.4	0.024	140.0	78.0	1.4735	1.1E-07	0.02227	1.35466	-4.15534
0.4	0.026	140.0	78.0	1.4651	0.0E-01	0.02497	1.34652	-3.991C8
0.5	0.030	140.0	78.0	1.4565	1.1E-07	0.02766	1.33868	-3.85234
0.6	0.040	140.0	78.0	1.4463	5.8E-08	0.03033	1.33109	-3.73207
0.8	0.060	140.0	78.0	1.41C1	0.0E-01	0.04346	1.25557	-3.33737
1.2	0.080	140.0	78.0	1.3117	0.0E-01	0.06674	1.22317	-3.00266
1.5	0.100	140.0	78.0	1.2776	1.0E-07	0.09281	1.17441	-2.89475
1.8	0.120	135.0	78.0	1.2151	0.0E-01	0.11572	1.11677	-2.88032
2.1	0.140	123.9	78.0	1.1532	9.6E-06	0.13749	1.05986	-2.69335
2.4	0.160	112.7	78.0	1.0995	0.0E-01	0.15817	1.01051	-2.24057
2.7	0.180	101.5	78.0	1.0557	0.0E-01	0.17796	0.97030	-1.77570
3.0	0.200	90.4	78.0	1.0224	9.5E-06	0.19705	0.93970	-1.27665
3.3	0.220	79.2	78.0	1.000e	0.0E-01	0.21562	0.91982	-0.71880
3.6	0.240	78.0	78.0	1.001e	4.8E-03	0.25223	0.92076	0.47856
4.0	0.260	78.0	78.0	1.0114	3.7E-03	0.27073	0.92954	0.39951
4.3	0.280	78.0	78.0	1.0153	2.0E-03	0.28940	0.93687	0.335C1
4.6	0.300	78.0	78.0	1.0260	2.2E-03	0.30820	0.94311	0.28072
4.9	0.320	78.0	78.0	1.0316	1.0E-03	0.32711	0.94815	0.23472
5.2	0.340	78.0	78.0	1.0393	1.4E-03	0.34612	0.95244	-0.19522
5.5	0.360	78.0	78.0	1.0441	1.1E-03	0.36521	0.95599	0.16062
5.6	0.360	78.0	78.0	1.0433	8.7E-04	0.38436	0.95890	0.13044
6.1	0.400	78.0	78.0	1.0456	6.0E-04	0.40356	0.96123	0.10319
6.4	0.420	78.0	78.0	1.0476	5.2E-04	0.42280	0.96304	0.07834
6.7	0.440	78.0	78.0	1.0453	3.9E-04	0.44206	0.96438	0.05526
7.0	0.460	78.0	78.0	1.0502	2.7E-04	0.46137	0.96526	0.03347
7.3	0.480	78.0	78.0	1.0567	1.7E-04	0.48068	0.96572	0.01243
7.6	0.500	78.0	78.0	1.0598	8.1E-05	0.50000	0.96576	-0.00826

ORIGINAL PAGE IS
OF POOR QUALITY

Appendix v. FORTRAN PROGRAM SF3

This computer program calculates the two-dimensional stress distribution at the end of the adhesive. The boundary stresses are represented by polynomial approximations to facilitate calculating their Fourier series coefficients.

```

C THIS PROGRAM CALCULATES THE STRESS DISTRIBUTION IN A RECTANGULAR REGION.
C THE BOUNDARY CONDITIONS ON THE UPPER AND LOWER SURFACES ARE STRESSES
C REPRESENTED AS FOURIER SERIES.
DIMENSION ATNOR(01300),ATSHR(01300),ANMOR(01300),ABSMW(01300),
1 C1CSF(300),C2CSF(300),C3CSF(300),C4CSF(300),
2 C1SSF(300),C2SSF(300),C3SSF(300),C4SSF(300)
REAL L
CALL ASSIGN(6, '878P3.DAT')
PI=3.141592654
ITERM=300
L=3.0
ALPHA=0.020
TALF=TAN(ALPHA)
T=0.2
Y=0.1
T=YY
C DEFINE THE POLYNOMIAL COEFFICIENTS FOR THE SHEAR STRESS DISTRIBUTION
C ON THE UPPER (TOP) SURFACE OF THE RECTANGULAR REGION:
C FOR THE LEFT SIDE, 0.8<=X<1.3
PTL0=70.7124
PTL1=-326.6084
PTL2=506.9503
PTL3=-350.0967
PTL4=81.2500
C FOR THE RIGHT SIDE, 1.35<=X<3.0
PTR0=19.952
PTR1=-23.625
PTR2=12.746
PTR3=-3.2254
PTR4=0.31475
C POLYNOMIAL COEFFICIENTS FOR SHEAR STRESS ON THE BOTTOM:
C FOR THE LEFT SIDE, 0.8<=X<2
PMSL0=31.492691
PMSL1=-104.790309
PMSL2=122.251273
PMSL3=-57.846437
PMSL4=9.493152
C FOR THE RIGHT SIDE, 2<=X<3
PMSR0=PTR0
PMSR1=PTR1
PMSR2=PTR2
PMSR3=PTR3
PMSR4=PTR4
C POLYNOMIAL COEFFICIENTS FOR NORMAL STRESS ON THE TOP:
PTNL0=TALF*PTL0
PTNL1=TALF*PTL1
PTNL2=TALF*PTL2
PTNL3=TALF*PTL3
PTNL4=TALF*PTL4
PTNR0=TALF*PTR0
PTNR1=TALF*PTR1
PTNR2=TALF*PTR2
PTNR3=TALF*PTR3
PTNR4=TALF*PTR4
C POLYNOMIAL COEFFICIENTS FOR THE NORMAL STRESSES ON THE BOTTOM:
C FOR THE LEFT SIDE, 0.8<=X<2
PBNL0=23.94353
PBNL1=-84.191958
PBNL2=104.403470
PBNL3=-53.417605
PBNL4=9.623233
C FOR THE RIGHT SIDE, 2<=X<3
PBNR0=-4.32591
PBNR1=8.62584
PBNR2=-1.68029
PBNR3=30.18728
PBNR4=0.00430
C POLYNOMIALS FOR NORMAL STRESSES REQUIRED FOR MOMENT EQUILIBRIUM:
C FOR THE LEFT SIDE, 0.8<=X<1.8
PMOML0=225.00000
PMOML1=-80.3721
PMOML2=883.7209
PMOML3=-27.9070
PMOML4=0.0
C FOR THE RIGHT SIDE, 1.8<=X<2.0
PMOMR0=155.5555
PMOMR1=-268.6666
PMOMR2=150.0000
PMOMR3=-27.7778
PMOMR4=0.0

```

C CALCULATE THE ZEROETH FOURIER COEFFICIENTS FOR THE NORMAL STRESSES

```

ATNOR(0)=ATNL0
1   ((2.0/L)*(PTR0+3.00*PTR1+3.00*2/2.0*PTR2+3.00*3/3.0
1   +PTR3+3.00*4/4.0*PTR4+3.00*5/5.0)
2   -(2.0/L)*(PTR0+1.38*PTR1+1.38*2/2.0*PTR2+1.38*3/3.0
2   +PTR3+1.38*4/4.0*PTR4+1.38*5/5.0)
3   +(2.0/L)*(PTL0+1.38*PTL1+1.38*2/2.0*PTL2+1.38*3/3.0
3   +PTL3+1.38*4/4.0*PTL4+1.38*5/5.0)
4   -(2.0/L)*(PTL0+0.80*PTL1+0.80*2/2.0*PTL2+0.80*3/3.0
4   +PTL3+0.80*4/4.0*PTL4+0.80*5/5.0))
ABNOR(0)=(2.0/L)*((PBNL0+PMODL0)=1.0
1   +(PBNL1+PMODL1)=1.0*2/2.0
1   +(PBNL2+PMODL2)=1.0*3/3.0
2   +(PBNL3+PMODL3)=1.0*4/4.0
2   +(PBNL4+PMODL4)=1.0*5/5.0)
-(2.0/L)*((PBNL0+PMODL0)=0.8
3   +(PBNL1+PMODL1)=0.8*2/2.0
3   +(PBNL2+PMODL2)=0.8*3/3.0
4   +(PBNL3+PMODL3)=0.8*4/4.0
4   +(PBNL4+PMODL4)=0.8*5/5.0)
+(2.0/L)*((PBNL0+PMODR0)=2.0
1   +(PBNL1+PMODR1)=2.0*2/2.0
1   +(PBNL2+PMODR2)=2.0*3/3.0
2   +(PBNL3+PMODR3)=2.0*4/4.0
2   +(PBNL4+PMODR4)=2.0*5/5.0)
-(2.0/L)*((PBNL0+PAODR0)=1.4
3   +(PBNL1+PAODR1)=1.4*2/2.0
3   +(PBNL2+PAODR2)=1.4*3/3.0
4   +(PBNL3+PAODR3)=1.4*4/4.0
4   +(PBNL4+PAODR4)=1.4*5/5.0)
+(2.0/L)*((PBNL0+PBMR1)=3.0*2/2.0*PBMR2+3.00*3/3.0
4   +PBMR3=3.00*4/4.0*PBMR4+3.00*5/5.0)
-(2.0/L)*((PBNL0+PBMR1)=2.0*2/2.0*PBMR2+2.00*3/3.0
4   +PBMR3=2.00*4/4.0*PBMR4+2.00*5/5.0)

```

C CALCULATE THE STRESS FUNCTION COEFFICIENTS FOR THE NORMAL STRESSES:
 C (THIS IS THE STRESS FUNCTION SOLUTION WHICH ACCOUNTS FOR THE DIFFERENCE
 C IN THE UPPER AND LOWER AVERAGE NORMAL STRESSES)

```

B3R(ABNOR(0)=ATNOR(0))/2.0/(YB-YT)
A2R(ATNOR(0)/2.0-93+YT

```

C CALCULATE THE ZEROETH FOURIER COEFFICIENTS FOR THE SHEAR STRESSES:

```

ATSHR(0)=(2.0/L)*(PTR0+3.00*(PTR1+83)+3.00*2/2.0*PTR2+3.00*3/3.0
1   +PTR3+3.00*4/4.0*PTR4+3.00*5/5.0)
2   -(2.0/L)*(PTR0+1.38*(PTR1+83)+1.38*2/2.0*PTR2+1.38*3/3.0
2   +PTR3+1.38*4/4.0*PTR4+1.38*5/5.0)
3   +(2.0/L)*(PTL0+1.38*(PTL1+83)+1.38*2/2.0*PTL2+1.38*3/3.0
3   +PTL3+1.38*4/4.0*PTL4+1.38*5/5.0)
4   -(2.0/L)*(PTL0+0.80*(PTL1+83)+0.80*2/2.0*PTL2+0.80*3/3.0
4   +PTL3+0.80*4/4.0*PTL4+0.80*5/5.0)
5   +(2.0/L)*(n3=0.8*2/2.0)
ABSHR(0)=(2.0/L)*(PBSR0+3.0*(PBSR1+83)+3.00*2/2.0*PBSR2+3.00*3/3.0
1   +PBSR3+3.00*4/4.0*PBSR4+3.00*5/5.0)
2   -(2.0/L)*(PBSR0+2.0*(PBSR1+83)+2.00*2/2.0*PBSR2+2.00*3/3.0
2   +PBSR3+2.00*4/4.0*PBSR4+2.00*5/5.0)
3   +(2.0/L)*(PBSL0+2.0*(PBSL1+83)+2.00*2/2.0*PBSL2+2.00*3/3.0
3   +PBSL3+2.00*4/4.0*PBSL4+2.00*5/5.0)
4   -(2.0/L)*(PBSL0+0.8*(PBSL1+83)+0.80*2/2.0*PBSL2+0.80*3/3.0
4   +PBSL3+0.80*4/4.0*PBSL4+0.80*5/5.0)
5   +(2.0/L)*(n3=0.8*2/2.0)

```

C CALCULATE THE FOURIER COEFFICIENTS FOR THE TOP STRESS DISTRIBUTION:
 DO 1 NBT1,1TERMS

```

1   RETABNPT1/L
ATSHR(N)=2.0*AN(L,BETA,PTR0,PTR1+83,PTR2,PTR3,PTR4,3.0)
1   -2.0*AN(L,BETA,PTR0,PTR1+83,PTR2,PTR3,PTR4,1.38)
2   +2.0*AN(L,BETA,PTL0,PTL1+83,PTL2,PTL3,PTL4,1.38)
3   -2.0*AN(L,BETA,PTL0,PTL1+83,PTL2,PTL3,PTL4,0.8)
4   +2.0*AN(L,BETA,0.0,83,0.0,0.0,0.0,0.0,0.0)
5   -2.0*AN(L,BETA,0.0,83,0.0,0.0,0.0,0.0,0.0)
ATNOR(N)=2.0*AN(L,BETA,PTNL0,PTNL1,PTNL2,PTNL3,PTNL4,3.0)
1   -2.0*AN(L,BETA,PTNL0,PTNL1,PTNL2,PTNL3,PTNL4,1.38)
2   +2.0*AN(L,BETA,PTNL0,PTNL1,PTNL2,PTNL3,PTNL4,0.8)
3   -2.0*AN(L,BETA,PTNL0,PTNL1,PTNL2,PTNL3,PTNL4,0.0)

```

1 CONTINUE

C CALCULATE THE FOURIER COEFFICIENTS OF THE BOTTOM STRESS DISTRIBUTION:

```

DO 2 N=1,ITERMS
BFTAN=PI/L
ABSHN(N)=2.0*AN(L,BETA,PBSR0,PBSR1+BS3,PBSR2,PBSR3,PBSR4,3.0)
1 -2.0*AN(L,BETA,PBSR0,PBSR1+BS3,PBSR2,PBSR3,PBSR4,2.0)
2 +2.0*AN(L,BETA,PBSL0,PBSL1+BS3,PBSL2,PBSL3,PBSL4,2.0)
3 -2.0*AN(L,BETA,PBSL0,PBSL1+BS3,PBSL2,PBSL3,PBSL4,0.0)
4 +2.0*AN(L,BETA,0.0,B3,0.0,0.0,0.0,0.0)
5 -2.0*AN(L,BETA,0.0,B3,0.0,0.0,0.0,0.0)
ABNOR(N)=2.0*AN(L,BETA,PBNR0,PBNR1,PBNR2,PBNR3,PBNR4,3.0)
1 -2.0*AN(L,BETA,PBNR0,PBNR1,PBNR2,PBNR3,PBNR4,2.0)
2 +2.0*AN(L,BETA,PBNL0+PM0H20,PBNL1+PM0H11,PBNL2+PM0H22,
3 PBNL3+PM0H23,PBNL4+PM0H24,2.0)
4 -2.0*AN(L,BETA,PBNL0+PM0H20,PBNL1+PM0H11,PBNL2+PM0H22,
5 PBNL3+PM0H23,PBNL4+PM0H24,1.0)
6 +2.0*AN(L,BETA,PBNL0+PM0H20,PBNL1+PM0H11,PBNL2+PM0H22,
7 PBNL3+PM0H23,PBNL4+PM0H24,1.0)
8 -2.0*AN(L,BETA,PBNL0+PM0H20,PBNL1+PM0H11,PBNL2+PM0H22,
9 PBNL3+PM0H23,PBNL4+PM0H24,0.0)

```

2 CONTINUE

C CHECK FOURIER COEFFICIENTS:

```

0 WRITE(6,111)
0111 FORMAT(T5,' ',T14,'ATNOR',T32,'ATSHR',T50,'ABNOR',T68,'ABSHR')
0 DO 10 N=0,ITERMS
0 WRITE(6,100) N,ATNOR(N),ATSHR(N),ABNOR(N),ABSHR(N)
010 CONTINUE
0 WRITE(6,110)
0110 FORMAT(T9,' ',T20,'TAUTN',T32,'TAUTS',T44,'TAUBN',T56,'TAUBS')
0 DO 4 NX=30,30
4 NX=0.1
4 TAUTN=ATNOR(0)/2.0
4 TAUTS=ATSHR(0)/2.0
4 TAUBN=ABNOR(0)/2.0
4 TAUBS=ABSHR(0)/2.0
0 DO 3 N=1,ITERMS
0 BETAN=PI*X/L
0 C=COS(BETAN)
0 TAUTN=TAUTN+C*ATNOR(N)
0 TAUTS=TAUTS+C*ATSHR(N)
0 TAUBN=TAUBN+C*ABNOR(N)
0 TAUBS=TAUBS+C*ABSHR(N)
03 CONTINUE
0 WRITE(6,101) X,TAUTN,TAUTS,TAUBN,TAUBS
04 CONTINUE
C

```

C CALCULATE SOLUTION COEFFICIENTS:

```

00 6 N=1,ITERMS
0 ETABN=PI/L
0 S=SIHN(BETA+YT)
0 C=COSH(BETA+YT)
A11=2.0*BETA+**2+S
A12=2.0*BETA+(S+BETA+YT+C)
A21=2.0*BETA+**2+C
A22=2.0*BETA+**2+YT+S
DET=A11*A22-A12*A21
B1=ABNOR(N)-ATSHR(N)
B2=0.0
C1SSF(N)=(B1+A22-B4*A12)/DET
C2SSF(N)=(B4*A11-B1*A21)/DET
B1=0.0
B4=-(ATNOR(N)+ABNOR(N))
C1CSF(N)=(B1+A22-B4*A12)/DET
C2CSF(N)=(B4*A11-B1*A21)/DET
A11=2.0*BETA+**2+C
A12=2.0*(BETA+C+BETA+**2+YT+S)
A21=2.0*BETA+**2+S
A22=2.0*BETA+**2+YT+C
DET=A11*A22-A12*A21
B2=-(ATSHR(N)+ABSHR(N))
B3=0.0
C2SSF(N)=(B2*A22-B3*A12)/DET
C3SSF(N)=(B3*A11-B2*A21)/DET
B2=0.0
B3=ABNOR(N)-ATNOR(N)
C2CSF(N)=(B2*A22-B3*A12)/DET
C3CSF(N)=(B3*-B2*A21)/DET
6 CONTINUE

```

```

C CALCULATE THE STRESS FUNCTION COEFFICIENTS FOR THE NORMAL STRESSES:
C (THIS IS THE STRESS FUNCTION SOLUTION WHICH ACCOUNTS FOR THE DIFFERENCE
C IN THE UPPER AND LOWER AVERAGE NORMAL STRESSES)
SF83=(ABNOR(0)-ATNOR(0))/2.0/(YB-YT)
SFA2=ATNOR(0)/2.0-SF83+YT
C
C CALCULATE THE STRESS FUNCTION COEFFICIENTS TO CORRECT THE LINEARLY
C INCREASING NORMAL STRESSES IN THE X-DIRECTION:
C (THIS STRESS FUNCTION ALSO MAKES THE X-DIRECTION NORMAL STRESSES ZERO
C AT THE ENDS AND MAKES THE SHEAR STRESSES CONSTANT AT THE ENDS)
SF03=182.3591
SF04=-107.5550
SF82=-SF04/2.0+YB*2
C
C CALCULATE STRESSES:
D      WRITE(6,112)
112    FORMAT(8,'NONE',T20,'XTN0',T32,'TAU1',T44,'TAU2',T56,'TAU12')
DO 7 NY=10,10,2
DO 7 NX=0,30
Y=NY*0.1
X=NX*0.1
SIGX=SF03+Y+SF04*X+Y
SIGY=SF83+Y+SFA2
TAUXY=ATSHR(0)/2.0-SF83*X-SF82-SF04/2.0*Y*2
DO 8 N=1,ITERMS
B=PI/L
B2=B*2
S=SIN(B*Y)
C=COSH(B*Y)
SIGX=SIGX
1 +SIN(B*X)*(C1CSF(N)+B2*C+C2CSF(N)+B2*S+C3CSF(N)+B*(2.0*S+B*Y+C)
2 +C4CSF(N)+B*(2.0*C+B*Y+S))
3 +COS(B*X)*(C1CSF(N)+B2*C+C2CSF(N)+B2*S+C3CSF(N)+B*(2.0*S+B*Y+C)
4 +C4CSF(N)+B*(2.0*C+B*Y+S))
SIGY=SIGY
1 -B2*SIN(B*X)*(C1CSF(N)+C+C2CSF(N)+S+C3CSF(N)+Y+C+C4CSF(N)+Y+S)
2 -B2*COS(B*X)*(C1CSF(N)+C+C2CSF(N)+S+C3CSF(N)+Y+C+C4CSF(N)+Y+S)
TAUXY=TAUXY
1 -B*COS(B*X)*(C1CSF(N)+B*S+C2CSF(N)+B+C+C3CSF(N)+(C+B*Y+S)
2 +C4CSF(N)+(S+B*Y+C))
3 +B*SIN(B*X)*(C1CSF(N)+B*S+C2CSF(N)+B+C+C3CSF(N)+(C+B*Y+S)
4 +C4CSF(N)+(S+B*Y+C))
8 CONTINUE
WRITE(6,101) X,Y,SIGX,SIGY,TAUXY
7 CONTINUE
1000 CONTINUE
100  FORMAT(8X,I3,SE18.4)
101  FORMAT(8X,5F12.6)
END
FUNCTION AN(L,BETA,P0,P1,P2,P3,P4,X)
REAL L
AN=(1.0/L)*(P0/BETA+P1*X/BETA+P2*(BETA**2*X**2-2.0)/BETA**3
1 +P3*(BETA**2*X**3-6.0*X)/BETA**3
2 +P4*(BETA**4*X**4-12.0*BETA**2*X**2+24.0)/BETA**5)
3 *SIN(BETA*X)
4 +(1.0/L)*(P1/BETA**2+2.0*B2*X/BETA**2
5 +P3*(3.0*BETA**2*X**2-6.0)/BETA**4
6 +P4*(4.0*BETA**2*X**3-24.0*X)/BETA**4)*COS(BETA*X)
RETURN
END
FUNCTION BN(L,BETA,P0,P1,P2,P3,P4,X)
REAL L
BN=(1.0/L)*(P1/BETA**2+2.0*B2*X/BETA**2
1 +P3*(3.0*BETA**2*X**2-6.0)/BETA**4
2 +P4*(4.0*BETA**2*X**3-24.0*X)/BETA**4)*SIN(BETA*X)
3 +(1.0/L)*(-P0/BETA-P1*(1/BETA-P2*(BETA**2*X**2-2.0)/BETA**3
4 -P3*(BETA**4*X**4-12.0*BETA**2*X**2+24.0)/BETA**5)
5 +P4*(BETA**4*X**4-12.0*BETA**2*X**2+24.0)/BETA**5)
6 *COS(BETA*X)
RETURN
END

```

ORIGINAL PAGE IS
OF POOR QUALITY

Appendix vi. FORTRAN PROGRAM DEFLCOMP

This program calculates the deflection, location of the neutral axis, bending rigidity (EI), moment and top and bottom strains of an adhesive'y bonded scarf joint with a doubler. It treats the specimen as a layered beam at each cross section.

```
1000 $RESET FREE
1010 *SET AUTOBIND
1020 C THIS PROGRAM CALCULATES THE DEFLECTION, LOCATION OF THE NEUTRAL
1030 C AXIS, BENDING STIFFNESS (EI), MOMENT AND TOP AND BOTTOM STRAINS OF
1040 C AN ADHESIVELY BONDED SCARF JOINT WITH A DOUBLER. IT TREATS THE
1050 C SPECIMEN AS A LAYERED BEAM AT EACH CROSS SECTION. IT ACCOUNTS FOR
1060 C VARIABLE ADHESIVE THICKNESS IN ALL ADHESIVE LAYERS AND FOR THE
1070 C UNFLAT LOWER SURFACE CAUSED BY VARIABLE THICKNESS IN THE SCARF
1080 C JOINT ITSELF.
1090 LOGICAL RKBSTA
1100 COMMON /RKBSTA/ SP,HMIN,HMAX,HC,AB,SG,Q(1609)
1110 REAL I1,I2,I3,I4,IS,LJ1,LJ2,LJ3,LJ4,L1,L2,M,N,MOD,NU12,
1120 1,NUMC,NUMR,NUM,NUM1,NUM2
1130 DIMENSION H(20),HR(20),E(20),ER(20),THETAR(20),THETAC(20)
1140 C--SET SPECIMEN GEOMETRY, PHYSICAL PROPERTIES AND LOAD
1150 C DAT IS DOUBLER ADHESIVE THICKNESS,
1160 C SAT IS SCARF ADHESIVE THICKNESS
1170 C DOUBT IS DOUBLER THICKNESS
1180 C HCOM IS THE THICKNESS OF THE ORIGINAL DAMAGED MATERIAL
1190 C DOL IS THE DOUBLER OVERLAP
1200 C EC,EE,ED ARE YOUNG'S MODULI OF THE COMPOSITE, ADHESIVE AND DOUBLER
1210 C GAMMA IS THE ANGLE OF THE SURFACES OF THE SCARF ADHESIVE DUE TO
1220 C VARYING THICKNESS.
1230 C LJ1 IS DAMAGE HALF LENGTH
1240 C TFLYC AND TFLYR ARE THE FLY THICKNESSES OF THE ORIGINAL LAMINATE
1250 C AND THE REPLACEMENT PIECE,
1260 C H(I) AND HR(I) ARE THE COORDINATES OF THE BOTTOMS OF THE I-TH
1270 C PLIES IN THE ORIGINAL LAMINATE AND THE REPLACEMENT PIECE.
1280 C NPLYC AND NPLYR ARE THE NUMBER OF PLIES IN THE ORIGINAL LAMINATE
1290 C AND THE REPLACEMENT PIECE.
1300 TPLYC=0.138
1310 TPLYR=0.138
1320 NPLYC=18
1330 NPLYR=18
1340 ALPHA=6.0
1350 DOUBT=0.62
1360 DATI=0.30
1370 DATLJ1=0.30
1380 DATLJ2=0.30
1390 DATLJ3=0.36
1400 DATLJ4=0.36
1410 DATL1=0.14
1420 SATLJ2=0.32
1430 SATLJ3=0.22
1440 LJ1=12.5
1450 DOL=25.0
1460 L2=120.0
1470 R=25.0
1480 EE=3450.0
1490 ED=63500.0
1500 C CALCULATE PLY MODULI- (ASSUMING SIGMAX IS NON-ZERO AND
1510 C SIGMAY=EPSILONXY=0)
1520 E11=117000.0
1530 E22=9300.0
1540 NU12=0.3
1550 G12=4500.0
1560 THETAC(1)= 0.0; THETAR(1)= 0.0
1570 THETAC(2)= 0.0; THETAR(2)= 0.0
1580 THETAC(3)= 45.0; THETAR(3)= 45.0
1590 THETAC(4)=-45.0; THETAR(4)=-45.0
1600 THETAC(5)= 90.0; THETAR(5)= 90.0
1610 THETAC(6)= 45.0; THETAR(6)= 45.0
1620 THETAC(7)=-45.0; THETAR(7)=-45.0
1630 THETAC(8)= 0.0; THETAR(8)= 0.0
1640 THETAC(9)= 0.0; THETAR(9)= 0.0
1650 THETAC(10)= 0.0; THETAR(10)= 0.0
1660 THETAC(11)= 0.0; THETAR(11)= 0.0
1670 THETAC(12)=-45.0; THETAR(12)=-45.0
1680 THETAC(13)= 45.0; THETAR(13)= 45.0
1690 THETAC(14)= 90.0; THETAR(14)= 90.0
1700 THETAC(15)=-45.0; THETAR(15)=-45.0
1710 THETAC(16)= 45.0; THETAR(16)= 45.0
```

```

1720      THETAC(17)= 0.0  THETAR(17)= 0.0
1730      THETAC(18)= 0.0  THETAR(18)= 0.0
1740      DO 302 I=1,NPLYC
1750      E(I)=EPLY(THETAC(I),E11,E22,NU12,B12)
1760      302 CONTINUE
1770      DO 303 I=1,NPLYR
1780      ER(I)=EPLY(THETAR(I),E11,E22,NU12,B12)
1790      303 CONTINUE
1800 C  CALCULATE SUMS FOR THE COMPOSITES:
1810 C  FOR THE ORIGINAL LAMINATE,
1820      H(1)=0.0
1830      NUMC=0.0
1840      DENOMC=0.0
1850      DO 300 I=1,NPLYC
1860      R=FLOAT(I)
1870      H(I+1)=R*TPLYC
1880      NUMC=E(I)*(H(I+1)+H(I))*(H(I+1)-H(I))+NUMC
1890      DENOMC=E(I)*(H(I+1)-H(I))+DENOMC
1900      300 CONTINUE
1910      HCOM=H(NPLYC+1)
1920 C  FOR THE REPLACEMENT PIECE,
1930      NUMR=0.0
1940      DENR=0.0
1950      HR(1)=0.0
1960      DO 301 I=1,NFLYR
1970      R=FLOAT(I)
1980      HR(I+1)=R*TPLYR
1990      NUMR=R(I)*(HR(I+1)+HR(I))*(HR(I+1)-HR(I))+NUMR
2000      DENR=E(I)*(HR(I+1)-HR(I))+DENR
2010      301 CONTINUE
2020      HTOPR=R(NFLYR+1)
2030      WRITE (6,205)
2040      205 FORMAT ('      ENTER LOAD FORCE IN NEWTONS AND INITIAL DEFLECTION'
2050      '      IN MM.')
2060      READ (5,/) F,Z0
2070      WRITE (6,202) LJ1,ALPHA,DOL,F
2080      202 FORMAT(1X/1X/3X*DEFLECTION OF A SCARF JOINT WITH DOUBLER*/1X/
2090      1 2X*DAMAGE HALF LENGTH IS 'F5.2' MM'
2100      1 2X*SCARF ANGLE IS 'F4.1' DEGREES'
2110      3 2X*DOUBLER OVERLAP IS 'F4.1' MM'
2120      3 2X*LOAD FORCE IS 'F8.2' NEWTONS  */1X/
2130      4 3X* POSITION DEFLECTION NEUT AXIS   EI      MOMENT*
2140      5 7X*MICRO STRAIN*/58X*TOP*4X*BOTTOM*
2150      6 3X*   MM      MM      MM      */
2160      ALPH=ALPHA*3.141592654/180.0
2170      TA=TAN(ALPH)
2180      LJ2=LJ1+SATLJ2/SIN(ALPH)
2190      LJ3=LJ1+HCOM/TA
2200      LJ4=LJ2+HCOM/TA
2210      L1=LJ3*DOL
2220      GAMMA=ATAN((SATLJ3-SATLJ2)*COS(ALPH)/(LJ3+SATLJ3*SIN(ALPH)-LJ2))
2230      SGAM=SIN(GAMMA)
2240      TGAM=TAN(GAMMA)
2250      800 CONTINUE
2260 C--SET INITIAL VALUES
2270      ILL RKRST
2280      SG=1.0E-09
2290      Y=0.0
2300      SP=0.0
2310      Z=Z0
2320      DZDY=0.0
2330 C--CALCULATE SECTION PROPERTIES: EI AND ECCENTRICITY, ECC.
2340      1000 IF (Y .GE. 0.0 .AND. Y .LT. LJ1) GO TO 501
2350      IF (Y .GE. LJ1 .AND. Y .LT. LJ2) GO TO 502
2360      IF (Y .GE. LJ2 .AND. Y .LT. LJ3) GO TO 503
2370      IF (Y .GE. LJ3 .AND. Y .LT. LJ4) GO TO 504
2380      IF (Y .GE. LJ4 .AND. Y .LT. L1) GO TO 505
2390      IF (Y .GE. L1) GO TO 506
2400      501 H3=HTOPR
2410      H4=H3+DATI+Y*(DATLJ1-DATI)/LJ1
2420      H5=H4+DOURT
2430      ZZERO=(L2-LJ2)*SGAM

```

```

2440 C CALCULATE THE NEUTRAL AXIS COORDINATE, T
2450     N=(ED*(H5-H4)*(H4+H5)+EE*(H4-H3)*(H3+H4)+NUMR)
2460     D=(2.0*(ED*(H5-H4)+EE*(H4-H3)+DENR))
2470     T=N/D
2480 C CALCULATE EI FOR THE COMPOSITE REPLACEMENT PIECE
2490     EIC=0.0
2500     DO 311 I=1,NPLYR
2510     HD=H(I+1)-H(I)
2520     R=T-(H(I)+HD/2.0)
2530     PMOI=B*HD*HD*HD/12.0+B*HD*R*R
2540     EIC=ER(I)*PMOI+EIC
2550 311 CONTINUE
2560     HD=H4-H3
2570     R=T-(H3+HD/2.0)
2580     I2=B*HD*HD*HD/12.0+B*HD*R*R
2590     HD=H5-H4
2600     R=T-(H4+HD/2.0)
2610     I3=B*HD*HD*HD/12.0+B*HD*R*R
2620     EI=EIC+EE*I2+ED*I3
2630     ECC=T-HCOM/2.0+ZZERO
2640     S=0.5*D
2650     TT=T-HS
2660     GO TO 600
2670 502 H2=HTOPR
2680     H2=(Y-LJ1)*TA
2690     H4=H3+DATLJ1+(Y-LJ1)*(DATLJ2-DATLJ1)/(LJ2-LJ1)
2700     H5=H4+DOUTR
2710     ZZERO=(L2-LJ2)*SGAM
2720 C CALCULATE THE NEUTRAL AXS COORDINATE, T.
2730     IL=INT(H2/TPLYR)
2740     DENOM=0.0
2750     NUM=0.0
2760     IF (IL.EQ. 0) GO TO 621
2770     DO 321 I=1,IL
2780     NUM=ER(I)*(HR(I+1)+HR(I))*(HR(I+1)-HR(I))+NUM
2790     DENOM=ER(I)*(HR(I+1)-HR(I))+DENOM
2800 321 CONTINUE
2810 621 CONTINUE
2820     NUM=ER(IL+1)*(H2+HR(IL+1))*(H2-HR(IL+1))+NUM
2830     DENOM=ER(IL+1)*(H2-HR(IL+1))+DENOM
2840     NUM=NUMR-NUM
2850     DENOM=DENR-DENOM.
2860     N=(ED*(H5-H4)*(H5+H4)+EE*(H4-H3)*(H3+H4)+NUM
2870     +EE*H2*H2)
2880     D=(2.0*(ED*(H5-H4)+EE*(H4-H3)+DENOM+EE*H2))
2890     T=N/D
2900 C CALCULATE EI FOR THE REVELED COMPOSITE REPLACEMENT PIECE
2910     EIC=0.0
2920     IF=IL+2
2930     IF (IP .GT. NPLYR) GO TO 622
2940     DO 322 I=IF,NPLYR
2950     HD=HR(I+1)-HR(I)
2960     R=T-(HR(I)+HD/2.0)
2970     PMOI=B*HD*HD*HD/12.0+B*HD*R*R
2980     EIC=ER(I)*PMOI+EIC
2990 322 CONTINUE
3000 622 CONTINUE
3010     HD=HR(IL+2)-H2
3020     R=T-(H2+HD/2.0)
3030     PMOI=B*HD*HD*HD/12.0+B*HD*R*R
3040     EIC=ER(IL+1)*PMOI+EIC
3050     HD=I2 -
3060     R=T-HD/2.0
3070     I1=B*HD*HD*HD/12.0+B*HD*R*R
3080     HD=H4-H3
3090     R=T-(H3+HD/2.0)
3100     I3=B*HD*HD*HD/12.0+B*HD*R*R
3110     HD=H5-H4
3120     R=T-(H4+HD/2.0)
3130     I4=B*HD*HD*HD/12.0+B*HD*R*R
3140     EI=EE*I1+EIC+EE*I3+ED*I4
3150     ECC=T-HCOM/2.0+ZZERO

```

```

3160      S=0.5*D
3170      TT=T-HS
3180      GO TO 600
3190 50:  SEAM=(Y-LJ2)*TGBAM
3200      H1=(Y-LJ2)*TA
3210      H2=H1+SATLJ2
3220      H3=TOPR+SEAM
3230      H4=H3+DATLJ2+(Y-LJ2)*(DATLJ3-DATLJ2)/(LJ3-LJ2)
3240      HS=H4+DOUBT
3250      ZZERO=(L2-Y)*SGAM
3260 C  CALCULATE THE NEUTRAL AXIS COORDINATE+T:
3270      ILT=INT(H2/TPLYR)
3280      ILB=INT(H1/TPLYC)
3290 C  FOR THE ORIGINAL LAMINATE:
3300      NUM1=0.0
3310      DENOM1=0.0
3320      IF (ILB .EQ. 0) GO TO 631
3330      DO 331 I=1,ILB
3340      NUM1=E(I)*(H(I+1)+H(I))*(H(I+1)-H(I))+NUM1
3350      DENOM1=E(I)*(H(I+1)-H(I))+DENOM1
3360 331  CONTINUE
3370 631  CONTINUE
3380      NUM1=E(ILB+1)*(H1+H(ILB+1))*(H1-H(ILB+1))+NUM1
3390      DENOM1=E(ILB+1)*(H1-H(ILB+1))+DENOM1
3400 C  FOR THE REPLACEMENT PIECE:
3410      NUM2=0.0
3420      DENOM2=0.0
3430      ILTR=ILT+2
3440      IF (ILTR .GT. NPLYR) GO TO 632
3450      DO 332 I=ILTR,NPLYR
3460      NUM2=ER(I)*(HR(I+1)+HR(I)+2.0*SEAM)*(HR(I+1)-HR(I))+NUM2
3470      DENOM2=ER(I)*(HR(I+1)-HR(I))+DENOM2
3480 332  CONTINUE
3490 632  CONTINUE
3500      NUM2=ER(ILT+1)*(HR(ILT+2)+H2+2.0*SEAM)*(HR(ILT+2)-H2)+NUM2
3510      DENOM2=ER(ILT+1)*(HR(ILT+2)-H2)+DENOM2
3520      H=(ED*(HS-H4)*(H4*HS)+EE*(H4-H3)*(H3+H4)+NUM2
3530      1 +EE*(H2+SEAM-H1)*(H1+H2+SEAM)+NUM1)
3540      D=(2.0*(ED*(HS-H4)+EE*(H4-H3)+DENOM2+EE*(H2+SEAM-H1)+DENOM1))
3550      T=N/D
3560 C  CALCULATE EI FOR THE ORIGINAL LAMINATE
3570      EIC1=0.0
3580      IF (ILB.EQ. 0) GO TO 633
3590      DO 333 I=1,ILB
3600      HD=H(I+1)-H(I)
3610      R=T-(H(I)+HD/2.0)
3620      PMOI=R*HD*HD*HD/12.0+B*HD*R*R
3630      EIC1=E(I)*PMOI+EIC1
3640 333  CONTINUE
3650 633  CONTINUE
3660      HD=H1-H(ILB+1)
3670      R=T-(H(ILB+1)+HD/2.0)
3680      PMOI=B*HD*HD*HD/12.0+B*HD*R*R
3690      EIC1=E(ILB+1)*PMOI+EIC1
3700      HD=H2+SEAM-H1
3710      R=T-(H1+HD/2.0)
3720      I2=B*HD*HD*HD/12.0+B*HD*R*R
3730 C  CALCULATE EI FOR THE REPLACEMENT PIECE
3740      EIC2=0.0
3750      ILTR=ILT+2
3760      IF (ILTR .GT. NPLYR) GO TO 634
3770      DO 334 I=ILTR,NPLYR
3780      HD=HR(I+1)-HR(I)
3790      R=T-(HR(I)+HD/2.0+SEAM)
3800      PMOI=B*HD*HD*HD/12.0+B*HD*R*R
3810      EIC2=ER(I)*PMOI+EIC2
3820 334  CONTINUE
3830 634  CONTINUE
3840      HD=HR(ILT+2)-H2
3850      R=T-(H2+SEAM+HD/2.0)
3860      PMOI=B*HD*HD*HD/12.0+B*HD*R*R
3870      EIC2=ER(ILT+1)*PMOI+EIC2

```

```
3880      HD=H4-H3
3890      R=T-(H3+HD/2.0+SEAM)
3900      I4=B*HD*HD*HD/12.0+B*HD*R*R
3910      HD=H5-H4
3920      R=T-(H4+HD/2.0)
3930      IS=B*HD*HD*HD/12.0+B*HD*R*R
3940      EI=EIC1+EE*I2+EIC2+EE*I4+ED*I5
3950      ECC=T-HCOM/2.0+ZZERO
3960      S=0.5*D
3970      TT=T-H5
3980      GO TO 600
3990 501 H3=(Y-LJ2)*TA
4000      H4=(LJ3-LJ2)*TA+SATLJ3+DATLJ3+
4010      1  (Y-LJ3)*(DATLJ4+HCOM)-((LJ3-LJ2)*TA+SATLJ3+DATLJ3))/(LJ4-LJ3)
4020      H5=H4+DOUBT
4030      ZZERO=(L2-Y)*SGAM
4040 C CALCULATE THE NEUTRAL AXIS COORDINATE, T:
4050      IL=INT(H3/TPLYC)
4060      NUM=0.0
4070      DENOM=0.0
4080      ILR=IL+2
4090      IF (ILR.GT. NPLYC) GO TO 641
4100      DO 341 I=ILR,NPLYC
4110      NUM=E(I)*(H(I+1)+H(I))*(H(I+1)-H(I))+NUM
4120      DENOM=E(I)*(H(I+1)-H(I))+DENOM
4130      341 CONTINUE
4140      641 CONTINUE
4150      NUM=E(IL+1)*(H(ILR)+H3)*(H(ILR)-H3)+NUM
4160      DENOM=E(IL+1)*(H(ILR)-H3)+DENOM
4170      NUM=NUMC-NUM
4180      DENOM=DENOMC-DENOM
4190      N=(ED*(H5-H4)*(H4+H5)+EE*(H4-H3)*(H3+H4)+NUM)
4200      D=(2.0*(ED*(H5-H4)+EE*(H4-H3)+DENOM))
4210      T=N/D
4220 C CALCULATE ET FOR THE BEVELED ORIGINAL LAMINATE:
4230      EIC=C.0
4240      IF (IL .EQ. 0) GO TO 642
4250      DO 342 I=1,IL
4260      HD=H(I+1)-H(I)
4270      R=T-(H(I)+HD/2.0)
4280      PMOI=B*HD*HD*HD/12.0+B*HD*R*R
4290      EIC=E(I)*PMOI+EIC
4300      342 CONTINUE
4310      642 CONTINUE
4320      HD=H3-H(IL+1)
4330      R=T-(H3-HD/2.0)
4340      PMOI=B*HD*HD*HD/12.0+B*HD*R*R
4350      EIC=E(IL+1)*PMOI+EIC
4360      HD=H4-H3
4370      R=T-(H3-HD/2.0)
4380      I2=B*HD*HD*HD/12.0+B*HD*R*R
4390      HD=H5-H4
4400      R=T-(H4+HD/2.0)
4410      I3=B*HD*HD*HD/12.0+B*HD*R*R
4420      EI=EIC+EE*I2+ED*I3
4430      ECC=T-HCOM/2.0+ZZERO
4440      S=0.5*D
4450      TT=T-H5
4460      GO TO 600
4470 502 H3=HCON
4480      H4=H3+DATLJ4+(Y-LJ4)*(DATL1-DATLJ4)/(L1-LJ4)
4490      H5=H4+DOUBT
4500      ZZERO=(L2-Y)*SGAM
4510 C CALCULATE THE NEUTRAL AXIS COORDINATE, T:
4520      N=(ED*(H5-H4)*(H4+H5)+EE*(H4-H3)*(H3+H4)+NUMC)
4530      D=(2.0*(ED*(H5-H4)+EE*(H4-H3)+DENOMC))
4540      T=N/D
4550 C CALCULATE EI FOR THE COMPOSITE:
4560      EIC=0.0
4570      DO 351 I=1,NPLYC
4580      HD=H(I+1)-H(I)
4590      R=T-(H(I)+HD/2.0)
```

```

4600      PMOI=B*HD*HD*HD/12.0+B*HD*R*R
4610      EIC=E(I)*PMOI+EIC
4620  351 CONTINUE
4630      HD=H4-H3
4640      R=T-(H3+HD/2.0)
4650      I2=B*HD*HD*HD/12.0+B*HD*R*R
4660      HD=H5-H4
4670      R=T-(H4+HD/2.0)
4680      I3=B*HD*HD*HD/12.0+B*HD*R*R
4690      EI=EIC+EE*I2+ED*I3
4700      ECC=T-HCOM/2.0+ZZERO
4710      S=0.5*D
4720      TT=T-H5
4730      GO TO 600
4740  506 CONTINUE
4750  C  CALCULATE THE NEUTRAL AXIS COORDINATE, T:
4760      T=NUMC/(DENOMC*2.0)
4770  C  CALCULATE EI
4780      EIC=0.0
4790      DO 361 I=1,NPLYC
4800      HU=(H(I+1)-H(I))
4810      R=T-(H(I)+HD/2.0)
4820      PMOI=B*HD*HU*HU/12.0+B*HD*R*R
4830      EIC=E(I)*PMOI+EIC
4840  361 CONTINUE
4850      EI=EIC
4860      ZZERO=(L2-Y)*SGAM
4870      ECC=2*ZERO
4880      S=DENOMC
4890      TT=T-HCOM
4900  C--INTEGRATE EQUATIONS
4910      600 Y=RKRI(Y,1.0)
4920      M=F8(Z+ECC)
4930      D2ZDY2=M/EI
4940      DZDY=RKB8U(DZDY,D2ZDY2)
4950      Z=RKB8U(Z,DZDY)
4960      IF (RKRSTA (.FALSE.)) GO TO 1000
4970      FEM=F8(T-HCOM/2.0)
4980      FEC=M-FEM
4990      EBOT=T*M/EI
5000      ETOP=T*M/EI
5010      EFORCE=F/S/B
5020      BSTRN=(EBOT+EFORCE)*1.0E06
5030      TSTRN=(ETOP+EFORCE)*1.0E06
5040      WRITE (6,200) Y,Z,T,EI,M,TSTRN,BSTRN
5050  200 FORMAT (3X,F6.1,3X,F10.6,F10.5,1X,1P2E10.3,0P2F9.1)
5060      SP=SF+0.2
5070      IF (Y .GE. L2) GO TO 700
5080      GO TO 1000
5090  700 CONTINUE
5100      END
5110  C  EPLY IS THE MODULUS OF A GIVEN PLY
5120      FUNCTION EPLY(THETA,E11,E22,NU12,G12)
5130      REAL M,N,M2,N2,M4,N4,NU21,NU12,NUNU,EPLY
5140      PI=3.141592654
5150      THETAR=THETA*PI/180.0
5160      M=COS(THETAR)
5170      N=SIN(THETAR)
5180      M2=M*M
5190      M4=M2*M2
5200      N2=N*N
5210      N4=N2*N2
5220      NU21=NU12*E22/E11
5230      NUNU=1.0-NU12*NU21
5240      Q11=E11/NUNU
5250      Q12=NU12*E22/NUNU
5260      Q22=E22/NUNU
5270      Q66=G12
5280      Q11P=M4*Q11+2.0*M2*N2*(Q12+2.0*Q66)+N4*Q22
5290      Q22P=N4*Q11+2.0*M2*N2*(Q12+2.0*Q66)+M4*Q22
5300      Q12P=M2*N2*(Q11+Q22-4.0*Q66)+(M4+N4)*Q12
5310      EPLY=(Q11P*Q22P-Q12P*Q12P)/Q22P
5320      RETURN
5330      END

```